Deciphering olfactory epithelium development : from cell type diversity to morphogenesis

Raphaël Aguillon

Université Fédérale

Toulouse Midi-Pyrénées

THÈSE

En vue de l'obtention du

DOCTORAT DE L'UNIVERSITÉ DE TOULOUSE

Délivré par :

Université Toulouse 3 Paul Sabatier

Présentée et soutenue par :
Raphaël Aguillon

le 15 Décembre 2017

Titre :

Décrypter la formation de l'épithélium olfactif : de la diversité cellulaire à la morphogenèse.

École doctorale et discipline ou spécialité :

ED n°151 Biologie - Santé - Biotechnologie
Biologie du Développement

Unité de recherche :

Centre de Biologie du Développement UMR5547

Directeur/trice(s) de Thèse :

Dr Patrick Blader
Dr Julie Batut

Jury :

Pr Cathy Soula	UT3 - Toulouse	Présidente du Jury
Dr Patrick Blader	UT3 - Toulouse	Directeur de thèse
Dr Julie Batut	UT3 - Toulouse	Co-Directrice de thèse
Dr Muriel Perron	UPSUD - Paris	Rapportrice
Dr Alexandre Pattyn	INM - Montpellier	Rapporteur
Dr Nicolas David	IBENS - Paris	Rapporteur

La mer
Qu'on voit danser le long des golfes clairs
A des reflets d'argent
La mer
Des reflets changeants
Sous la pluie

On dit merci qui ?

Je voudrais tout d'abord remercier l'ensemble des membres de mon jury de thèse pour avoir pris le temps de m'écouter et de discuter de mes travaux.

CBD, Dès ma première année à la fac, j'ai commencé à trainer dans le 4R3 et puis de façon plus progressive dans les couloirs du CBD. Je me sens bien avec vous ! Je vous embrasse tous et toutes. Un ptit mot spécial pour Corinne Benassayag : Je ne sais pas si tu te souviens mais c'est après t'avoir rencontré en L1 lors d'un interview pour un module d'insertion professionnel que j'ai su que je voulais devenir chercheur !

Aurélie

Clément

Patrick, je n'ai pas vraiment de point de comparaison, mais je doute qu'il puisse exister un meilleur directeur de thèse que toi. Haut les cœurs Pat Ps : n'hésite pas à me contacter si tu as des questions ou des difficultés en Biomol. Bitch un jour, Bitch toujours.

Juju, ma binôme. Ma co-directrice de thèse. Et puis bien plus que ça. Cela me parait presque ridicule de te remercier en quelques mots...t'es géniale et j'espère avoir acquis un peu de toi pendant ces 3 années. Fais attention à toi, et moi je ferai pareil. Qui sait quelle surprise nous réserve l'avenir.

Brice

Quentin

Elsa

P&P : ...haha

Isabelle

Marie

Pauline

Arnaud

Stéphanie

Laurence

Myriam, Elise, Laurence, Aurélie, Véro, Aurore, Aurore, Claire...Coucou la ptite famille de la poiscaille. J'ai baigné dans vos eaux pendant 6 ans. J'ai grandi avec vous et j'aime bien le jeune scientifique que je suis devenu. Je vous embrasse

Kris

Mes amours des premières années de fac, vous êtes encore là et je vous aime

Sarah, Gautier, Alex, Hayssam Mes doudous, vous me manquez. Surtout, éclatez-vous :)

Claire

Sylvanie

Elodie

Anna

François

Pascale, finalement, c'est grâce à toi que j'en suis là. Docteur en BDA. Quelle blague, tu m'as bien eu ! Mais merci quand même. Ma Pascale, respire un bon coup et fonce. Quant à moi, je continuerai à t'écouter sans prendre de notes.

Florian

Laurence

Sandra

Marie

Pascale

Guillaume

Raphaël

Myriam

Audrey

Valérie

Patrick

Anthony, tu y es pour beaucoup dans qui je suis aujourd'hui. Merci pour toutes ces pages vécues.

Aurore

Antoine, jamais je n'oublierai ces douces fourmis qui nous ont porté ensemble. A demain !

Ma jolie famille. de votre amour Je vous en serai toujours reconnaissant, je vous aime profondément. Un spécial pour Maman : sans toi, je ne serai pas bien loin.
T'es merveilleuse. Merci. Je t'aime.

Julie

Suzanne

Philippe

Jérémie

Roxanne

Lu

Marion

Adrien

Delphine

Pauline

A tous mes amis proches ou loin, du passé, du présent et du futur. Je suis à vous, vous à moi.

Julie

Rémi

Ma famille M2R, je vous embrasse tous ! Je n'ai pas toujours été là mais avec moi c'est pas loin des yeux, loin du coeur.

Christopher

Poppy

Laura

Je n'ai pas mentionné beaucoup de personnes car j'aurai bien peur d'en oublier. Si vous m'avez croisé au cours de mon existence et que vous m'avez fait sourire alors ces remerciements vous concernent. Merci !

Sommaire

I. Introduction

La capacité d'un organisme à interagir avec son environnement repose sur son aptitude à percevoir, à intégrer et à répondre à un stimulus externe. La représentation du monde que se fait un individu est donc inhérente à son équipement sensoriel. Le fondateur de l'éthologie, Jacob von Uexküll, suggère qu'il y a donc autant de réalités possibles (*Umwelt*) que d'espèces animales et illustre cette approche en suggérant à ses lecteurs cette représentation: « *blow, in fancy, a soap bubble around each creature to represent its own world, filled with the perceptions which it alone knows* » (Uexkull, 1934).

L'univers sensoriels de l'espèce humaine repose sur l'intégration de cinq modalités: la vue, le toucher, l'ouïe, le goût et l'**odorat**. Chacun de ces sens repose sur des organes sensoriels dont le rôle et de détecter une variation de l'environnement (longueur d'onde, pression, vibration, pH, molécule) et de la convertir en un signal (influx nerveux) interprétable par le système nerveux central (fig.1). Ces organes sont composés d'une variété de cellules sensorielles jouant le rôle de capteur pour notre cerveau. Privés de ces cellules, nous serions enfermés dans notre propre corps sans aucun moyen de prendre part au monde qui nous entoure.

Au cours de mes travaux de thèse, je me suis intéressé à la construction de l'organe sensoriel olfactif : la genèse de sa **forme** et de la **diversité** des cellules qui le composent. Afin de questionner les mécanismes biologiques à la base de ces processus j'ai étudié le développement de l'organe olfactif de l'embryon du **poisson zèbre**. J'ai volontairement orienté l'introduction suivante selon un point de vue essentiellement anatomique de manière à ce que le lecteur puisse assimiler au mieux l'apport de mes travaux de recherche aux connaissances actuelles, mais il va de soi que forme et fonction ne sont que les deux faces d'une même pièce.

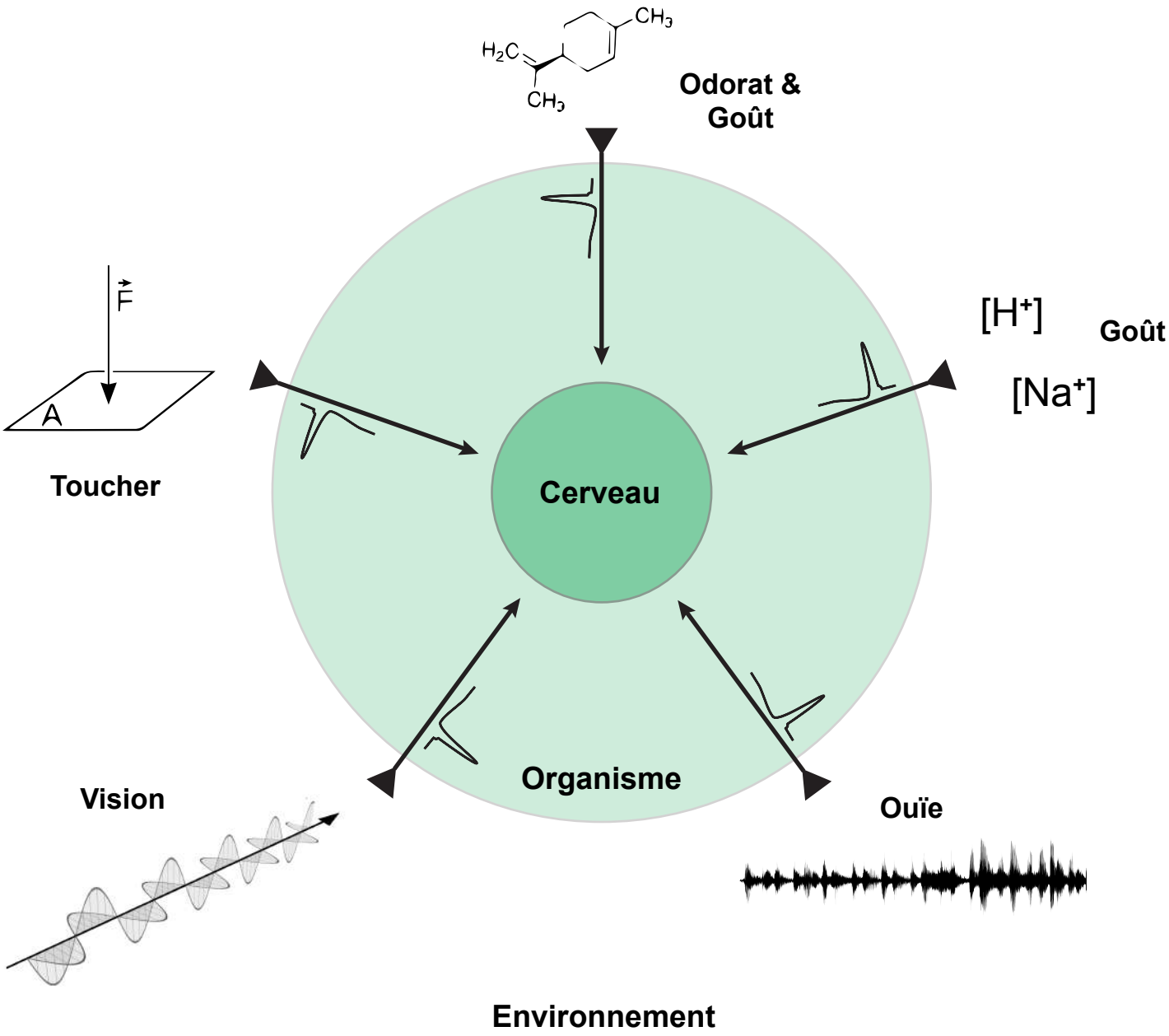

Figure 1 : Les organes sensoriels traduisent les propriétés physico-chimiques de l'environnement sous forme d'influx nerveux.
Les flèches représentent les voies sensorielles. Les cellules capteurs sont situées en périphérie de l'organisme ( ). Ells convertissent les propriétés physico-chimiques de l'environnement en influx nerveux ( ) que le cerveau peut interpréter pour adapter son comportement.

1.1 Système olfactif chez l'Homme

1.1.1 Epithélium olfactif principal

Chez les Vertébrés, l'organisation du système olfactif est stéréotypée avec une organisation tripartite en trois couches de neurones successives (Wislon & Mainen, 2006). La première couche est celle des organes récepteurs olfactifs : **L'épithélium olfactif (OE)** reposant sur du tissu conjonctif et dont l'ensemble forme la muqueuse olfactive (OM) situé dans la cavité nasale (fig.2A)**.** Chez l'homme on retrouve dans cette première couche 5 populations que je présente selon leur position apico-basale (fig.2B):

- Les **neurones récepteurs olfactifs ciliés** (**cORN**, également appelés neurones sensoriels olfactifs ciliés) ont une morphologie bipolaire présentant une dendrite apicale ciliée et un axone (Chen *et al*, 2014). La perception d'une odeur est initiée dans la dendrite par un récepteur olfactif de type GPCR (G-protein coupled receptor) couplé aux protéines G. Un cORN n'exprime qu'un unique allèle au sein d'un répertoire contenant 384 gènes olfactifs (Olender *et al*, 2016). Ce mécanisme confère une sélectivité à chaque cORN. Dans le règne animal les récepteurs olfactifs sont classés en 4 familles :

    - **OR**: Odorant Receptor
    - **TAAR:** Trace Amine-Associated Receptor
    - **V1R/Ora**: Vomeronasal Receptor de type 1/Olfactory receptor genes related to class A
    - **V2R/OlfC**: et Vomeronasal Receptor de type 2/Olfactory C family G-protein coupled receptor

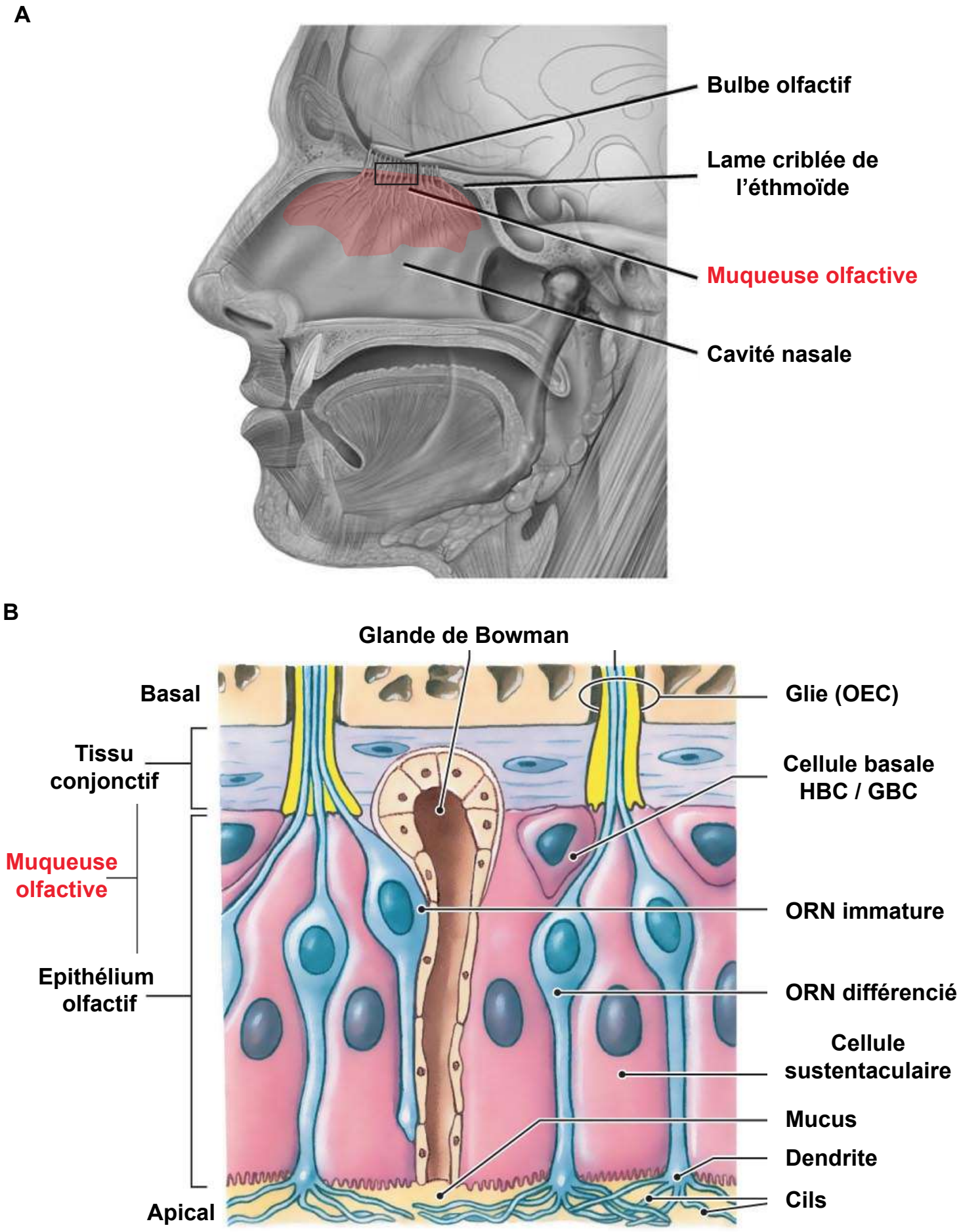

Figure 2 : Histologie de la muqueuse olfactive chez l'Homme.
En **A**, situation anatomique de la muqueuse olfactive dans la cavité nasale, marquée en rouge (adapté de https://commons.wikimedia.org/wiki/File%3AHead_olfactory_nerve.jpg).
En **B**, populations cellulaires de la muqueuse olfactive. (adapté de http://thesistut.com/olfactory-nerve-anatomy.html). **OEC**: cellule gliale olfactive engainante, **HBC**: cellule basale horizontale, **GBC**: cellule basale globose, **ORN**: neurone olfactif

Les cORN n'expriment que des récepteurs de type OR ou TAAR. Les familles V1R/Ora et V2R/OlfC sont un cas particulier dont on parlera un peu plus tard. La liaison d'une molécule odorante à un de ces récepteurs aboutit à la génération d'un potentiel d'action du cORN via une cascade de transduction bien définie : l'activation du récepteur libère la protéine G, qui active l'enzyme AC (Adenylate Cyclase). La production d'AMPc (Adenosine monophosphate cyclic) par l'AC provoque l'ouverture de canaux ioniques entrainant l'influx de charges positives (Na^+ et Ca^{2+}) et l'efflux de charges négatives (Cl^-) générant l'hyperpolarisation du neurone olfactif (fig.3A) (Hatt *et al*, 2004).

- Les **cellules sustentaculaires** sont de structure colonnaire et présentent à leur surface apicale des microvillosités en contact avec le milieu extérieur. Elles assurent une fonction de soutien de l'OE et joueraient notamment un rôle essentiel pour l'homéostasie des ORN (Chen *et al*, 2014).

- Les **cellules basales** sont situées dans la partie basale de l'épithélium et permettent le renouvellement constant des cellules de l'OE exposés aux agressions du milieu extérieur. Il existe chez le rongeur deux types de cellules basales. Les cellules horizontales (HBC) et les cellules globoses (GBC). Suite à la mitose, les HBC produisent des GBC et se renouvellent. Ce sont des cellules souches adultes. Les GBC, positionnées au-dessus, sont les cellules progénitrices de l'OE. Contrairement aux HBC, ce n'est que récemment que les GBC ont été identifiées chez l'homme grâce à des marqueurs utilisés chez les rongeurs (Holbrook *et al*, 2011).

- Les **glandes de Bowman** (BG) sont des structures cellulaires tubulo-alveolaires, localisées dans le tissu conjonctif et traversant l'OE, dont la lumière débouche sur la face apicale. Elles sécrètent un mucus recouvrant les dendrites des ORN favorisant la diffusion des molécules odorantes (Chen *et al*, 2014).

-

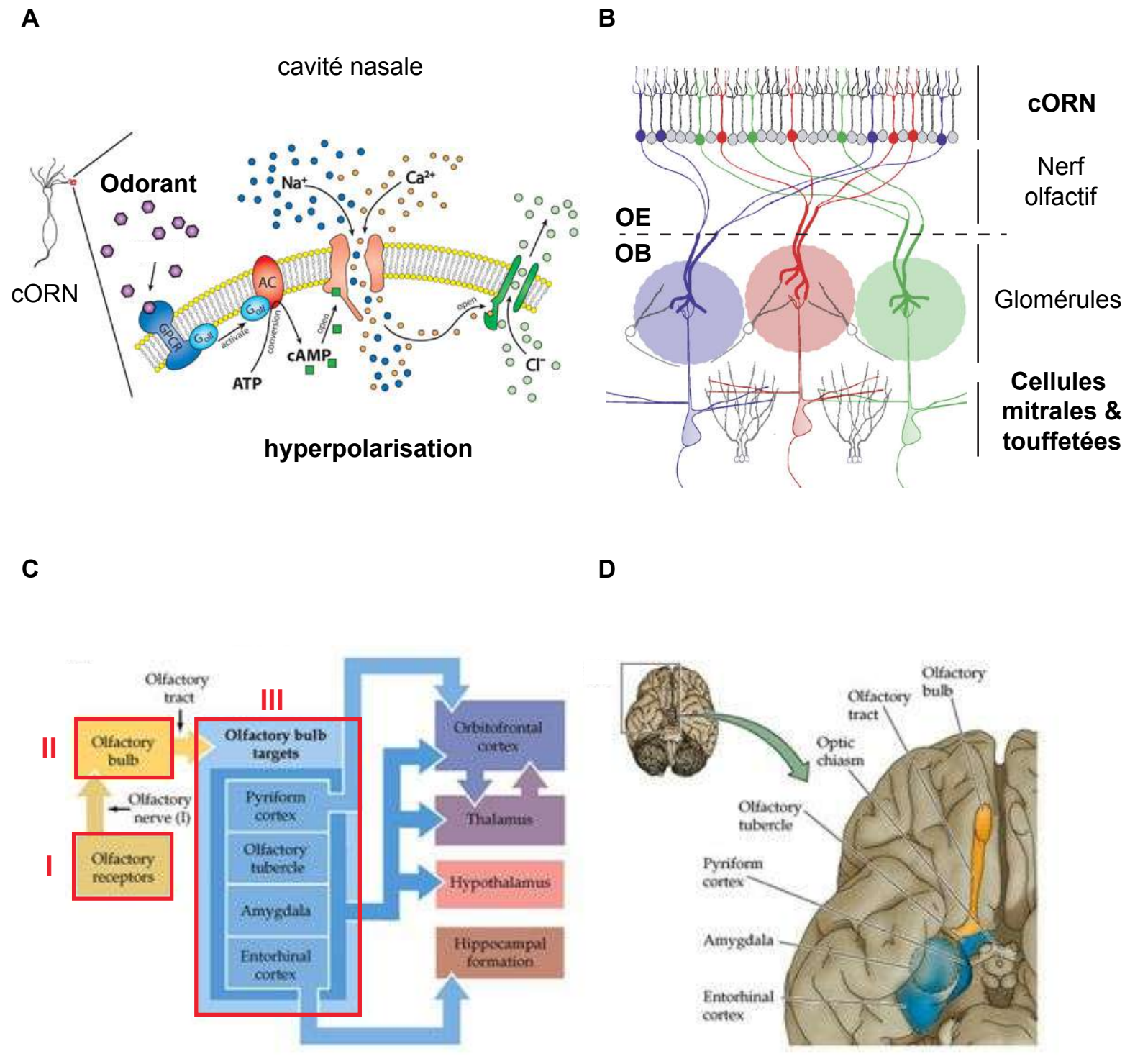

Figure 3: Du récepteur olfactif au néocortex.
En **A**, signalisation intracellulaire en réponse à l'activation d'un récepteur olfactif (adapté de http://www.mdc-berlin.de). En **B**, les ORN exprimant le même récepteur olfactif font synapses sur le même glomérule dans le bulbe olfactif (adapté de Gathpande, 2009). En **C**, structures cérébrales impliquées dans le traitement de l'information olfactive. Organisation tripartite du système olfactif souligné en rouge. En **D**, vue anatomique des voies olfactives centrales (adapté de Purves, 2008). **OE**: épithélium olfactif, **OB**: bulbe olfactif, c**ORN**: neurone olfactif cillié.

- Les **cellules olfactives engainantes** (OEC) sont des cellules gliales associées aux axones des ORN. Les ORN ont une durée de vie de 1 à 2 mois, il y a donc un renouvellement permanent du nerf olfactif. On sait maintenant que les OEC favorisent ce processus en stimulant la croissance axonale. Les propriétés de cette population gliales sont également évaluées pour la régénération de la moelle épinière chez l'animal et l'homme depuis une dizaine d'années (Ekberg *et al*, 2012).

Les axones des ORN quittent la muqueuse olfactive, traverse la lame criblée de l'ethmoïde (fig.2A) et rejoignent **le bulbe olfactif** (OB) pour connecter la seconde couche de neurones: les cellules mitrales et toufettées. Ce premier relais synaptique de la voie olfactive a lieu dans les **glomérules** qui sont des amas synaptiques protégés par une capsule gliale (Haberly, 2001). Etonnamment, les NRO exprimant le même récepteur sont répartis de façon homogène dans l'OE mais leurs projections axonales convergent sur le même glomérule (fig.3B). Il s'agit de la règle 1R:1N:1G du système olfactif : « un récepteur = un neurone = un glomérule », initialement découvert chez le rat par le laboratoire de Richard Axel (Vassar *et al*, 1994). Le bulbe olfactif est donc une **représentation odotopique** de l'environnement. Cela signifie que chaque odotope (ensemble des ligands pour un même récepteur olfactif) est spatialement localisé dans le OB (fig.3D), et ce de façon conservée entre les individus. Chez le poisson zèbre, l'observation de l'activité neuronale dans le bulbe olfactif permet ainsi de prédire la qualité et même la concentration de l'odeur perçue par l'OE (Friedrich *et al*, 1997).

Enfin, la dernière et troisième couche : **les centres olfactifs supérieurs**. De façon schématique, les cellules du bulbe olfactif projettent directement sur le système limbique (LS) qui est une composante majeure du traitement de l'information olfactive (Haberly, 2001). L'information est ensuite relayée d'une part dans l'hypothalamus et d'autre part dans le thalamus pour enfin terminer dans le néocortex (fig.3C). Contrairement aux autres modalités sensorielles, l'information olfactive passe d'abord par les centres de la mémoire et des émotions (LS) avant d'être traitée par le cortex qui assure la discrimination et la reconnaissance de l'odeur (Mainland *et al*, 2014).

La perception des signaux chimiques par le système olfactif ne permet pas seulement de reconnaitre des molécules odorantes liées au comportement alimentaire. En effet, chez les animaux ce sens est également impliqué dans la reconnaissance des congénères, partenaires sexuels ou encore des prédateurs via la perception de phéromones. Les phéromones sont des substances chimiques produites et libérées dans l'environnement par un organisme capables de générer une modification physiologique ou comportemental chez un autre organisme de la même espèce. Nous savons que l'espèce humaine ne fait pas exception et réagit également à ces composés. Cependant le mode de perception reste encore inconnu. Chez les mammifères, il existe d'autres systèmes olfactifs situés dans la cavité nasale impliqués notamment dans la perception des phéromones (Storan & Key, 2006 ; Tian & Ma, 2004 ; D'Aniello *et al*, 2017). L'un de ces systèmes est conservé chez l'homme.

1.1.2 Système olfactif accessoire

L'organe voméronasal (VNO), appelé également organe de Jacobson, est apparu avec les vertébrés terrestres. Cet organe tient son nom de sa position anatomique. Le VNO est localisé sur la face dorsale de l'os vomer à la base du septum nasal. Il est contenu dans une cavité en contact avec le milieu extérieur via un canal débouchant dans la cavité buccale et/ou nasale selon l'espèce considérée. Il est formé d'un neuro-épithélium contenant des ORN dont la dendrite diffère du cORN, il y a à sa surface des microvillosités (mORN). Les **mORN** expriment les récepteurs V1R/Ora et V2R/OlfC et leurs axones projettent sur le bulbe olfactif accessoire (AOB) (fig.4A) (Brignall & Cloutier, 2015). La fonction du VNO n'est pas encore clairement élucidée mais est associée à l'activation de comportements innés (sociaux et sexuels) chez le rongeur via la détection de phéromones (Pérez-Gomez *et al*, 2014). Bien que cet organe soit présent chez l'homme au cours de la gestation, il dégénérerait et serait non fonctionnel chez l'adulte (Smith & Bhatnagar, 2000 ; Bhatnagar & Smith, 2001) (fig.4B). En effet, les gènes V1R et V2R codant les récepteurs olfactifs spécifiques du VNO sont mutés et non fonctionnels (D'Aniello *et al*, 2017). Bien que les mORN soient identifiables lors du développement embryonnaire ils sont absents chez l'adulte. Il n'y a pas d'axones et pas d'AOB non plus. Cependant, les cellules restantes ont des microvillosités sur leur face apicale,

A

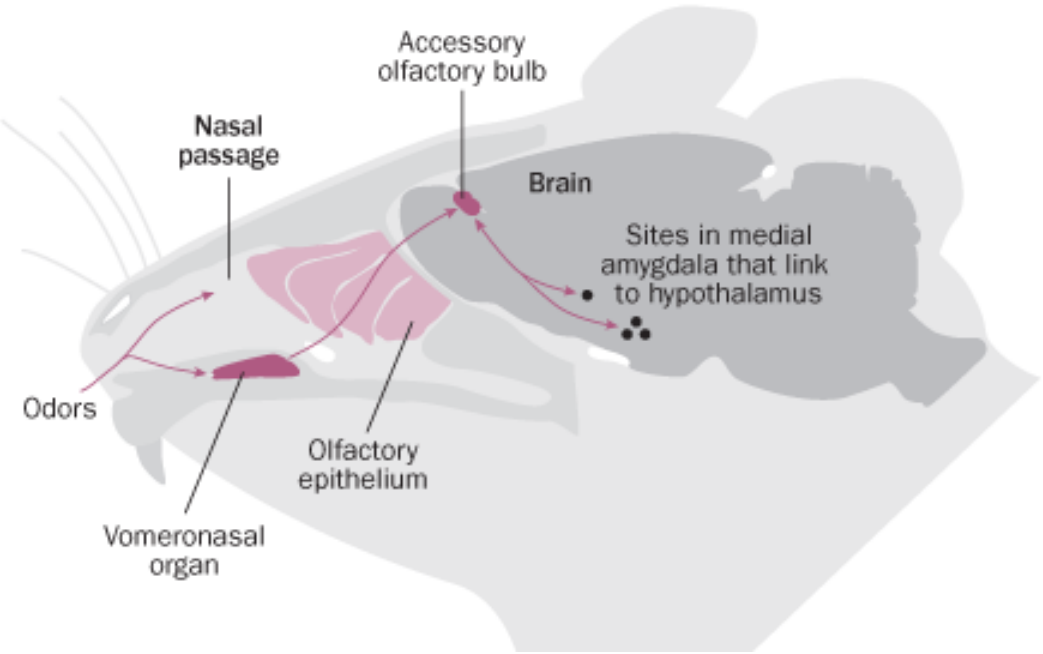

B

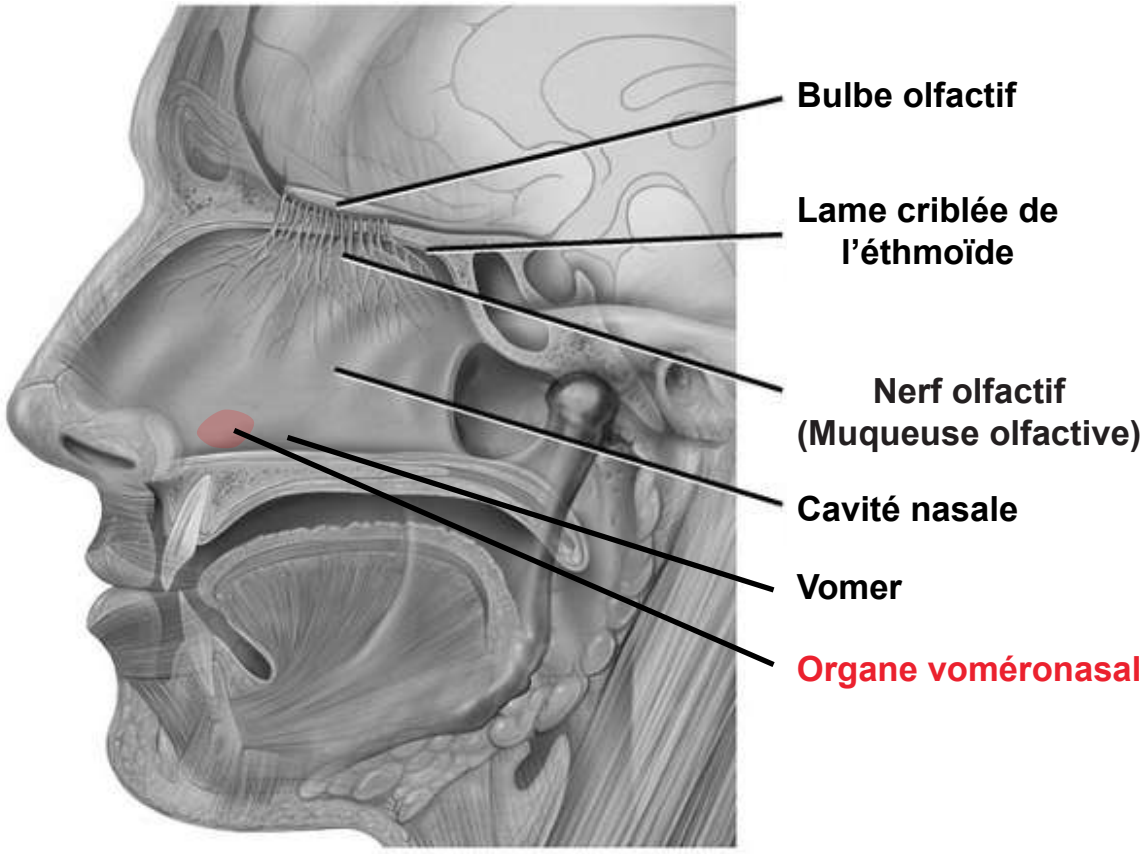

Figure 4 : L'organe voméronasale est conservé chez l'Homme.
En **A**, organisation du système olfactif accessoire chez le rongeur
(adapté de http://78.media.tumblr.com)
En **B**, situation anatomique de l'organe voméronasal dans la cavité nasale, marqué en rouge
(adapté de https://commons.wikimedia.org).

sont associées à des capillaires sur leur face basale et expriment un marqueur de cellules endocrines CaBP (Calcium-Binding Protein) (Wessels *et al*, 2014). Cette observation anatomique suggèrent une fonction endocrine potentielle du VNO chez l'homme et pourrait être l'origine de certaines réponses physiologiques observées après exposition à des phéromones (Monti-Bloch *et al*, 1998). Enfin, on ne peut exclure une fonction développementale de cet organe qui pourrait expliquer sa conservation chez l'Homme et sa courte durée de vie.

J'ai développé dans cette partie la structure générale du système olfactif chez l'Homme en insistant davantage sur l'aspect anatomique que fonctionnel. Ceci dans le but de mettre en lumière que ce circuit nerveux repose sur l'intégration de nombreux types cellulaires ayant chacun un rôle dans la perception olfactive. L'altération de ce système, qu'elle soit innée ou acquise, peut perturber ou empêcher l'odorat de fonctionner et avoir des conséquences bien plus importantes que la seule perte de la modalité sensorielle.

1.2 Troubles de l'olfaction

On considère que **20% de la population mondiale** présente des troubles de l'odorat (Croy *et al*, 2014). Selon les auteurs il s'agirait d'une estimation inférieure à la réalité car la perception olfactive est un processus en grande partie inconscient. Ainsi de nombreuses personnes ayant des troubles modérés peuvent vivre des années sans s'en rendre compte. Cependant, cela peut avoir une incidence sur leur santé. En effet, des patients ayant subi une lésion entrainant une **perte de l'odorat** ont davantage de chance de présenter des signes de **dépression**. Et la réciproque est également vraie. Les patients dépressifs présentent plus souvent des troubles de l'odorat que le reste de la population (Kholi *et al*, 2016). La causalité de cette relation n'est pas encore établie. Cependant comme nous avons vu précédemment, les centres supérieurs de l'odorat et le système limbique partagent de nombreuses structures cérébrales. On peut supposer que cette relation anatomique peut être l'un des substrats de cette corrélation. La perte d'odorat peut donc affecter plus largement la qualité de vie des patients en étant associée à des signes de dépression, en diminuant l'attrait pour la nourriture ou encore en générant de l'anxiété liée à l'incapacité à déceler des dangers pour soi ou l'entourage (incendie ou fuite de gaz) (Croy *et al*, 2014).

1.2.1 Un odorat, des troubles

Tous les troubles olfactifs ne sont pas équivalent et peuvent affecter le quotidien des patients de façons bien différentes. Il existe 4 types de troubles répartis en deux catégories : qualitative et quantitative.

Ainsi, les troubles **qualitatifs :** ils sont difficiles à mettre en évidence mais peuvent tout de même altérer fortement la qualité de vie des patients. La **phantosmie** induit la perception d'une odeur absente de l'environnement alors que la **parosmie** se traduit par la déformation perceptive d'une odeur déjà connue. La prévalence de ces troubles est plus importante dans les contextes de dégénérescence ou régénération du système olfactif (Leopold *et al*, 2002).

Alors que les troubles **quantitatifs** entrainent une diminution (**hyposmie**) ou absence (**anosmie**) des capacités olfactives du patient. Ces troubles apparaissent principalement à la suite de lésions traumatiques ou infectieuses. Mais pour 4% des patients ce trouble est inné, il s'agit d'**anosmies congénitales** (Croy *et al*, 2014).

1.2.2 Le syndrome de Kallmann

Le syndrome de Kallmann (KS) ou dysplasie olfacto-génitale de Kallmann-De Morsier est une maladie génétique du développement caractérisée par l'association d'un **hypogonadisme hypogonadotrope** (HH) et d'une **anosmie** ou hyposmie avec hypotrophie des bulbes olfactifs (Boehm *et al,* 2015). L'incidence de ce syndrome est de 1/10 000 avec une prévalence plus importante pour les hommes. Les manifestations cliniques du syndrome sont: un micropenis, une cryptorchidie, l'absence de puberté spontanée ainsi qu'un déficit partiel ou complet de la perception des odeurs. Les deux signes cardinaux sont l'HH et l'anosmie mais on peut retrouver également différents symptômes associés tels que: des troubles de l'audition, de la motricité oculaire, une fente palatine, des déformations des doigts ou encore une dysgénésie rénale. De nombreux gènes ont été associés au KS et peuvent expliquer cette variabilité des symptômes mais tous ont en commun une fonction dans le développement précoce du système reproducteur, processus indissociable du développement olfactif (Forni *et al*, 2015).

1.2.3 Bases développementales de l'association HH-Anosmie

L'étonnante association de ces deux signes cliniques (HH et anosmie) est éclairée par la relation topographique étroite qu'ont le **nerf olfactif/voméronasal (ON/V)** en développement et la population neuronale responsable du contrôle de la fertilité, les neurones à gonadolibérine (**GnRH,** Gonadotrophin Releasing Hormon**)**.
Chez l'Homme, ces neurones hypothalamiques sont localisés dans le noyau pré-optique. Ils contrôlent l'activité des cellules hypophysaires gonadotropes (**LH**, Luteinizing Hormon et **FSH**, Follicule Stimulating Hormon) via la sécrétion du neuropeptide GnRH (fig.5A) (Forni *et al*, 2015). On les retrouve également dans le nerf terminal reliant directement l'OE à l'hypothalamus mais dont la fonction n'est pas

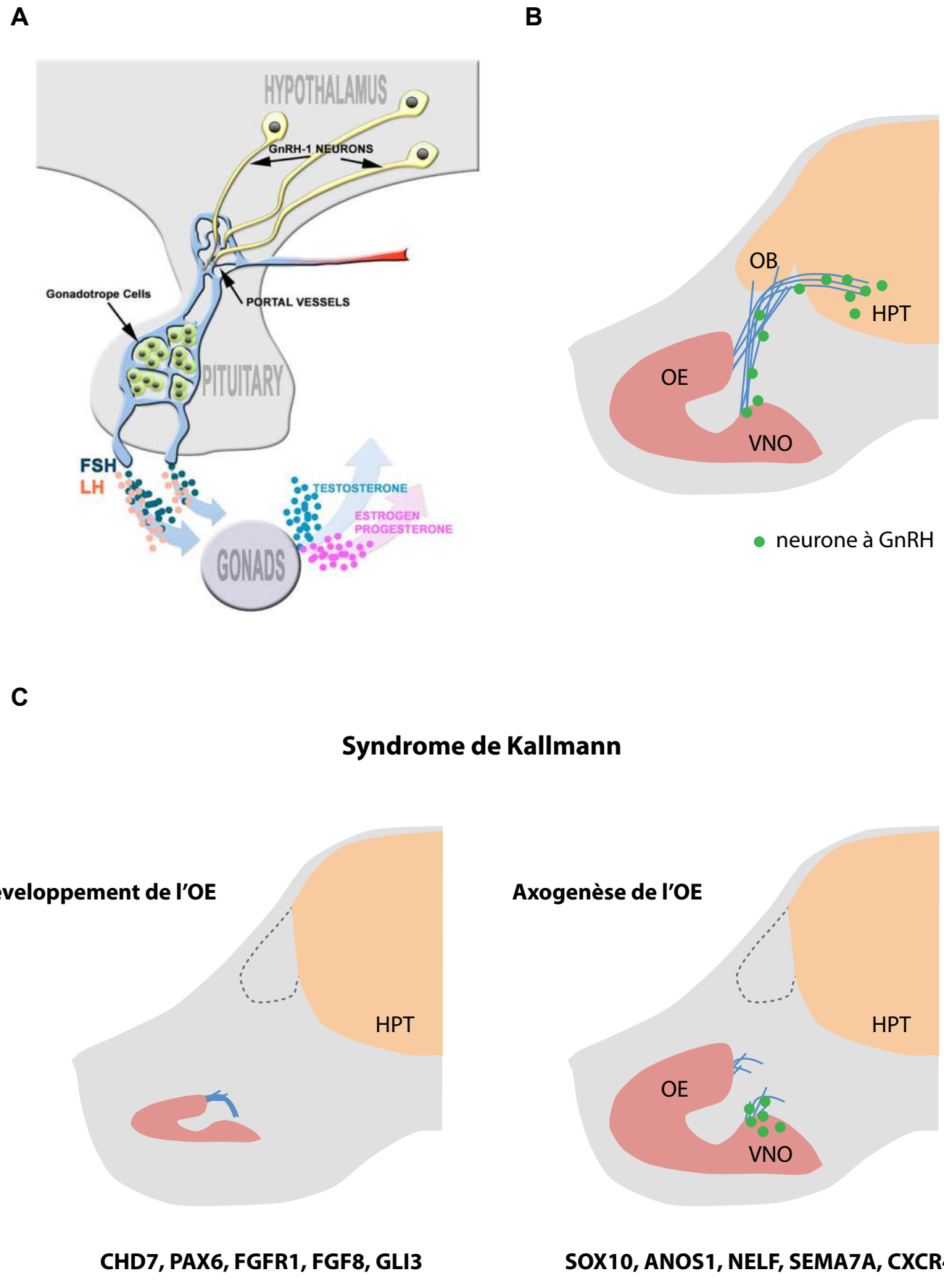

Figure 5: Système neuronal GnRH : Fonction, Développement et Syndrome de Kallmann
En **A**, les neurones hypothalamiques à GnRH régulent les hormones sexuelles. En **B**, les neurones à GnRH migrent le long du nerf olfactif/terminal pour atteindre le cerveau. En **C**, gènes requis pour le développement des neurones à GnRH (adapté de Forni & Wray, 2015). **OE**: épithélium olfactif, **OB**: bulbe olfactif, **VNO**: organe voméronasal, **HPT**: hypothalamus.

clairement définie (D'Aniello *et al*, 2017). Bien que situés dans le système nerveux central les neurones à GnRH trouvent leur origine embryonnaire en périphérie (Wray *et al*, 1989 ; Schwanzel-Fukuda *et al*, 1989 ; Casoni *et al*, 2016).

Précocement, les neurones olfactifs et à GnRH sont localisés dans la **placode olfactive**, structure embryonnaire commune à l'OE et au VNO. Les GnRH empruntent le ON/V en développement pour accéder au système nerveux central et enfin coloniser le nerf terminal et l'hypothalamus (fig.5B). Si ce nerf ne peut se former correctement, les neurones à GnRH ne peuvent entreprendre leur migration. Considérant les interactions requises pour ce processus, le nombre de facteurs potentiels pouvant l'altérer de façon directe ou indirecte devient alors difficile à évaluer. A ce jour, on ne peut identifier une mutation génétique causale que chez seulement 40% des patients (Mitchell *et al,* 2011).

1.2.4 Bases génétiques du syndrome de Kallmann.

Comme nous l'avons vu précédemment, le développement du système GnRH est indissociable du système olfactif. De fait, la plupart les facteurs impliqués dans le développement de l'épithélium olfactif (de la production des cellules olfactives à la formation du ON/V) peuvent être à l'origine du KS. Parmi les 18 gènes identifiés chez les patients KS (Boehm *et al,* 2015), on retrouve effectivement: **FGF8 (**Fibroblast growth factor 8), **FGFR1** (Fibroblast growth factor receptor 1), **PAX6** (Paired box protein 6) ou **CHD7** (Chromodomain-helicase DNA binding protein 7) impliqués dans la production des neurones olfactifs ou plus largement dans la morphogenèse crânio-faciale chez la souris et le poisson zèbre (fig.5C). On retrouve également des facteurs nécessaires à la formation du ON/V comme **ANOS1** (Anosmin 1), **NELF** (Nasal embryonic luteinizing hormone-releasing hormone factor), **SEMA7A** (Semaphorin 7A) et **SOX10** (SRY-box 10) (Forni *et al*, 2016).

L'analyse du génome de 48 patients KS a récemment permis d'identifier 19 nouveaux gènes mutés (Quaynor *et al*, 2016). Parmi ces gènes on retrouve **GLI3** (GLI-Kruppel family member 3) qui est un composant de la voie de signalisation Hedgehog déjà connu dans le développement du nerf olfactif chez la souris (Balmer & Lamantia, 2004). On retrouve également le gène **CXCR4** (CXC motif receptor 4) qui participe à la formation de l'épithélium olfactif, du nerf olfactif et aussi à la migration des neurones à GnRH chez la souris (Schwarting *et al,* 2006; Toba *et al*,

2008) et le poisson zèbre (Miyasaka *et al*, 2007; Palevitch *et al,* 2010). L'analyse du génome des patients KS permet de fournir de précieuses informations sur les potentielles bases génétiques, mais seule l'étude fonctionnelle grâce aux modèles animaux permet de comprendre le rôle de ces facteurs sur la pathogenèse.

1.2.5 Modèles d'études animaux du syndrome de Kallmann

La migration des GnRH au cours du développement embryonnaire a été découverte chez le modèle murin (Wray *et al*, 1989; Schwanzel-Fukuda *et al*, 1989). Au cours des 30 dernières années, les études effectuées sur ce modèle ont permis de découvrir de nombreux facteurs impliqués dans ce processus conservé chez tous les vertébrés (Forni *et al,* 2015). Cependant, un autre modèle d'étude s'est rapidement développé dans ce champ de recherche: le poisson zèbre.
Le premier gène identifié comme responsable du KS est *kal-1* (Hardelin *et al,* 1992). Il s'agit d'une protéine sécrétée associée à la matrice extracellulaire impliquée dans la régulation de l'activité de la voie FGF (Korsensky & Ron, 2016). Cependant, ce gène est absent du génome murin. Chez le poisson zèbre, il y a deux gènes paralogues *kal-1a* et *kal-1b* identifiés et leur perte de fonction par Morpholino (outil de perte de fonction, pour revue : Housden *et al*, 2017) altère la fasciculation du nerf olfactif et la formation des synapses dans le OB (Ardouin *et al,* 2000, Yanicostas *et al,* 2009). Bien que phylogénétiquement plus éloigné de l'Homme, ce modèle génétique présente la particularité d'être transparent au cours du développement embryonnaire offrant ainsi l'unique contexte dans lequel les neurones à GnRH peuvent être suivi en temps réel *in vivo* (Abraham *et al,* 2008 ; Abraham *et al,* 2009).

Dans le laboratoire, nous étudions le développement de l'épithélium olfactif grâce au poisson zèbre. Dans la partie suivante, je propose une description du développement de cet organe basée sur 30 ans d'études expérimentales chez le poisson zèbre et appuyée par des données obtenues chez la souris et le xénope.

1.3 Développement de l'épithélium olfactif du poisson zèbre

Chez **les poissons,** les narines situées sur la face dorsale de la tête sont indépendantes des voies respiratoires. Contrairement à l'espace humaine, il n'existe qu'**un système olfactif**. Dans chaque narine se trouve un ensemble de lamelles organisées en rosette et jointes par un raphé central (fig.10A). Chaque lamelle contient deux régions: les zones latérales, non sensorielles et en position médiane l'épithélium olfactif sensoriel (Hansen & Zeiske, 1993). La **construction** de cet organe est un processus **très rapide** (environ 20 heures, du début de la gastrulation jusqu'à la morphologie en rosette) mais qui repose sur une série d'inductions, de mouvements cellulaires et différenciations parfois concomitants mais surtout finement régulés spatio-temporellement. Au cours de ce chapitre j'ai donc pris la liberté de décrire ces processus de façon séquentielle.

1.3.1 La bordure neurale

1.3.1.1 La frontière dorso-ventrale de l'ectoderme.

A la fin de la gastrulation, lorsque les feuillets embryonnaires sont morphologiquement identifiables l'ectoderme est régionalisé sur l'axe dorso-ventral. Le système nerveux central sera issu du développement de l'ectoderme dorsal qualifié de neural alors que la partie ventrale produira l'épiderme. A l'interface entre ces deux zones se trouve un territoire frontière appelé **bordure neurale** d'où émergera non seulement les **crêtes neurales** mais également les **placodes crâniales** générant une importante diversité de destinée ectodermique telle que l'épithélium olfactif, le système nerveux périphérique, les mélanocytes ou encore les glandes surrénales pour n'en citer que quelques-unes (Aguillon *et al,* 2016 ; Schlosser, 2014 ; Dupin & Le Douarin, 2014). Dans cette partie je décris en détail les étapes précoces conduisant à la formation du territoire olfactif ainsi qu'une brève description des crêtes neurales céphaliques.

1.3.1.2 BMP définie la bordure neurale

La régionalisation dorso-ventral de l'ectoderme est principalement sous contrôle de la voie BMP (Bone morphogenetic protein). Au début de la gastrulation, son activité est élevée dans la région ventrale et nulle en dorsal. La localisation de la bordure neurale (NB), à mi-chemin sur l'axe dorso-ventral suggère qu'un niveau intermédiaire d'activité de la voie BMP est nécessaire à son induction (fig.6A) (Neave *et al,* 1997 ; Nguyen *et al,* 1998; Tucker *et al,* 2008, Schumacher *et al,* 2011). Cependant le niveau d'activité au sein de la bordure neurale varie au cours de la gastrulation suggérant que ce territoire est hétérogène. L'utilisation de l'imagerie en temps réel associé à la lignée transgénique reportrice de l'activité de la voie *Tg(BMPRE :mRFP)*^{cj100Tg} confirme que la partie la plus antérieure de la bordure neurale devient inhibée contrairement à la zone postérieure (Ramel & Hill, 2012). Cette subdivision apparait au cours de la gastrulation et reflète deux nouveaux territoires: la **région préplacodale (PPR)** en antérieur et le territoire des crêtes neurales (NC) en postérieur (fig.6). Cette régulation est due notamment à l'expression de l'antagoniste BAMBIb (BMP and activin membrane bound inhibitor b) induit par le facteur de transcription Dlx3b (Distal-less homeobox 3 b) spécifiquement exprimé par la PPR au cours de la gastrulation (fig.6A). En parallèle, le maintien de l'activité BMP dans la partie postérieure est assuré par l'expression du gène *cvl2* (Crossveinless 2) (Reichert *et al,* 2013).

1.3.2 Région pré-placodale et territoire olfactif

1.3.2.1 Spécification de la région pré-placodale

De façon générale, un territoire embryonnaire se définit par l'expression spatio-temporelle d'un set de gènes spécifiques. Un ensemble de gènes exprimés dans la région ventrale ***tfap2a*** (Transcription factor activator 2a*),* ***tfap2c*** (Transcription factor activator 2c)*,* ***gata3*** (GATA binding factor 3) *,* ***foxi1*** *(*Forkhead box I1) et dans la région dorsale *pax3a (*Paired box 3a), *zic3* (Zinc finger of the cerebellum 3) (Schlosser, 2014) qui se retrouvent co-exprimés dans la NB (fig.A). Cependant l'expression de ces gènes n'est pas homogène dans la bordure neurale, de fait la voie BMP ne peut à elle-seule expliquer cette complexité. En fait, l'identité de cette

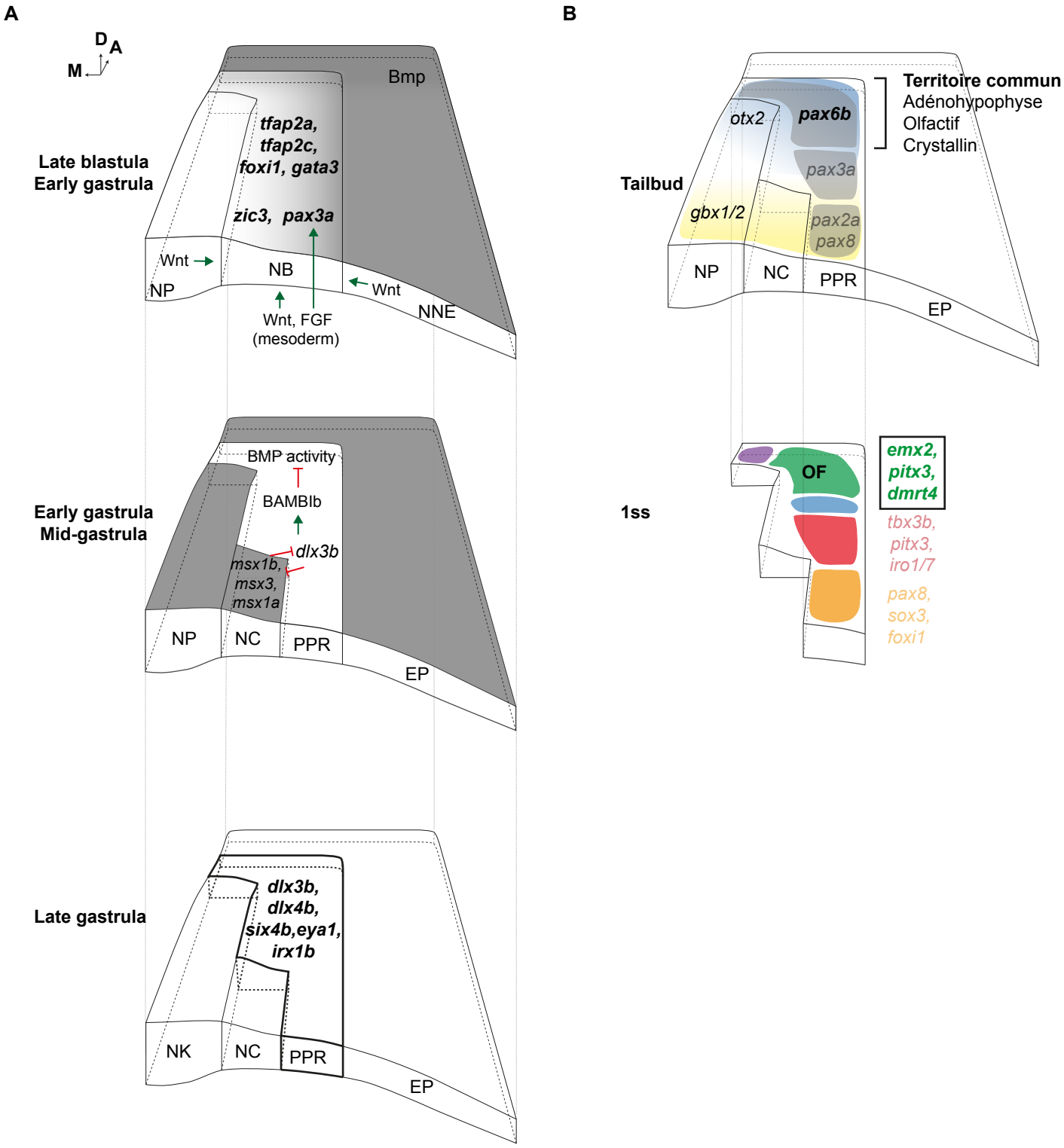

Figure 6 : De la bordure neurale au territoire olfactif: topographie génétique
L'activité intermédiaire de la voie BMP définie la bordure neurale au début de la gastrulation (**A).** L'inhibition de la voie BMP est ensuite nécessaire à la spécification de la PPR.
En **B**, le territoire olfactif est issu de la partie antérieure de la PPR qui au commune au lignage adenohypophysaire et crystalinienne. **NP**: plaque neural, **NB**: bordure neurale, **NNE**: ectoderme non neural, **NC**: crêtes neurales, **PPR**: région pré-placodale, **EP**: ectoderme épidermique, **NK**: gouttière neurale (adapté de Aguillon *et al*, 2016).

bordure neurale est le résultat de l'intégration la voie BMP et des voies de signalisation FGF, Wnt et RA (fig.6A):

- La **voie FGF** est nécessaire à la formation de la PPR (Ahrens & Schlosser, 2005; Villanueva *et al,* 2002; Litsiou *et al,* 2005). Le facteur *cvl2* induit par Dlx3b et Dlx4b génère la compétence pour répondre à la signalisation FGF dans la PPR via la régulation des récepteurs au FGF et des cibles de la voie (Esterberg & Fritz, 2009). L'utilisation de transgènes inductibles à la chaleur (heat-shock) associée à un inhibiteur pharmacologique révèle que le FGF associé à l'atténuation de BMP est suffisant pour induire l'expression des marqueurs de la PPR dans l'ectoderme non neural. Ces résultats confirment ce qui a été observé dans les embryons de xénope et de poulet (Kwon *et al,* 2010; Ahrens *et al,* 2005; Litsiou *et al,* 2005). Enfin le facteur PDGFa (Platelet derived growth factor a), exprimé dorsalement pendant la gastrulation semble agir de façon partiellement redondante au FGF pendant la spécification de la PPR (Kwon *et al,* 2010).

- La **voie Wnt** (Wingless type) semble être un facteur antagoniste de la spécification de la PPR. Chez le poisson-zèbre, Wnt et ses antagonistes sont exprimés par la plaque neurale antérieure et le mésendoderme sous-jascent générant un gradient d'activité «faible en antérieur et élevé en posterieur» (Cavodeassi *et al,* 2014). De plus, Il a été démontré que les gènes requis pour la spécification de la bordure neurale *pax3a* et *zic3* contiennent des éléments de régulation intégrant les activités des voies Wnt, FGF et BMP (Garnett *et al,* 2012).

- La **voie RA** (Retinoic acid) est également requise pour induire l'expression des marqueurs de la PPR chez les vertébrés. En effet, chez le xénope, l'enzyme de synthèse du RA Raldh2 (retinaldehyde dehydrogenase 2) est exprimé par la PPR et cette signalisation limite le développement de la PPR à la tête (Shiotsugu *et al,* 2004). Reste à déterminer si ce mécanisme est conservé chez le poisson zèbre.

1.3.2.2 Réseau de gènes à l'origine de la région pré-placodale

La combinatoire des voies de signalisation précédemment décrite permet l'expression des marqueurs de la PPR Tfap2a, Tfap2c, Gata3 et Foxi1 qui sont tous requis pour établir la **compétence préplacodale** de l'ectoderme non neural (Kwon *et al,* 2010; Bhat *et al,* 2013). La perte de fonction combinée de ces facteurs entraine la perte des marqueurs tardifs de la PPR ainsi que des défauts de développement des placodes crâniales (Kwon *et al,* 2010). L'activité de la voie BMP est en fait seulement requise précocement pour induire l'expression de ces marqueurs qui deviennent alors indépendant de la voie. L'utilisation conjointe de transgènes inductibles associée à l'inhibition transitoire de la voie BMP montre que ces 4 facteurs forment un réseau génique qui s'auto-entretient (Bhat *et al,* 2013). Ces facteurs maintiennent leur expression et contribuent via *dlx3b* à l'atténuation de la voie BMP dans la PPR (Yao *et al,* 2014) (fig.6A).

Les gènes spécifiquement exprimés dans la PPR en aval des facteurs de compétences décrits précédemment comprennent les facteurs des familles *Eyes absent (Eya)/Sine oculis, (Six)/Dachshund (Dach), Distalless (Dlx),* and *Iroquois (Irx)* (Ahrens *et al,* 2005, Bhat *et al,* 2013, Glavic *et al,* 2003, Kwon *et al,* 2010, Litsiou *et al,* 2005, Nguyen *et al,* 1998) (fig.6A). Chez le poisson zèbre *dlx3b* et le marqueur le plus précoce de la PPR, exprimé dès 8 heures après la fécondation (8 hpf) dans l'ectoderme non neural et dont l'expression augmente jusqu'à la fin de la gastrulation (Akimenko *et al,* 1994; Esterberg & Fritz, 2009; Solomon & Fritz, 2002; Woda *et al,* 2003). Dès 10 hpf, *six4b* et *eya1* sont exprimés dans la PPR (Bhattacharyya et al, 2004). Chez la souris, le poisson et le xénope, ces facteurs sont essentiels pour la formation des organes sensoriels notamment par la régulation de la neurogenèse (Bricaud *& Collazo,* 2006, Nica *et al,* 2006, Kozlwski *et al,* 2005, Ikeda *et al,* 2002, Laclef *et al,* 2003, Li *et al,* 2003, Ozaki *et al,* 2002, Xu *et al,* 1999, Zheng *et al,* 2003, Zou *et al,* 2004, Riddiford *et al,* 2017). Enfin *irx1b* est également exprimé dès 10 hpf et est requis pour la spécification de la PPR (Lecaudey *et al,* 2005, Glavic *et al,* 2003).

1.3.2.3 Genèse du territoire olfactif au sein de la PPR

J'ai précédemment décrit les facteurs spécifiques de la PPR, requis pour établir son identité. Dans ce paragraphe, je vais décrire quels sont les facteurs connus du lors de la formation du territoire olfactif au sein de la PPR.

Les signaux issus du mésendoderme sont nécessaires à la formation des placodes olfactives chez l'embryon de poisson zèbre et du poulet (Devos *et al,* 2002, Lleras-Forero *et al,* 2013). Par exemple, l'expression de *pax6b* est induite dans les progéniteurs placodaux antérieurs par les neuropeptides somatostatine et nociceptine. De même, la voie FGF issu du mésoderme crânial postérieur limite l'identité antérieure de la PPR (fig.6B) (Lleras-Forero *et al,* 2013)

Un autre marqueur du domaine antérieur est *pitx3* (Pituitary homeobox 3) (Zilinski *et al,* 2005). Cependant la perte de fonction par Morpholino de ce gène affecte le développement de l'œil mais pas celui de l'épithélium olfactif (Shi *et al,* 2005). Chez le xénope, *Dmrt4* (doublesex and mad-3-related transcription factor 4) marque également le domaine placodal antérieur (Huang *et al,* 2005) et la réduction de son activité affecte la neurogenèse olfactive. Chez le Medaka, un autre modèle poisson, *dmrt4* est aussi exprimé dans le système olfactif en développement (Winkler *et al,* 2004). Enfin trois membres de la famille des facteurs de transcription *emx* (empty spiracles homeobox 1) sont exprimés dans le domaine placodal antérieur et de façon plus spécifique dans le territoire olfactif. Cependant aucune donnée fonctionnelle n'est disponible (Viktorin *et al,* 2009) (fig.6B). Pour conclure, nous connaissons quelques facteurs exprimés précocement dans le territoire olfactif mais il n'y a quasiment aucune étude fonctionnelle effectuée à ce stade du développement de l'OE chez le poisson zèbre. En parallèle de la formation du territoire olfactif émerge également celui des crêtes neurales céphaliques dans la bordure neurale qui s'avère être un partenaire indissociable du développement olfactif.

1.3.3 Les crêtes neurales céphaliques

Le second lignage de la bordure neurale est celui des crêtes neurales (NC). Il s'agit d'une population cellulaire propre aux vertébrés ayant des capacités de migration et de différenciation sans équivalent leur permettant de quitter leur site de spécification,

d'envahir l'embryon et de participer à la formation de très nombreux organes (Dupin & Le Douarin, 2014).

La genèse du territoire des crêtes neurales repose sur la combinaison du module de gènes requis pour la bordure neural précédemment décrit et des mêmes voies de signalisation que pour la PPR. A la différence que durant la gastrulation les voies BMP, Wnt, FGF et RA induisent toutes l'identité NC. La combinaison des voies associée aux facteurs exprimés dans la bordure neurale permet donc l'expression d'un module de gènes comprenant notamment *snail2*, *foxd3* (Forkhead box d3) et *sox10* requis pour la spécification des NC (fig.7) (Barallo-Gimeno *et al,* 2004). Une fois les NC spécifiées, un autre module de gènes va permettre d'initier leur migration vers 12 hpf (fig.7).

Le territoire des NC est hétérogène sur l'axe Antéro-Posterieur (AP) et je vais uniquement décrire les crêtes neurales céphaliques (CNC) qui participent au développement crânio-facial (Mork *et al,* 2015). Les CNC sont des partenaires indiscutables des placodes crâniales chez tous les animaux étudiés (Steventon *et al,* 2014). Bien que leur rôle dans le développement de l'OE chez le poisson zèbre soit encore peu compris, j'ai intégré les connaissances actuelles dans la partie suivante traitant de la morphogenèse des placodes olfactives.

1.3.4 Morphogenèse de la placode olfactive

La morphogenèse est un processus au cours duquel les cellules changent de position et de morphologie dans l'espace et le temps afin de constituer un organe ou un tissu. Par définition une placode crâniale est un épaississement local de l'ectoderme non neural participant exclusivement à la formation des structures sensorielles (Streit, 2008). Précédemment j'ai décrit la genèse du territoire olfactif au sein de la PPR. Dans la partie suivante, je propose une description morphologiques et moléculaires de la formation de la placode à partir de ce territoire constitué de progéniteurs.

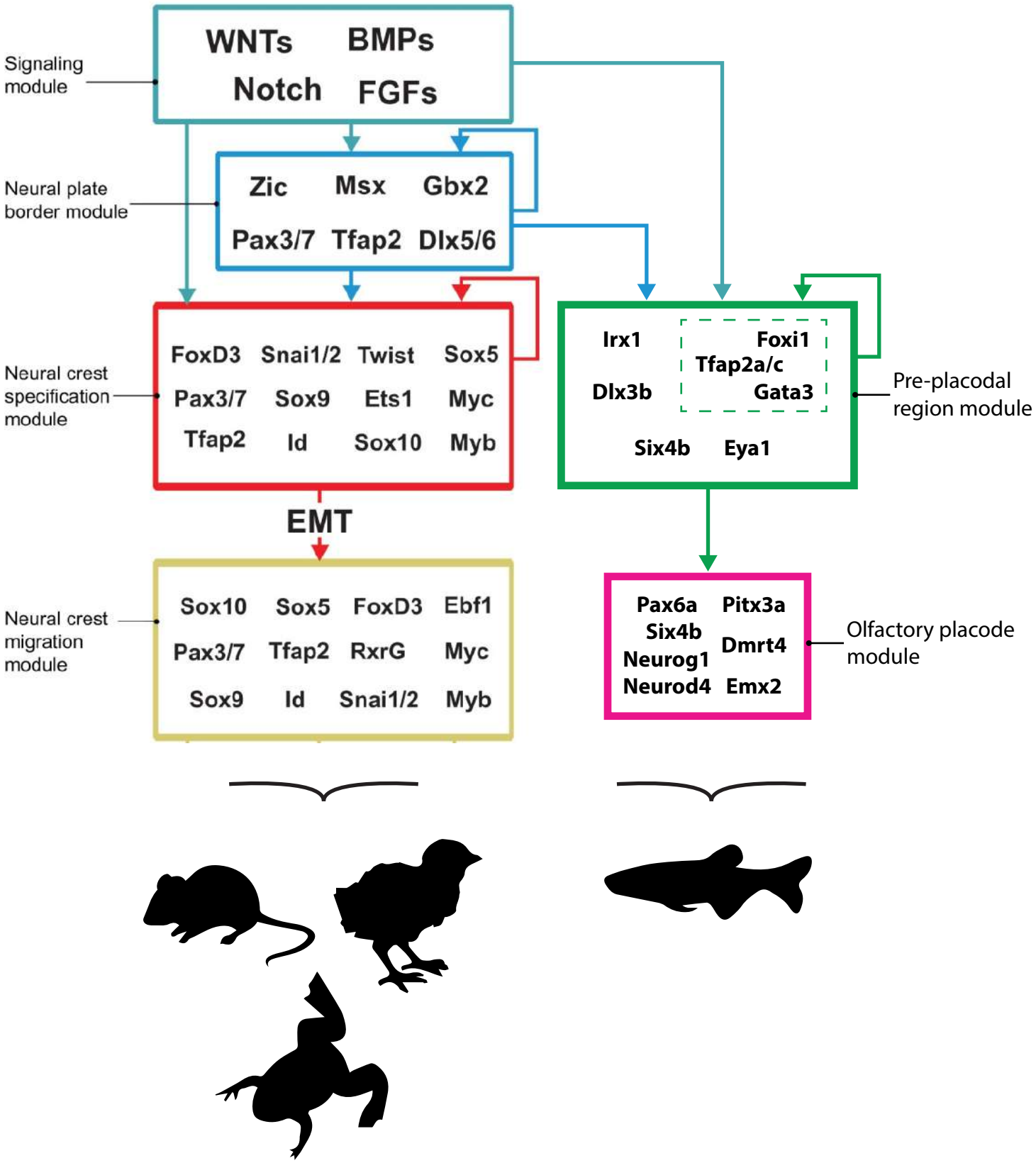

Figure 7: De la bordure neurale au territoire olfactif : modules génétiques chez les vertébrés.
Modules génétiques mis en place pour le développement de la bordure neurale et de ses dérivés : les crêtes neurales (souris, xénope, poulet) et la région préplacodale avec le territoire olfactif (poisson zèbre). (adapté de Simoes-cortes & Bronner, 2015 ; Wheeler & Brändli, 2009).

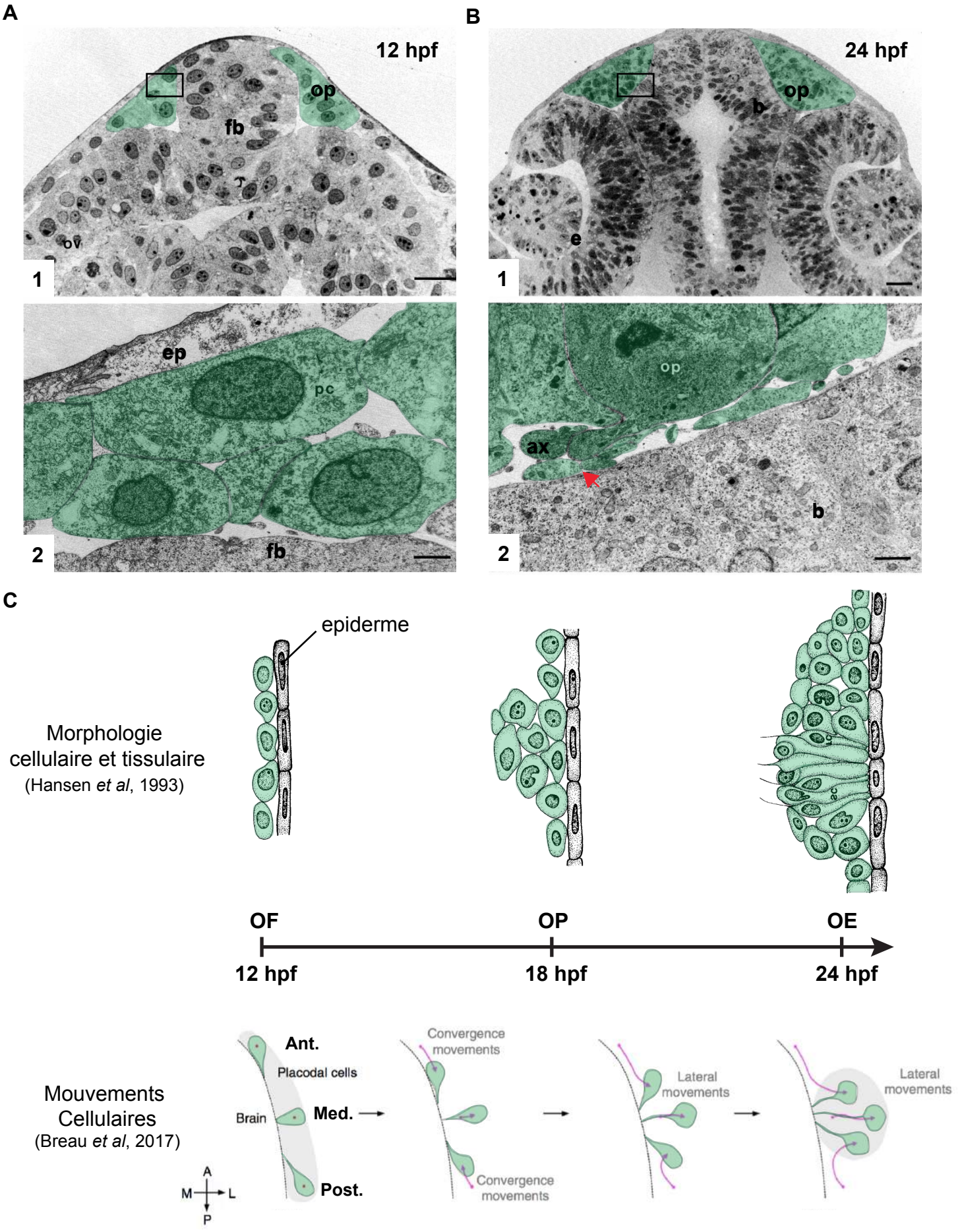

Figure 8: Morphogenèse de l'épithélium olfactif
En **A**, territoire olfactif à 12 hpf. En **B**, épithélium olfactif à 24 hpf (échelle : **1** à 20um et **2** à 2um, MET). (adapté de Hansen *et al*, 1993). En **C**, représentation schématique des changements morphologiques cellulaires et tissulaires ainsi que des mouvements cellulaires de 12 hpf à 24 hpf.
op: placode olfactive, **fb**: télencéphale, **ov**: vésicule optique, **ep**: épiderme, **pc**: progéniteur olfactif **b**: cerveau, **e**: oeil, **ax**: axone, **OF**: territoire olfactif, **Flèche rouge**: projections axonales olfactives.

*1.3.4.*1 Anatomie descriptive

Le développement précoce de la placode olfactive du poisson zèbre a été décrit pour la première fois en 1993 par microscopie électronique à transmission (Hansen & Zeiske, 1993). Au stade 10-12 hpf, une couche cellulaire située entre l'épiderme et la plaque neurale que les auteurs décrivent comme une **couche sub-épidermique** a été mise en évidence (fig.8A, 8C). L'absence de jonctions cellulaires visibles avec les couches adjacentes suggère que ces cellules forment une entité anatomique **distincte** de la plaque neurale et de l'épiderme (fig.8A, 8C). Au cours des heures qui suivent, les cellules sub-épidermiques s'accumulent dans la cavité formée entre la rétine et le prosencéphale pour former la **placode**. Les auteurs n'observent aucune mitose qui pourrait suggérer un lignage commun avec l'épiderme ou la plaque neurale. A partir de 24hpf, les cellules sont polarisées et présentent un prolongement membranaire en direction du tube neural (fig.8B, 8C). Dans les 3 heures qui suivent, les cellules acquièrent une morphologie bipolaire typique des ORN. A 27 hpf, l'ensemble des prolongements membranaires sont fasciculés et s'étendent jusqu'au système nerveux central (CNS) pour former le nerf olfactif. L'analyse ultérieure de la formation de la placode olfactive par Whitlock and Westferfield (2000) suggère pourtant une origine commune avec le prosencéphale. Les auteurs ont marqué des cellules du territoire olfactif présomptif à l'aide de marqueur fluorescent et observé un marquage non seulement dans des neurones de l'OE mais aussi dans le télencéphale à 24 hpf. Cependant l'étude citée précédemment révèle que les cellules du territoire olfactif sont voisines de la plaque neurale. Malgré la technicité employée on ne peut exclure un marquage non spécifique amenant à la conclusion d'un lignage commun. Cette étude révèle cependant qu'au sein du territoire olfactif, la position d'une cellule prédéfinit dans une certaine mesure sa position finale dans l'épithélium olfactif à 24hpf. Les auteurs proposent ainsi le terme de **convergence** pour définir le déplacement des cellules placodales sur l'axe AP.

Grace au développement de l'imagerie, la description des processus morphogénétiques a pu acquérir une résolution spatio-temporelle inédite. Les travaux de Bréau *et al,* (2017) proposent une description des trajectoires des neurones olfactifs pionniers au cours de ce processus de convergence (fig.8C). Le territoire olfactif est divisé en trois zones : antérieure, médiane et postérieure. De façon attendue, en fonction de la position sur l'axe AP, les cellules ne se dirigent pas

dans la même direction. La zone médiane est définie par la position finale de la placode olfactive. Ainsi dans le territoire olfactif les cellules des zones antérieure et postérieure se déplacent en direction de la zone médiane pour former la placode (fig.8C).

1.3.4.2 Bases moléculaires de la convergence

La formation de la placode repose sur le **déplacement** des progéniteurs répartis dans le territoire olfactif. Jusqu'aux travaux de Miyasaka *et al,* (2007) les mécanismes contrôlant ce processus de convergence étaient inconnus. Les auteurs ont découvert qu'il repose notamment sur l'expression de ***cxcr4b*** par ces cellules dès 10 hpf. Ce gène code pour un récepteur membranaire impliqué dans la **migration** de nombreux types cellulaires au cours du développement (Bussmann *et al,* 2015). L'expression du récepteur est maintenue dans les cellules pendant tout le processus de convergence, puis son expression sera progressivement restreinte aux cellules en position basale au sein de la placode. Dans ce contexte son ligand (Cxcl12a) serait une protéine diffusible exprimée par les cellules de la plaque neurale antérieure et dont le patron d'expression se restreint progressivement aux cellules à proximités des placodes olfactives (Miyasaka *et al*, 2007). Dans le mutant pour *cxcr4b,* comme dans le gain de fonction de *cxcl12a*, le déplacement des cellules placodales est affecté lors de la convergence conduisant à leur localisation anormale sur l'axe dorso-ventral. Ainsi le **positionnement** des cellules au cours de la convergence est gouverné par le couple Cxcr4b-Cxcl12a (fig.9A, 9C). Les travaux de Bréau *et al,* (2017), suggèrent que les déplacements de ces cellules soient un processus actif. En effet, au cours de la convergence les cellules antérieures présentent des protrusions membranaires de types filopodes et lamellipodes dirigés dans le sens du déplacement (fig.9B). Ces protrusions sont caractérisées par une activité de la myosin II ainsi qu'une polymérisation d'actines élevées. Enfin la perte de fonction des protéines GTPases, essentielles aux processus de migration cellulaire, Rac ou Rho perturbe le déplacement des cellules de façon similaire à ce qui peut être observée dans le mutant pour *cxcr4b*. Il aurait été intéressant d'inclure l'analyse du mutant pour *cxcr4b* dans cette étude. En effet, il est tentant de positionner ce module moléculaire nécessaire à la migration en aval du récepteur Cxcr4b pour assurer le processus de convergence. De plus un défaut de **projection**

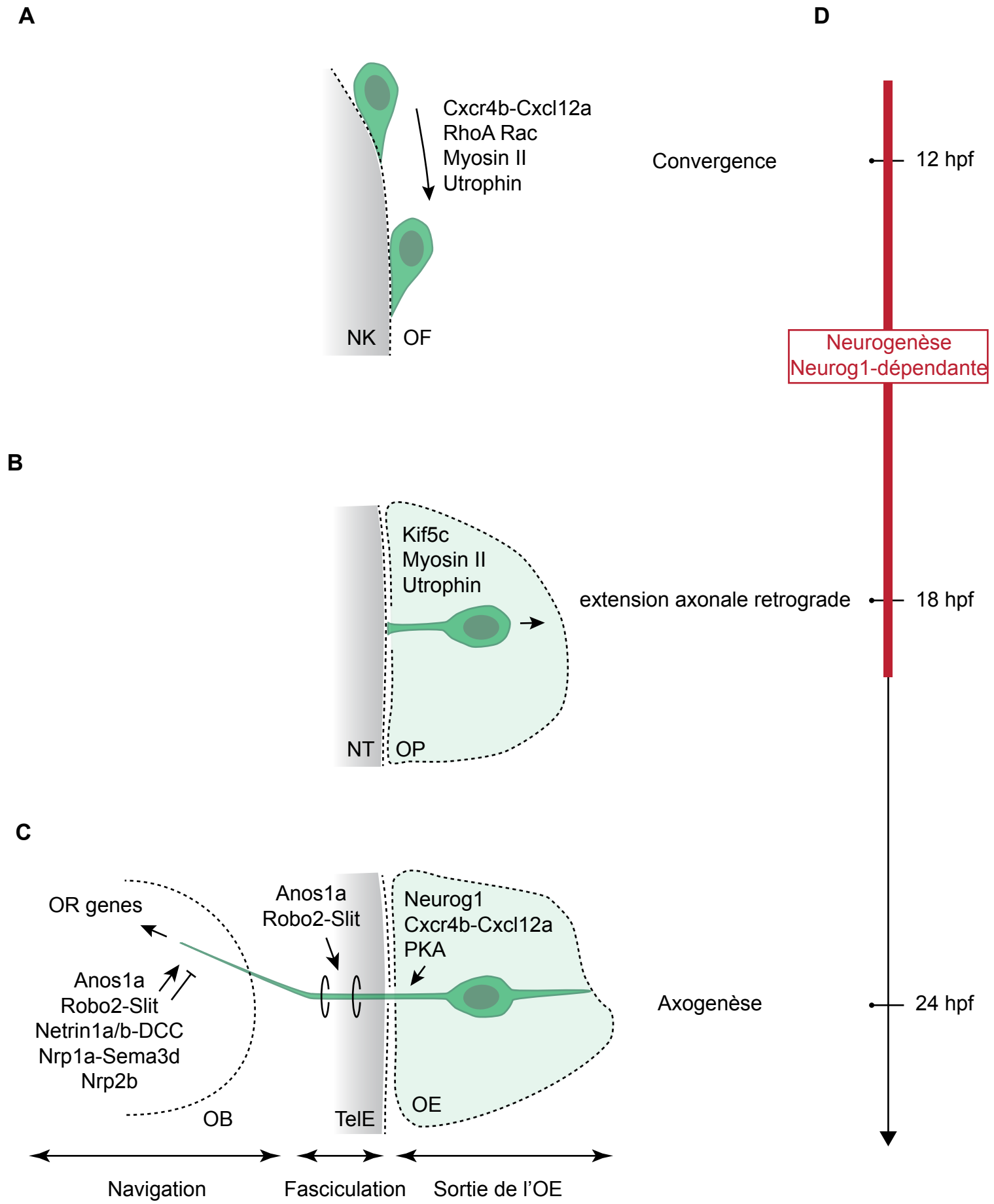

Figure 9: Bases moleculaires du comportement cellulaire lors de la formation de l'OE.
En **A**, les progéniteurs olfactifs convergent dès 12 hpf pour former la placode à 18 hpf. En **B**, initiation de l'axogenèse des ORN dans la placode à 18 hpf. En **C**, l'établissement du nerf olfactif necessite trois étapes: sortie de l'axone de l'OE puis sa fasciculation et sa navigation. **NK:** gouttière neurale, **OF**: territoire olfactif, **NT**: Tube neural, **OP**: placode olfactif, **OB**: bulbe olfactif, **TelE**: Télencéphale, **OE**: épithélium olfactif.

des cORN a été observé dès le stade 24 hpf dans le mutant pour *cxcr4b* (Miyasaka *et al*, 2007). Ce phénotype présente la particularité de ne pas être pénétrant (Seulement 30% des placodes sont affectées) et d'être défini par une absence complète de nerf olfactif. Cette fonction de Cxcr4b dans ces deux processus (fig.9A, 9C) permet de proposer deux hypothèses :

- Soit le couple Cxcr4b-Cxcl12a est requis pour le positionnement et l'axogenèse des cellules olfactives de façon indépendante.

- Soit le positionnement est un prérequis à l'axogenèse.

L'étude des mécanismes moléculaires de la convergence suggère que ce processus nécessite la migration orientée des cellules du territoire olfactif pour former la placode. De plus la mise en évidence d'un acteur commun entre convergence et axogenèse suggère une interdépendance de ces processus que je traite dans la partie suivante.

1.3.4.3 Convergence, initiation de l'axogenèse et polarité

Dès l'initiation de la convergence à 12 hpf les progéniteurs sont morphologiquement polarisés. Ils présentent des protrusions membranaires dirigées dans le sens de migration. Lorsqu'ils atteignent leur position finale ces protrusions se stabilisent sur la surface basale du tube neural. A partir de 18 hpf, on observe une translocation médio-latérale des corps cellulaires qui maintiennent le contact membranaire avec la surface basale du tube neural (fig.9A-B). Les forces physiques impliquées dans le déplacement du corps cellulaire proviennent des cellules olfactives voisines ainsi que des tissus environnants. Ainsi la protrusion s'allonge et la localisation de la protéine de fusion Kif5c560-YFP (Kinesin family member 5c, marqueur intracellulaire axonal) révèle qu'il s'agit de l'axone en formation. Ce processus d'axogenèse non canonique nommé «extension axonale rétrograde » semble être à l'origine des projections des premiers neurones olfactifs (Bréau et al, 2017). Nous avons vu dans la partie précédente que le couple Cxcr4b/Cxcl12a est impliqué à la fois dans la convergence et dans l'axogenèse. L'analyse du comportement cellulaire supporte l'hypothèse que ces deux processus sont bien liés.

Cette transition entre la convergence et l'axogenèse est accompagnée de la mise en place de l'axe apico-basal (AB) de la placode. A 16 hpf la lame basale devient détectable entre la placode et le télencéphale. Cette identité basale apparaissant de façon conjointe au passage des crêtes neurales céphaliques on peut supposer qu'elles y participent. Enfin l'identité apicale devient apparente à partir de 18 hpf via la localisation de Pard3 (Partitioning-defective protein 3, marqueur intracellulaire apical) (Torres-paz *et al,* 2014). A ce jour, nous n'avons aucune connaissance sur les relations entre le processus de convergence-initiation de l'axogenèse, la mise en place de la polarité de la placode et la migration des CNC.

L'ensemble de ces étapes est à la base de la structure en épithélium de l'OE. Dans la partie suivante, je décris les facteurs impliqués dans la mise en place des projections olfacto-bulbaires : le nerf olfactif.

1.3.4.4 Axogenèse olfacto-bulbaire

Le nerf olfactif est une structure complexe. Les axones des ORN sont organisés en faisceaux à la sortie de l'OE, traversent les lames basales (de l'OE et du SNC), entrent dans le télencéphale, atteignent l'OB puis se séparent pour atteindre les différents glomérules (fig.3B, 9C). Finalement cette description anatomique récapitule schématiquement le développement de ce nerf dont je présente ici les acteurs connus.

La **sortie** des axones olfactifs de l'OE est dépendante de l'activité de la PKA (cAMP protein kinase) (fig.9C). En effet sa perte de fonction empêche les axones d'entrer dans le télencéphale (Yoshida *et al*, 2002). Ce phénotype d'axogenèse est similaire à celui observé dans le mutant pour *cxcr4b* suggérant une interaction entre ces deux facteurs (Miyasaka *et al*, 2007).

La **fasciculation** des axones dépend du récepteur membranaire Robo2 (Roundabout 2) exprimé par les ORN ainsi que du facteur secrété Anos1a (Miyasaka *et al,* 2003 ; Yanicostas *et al*, 2009) (fig.9C).

La **navigation** des cônes de croissance des axones olfactifs est régulée par un ensemble de facteur attractifs et répulsifs (fig.9C). Les récepteurs Nrp1a (Neuropilin 1a), Nrp2b (Neuropilin 2b), DCC (Deleted in colorectal carcinoma), Robo2 exprimés par les ORN sont activés par leur ligands respectifs Sema3D

(Semaphorin 3D), Netrin1a, Netrin1b et Slit1, Slit2, Slit4 exprimés différentiellement dans l'OB (Taku *et al*, 2016 ; Lakhina *et al*, 2012 ; Miyasaka *et al,* 2003). Le facteur Anos1a est également requis pour le ciblage des glomérules (Yanicostas *et al*, 2009). Ces facteurs assurent l'orientation des axones dans différents compartiments du OB, mais le ciblage précis des axones olfactifs sur les glomérules repose le récepteur olfactif spécifiquement exprimé par l'ORN. En effet, lors de la mise en évidence de la règle 1R/1N/1G chez le rongeur, les auteurs ont remarqué que les récepteurs olfactifs sont également localisés dans les cônes de croissance des axones (Vassar *et al*, 1994). La perte de fonction conditionnelle du récepteur olfactif inhibe la connexion de l'ORN vers le glomérule. De même la substitution de la séquence codante d'un récepteur olfactif par celle d'un autre récepteur entraine *de facto* la connexion de l'ORN sur le glomérule correspondant au nouveau récepteur (Wang *et al*, 1998). Chez l'embryon de poisson zèbre ce processus est également conservé, bien qu'initialement ce soit davantage le type de récepteur olfactif plutôt que le récepteur lui-même qui impose le choix parmi les proto-glomérules (forme immature du glomérule) (Shao *et al,* 2017).

Nous avons vu jusqu'à présent toutes les étapes nécessaires à la formation de l'OE, de sa spécification jusqu'à l'établissement des connections avec le bulbe olfactif. Cependant la fonction d'un organe ne repose pas uniquement sur son anatomie mais également sur l'ensemble des populations cellulaires qui le compose. Les ORN sont les acteurs principaux de la perception olfactive. Au cours de la prochaine partie, je décris quels sont les mécanismes connus régulant la neurogenèse olfactive embryonnaire chez le poisson zèbre.

1.3.5 Neurogenèse de la placode olfactive

La production des neurones au cours du développement repose sur la régulation de plusieurs étapes préalablement à leur différenciation terminale. Alors que les progéniteurs neuraux effectuent leur dernière division ils s'engagent vers un destin donné afin de produire un des nombreux sous-types neuronaux. De façon générale, dans le système nerveux central les neurones post-mitotiques quitte la zone des progéniteurs et migrent jusqu'à leur site d'intégration où ils se différencieront. Les facteurs de transcriptions proneuraux qui appartiennent à la famille des bHLH (basic

Helix Loop Helix) sont exprimés dans les progéniteurs en prolifération où ils jouent un rôle essentiel dans le programme de différenciation neuronal (Castro *et al,* 2011). Comme chez la souris et le xénope, la neurogenèse olfactive précoce est sous le contrôle de facteurs proneuraux chez le poisson-zèbre (Cau *et al,* 1997 ; Burns *et al,* 2002 ; Madelaine *et al,* 2011). Dès 8 hpf, le proneural Neurogénine1 (Neurog1) est exprimé dans une population de cellules organisées en fer à cheval similaire au territoire olfactif. A 24 hpf, dans le mutant pour *neurog1,* il manque 50% des neurones olfactifs précoces, un défaut d'expression des marqueurs de différenciation et une absence complète des projections axonales (fig.9D). La présence d'une partie de la population suggère l'expression d'un autre facteur partiellement redondant qui compenserait la perte d'activité de Neurog1. Le facteur Neurod4 est exprimé dès 11 hpf par les progéniteurs olfactifs et bien que son expression soit retardée à 17 hpf dans le mutant pour *neurog1* cela est suffisant pour maintenir partiellement la neurogenèse. En effet l'injection d'un Morpholino contre Neurod4 dans le mutant *neurog1* permet d'éliminer quasiment toutes les cellules à 24 hpf (Madelaine *et al,* 2011). Les facteurs bHLH sont connus pour être exprimés en cascade au cours du développement neural (Castro *et al,* 2011) et il semblerait que ce soit également le cas dans ce contexte. Ainsi, Les progéniteurs olfactifs expriment séquentiellement les facteurs proneuraux *neurog1* et *neurod4* à partir de 8 hpf et maintiennent leur expression pendant le processus de convergence et ce jusqu'au début de la différenciation des premiers neurones olfactifs à 19 hpf (Madelaine *et al,* 2011). La morphogenèse et la neurogenèse sont donc deux processus concomitants (fig.9). Les progéniteurs doivent ainsi se diviser et produire des neurones tout en participant à la construction de l'OE.

Nous avons vu comment l'épithélium olfactif et le nerf olfactif sont construits au cours du développement et quels sont les acteurs impliqués dans la production des neurones olfactifs. Au début de l'introduction, j'ai présenté l'ensemble des types cellulaires olfactifs connus chez l'Homme (fig.2B). Dans la partie suivante, je présente l'état des connaissances actuelles sur l'origine de la diversité cellulaire chez le poisson zèbre (fig.10B).

A

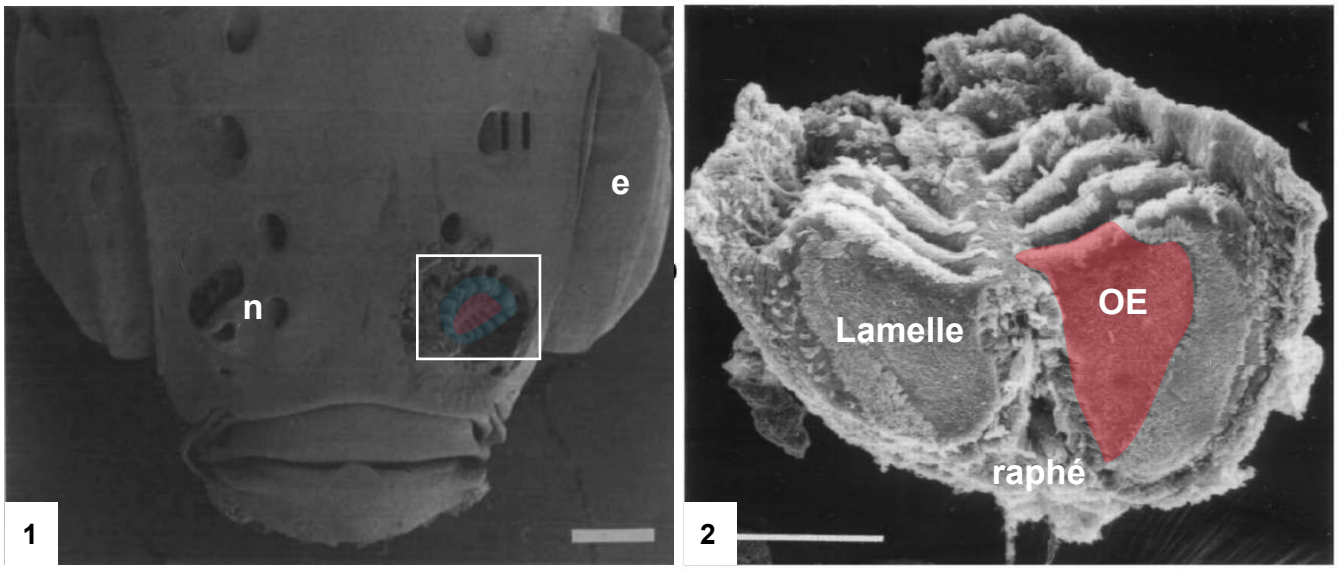

B

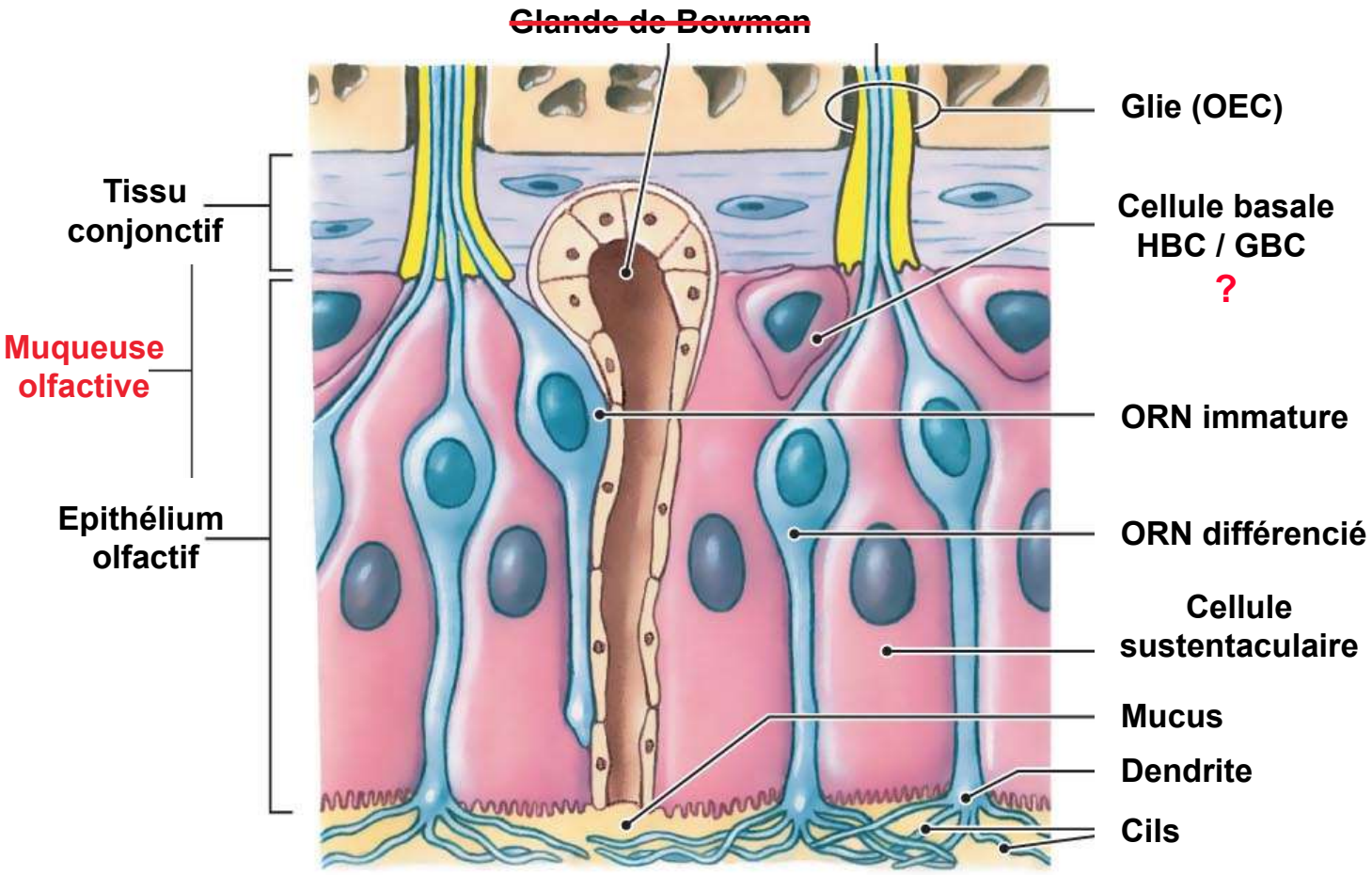

Figure 10: Histologie de l'épithélium olfactif chez le poisson zèbre.
En **A**, situation anatomique de l'épithélium olfactif dans la cavité nasale, épithélium olfactif sensoriel mis en évidence en rouge. En **1**, vue dorsale de la tête d'un poisson zèbre agé de 6 mois. En **2**, structure en lamelles de l'organe olfactif (adapté de Hansen & Zeiske, 1993).
En **B**, populations cellulaires de la muqueuse olfactive. Seule la glande de Bowman n'existe pas chez le poisson zèbre (adapté de http://thesistut.com/olfactory-nerve-anatomy.html). **n**: narine, **e**: oeil, **oe**: épithélium olfactif, **OEC**: cellule gliale olfactive engainante, **HBC**: cellule basale horizontale, **GBC**: cellule basale globose, **ORN**: neurone olfactif.

1.3.6 Diversité et développement des populations de l'épithélium olfactif

La fonction d'un organe repose sur l'organisation dans l'espace d'une variété de types cellulaires organisés en tissus, eux-mêmes structurés en organe. J'ai précédemment décrit les différentes étapes du développement de l'épithélium olfactif. Dans cette partie je présente l'ensemble des types cellulaires identifiés dans l'embryon du poisson zèbre de façon identique à l'Homme, selon leur position sur l'axe apico-basal dans l'OE (fig.10B et 11C):

- Il existe 4 types d'**ORN** dans l'OE chez le poisson zèbre :

    - **Ciliés** (cORN ou OSN): Chez le poisson zèbre, la protéine OMP (Olfactory Marker Protein) est le marqueur des cORN et son expression est détectable à partir de 24 hpf dans l'OE (Madelaine *et al,* 2011). La lignée transgénique *Tg(-2.0ompb:gap-YFP)*^{rw32Tg} permet de suivre la mise en place de leurs projections axonales qui atteignent le télencéphale à partir de 27 hpf (Sato *et al,* 2005) les cORN expriment les récepteurs olfactifs de type OR et TAAR. Leur différenciation et axogenèse sont dépendantes du couple Neurog1-Neurod4 (Madelaine *et al,* 2011).

    - **A microvillosités** (mORN): Chez le poisson zèbre, les récepteurs olfactifs exprimés par les mORN sont de type V1R/Ora et V2R/OlfC. Ils sont caractérisés par l'expression de *trcp2b* (transient receptor potential cation channel 2b) dès 24 hpf dans l'OE (von Niederhäusern *et al,* 2013). La lignée transgénique *Tg(-4.5trpc2b :gapVENUS)*^{rw037Tg} permet également de suivre leurs projections axonales (Sato *et al,* 2005). La majorité des mORN expriment également le transgène *Tg(-4.9sox10 :GFP)*^{ba2Tg} suggérant une origine mixte placode/CNC de cette population (Saxena *et al,* 2013). L'analyse du lignage par photoconversion des CNC conforte cette hypothèse. Cependant, l'étude de la contribution des CNC via l'utilisation d'une autre lignée transgénique *Tg(-*

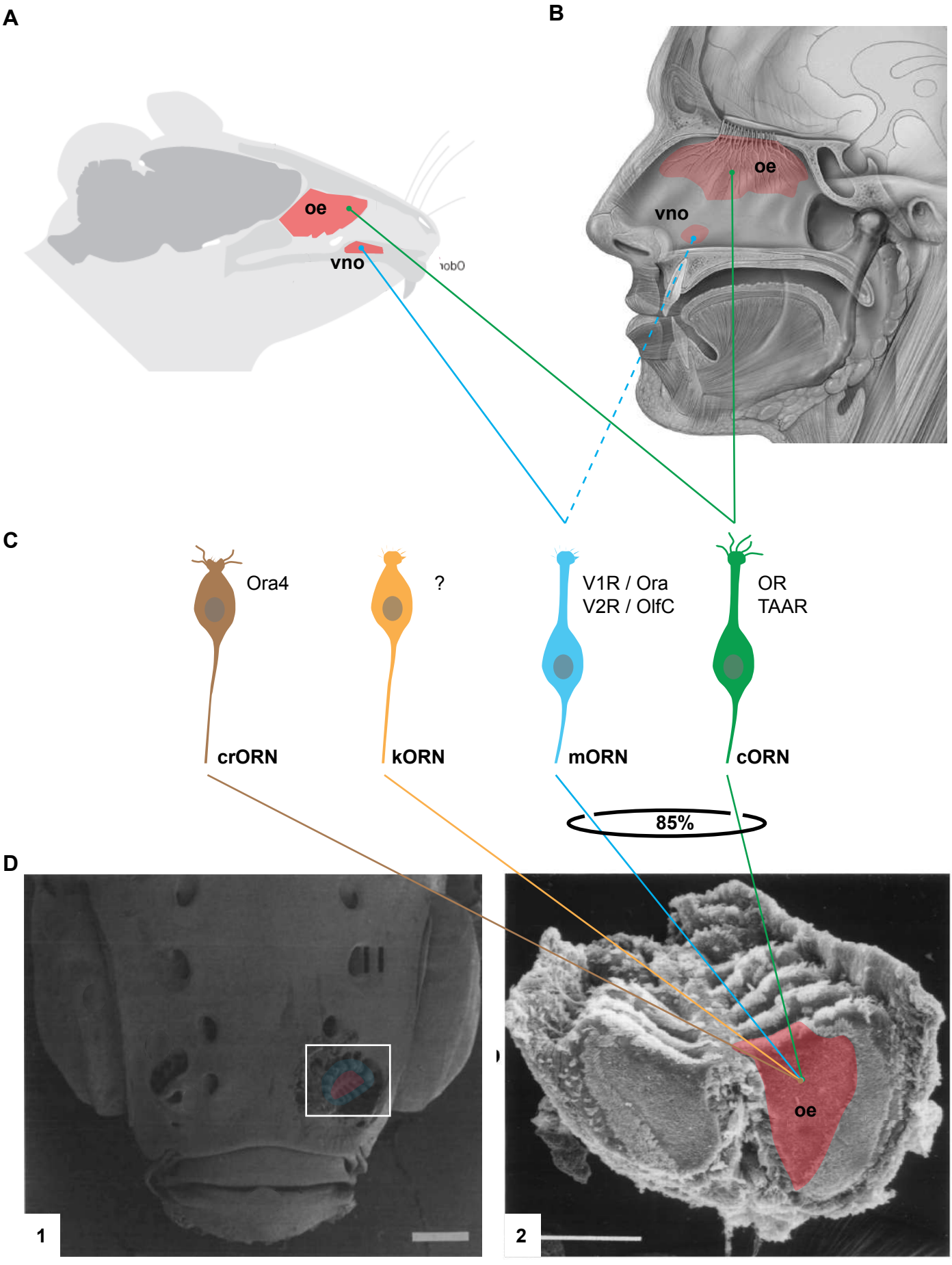

Figure 11: Répartition des classes d'ORN dans le système olfactif chez la souris, l'Homme et le poisson zèbre.
Les organes olfactifs sensoriels sont soulignés en rouge chez la souris (**A**,adapté de http://78.media.tumblr.com), l'Homme (**B**, adapté de https://commons.wikimedia.org) et le poisson zèbre (**D**, Hansen & Zeiske, 1993). En **C**, classes d'ORN chez les vertébrés et leurs récepteurs olfactifs associés. trait en pointillé: présence seulement chez l'embryon.**oe**: épithélium olfactif, **vno**: organe voméronasal.

7.2sox10 :mRFP)^{vu234Tg} ne montre aucune co-expression avec les mOSN (Harden *et al,* 2012). Cette étude remet donc en cause l'origine mixte des mORN et génère des interrogations quant à l'utilisation des lignées transgéniques comme outil de lignage.

- **A cryptes** (crORN) et **à casquettes** (kORN) : ils ne représentent que 15% des ORN. Ils ont une morphologie distincte des cORN et mORN et expriment des marqueurs spécifiques (Biechl *et al,* 2016 ; Ahuja *et al,* 2014). Etonnamment, les crORN n'expriment qu'un seul récepteur olfactif *ora4* de la famille V1R/Ora (Oka *et al,* 2012) et sont impliqués dans la reconnaissance des congénères génétiquement apparentés (Ahuja & Korshing, 2014 ; Biechl *et al,* 2016). Il n'y a pour le moment aucune donnée sur leur développement.

- Les **neurones pionniers/olfactifs précoces (EON)** sont des neurones unipolaires situés en position basale dans l'OE, ils sont différenciés à partir de 19 hpf, forment les premières connections avec le télencéphale dès 24 hpf pour finalement entrer en apoptose vers 72 hpf (Whitlock *et al,* 1998 ; Dynes *et al,* 1998). Les progéniteurs de cette population sont identifiables dès 12 hpf car expriment le transgène *Tg(-8.4neurog1 :GFP)*^{sb1Tg} (Blader *et al*, 2004 ; Bréau *et al,* 2017). Comme décrit précédemment, la production des EON et leur différenciation dépendent du couple de proneuraux Neurog1-Neurod4 (Madelaine *et al,* 2011). Ils ont une fonction d'échafaudage pour les axones des ORNs, en effet leur ablation physique ou génétique inhibe la formation du nerf olfactif (Whitlock *et al,* 1998 ; Madelaine *et al,* 2011).

- Les **cellules basales** n'ont pas encore été identifiées chez l'embryon. Chez l'adulte, on sait cependant que l'OE est capable de se régénérer suite à une lésion chimique et contient une population de cellules présentant des caractéristiques de progéniteurs (Huang *et al,* 1998 ; Iqbal *et al,* 2010).

- Les **cellules olfactives engainantes** ont été caractérisées chez l'adulte par immunohistochimie (Lazzari *et al,* 2014) mais aucune étude n'a été faite sur leur développement embryonnaire.

- Les **neurones à GnRH** sont des neurones unipolaires exprimant le gène *gnrh3* et le transgène *Tg(-2.4gnrh3 :eGFP)*^{zf103} à partir *de* 24 hpf. Ils sont localisés dans la partie basale de l'OE (Whitlock *et al,* 2005 ; Zhao *et al,* 2013). Bien que localisés précocement dans l'OE, ces neurones sont issus des crêtes neurales céphaliques (Whitlock *et al,* 2003). En effet, ils expriment également le marqueur des NC *sox10* et leur nombre est réduit suite à l'injection combinée des Morpholino ciblant *sox10* et *foxd3.* Cependant l'origine embryonnaire de ces neurones est à ce jour sujet à controverses. Chez le poulet et le xénope ils sont issus des placodes olfactives alors que chez la souris leur origine est mixte OP/CNC (Forni *et al,* 2015).

L'épithélium olfactif de l'embryon de poisson zèbre contient donc un équipement cellulaire tout à fait équivalent à celui de l'Homme (fig.11). Grace aux connaissances accumulées depuis ces 30 dernières années la communauté dispose d'un modèle d'étude unique pour étudier le développement de l'OE chez les vertébrés. Il est ainsi possible d'interroger l'ensemble des mécanismes biologiques œuvrant notamment à la genèse de cette diversité cellulaire mais aussi à la formation du nerf olfactif. L'approfondissement de ce savoir fournira sans aucun doute un socle de connaissances utiles et nécessaires pour développer des approches thérapeutiques pour la restauration de la fonction olfactive.

II. Résutats

Durant ma thèse, je me suis tout d'abord intéressé à comprendre l'origine de l'hétérogénéité des populations neurales (Aguillon et al., en révision, eLife).

Puis j'ai mis en évidence la mécanistique d'action de Neurog1 dans la morphogenèse de l'OE (Aguillon et al., en préparation).

2.1 Cell-type heterogeneity in the zebrafish olfactory placode is generated from progenitors within preplacodal ectoderm

Résumé des travaux

L'épithélium olfactif du poisson zèbre est constitué d'une variété de types cellulaires générés précocement au cours du développement embryonnaire. La neurogenèse de l'OE est gouvernée par le couple de facteur bHLH Neurog1 et Neurod4. Les EON sont les premiers neurones à se différencier et à projeter dans le bulbe olfactif. Des travaux antérieurs révèlent qu'une partie de ces neurones entrent en apoptose après seulement quelques jours de développement suggérant une hétérogénéité au sein de cette population. Dans le but de caractériser l'origine des EON nous avons analysé les profils d'expression de différents marqueurs déjà décrits pour être exprimés dans des sous-populations neuronales. Ainsi nous avons découvert que les facteurs Islet1/2 sont spécifiquement exprimés dans les cellules de l'OE marquées par le transgène *Tg(-2.4gnrh3 :eGFP)*^{zf103}. Bien que localisés précocement dans l'OE, il a été montré que les neurones à GnRH3 dériveraient des CNC. Nous avons alors analysé l'expression de Islet1/2 dans un contexte de défaut de différenciation des CNC (mutant *sox10*). Contrairement à ce qui a été décrit dans le morphant contre *sox10*, le nombre de neurones à GnRH3 ne varie pas, remettant en question leur origine CNC. En combinant différentes approches de lignage, comprenant notamment le suivi des cellules par imagerie en temps réel, nous avons montré que les neurones à GnRH3 sont en réalité issus de la PPR antérieure. Ces multiples approches suggèrent que les CNC ne contribuent pas de façon significative aux populations olfactives. Nous avons donc décidé de revisiter le lignage des mORN,

provenant également des CNC dont l'origine est en réalité la PPR. Nos résultats suggèrent que l'hétérogénéité cellulaire de l'EO est générée par la PPR sans contribution significative des CNC.

Cell-type heterogeneity in the zebrafish olfactory placode is generated from progenitors within preplacodal ectoderm

Raphaël Aguillon[1§], Julie Batut[1§], Arul Subramanian[2], Romain Madelaine[1#], Pascale Dufourcq[1], Thomas F. Schilling[2] and Patrick Blader[1*]

[1] Centre de Biologie du Développement (CBD, UMR5547), Centre de Biologie Intégrative (CBI, FR3743), Université de Toulouse, CNRS, UPS, 31062, France.
[2] Department of Developmental and Cell Biology, 4109 Natural Sciences II, University of California, Irvine, CA 92697-2300, USA.

[#] Present address: Beckman Center, Stanford University School of Medicine, Stanford, CA 94305
[§] These authors contributed equally.
[*]For correspondence: patrick.blader@univ-tlse3.fr

Abstract

Vertebrate olfactory placodes consists of a variety of neuronal populations, which are thought to have distinct embryonic origins. In the zebrafish, while ciliated sensory neurons arise from preplacodal ectoderm (PPE), previous lineage tracing studies suggest that both Gonadotropin releasing hormone 3 (Gnrh3) and microvillous sensory neurons derive from cranial neural crest (CNC). We find that the expression of Islet1/2 is restricted to Gnrh3 neurons associated with the olfactory placode. Unexpectedly, however, we find no change in Islet1/2+ cell numbers in *sox10* mutant embryos, calling into question their CNC origin. Lineage reconstruction based on backtracking in time-lapse confocal datasets, and confirmed by photoconversion experiments, reveals that Gnrh3 neurons derive from the anterior/medial PPE. Similarly, all of the microvillous sensory neurons we have traced arise from preplacodal progenitors. Our results suggest that rather than originating from separate ectodermal populations, cell-type heterogeneity is generated from overlapping pools of progenitors within the preplacodal ectoderm.

Introduction

A fundamental question in developmental neurobiology is how different neuronal subtypes arise from fields of pluripotent progenitors. At the end of gastrulation, the anterior neural plate border of vertebrate embryos gives rise to two specialized regions of ectoderm: the preplacodal ectoderm (PPE) that will ultimately produce the cranial placodes, and the cranial neural crest (CNC). Specification of the PPE is achieved through the action of so-called preplacodal competence factors such as *tfap2a*, *tfap2c*, *foxi1* and *gata3* (Kwon et al., 2010). During a similar time-window, key neural crest specifier genes, such as *foxd3* (Lister et al., 2006; Montero-Balaguer et al., 2006; Stewart et al., 2006), *tfap2a* (Barrallo-Gimeno et al., 2004) and *sox10* (Dutton et al., 2001) establish the CNC fate. Cranial placodes subsequently arise via the condensation of specific regions within the PPE along the anteroposterior axis, with the adenohypophyseal and olfactory placodes forming anteriorly, the lens and trigeminal placodes forming at an intermediate position and the otic and epibranchial placodes forming posteriorly (for reviews see (Steventon et al., 2014; Aguillon et al., 2016)). Concomitantly, CNC cells delaminate and migrate throughout the head, where they have been reported to contribute to a large number of cell types, including neurons associated with derivatives of the cranial placodes. These include

sensory neurons of the various peripheral sensory ganglia (D'Amico-Martel and Noden, 1983; Harlow and Barlow, 2007), as well as sensory and neurosecretory cells of the olfactory system (Whitlock et al., 2003; Saxena et al., 2013). This dual embryonic (PPE/CNC) origin for olfactory neurons may have critical developmental and functional consequences.

In zebrafish embryos, olfactory neurons are generated in two waves, early olfactory neurons (EON) and olfactory sensory neurons (OSN), under the redundant control of the bHLH proneural transcriptions factors Neurog1 and Neurod4 (Madelaine et al., 2011). EONs act as pioneers for the establishment of projections from the olfactory placode to the olfactory bulb. Once OSN projections are established, a subset of EONs dies by apoptosis (Whitlock and Westerfield, 1998) suggesting the existence of distinct subtypes of neurons within the population, but specific markers for these different neurons have yet to be described. Neural subtype heterogeneity is also detected early within the OSN population; in zebrafish the predominant subtypes are ciliated sensory neurons that have long dendrites and express olfactory marker protein (OMP) and microvillous sensory neurons, which have short dendrites and express the Transient receptor potential cation channel, subfamily C, member 2b (Trpc2b)(Hansen and Zeiske, 1998; Sato et al., 2005). A third neural subtype associated with the early olfactory placode in zebrafish expresses *gonadotropin releasing hormone 3* (*gnrh3*). Rather than projecting exclusively to the olfactory bulb, Gnrh3 neurons send their axons caudally to various brain regions, including the hypothalamus (Abraham et al., 2008). While laser-ablating Gnrh3+ cells leads to sterility, animals homozygous for TALEN-induced mutations of *gnrh3* are fertile, pointing to the need of identifying other genes expressed in these cells that might underlie the differences between these phenotypes (Abraham et al., 2010; Spicer et al., 2016).

Although the major neural cell types associated with the olfactory epithelium appear to be conserved across vertebrates, there is no coherent vision as to their lineage origin between species. For instance, while Gnrh cells associated with the developing olfactory placode are reported to be of preplacodal origin in chick, in the zebrafish they have been shown to derive from the neural crest (Whitlock et al., 2003; Sabado et al., 2012); in mouse, Cre/*lox* experiments suggest that Gnrh cells are of mixed lineage origin, coming from both the ectoderm and CNC (Forni et al., 2011). To identify additional markers of cell-type heterogeneity in the developing

zebrafish olfactory placode we screened expression of molecules known to label discreet sets of neurons in other regions of the nervous system. We found that an antibody that recognizes the Islet family (Islet1/2) of LIM-homeoproteins labels Gnrh3 neurons in the olfactory placode from an early developmental stage (Ericson et al., 1992). With this new marker we find no change in the numbers of Islet1/2+ cells in the olfactory system in *sox10*$^{-/-}$ mutants, which are deficient in many CNC lineages. This is in contrast with previous studies and calls into question the proposed CNC origin of Gnrh+ cells. Consistent with these findings, lineage reconstructions of time-lapse confocal movies show that most if not all Gnrh3+ neurons, as well as microvillous sensory neurons, derive from the PPE. Thus, cell-type heterogeneity within the olfactory placode is likely established entirely from progenitors within the PPE.

Results

Islet1/2 expression in Gnrh3 neurons in the olfactory placode is unaffected in *sox10* mutants

Heterogeneity in neuronal subtypes is apparent in the zebrafish olfactory placode from early developmental stages (Whitlock and Westerfield, 1998; Whitlock and Westerfield, 2000; Whitlock et al., 2003; Sato et al., 2005; Madelaine et al., 2011; Saxena et al., 2013). While searching for novel markers of this heterogeneity, we found that at 48 hours post-fertilization (hpf) immunoreactivity to the Islet1/2 monoclonal antibody 39.4D5 is restricted to a small group of cells in the olfactory placode at the interface with the telencephalon (Figure 1A). The number and position of these Islet1/2+ cells resembles expression of *gonadotropin releasing hormone 3* (*gnrh3*) (Gopinath et al., 2004). To determine if they are the same cells, we examined expression of Islet1/2 in a transgenic line expressing enhanced GFP (eGFP) under the control of the *gnrh3* promoter, which recapitulates the endogenous expression of *gnrh3* in the olfactory placode (Abraham et al., 2008). Our results reveal a complete overlap between eGFP expression from the *Tg(gnrh3:eGFP)* transgene and Islet1/2 (Figure 1A).

It has been reported that zebrafish Gnrh3+ neurons associated with the olfactory placode derive from cranial neural crest (CNC), and that impairing CNC specification through morpholino knock-down of the HMG transcription factor *sox10* dramatically reduces their number (Whitlock et al., 2003; Whitlock et al., 2005). Unexpectedly, we found no difference in Islet1/2+ cell numbers in embryos homozygous for a strong *sox10* mutant allele (*sox10*$^{t3/t3}$) relative to wildtype siblings (6.9+/-0.4 versus 6.8+/-0.3 cells per placode, n=16; Figure 1A and B; (Dutton et al., 2001)). Similarly, eGFP expression in embryos carrying the *Tg(gnrh3:eGFP)* transgene was unaffected in a *sox10*$^{t3/t3}$ mutant background (7.1+/-0.4 versus 7.2+/-0.3 cells per placode, n=16; Figure 1A,C); endogenous *gnrh3* expression was also unaffected in *sox10* mutant embryos, ruling out a transgene-specific effect (Figure 1 – figure supplement 1). Our results indicate that Islet1/2 is a novel marker of Gnrh3 neurons associated with the zebrafish olfactory placode, and that these cells do not require Sox10 for specification.

A previous study assessed the origin of zebrafish Gnrh3 neurons by DiI labeling of premigratory CNC followed by immunostaining for GnRH (Whitlock et al., 2003). To revisit the proposed CNC origin of these neurons, we chose a Cre/*lox*-

based approach coupled with analysis of Islet1/2 expression. Double-heterozygous embryos carrying both a *Tg(-28.5Sox10:Cre)* and *Tg(ef1a:loxP-DsRed-loxP-eGFP)* transgene display a permanent shift from DsRed to eGFP expression in CNC lineages (Kague et al., 2012). Despite widespread expression of eGFP throughout the heads of 48 hpf double-heterozygous *Tg(-28.5Sox10:Cre);Tg(ef1a:loxP-DsRed-loxP-egfp)* embryos, including in cells surrounding the olfactory placode, we did not detect eGFP;Islet1/2 double-positive cells in the placodes themselves (n=20; Figure 2). While these are negative results, when combined with the lack of defects in Islet1/2+ cell numbers in *sox10* mutants they lend further support against a CNC origin for Gnrh3 neurons in the developing zebrafish olfactory system.

Lineage reconstruction reveals an anterior preplacodal ectoderm origin for Gnrh3 neurons

Gnrh3+ neurons associate closely with the olfactory placode from early stages (Gopinath et al., 2004). However, a lack of Cre lines specific for placodal progenitors precluded using a Cre/*lox* approach to address if Gnrh3 neurons derive from these cells. As an alternative, we developed an unbiased backtracking approach using time-lapse confocal movies. Briefly, synthetic mRNAs encoding Histone2B-RFP (H2B-RFP) were injected into *Tg(gnrh3:eGFP)* transgenic embryos, which were subsequently imaged from 12-36 hpf (Figure 3A); delamination and migration of CNC begins approximately 2 hours after the initiation of the time-lapse acquisition, and eGFP from the transgene is robustly expressed at 36 hpf (Schilling and Kimmel, 1994; Abraham et al., 2008). The lineage of various populations of cells was then manually retraced by backtracking H2B-RFP+ nuclei to their position at the beginning of the time-lapse series using Imaris software (Figure 3A and Video 1). To test our approach relative to well-established fate maps already generated for zebrafish cranial placodes, we first backtracked H2B-RFP+ nuclei of gnrh3:eGFP-negative cells in the olfactory placode as well as lens cells, which can be identified at the end of the time-lapse series by their distinct morphology (Figure 3B,C). Consistent with previous lineage studies (Whitlock and Westerfield, 2000), we found that gnrh3:eGFP-negative cells of the olfactory placode derived from progenitors in the prelacodal ectoderm (PPE) at the anterior/lateral neural plate border (n=32 cells from 9 placodes; Figure 3B,E and Figure 3 - figure supplement 1). Also as expected from earlier studies (Dutta et al., 2005), the H2B-RFP+ nuclei of lens cells traced back to a

PPE domain posterior and slightly lateral to that of the olfactory placode progenitors (n=10 cells from 2 lenses; Figure 3C,E). In contrast to previous reports, the nuclei of gnrh3:eGFP-positive cells traced back to the most anterior/medial region of the PPE (n=30 cells from 9 placodes; Figure 3D,E and Figure 3 – figure supplement 1), rather than from a region posterior to the lens progenitors as would be expected for CNC cells.

To confirm the anterior/medial PPE origin of Gnrh3 neurons, we used photoconversion to label the cells. We loaded *Tg(gnrh3:eGFP)* embryos with NLS-mEos2 by mRNA injection and at 12 hpf photoconverted either the left or right half of the domain predicted by backtracking to contain precursors of Gnrh3 neurons at this stage. Photoconverted embryos were then allowed to develop until 36 hpf, at which stage we determined if any gnrh3:eGFP+ cells had photoconverted nuclei (NLS-mEos2^{PC}; Figure 4A-D). Photoconversion caused no changes in the number of gnrh3:eGFP+ cells (5.4+/-0.5 versus 5.2+/-0.6 cells per placode, n=9; Figure 4E). However, while on average less than one NLS-mEos2^{PC};gnrh3:eGFP+ double-labeled cell per placode was detected on the control side of the embryo (0.3+/-0.2 cells per placode, n=9), the entire gnrh3:eGFP+ population was double-labeled on the photoconverted side (4.6+/-0.3 cells per placode, n=9; Figure 4E). There was no statistical difference between the number of gnrh3:eGFP+ and eGFP/mEos2^{PC}-double-positive cells in the photoconverted side suggesting that all Gnrh3 neurons associated with the olfactory placode are derived from the anterior/medial PPE.

Microvillous sensory neurons also derive from the preplacodal ectoderm

Zebrafish microvillous sensory neurons, like their counterparts in the rodent vomeronasal organ, express Transient receptor potential cation channel, subfamily C, member 2 (Trpc2) and VR-type olfactory receptors (Sato et al., 2005). The expression of a *Tg(-4.5trpc2b:GAP-Venus)* transgene is reduced in *sox10* morphant embryos suggesting a CNC origin for microvillous sensory neurons in zebrafish (Saxena et al., 2013), similar to Gnrh3+ neurons. Given our results with Gnrh3 neurons in *sox10* mutants (Figure 1A,B; (Whitlock et al., 2005)), we also revisited the microvillous lineage. Indeed, we found that the expression of endogenous *trpc2b* was unaffected in *sox10* mutants (Figure 5 - figure supplement 1). We then backtracked eGFP+ neurons in the *Tg(-4.9sox10:eGFP)* transgenic background (Video 2; (Wada et al., 2005)); expression from this transgene has been shown to overlap almost

completely with that of *Tg(-4.5trpc2b:GAP-Venus)* (Saxena et al., 2013). As before, nuclei of randomly chosen eGFP-negative cells in the olfactory placode trace back to an anterior/lateral position in the PPE (n=44 cells from 7 placodes; Figure 5A,D and Figure 5 – figure supplement 2); backtracked lens cells also behaved as before (n=10 cells from 2 lenses; Figure 5B,D). Unexpectedly, backtracking revealed a similar anterior/lateral PPE origin for sox10:eGFP+ cells as their eGFP-negative neighbors (n=41 cells from 7 placodes; Figure 5C,D and Figure 5 – figure supplement 2).

Similar to the Gnrh3+ cells, we used photoconversion of NLS-mEos2 to confirm our backtracking results for the microvillous population. This time, however, photoconversion was focused on the left or right two-thirds of the anterior/lateral PPE of *Tg(-4.9sox10:eGFP)* embryos (Figure 6A,B). As before, the number of eGFP+ cells was unaffected by the photoconversion (8+/-0.6 versus 9.8+/-0.7 cells per placode, n=9 and 6 respectively; Figure 6C-E), and less than one NLS-mEos2^{PC};sox10:eGFP+ cell per placode was detected on the control side of the embryo (0.3+/-0.3 cells per placode, n=6; Figure 6E). On the photoconverted side, however, an average of just under 60% of the total sox10:eGFP+ population was also NLS-mEos2^{PC}-positive (4.6+/-0.6 cells per placode, n=9; Figure 6D,E). This is consistent with the fact that we photoconverted approximately two-thirds of the cells in the PPE that gives rise to the olfactory placode.

Taken together, our results obtained using a combination of backtracking and photoconversion, indicate that Gnrh3 and microvillous sensory neurons associated with the zebrafish olfactory placode derive from the anterior/medial and anterior/lateral PPE, respectively.

Discussion

As part of our ongoing studies into the mechanisms underlying neurogenesis in the early zebrafish olfactory placode (Madelaine et al., 2011), here we have investigated how different subtypes of olfactory neurons arise. Using a novel marker for Gnrh3 neurons we have revisited this lineage and its origins within the placode. By combining Cre/*lox*, backtracking in 4D confocal datasets and photoconversion, we show that Gnrh3+ neurons derive from progenitors in the PPE; similar live imaging techniques also indicate a PPE origin for microvillous sensory neurons. These results support a common PPE origin for all of the neuronal populations within the olfactory system and argue against any CNC contribution. More generally, they suggest a mechanism by which cellular heterogeneity arises progressively within a field of neuronal progenitors.

In zebrafish at least two Islet genes, *islet1* and *islet2b*, are expressed in the olfactory Gnrh3+ cells (R. Aguillon and P. Blader, unpublished data). Whether or not Islet transcription factors regulate the development of Gnrh3 neurons, similar to Islet1 in pancreatic β-cells, remains unknown (Ahlgren et al., 1997). If this is the case, the specification of endocrine lineages, like Gnrh3 olfactory cells and Insulin expressing β-cells, may be an ancestral role of Islet proteins, which were later co-opted into other lineages such as motor neurons in the spinal cord (Karlsson et al., 1990; Ericson et al., 1992; Appel et al., 1995). Our analysis also reassigns the Gnrh3 lineage to progenitors found in a domain of the PPE known to give rise to neurons of the adenohypophysis (Dutta et al., 2005) and proposed to generate hypothalamic Gnrh2 neurons (Whitlock et al., 2003). Whether or not this region of the zebrafish PPE provides an environment that promotes the production of neuroendocrine lineages remains an open question.

Lineage reconstruction experiments in the tunicate, *Ciona intestinalis,* recently demonstrated the existence of a proto-placodal ectoderm, equivalent to the vertebrate PPE, which gives rise to both sensory neurons and Gnrh cells (Abitua et al., 2015). We propose that the development of a Gnrh population from the anterior/medial PPE has been conserved during chordate evolution. Whether or not this conservation holds for other vertebrates, however, remains unclear. DiI labeling experiments in the chick suggest that GnRH cells derive from precursors of the olfactory placodes separate from the adenohypophysis (Sabado et al., 2012), while our study and others show that in zebrafish these two populations overlap

significantly in the PPE (reviewed in (Toro and Varga, 2007)). In mice Cre/*lox* lineage analysis suggests that GnRH cells associated with the olfactory system are of mixed origin, being derived 70% from the ectoderm and 30% from CNC (Forni et al., 2011). This does not appear to be the case in chick, however, as grafted neural folds expressing GFP do not contribute to the olfactory placode (Sabado et al., 2012). Furthermore, similar to our results in zebrafish no change in GnRH cells numbers is detected in *Sox10*-null mutant mice (Pingault et al., 2013). As the original lineage assignment in mouse was established using only a single ectodermal (*Crect*; (Reid et al., 2011)) and neural crest (*Wnt1Cre*; (Danielian et al., 1998)) Cre line, respectively, our results suggest that revisiting the lineage assignment in the mouse with other genetic tools or other approaches is needed.

The origin of zebrafish microvillous sensory neurons is controversial (Saxena et al., 2013; Torres-Paz and Whitlock, 2014). Our results indicate that this lineage is derived from progenitors in the PPE. Furthermore, they imply that the expression of eGFP in the olfactory placode of *Tg(sox10:eGFP)* embryos does not reflect a CNC origin for these cells but rather an ectopic site of transgene expression. Why ectopic expression of the transgene in the olfactory placode appears restricted to microvillous sensory neurons is unclear but highlights the need to be cautious when using transgenic tools in lineage analyses. In this regard, the backtracking approach we have developed provides a powerful alternative for ascertaining lineage assignments during zebrafish embryogenesis. While in this study we used transgenic lines to identify cell types for backtracking, with the caveats that this obliges, we have also backtracked cells identified using antibody markers. For this, cells for backtracking can be identified by comparing the 3D architecture of a tissue described by nuclear position at the end of a time-lapse series to that of the same embryo after fixation and antibody labeling. Our analysis also highlights difficulties with using morpholinos when studying tissues for which a detailed comparison between the morphant and mutant phenoptypes has not been undertaken. Thus, while *sox10* morphants recapitulate a variety of phenotypes described in strong alleles of *sox10* mutants (Dutton et al., 2001), our data suggests that this cannot be extrapolated to the olfactory placode.

In conclusion, our results argue that cell-type heterogeneity in the zebrafish olfactory placode is generated from progenitors within the PPE, and begin to provide coherence for the lineage assignment of olfactory neural subtypes between

vertebrate species. Identifying the mechanisms underlying the segregation of the various olfactory lineages from overlapping progenitor pools is an important avenue for future research.

Acknowledgments

This work was supported by the Centre National de la Recherche Scientifique (CNRS); the Institut National de la Santé et de la Recherche Médicale (INSERM); Université de Toulouse III (UPS); University of California, Irvine; National Institute of Health (NIH R01 DE13828 and AR67797 to TS); Fondation pour la Recherche Médicale (DEQ20131029166 to PB); Fédération pour la Recherche sur le Cerveau; and the French Ministère de la Recherche. We would like to thank Brice Ronsin and the Toulouse RIO Imaging platform (LITC), and Aurore Laire, Richard Brimicombe-Lefevre and Ines Gehring for fish husbandry. We thank the Alsina, Fisher, Granato, Kelsh, Neuhauss, and Zohar labs for providing fish lines and other reagents. We also thank Christian Mosimann, Tatjana Sauka-Spengler and Trevor Williams for comments and suggestions.

Materials and methods

Fish Husbandry and lines

Fish were maintained at the CBD (Toulouse) and UCI (Irvine) zebrafish facilities in accordance with the rules and protocols in place in the respective locations. The *sox10*^{t3}, *Tg(-2.4gnrh3:egfp)*^{zf103} and *Tg(-4.9sox10:eGFP)*^{ba2Tg} lines have previously been described (Dutton et al., 2001; Wada et al., 2005; Abraham et al., 2008), as were the *Tg(-28.5Sox10:Cre)*^{zf384} and *Tg(ef1a:loxP-DsRed-loxP-eGFP)*^{zf284} lines used for Cre/loxP-based lineage analyses (Kague et al., 2012). Embryos were obtained through natural crosses and staged according to (Kimmel et al., 1995).

In situ Hybridisation, Immunostaining and Microscopy

In situ hybridisation was performed as previously described (Oxtoby and Jowett, 1993). Antisense DIG-labelled probes for *gnrh3* (Abraham et al., 2008) and *trpc2b* (Von Niederhausern et al., 2013) were generated using standard procedures. In situ hybridisations were visualised using BCIP and NBT (Roche) as substrates.

Embryos were immunostained as previously described (Madelaine et al., 2011); primary antibodies used were chicken anti-GFP (1:1000; ab13970, Abcam,

USA), rabbit anti-GFP (1:1000; TP-401, Torrey Pines Biolabs, USA) and mouse anti-Islet1/2 (1:200; 39.4D5, Developmental Studies Hybridoma Bank, USA). Primary antibodies were detected using the following fluorescently conjugated secondary antibodies (1:1000): Alexa Fluor 680 conjugated donkey anti-mouse IgG (A10038, Molecular Probes, USA), Alexa Fluor 568 conjugated goat anti-mouse IgG (A-11004, Molecular Probes, USA), Alexa Fluor 488 conjugated goat anti-rabbit IgG (A-11034, Molecular Probes, USA) and Alexa Fluor 488 conjugated donkey anti-chicken IgY (703-486-155, Jackson ImmunoResearch, USA). Immunolabellings were counterstained with DAPI (1:1000; D1306, Life Technologies, USA). Fluorescently labelled embryos were imaged using an inverted Nikon Eclipse Ti Confocal and brightfield images were taken on a Nikon Eclipse 80i microscope. Images were analysed using ImageJ and Imaris 8.3 (Bitplane, Switzerland) software.

Live confocal imaging and lineages reconstruction

Embryos from the *Tg(gnrh3:egfp)*^{zf103} or *Tg(-4.9sox10:eGFP)*^{ba2Tg} transgenic lines were injected with synthetic mRNA encoding an H2B-RFP fusion protein. Resulting embryos were grown to 12 hpf, a stage preceding the delamination and anterior migration of cranial neural crest cells (Schilling and Kimmel, 1994). They were then dechorionated and embedded for imaging in 0.7% low-melting point agarose in embryos medium in 55mm round petri dish (Gosselin; BP-50). A time-lapse series of confocal stacks (1 µm slice/180 µm deep) was generated of the anterior neural plate and flanking non-neural ectoderm on an upright Leica SP8 Confocal microscope using a 25x HC FLUOTAR water-immersion objective (L25 x 0.95 W VISIR). Stacks were acquired each 8 min until 36 hpf, a stage when eGFP from either transgene is strongly expressed in the olfactory placode. The lineage of the various neuronal populations was subsequently reconstructed manually by backtracking H2B-RFP^{+} nuclei using Imaris 8.3 analysis software (Bitplane, Switzerland).

Photoconversion

Embryos from the *Tg(gnrh3:egfp)*^{zf103} and *Tg(-4.9sox10:eGFP)*^{ba2Tg} transgenic lines were injected with synthetic mRNA encoding an NLS-mEos2 (mEOS2 fused to a nuclear localization sequence) fusion protein (Sapede et al., 2012). Embryos were then grown to 12 hpf, dechorionated and embedded for photoconversion/imaging in

0.7% low-melting point agarose in embryos medium in 35mm circular petri dish (Nunc™; 153066) bearing a silicone sealed 22mm circular cover slip (Thermo Scientific™; 174977). Mounted embryos were first imaged for NLS-mEos2 expression prior photoconversion at very low laser levels (confocal stack 2 µm slice/80 µm deep). Subsequently, a region of interest (ROI) was photoconverted using a 405nm diode (100% laser, 41sec), after which embryos were imaged again to assess the extent of NLS-mEos2 conversion. Photoconversion and imaging was done on an inverted SP8 Leica confocal with an HC PL APO CS2 40x/1.3 oil objective. Full z-stacks were acquired for each photoconverted embryo 24h after the photoconversion (confocal stack 1 µm slice/80 µm deep) to determine the contribution of progenitors located in the ROI at the time of photoconversion to the Gnrh3 or microvillous lineages.

Statistical analysis

All statistical comparisons are indicated in figure legends including one sample and unpaired t-test performed using Prism (GraphPad.) The scatter dot plots were generated with Prism. Data are mean ± s.e.m. Two-tailed t-test *p<0.05, **p<0.01, ***p<0.005, ****p<0.0001.

Additional information

Funding

Funder	Grant reference number	Author
Fondation pour la Recherche Médicale	DEQ20131029166	Raphaël Aguillon Julie Batut Romain Madelaine Pascale Dufourcq Patrick Blader
National Institute of Health	AR67797 DE13828	Arul Subramanian Thomas F Schilling

The funders had no role in study design, data collection and interpretation, or the decision to submit the work for publication.

Author contributions

RA, JB, Conception and design, Acquisition, analysis and interpretation of data, Drafting or revising the article; AS, RM, PD, Acquisition, analysis and interpretation of data; TFS, PB, Conception and design, Analysis and interpretation of data, Drafting or revising the article.

Author ORCIDs

Arul Subramanian, http://orcid.org/0000-0001-8455-6804

Thomas F Schilling, http://orcid.org/0000-0003-1798-8695

Patrick Blader, http://orcid.org/0000-0003-3299-6108

Julie Batut, http://orcid.org/0000-0002-1984-2094

Ethics

Animal experimentation: The study was performed in strict accordance with French and European guidelines (Toulouse), and to the recommendations in the Guide for the Care and Use of Laboratory Animals of the National Institutes of Health (Irvine).

Toulouse, France: French veterinary service and national ethical committee approved the protocols in this study, with approval ID: A-31-555-01 and APAPHIS #3653-2016011512005922v6.

Irvine, USA: All of the animals were handled according to approved institutional animal care and use committee (IACUC) protocols (#2000-2149) of the University of California, Irvine. The renewal of this protocol was approved by the IACUC (Animal Welfare Assurance #A3416.01) on December 11, 2015.

All animal experiments were performed on embryos derived from natural spawnings and every effort was made to minimize suffering.

References

Abitua, P. B., Gainous, T. B., Kaczmarczyk, A. N., Winchell, C. J., Hudson, C., Kamata, K., Nakagawa, M., Tsuda, M., Kusakabe, T. G. and Levine, M. (2015) The pre-vertebrate origins of neurogenic placodes, *Nature* 524(7566): 462-5.

Abraham, E., Palevitch, O., Gothilf, Y. and Zohar, Y. (2010) Targeted gonadotropin-releasing hormone-3 neuron ablation in zebrafish: effects on neurogenesis, neuronal migration, and reproduction, *Endocrinology* 151(1): 332-40.

Abraham, E., Palevitch, O., Ijiri, S., Du, S. J., Gothilf, Y. and Zohar, Y. (2008) Early development of forebrain gonadotrophin-releasing hormone (GnRH) neurones and the role of GnRH as an autocrine migration factor, *J Neuroendocrinol* 20(3): 394-405.

Aguillon, R., Blader, P. and Batut, J. (2016) Patterning, morphogenesis, and neurogenesis of zebrafish cranial sensory placodes, *Methods Cell Biol* 134: 33-67.

Ahlgren, U., Pfaff, S. L., Jessell, T. M., Edlund, T. and Edlund, H. (1997) Independent requirement for ISL1 in formation of pancreatic mesenchyme and islet cells, *Nature* 385(6613): 257-60.

Appel, B., Korzh, V., Glasgow, E., Thor, S., Edlund, T., Dawid, I. B. and Eisen, J. S. (1995) Motoneuron fate specification revealed by patterned LIM homeobox gene expression in embryonic zebrafish, *Development* 121(12): 4117-25.

Barrallo-Gimeno, A., Holzschuh, J., Driever, W. and Knapik, E. W. (2004) Neural crest survival and differentiation in zebrafish depends on mont blanc/tfap2a gene function, *Development* 131(7): 1463-77.

D'Amico-Martel, A. and Noden, D. M. (1983) Contributions of placodal and neural crest cells to avian cranial peripheral ganglia, *Am J Anat* 166(4): 445-68.

Danielian, P. S., Muccino, D., Rowitch, D. H., Michael, S. K. and McMahon, A. P. (1998) Modification of gene activity in mouse embryos in utero by a tamoxifen-inducible form of Cre recombinase, *Curr Biol* 8(24): 1323-6.
Dutta, S., Dietrich, J. E., Aspock, G., Burdine, R. D., Schier, A., Westerfield, M. and Varga, Z. M. (2005) pitx3 defines an equivalence domain for lens and anterior pituitary placode, *Development* 132(7): 1579-90.
Dutton, K. A., Pauliny, A., Lopes, S. S., Elworthy, S., Carney, T. J., Rauch, J., Geisler, R., Haffter, P. and Kelsh, R. N. (2001) Zebrafish colourless encodes sox10 and specifies non-ectomesenchymal neural crest fates, *Development* 128(21): 4113-25.
Ericson, J., Thor, S., Edlund, T., Jessell, T. M. and Yamada, T. (1992) Early stages of motor neuron differentiation revealed by expression of homeobox gene Islet-1, *Science* 256(5063): 1555-60.
Forni, P. E., Taylor-Burds, C., Melvin, V. S., Williams, T. and Wray, S. (2011) Neural crest and ectodermal cells intermix in the nasal placode to give rise to GnRH-1 neurons, sensory neurons, and olfactory ensheathing cells, *J Neurosci* 31(18): 6915-27.
Gopinath, A., Andrew Tseng, L. and Whitlock, K. E. (2004) Temporal and spatial expression of gonadotropin releasing hormone (GnRH) in the brain of developing zebrafish (Danio rerio), *Gene Expr Patterns* 4(1): 65-70.
Hansen, A. and Zeiske, E. (1998) The peripheral olfactory organ of the zebrafish, Danio rerio: an ultrastructural study, *Chem Senses* 23(1): 39-48.
Harlow, D. E. and Barlow, L. A. (2007) Embryonic origin of gustatory cranial sensory neurons, *Dev Biol* 310(2): 317-28.
Kague, E., Gallagher, M., Burke, S., Parsons, M., Franz-Odendaal, T. and Fisher, S. (2012) Skeletogenic fate of zebrafish cranial and trunk neural crest, *PLoS One* 7(11): e47394.
Karlsson, O., Thor, S., Norberg, T., Ohlsson, H. and Edlund, T. (1990) Insulin gene enhancer binding protein Isl-1 is a member of a novel class of proteins containing both a homeo- and a Cys-His domain, *Nature* 344(6269): 879-82.
Kimmel, C. B., Ballard, W. W., Kimmel, S. R., Ullmann, B. and Schilling, T. F. (1995) Stages of embryonic development of the zebrafish, *Dev Dyn* 203(3): 253-310.
Kwon, H. J., Bhat, N., Sweet, E. M., Cornell, R. A. and Riley, B. B. (2010) Identification of early requirements for preplacodal ectoderm and sensory organ development, *PLoS Genet* 6(9): e1001133.
Lister, J. A., Cooper, C., Nguyen, K., Modrell, M., Grant, K. and Raible, D. W. (2006) Zebrafish Foxd3 is required for development of a subset of neural crest derivatives, *Dev Biol* 290(1): 92-104.
Madelaine, R., Garric, L. and Blader, P. (2011) Partially redundant proneural function reveals the importance of timing during zebrafish olfactory neurogenesis, *Development* 138(21): 4753-62.
Montero-Balaguer, M., Lang, M. R., Sachdev, S. W., Knappmeyer, C., Stewart, R. A., De La Guardia, A., Hatzopoulos, A. K. and Knapik, E. W. (2006) The mother superior mutation ablates foxd3 activity in neural crest progenitor cells and depletes neural crest derivatives in zebrafish, *Dev Dyn* 235(12): 3199-212.
Oxtoby, E. and Jowett, T. (1993) Cloning of the zebrafish krox-20 gene (krx-20) and its expression during hindbrain development, *Nucleic Acids Res* 21(5): 1087-95.
Pingault, V., Bodereau, V., Baral, V., Marcos, S., Watanabe, Y., Chaoui, A., Fouveaut, C., Leroy, C., Verier-Mine, O., Francannet, C. et al. (2013) Loss-of-function mutations in SOX10 cause Kallmann syndrome with deafness, *Am J Hum Genet* 92(5): 707-24.
Reid, B. S., Yang, H., Melvin, V. S., Taketo, M. M. and Williams, T. (2011) Ectodermal Wnt/beta-catenin signaling shapes the mouse face, *Dev Biol* 349(2): 261-9.
Sabado, V., Barraud, P., Baker, C. V. and Streit, A. (2012) Specification of GnRH-1 neurons by antagonistic FGF and retinoic acid signaling, *Dev Biol* 362(2): 254-62.
Sapede, D., Dyballa, S. and Pujades, C. (2012) Cell lineage analysis reveals three different progenitor pools for neurosensory elements in the otic vesicle, *J Neurosci* 32(46): 16424-34.
Sato, Y., Miyasaka, N. and Yoshihara, Y. (2005) Mutually exclusive glomerular innervation by two distinct types of olfactory sensory neurons revealed in transgenic zebrafish, *J Neurosci* 25(20): 4889-97.
Saxena, A., Peng, B. N. and Bronner, M. E. (2013) Sox10-dependent neural crest origin of olfactory microvillous neurons in zebrafish, *Elife* 2: e00336.
Schilling, T. F. and Kimmel, C. B. (1994) Segment and cell type lineage restrictions during pharyngeal arch development in the zebrafish embryo, *Development* 120(3): 483-94.
Spicer, O. S., Wong, T. T., Zmora, N. and Zohar, Y. (2016) Targeted Mutagenesis of the Hypophysiotropic Gnrh3 in Zebrafish (Danio rerio) Reveals No Effects on Reproductive Performance, *PLoS One* 11(6): e0158141.

Steventon, B., Mayor, R. and Streit, A. (2014) Neural crest and placode interaction during the development of the cranial sensory system, *Dev Biol* 389(1): 28-38.
Stewart, R. A., Arduini, B. L., Berghmans, S., George, R. E., Kanki, J. P., Henion, P. D. and Look, A. T. (2006) Zebrafish foxd3 is selectively required for neural crest specification, migration and survival, *Dev Biol* 292(1): 174-88.
Toro, S. and Varga, Z. M. (2007) Equivalent progenitor cells in the zebrafish anterior preplacodal field give rise to adenohypophysis, lens, and olfactory placodes, *Semin Cell Dev Biol* 18(4): 534-42.
Torres-Paz, J. and Whitlock, K. E. (2014) Olfactory sensory system develops from coordinated movements within the neural plate, *Dev Dyn* 243(12): 1619-31.
Von Niederhausern, V., Kastenhuber, E., Stauble, A., Gesemann, M. and Neuhauss, S. C. (2013) Phylogeny and expression of canonical transient receptor potential (TRPC) genes in developing zebrafish, *Dev Dyn* 242(12): 1427-41.
Wada, N., Javidan, Y., Nelson, S., Carney, T. J., Kelsh, R. N. and Schilling, T. F. (2005) Hedgehog signaling is required for cranial neural crest morphogenesis and chondrogenesis at the midline in the zebrafish skull, *Development* 132(17): 3977-88.
Whitlock, K. E., Smith, K. M., Kim, H. and Harden, M. V. (2005) A role for foxd3 and sox10 in the differentiation of gonadotropin-releasing hormone (GnRH) cells in the zebrafish Danio rerio, *Development* 132(24): 5491-502.
Whitlock, K. E. and Westerfield, M. (1998) A transient population of neurons pioneers the olfactory pathway in the zebrafish, *J Neurosci* 18(21): 8919-27.
Whitlock, K. E. and Westerfield, M. (2000) The olfactory placodes of the zebrafish form by convergence of cellular fields at the edge of the neural plate, *Development* 127(17): 3645-53.
Whitlock, K. E., Wolf, C. D. and Boyce, M. L. (2003) Gonadotropin-releasing hormone (GnRH) cells arise from cranial neural crest and adenohypophyseal regions of the neural plate in the zebrafish, Danio rerio, *Dev Biol* 257(1): 140-52.

Figure Legends

Figure 1. Islet1/2 labels Gnrh3 neurons of the olfactory placode and its expression is unaffected in *sox10* mutants.

(A) Single confocal sections of olfactory placodes from *Tg(gnrh3:eGFP)* embryos at 48 hpf, in either wildtype or *sox10*$^{t3/t3}$ mutants, labelled for the expression of Islet1/2 (magenta) and eGFP (green); nuclei are labelled with DAPI (grey). Embryos are viewed dorsally and the inset in the first panel shows a schematic representation of a 48 hpf embryonic head indicating the the region analysed. Dotted lines highlight the olfactory placodes and scalebars represent 15 μm.

(B) Counts of cells expressing Islet1/2 in either wildtype or *sox10*$^{t3/t3}$ mutant placodes (6.8+/-0.3 versus 6.9+/-0.4 cells per placode, n=16 placodes).

(C) Counts of cells expressing eGFP from the *Tg(gnrh3:eGFP)* transgene in either wildtype or *sox10*$^{t3/t3}$ mutant placodes (7.2+/-0.3 versus 7.1+/-0.4 cells per placode, n=16 placodes).

(B-C) Mean ± s.e.m. P values are calculated using a two-tailed Student's t-test, n.s. not significant.

The following figure supplement is available for figure 1:

Figure supplement 1. Expression of endogenous *gnrh3* in *sox10*$^{t3/t3}$ mutants and wildtype siblings.

Representative bright-field images of *in situ* hybridisation against endogenous *gnrh3* transcripts in wildtype or *sox10*$^{t3/t3}$ mutant placodes showing high and low numbers of expressing cells. The number of placodes binned for each category over the total number of placodes analysed is indicated. Dotted lines highlight the olfactory placodes and scalebars represent 20 μm.

The following source data is available for figure 1:

Source data 1. Islet+ cell number quantification.

Source data 2. eGFP+ cell number quantification.

Figure 2. Cre/*lox* lineage mapping of neural crest cells reveals contributions to cells surrounding the olfactory epithelium but not to Islet/Gnrh3+ neurons.

Single confocal sections of an olfactory placode from double-heterozygous *Tg(-28.5Sox10:Cre);Tg(ef1a:loxP-DsRed-loxP-egfp)* embryo at 48 hpf, labelled for the expression of Islet1/2 (magenta) and eGFP (green); nuclei are labelled with DAPI (grey). No eGFP;Islet1/2 double-positive cells are detected in the placodes. Embryos are viewed dorsally and the inset in the first panel shows a schematic representation of a 48 hpf embryonic head indicating the orientation of the region analysed. Dotted lines highlight the olfactory placode and scalebars represent 15 μm.

Figure 3. Lineage reconstruction reveals an anterior preplacodal ectoderm origin for Gnrh3 neurons: backtracking.

(A) Schematic representation of the backtracking strategy. Synthetic mRNAs encoding Histone2B-RFP (H2B-RFP) were injected into *Tg(gnrh3:eGFP)* transgenic embryos, which were subsequently imaged from 12 to 36 hpf. The lineages of various populations of cells were manually retraced by backtracking H2B-RFP+ nuclei to their position at the beginning of the time-lapse series.

(B-D) Confocal projections from a representative 4D dataset at 36, 28, 20 and 12 hpf showing the position of the nuclei backtracked from 10 gnrh3:eGFP-negative (B, pink), 10 lens (C, yellow) and 7 gnrh3:eGFP-positive (D, blue) cells at each timepoint. Scalebars represent 40 μm.

(E) Schematic representation of an embryonic head at 36 hpf and the anterior neural plate (NP, dark grey) and adjacent preplacodal ectoderm (light grey) at 12 hpf, dorsal views. The 36 hpf head shows the colour code of the backtracked lineages, and the position of backtracked nuclei at 12 hpf is indicated in the preplacodal ectoderm. The 12 hpf representation shows the results obtained from 9 placodes (5 embryos) for 30 gnrh3:eGFP-positive cells and 32 gnrh3:eGFP-negative cells; the 10 lens were backtracked from a pair of placodes in a single 4D dataset only.

The following figure supplements are available for figure 3:

Figure supplement 1. Backtracking data from individual *Tg(gnrh3:eGFP)* embryos.

Confocal projections extracted from 4D datasets at 36 and 12 hpf for all embryos analysed showing the position of the backtracked nuclei of gnrh3:eGFP-negative (pink) and gnrh3:eGFP-positive (blue) cells at both timepoints. Backtracked nuclei for

the lens were only performed for Embryo 1 and are not shown. Scalebars represent 40 μm.

Figure 4. Lineage reconstruction reveals an anterior preplacodal ectoderm origin for Gnrh3 neurons: photoconversion.
(A,B) Confocal projections of NLS-mEos2 loaded, *Tg(gnrh3:eGFP)* embryos at 12 hpf before (A) and after photoconversion (B). The first panel in (A) shows a schematic representation of the anterior neural plate (NP, dark grey) and adjacent preplacodal ectoderm (light grey) at 12 hpf indicating the origin of backtracked gnrh*3*:eGFP-positive cells (blue dots) and the photoconverted area (magenta square), which is also indicated on the confocal projection shown in (B) after photoconversion. Scalebars represent 30 μm.
(C,D) Single confocal sections of olfactory placodes from *Tg(gnrh3:eGFP)* embryos at 36 hpf showing the expression of eGFP from the transgene (cytoplasmic green), unconverted NLS-mEos2 (mEos2; nuclear green) and converted NLS-mEos2 ($mEos2^{PC}$; nuclear magenta). Insets in (C) and (D) shows a schematic representation of an embryonic head at 36 hpf indicating the region analysed (black rectangle). Scalebars represent 5 μm.
(E) Counts of cell expressing eGFP from the *Tg(gnrh3:eGFP)* transgene or eGFP and photoconverted mEos2 ($mEos2^{PC}$) on the control (Ctl) versus photoconverted (PC) sides of the embryo at 36 hpf. No difference in the number of eGFP-positive cells is apparent between the Ctl and PC conditions (5.2+/-0.6 versus 5.4+/-0.5 cells per placode, n=9 placodes). Conversely, while a number of cells equivalent to the entire gnrh3:eGFP+ population is also $mEos2^{PC}$-positive on the photoconverted side, virtually no eGFP/$mEos2^{PC}$-double positive cells are detected on the control side (4.6+/-0.3 versus 0.3+/-0.2 cells per placode, n=9 placodes). Mean ± s.e.m. P values are calculated using a two-tailed Student's t-test, n.s. not significant, ****p<0.0001.

The following source data is available for figure 4:
Source data 1. gnrh3:eGFP+ and $mEos2^{PC}$+ cell number quantification.

Figure 5. Microvillous sensory neurons derive from preplacodal precursors: backtracking.

(A-C) Confocal projections from a representative 4D dataset at 36, 28, 20 and 12 hpf showing the position of the nuclei backtracked from 10 sox10:eGFP-negative (A, pink), 10 lens (B, yellow) and 10 sox10:eGFP-positive (C, blue) cells at each timepoint. Scalebars represent 40 μm.

(D) Schematic representation of an embryonic head at 36 hpf and the anterior neural plate (NP, dark grey) and adjacent preplacodal ectoderm (light grey) at 12 hpf, dorsal views; the cranial neural crest (CNC) at the earlier stage is indicated. While the 36 hpf head shows the colour code of the backtracked lineages, the position of backtracked nuclei at 12 hpf is indicated in the preplacodal ectoderm. The 12 hpf schema represents the results obtained from 7 placodes (4 embryos) for 41 sox10:GFP-positive cells and 44 sox10:eGFP-negative cells; the 10 lens were backtracked from a pair of placodes in a single 4D dataset only.

The following figure supplements are available for figure 5:

Figure supplement 1. Expression of endogenous *trpc2b* is unchanged in *sox10*$^{t3/t3}$ mutant embryos relative to wildtype siblings.

Representative bright-field images of *in situ* hybridisation against endogenous *trpc2b* transcripts in wildtype or *sox10*$^{t3/t3}$ mutant placodes showing high and low numbers of expressing cells or no expressing cells. The number of placodes binned for each category over the total number of placodes analysed is indicated. Dotted lines highlight the olfactory placodes and scalebars represent 20 μm.

Figure supplement 2. Backtracking data from individual *Tg(sox10:eGFP)* embryos.

Confocal projections extracted from 4D datasets at 36 and 12 hpf for all embryos analysed showing the position of the backtracked nuclei of sox10:eGFP-negative (pink) and sox10:eGFP-positive (blue) cells at both timepoints. Backtracked nuclei for the lens were only performed for Embryo 1 and are not shown. Scalebars represent 40 μm.

Figure 6. Microvillous sensory neurons derive from preplacodal precursors: photoconversion.

(A,B) Confocal projections of NLS-mEos2 loaded, *Tg(-4.9sox10:eGFP)* embryos at 12 hpf before (A) and after photoconversion (B). The first panel in (A) shows a

schematic representation of the anterior neural plate (NP, dark grey), adjacent preplacodal ectoderm (light grey) and cranial neural crest (CNC) at 12 hpf indicating the origin of backtracked sox10:eGFP-positive cells and the photoconverted area (magenta square), which is also indicated on the projection shown in (B) after photoconversion. Scalebars represent 30 μm.

(C,D) Single confocal sections of olfactory placodes from *Tg(-4.9sox10:eGFP)* embryos at 36 hpf showing the expression of eGFP from the transgene (cytoplasmic green), unconverted NLS-mEos2 (mEos2; nuclear green) and converted NLS-mEos2 ($mEos2^{PC}$; nuclear magenta). Insets in (C) and (D) shows a schematic representation of an embryonic head at 36 hpf, dorsal view, indicating the area analysed (black rectangle). Scalebars represent 5 μm.

(E) Counts of cell expressing eGFP from the *Tg(-4.9sox10:eGFP)* transgene or eGFP and photoconverted mEos2 ($mEos2^{PC}$) on the control (Ctl) versus photoconverted (PC) sides of the embryo at 36 hpf. No difference in the number of eGFP-positive cells is apparent between the Ctl and PC conditions (9.8+/-0.7 versus 8+/-0.6 cells per placode, n=9 and 6, respectively). Conversely, while numerous sox10:eGFP+ cells are also $mEos2^{PC}$-positive on the photoconverted side, virtually no eGFP/$mEos2^{PC}$-double positive cells are detected on the control side (4.6+/-0.6 versus 0.3+/-0.3 cells per placode, n=9 and 6, respectively). Shown are mean ± s.e.m. P values are calculated using a two-tailed Student's t-test, n.s. not significant, ***p=0.0001.

The following source data is available for figure 6:

Source data 1. sox10:eGFP+ and $mEos2^{PC}$+ cell number quantification.

Video 1. Lineage reconstruction reveals an anterior preplacodal ectoderm origin for Gnrh3 neurons.

Movie showing an acquisition series and backtracking of a Gnrh3 neuron in an Histone2B-RFP loaded *Tg(gnrh3:eGFP)* transgenic embryo. The movie is divided into 5 parts: an acquisition phase, a phase showing a z-stack of the olfactory placode at 36 hpf, an initial backtracking phase, the unique mitosis detected during the backtracking, and a final backtracking phase. During backtracking, the nucleus being followed is labelled with a blue dot. During the mitosis, the sister cell is labelled with a

pink dot for three frames until the two sister nuclei fuse. The movie finishes with a schematic representation of the anterior neural plate and adjacent preplacodal ectoderm at 12 hpf showing the results obtained from backtracking 30 gnrh3:eGFP-positive cells. The cell backtracked in the movie is indicated (arrowhead).

Video 2. Microvillous sensory neurons derive from classical preplacodal precursors: backtracking.

Movie showing an acquisition series and backtracking of a mircovillous sensory neuron in an Histone2B-RFP loaded *Tg(sox10:eGFP)* transgenic embryo. The movie is divided into 5 parts: an acquisition phase, a phase showing a z-stack of the olfactory placode at 36 hpf, an initial backtracking phase, the unique mitosis detected during the backtracking, and a final backtracking phase. During backtracking, the nucleus being followed is labelled with a blue dot. During the mitosis, the sister cell is labelled with a pink dot for three frames until the two sister nuclei fuse. The movie finishes with a schematic representation of the anterior neural plate, the adjacent preplacodal ectoderm (light grey) and neural crest (CNC) at 12 hpf showing the results obtained from backtracking 41 sox10:eGFP-positive cells. The cell backtracked in the movie is indicated (arrowhead).

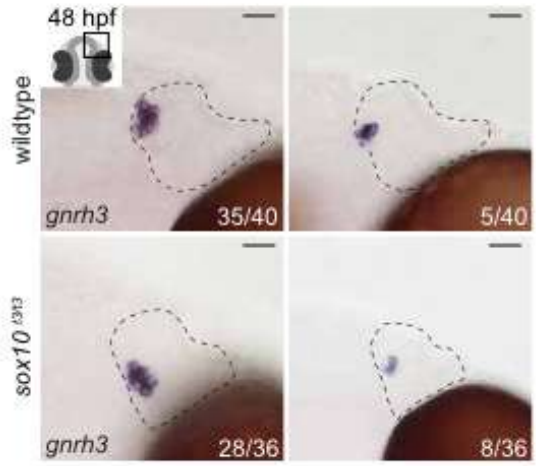

Aguillon et al., Figure 1 - figure supplement 1

Figure 1–source data 1. Islet+ cell number quantification.

	wildtype	*sox10t3/t3*
number of placode	16	16
minimum	4	5
25% Percentile	6.250	6
75% Percentile	7.750	8.750
maximum	9	10
Median	7	6
Mean	6.875	6.938
Std. Deviation	1.204	1.652
Std. Error	0.3010	0.4130

t-test	**two-tailed P value**	
wildtype versus *sox10t3/t3*	0.9027	n.s.

Figure 1–source data 2. eGFP+ cell number quantification

	wildtype	*sox10t3/t3*
number of placode	16	16
minimum	5	5
25% Percentile	6.250	6
75% Percentile	8	8.750
maximum	9	10
Median	7	7
Mean	7.250	7.125
Std. Deviation	1.125	1.708
Std. Error	0.2814	0.4270

t-test	**two-tailed P value**	
wildtype versus *sox10t3/t3*	0.8086	n.s.

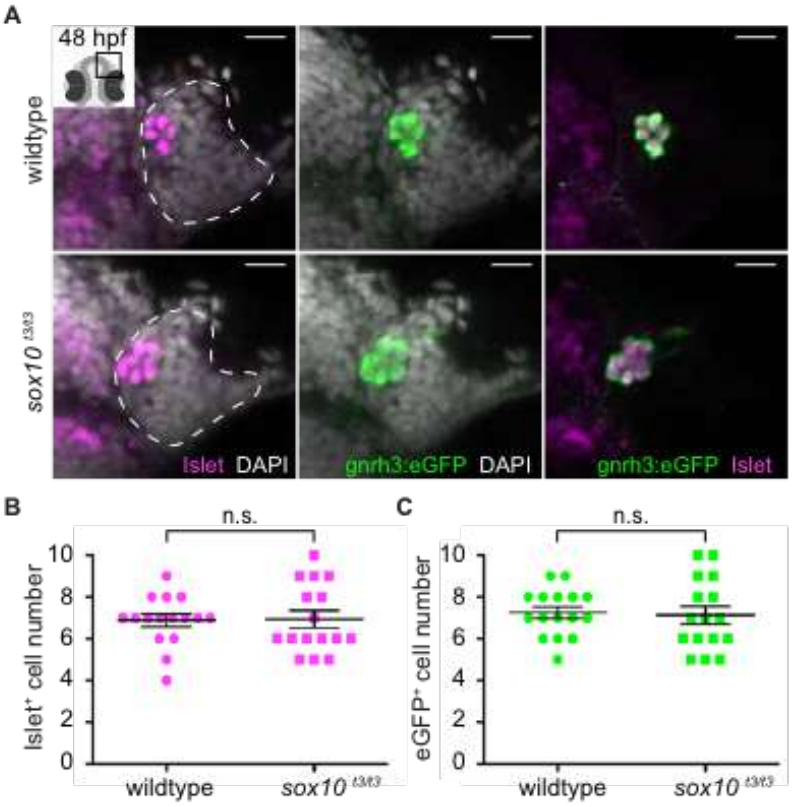

Aguillon et al., Figure 1

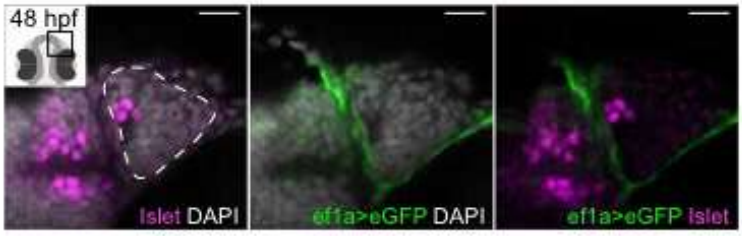

Aguillon et al., Figure 2

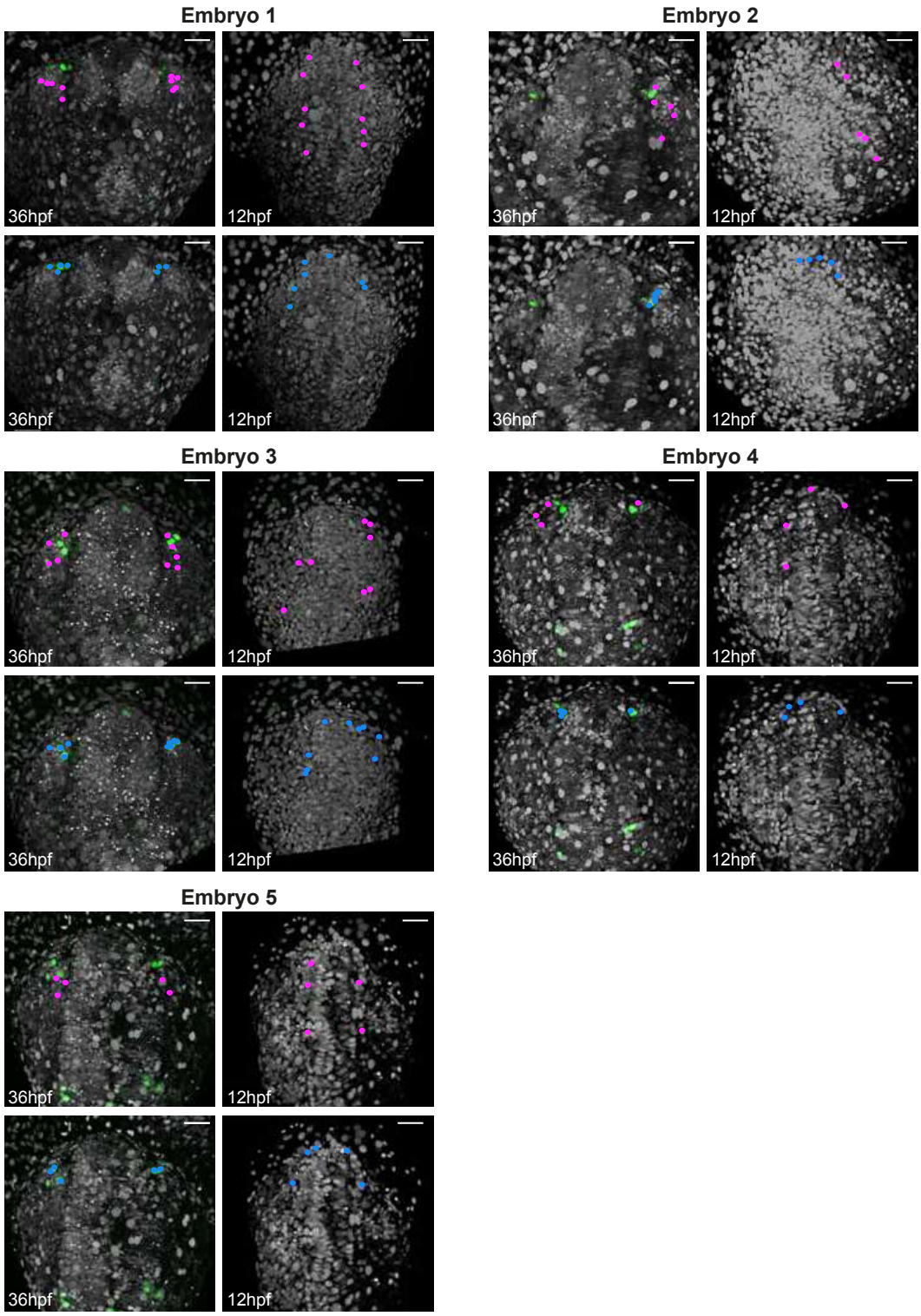

Aguillon et al., Figure 3 - figure supplement 1

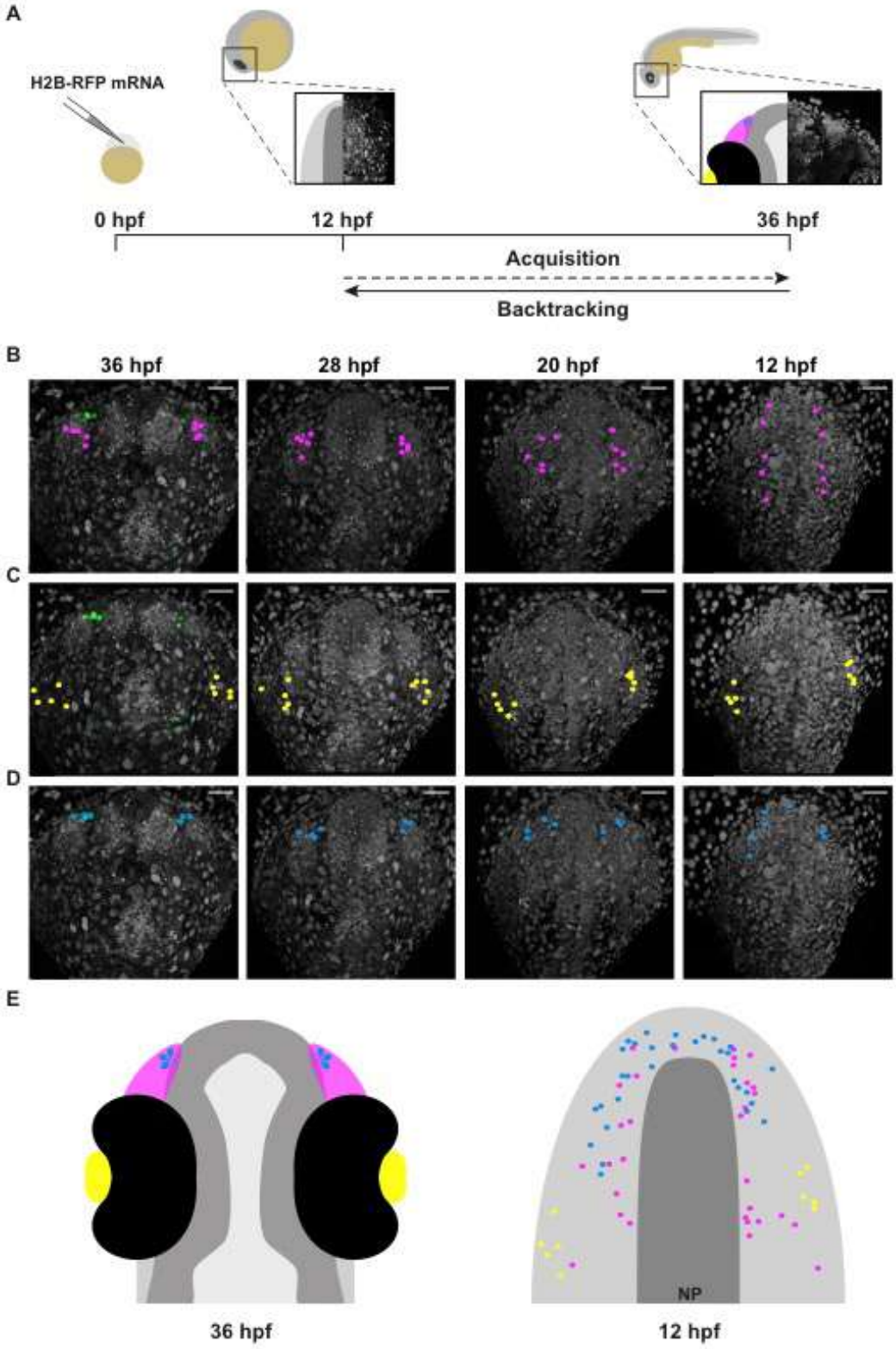

Aguillon et al., Figure 3

Figure 4–source data 1. gnrh3:eGFP+ and mEos2PC+ cell number quantification.

	Total (Ctl)	Total (PC)	mEos2PC (Ctl)	mEos2PC (PC)
number of placode	9	9	9	9
minimum	3	3	0	3
25% Percentile	4	4	0	4
75% Percentile	6.5	7	1	5.5
maximum	8	8	1	6
Median	5	5	0	5
Mean	5.222	5.444	0.3333	4.667
Std. Deviation	1.716	1.667	0.5	1
Std. Error	0.5720	0.5556	0.1667	0.3333

t-test	**two-tailed P value**	
Total (Ctl) versus Total (PC)	0.7843	n.s.
Total (PC) versus mEos2PC (PC)	0.2479	n.s.
mEos2PC (Ctl) versus mEos2PC (PC)	<0.0001	****

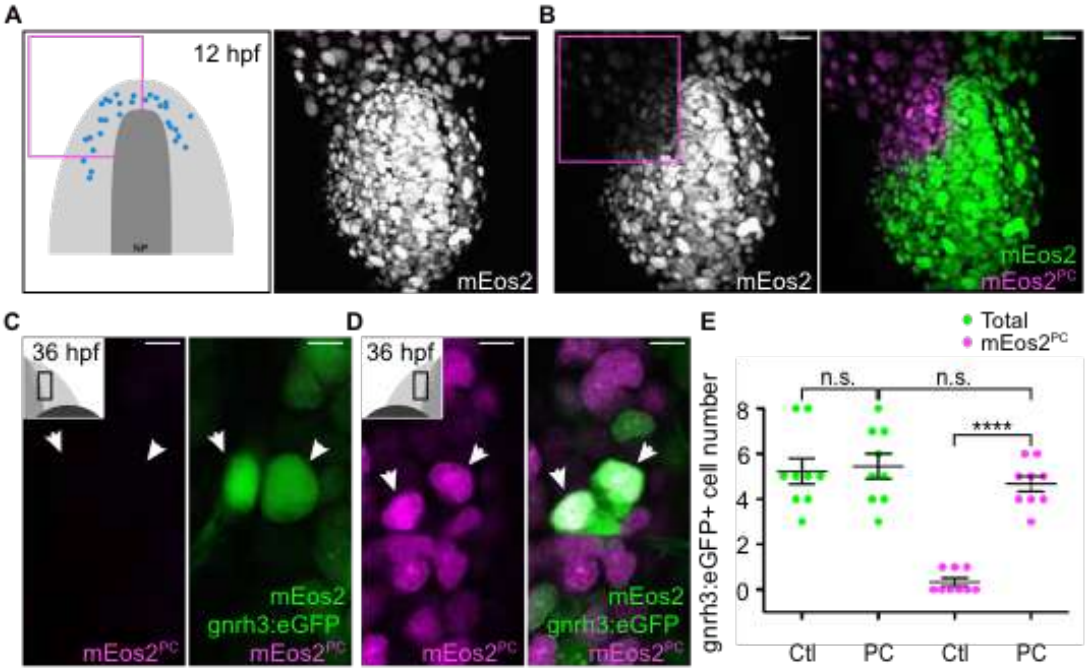

Aguillon et al., Figure 4

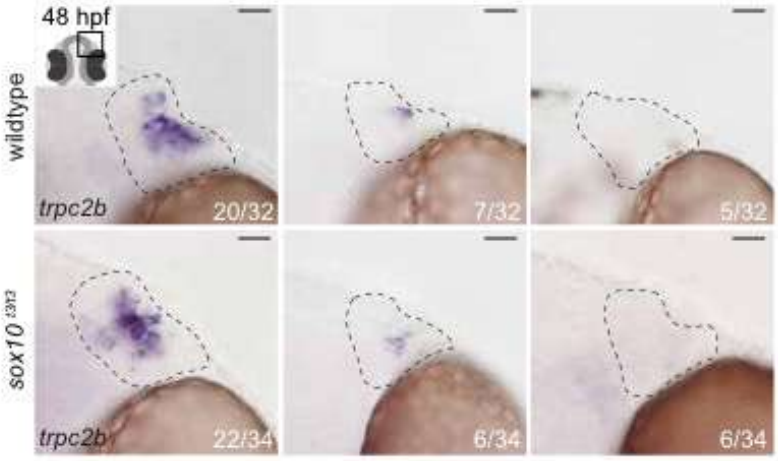

Aguillon et al., Figure 5 - figure supplement 1

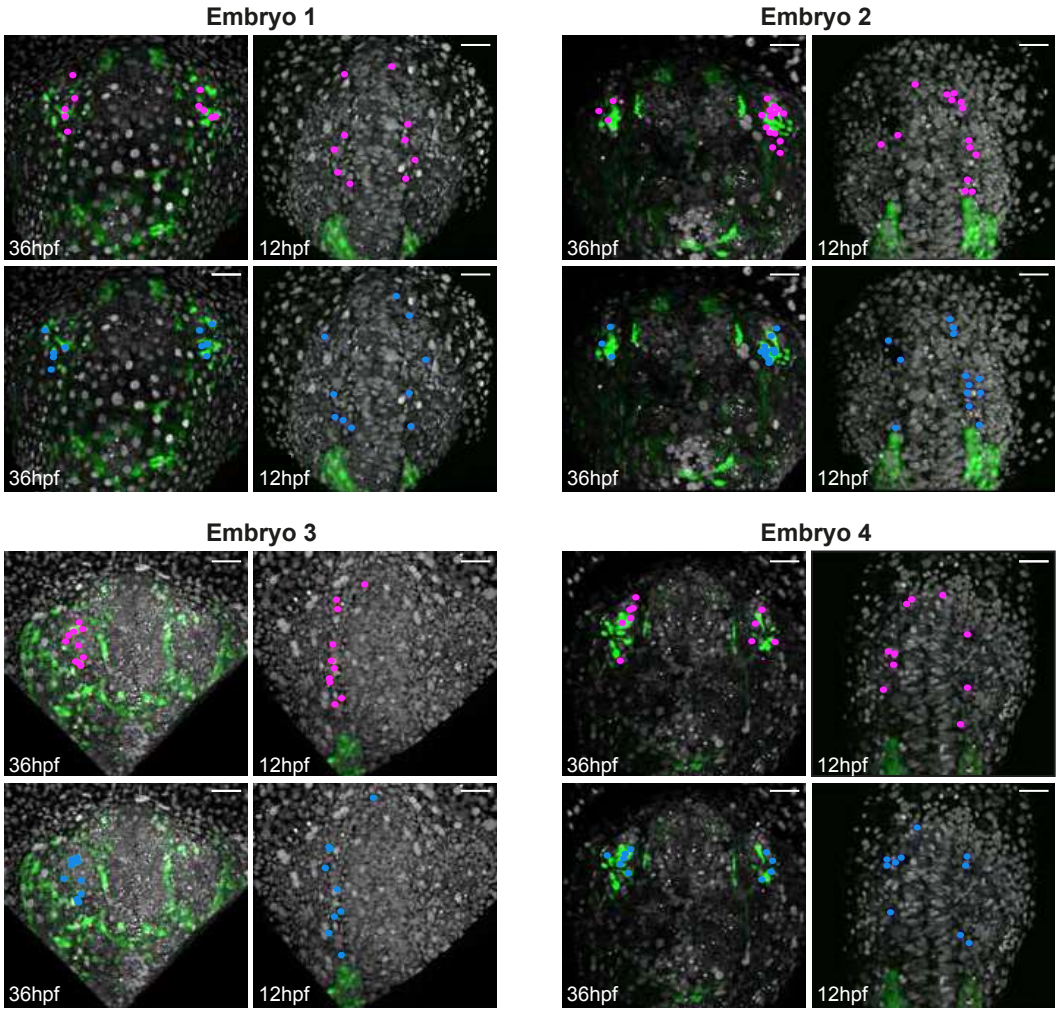

Aguillon et al., Figure 5 - figure supplement 2

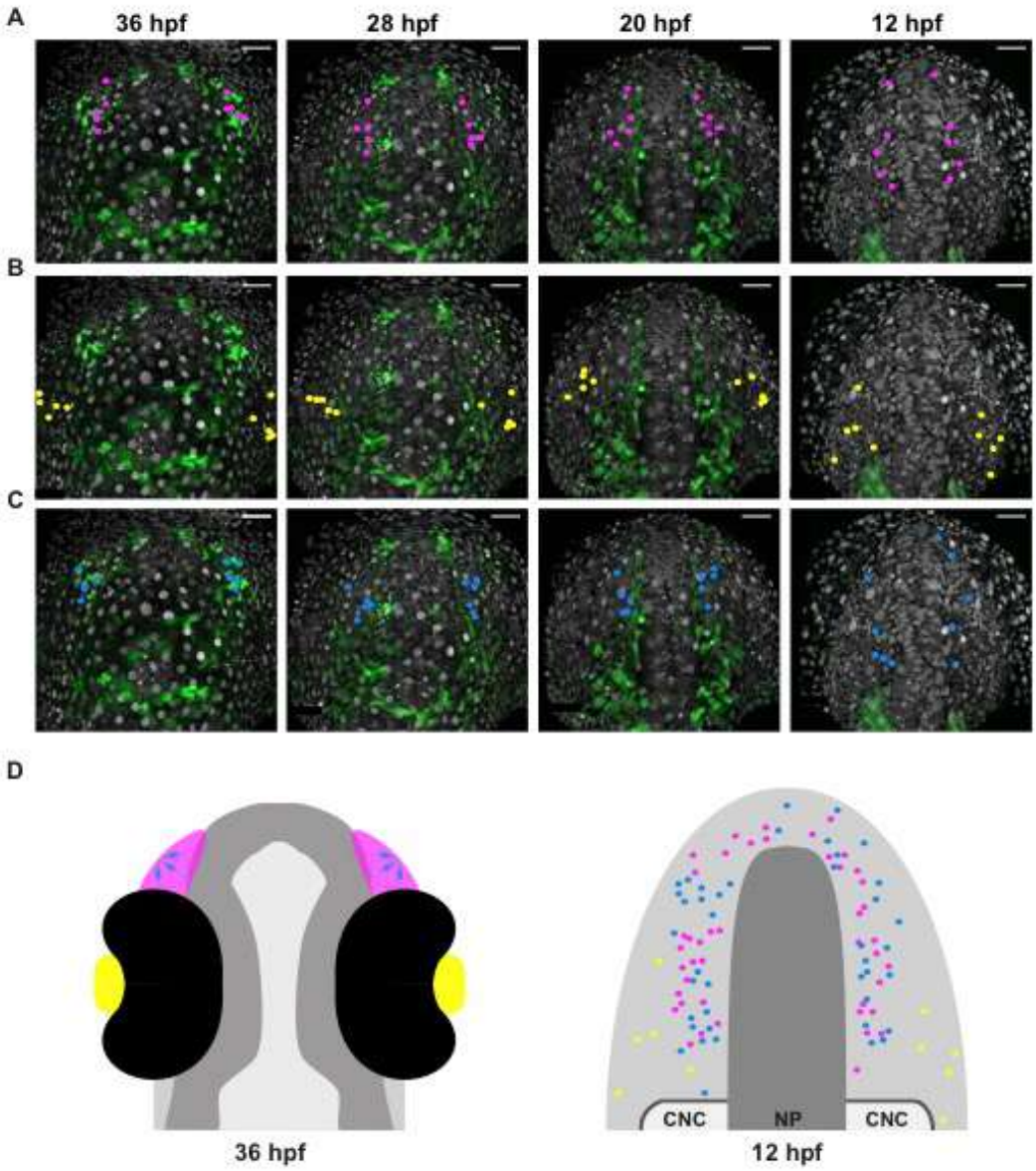

Aguillon et al., Figure 5

Figure 6–source data 1. sox10:eGFP+ and mEos2PC+ cell number quantification.

	Total (Ctl)	Total (PC)	mEos2PC (Ctl)	mEos2PC (PC)
number of placode	6	9	6	9
minimum	8	6	0	3
25% Percentile	8	6.5	0	4
75% Percentile	11.25	9	0.5	6
maximum	12	12	2	8
Median	10	8	0	4
Mean	9.833	8	0.3333	4.556
Std. Deviation	1.602	1.871	0.8165	1.810
Std. Error	0.6540	0.6236	0.3333	0.6035

t-test	**two-tailed P value**	
Total (Ctl) versus Total (PC)	0.0715	n.s.
mEos2PC (Ctl) versus mEos2PC (PC)	0.0001	***

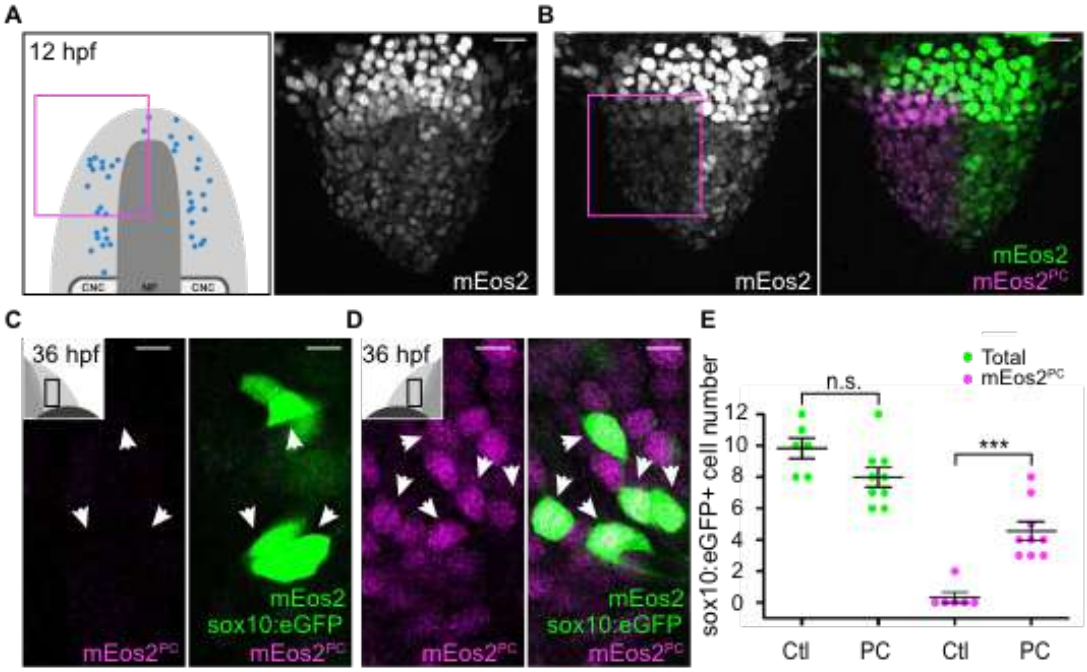

Aguillon et al., Figure 6

2.2 Neurog1 couples neurogenesis with morphogenetic movements during olfactory placode development

Résumé des travaux :

Le développement du système nerveux chez les vertébrés repose sur la production et la différentiation des neurones, leur migration et l'établissement des connections avec leurs cibles. Bien que les bases moléculaires de ces différents processus commencent à être bien connues, nous ne savons pas comment ils sont coordonnés. Nous avons précédemment montré que la neurogenèse de la placode olfactive du poisson zèbre requiert le facteur de transcription bHLH proneural Neurogenine1 (Neurog1). En parallèle de la première vague de neurogenèse, les cellules du territoire olfactif au sein de la région pré-placodale convergent pour former la placode olfactive.

Nos résultats révèlent que le comportement des neurones pionniers (EON) lors de la convergence est affecté dans le mutant pour *neurog1*. De façon intéressante, cette étape de la morphogenèse de la placode est affecté de façon similaire dans le mutant pour *cxcr4b* suggérant que ce gène pourrait être une cible de Neurog1. L'expression de *cxcr4b* est effectivement absente dans les cellules olfactives dans le mutant pour *neurog1* pendant les premières phases de la convergence. Nous avons réalisé une carte morphométrique résumant le déplacement des EON pendant la formation des placodes.

En combinant des approches classiques (analyse de promoteur & ChIP) et les techniques d'édition du génome (CrispR-Cas9) nous avons validé la régulation de *cxcr4b* par Neurog1. En effet, nous avons démontré que le proneural lie un cluster de E-box localisé à proximité du site d'initiation de la transcription du gène *cxcr4b.* Nos résultats suggèrent que les facteurs de transcription proneuraux coordonnent différents processus développementaux via la régulation de différents sets de gènes.

Neurog1 couples neurogenesis with morphogenetic movements during olfactory placode development

Raphaël Aguillon[1], Romain Madelaine[1†], Brice Ronsin[1], Caroline Halluin[1], Guturu Harendra[3], Sandra Link[4] Pascale Dufourcq[1], Holger Knaut[2], Gill Bergerano[3], Virginie Lecauday[4&], Julie Batut[1*] and Patrick Blader[1*]

[1] Centre de Biologie du Développement (CBD, UMR5547), Centre de Biologie Intégrative (CBI, FR 3743), Université de Toulouse, CNRS, UPS, 31062, France.
[2] Developmental Genetics Program and Kimmel Center for Stem Cell Biology, Skirball Institute of Biomolecular Medicine, New York University Langone Medical Center, 540 First Avenue, Skirball Institute 4-15, NY 10016, USA.
[3] Department of Computer Science, Department of Developmental Biology, Stanford University, Stanford, CA 94305, USA.
[4] BIOSS Centre for Biological Signalling Studies, Albert Ludwigs University of Freiburg, Freiburg im Breisgau, Germany.
[†] Present address: Beckman Center, Stanford University School of Medicine, Stanford, CA 94305
[&] Present address: Goethe-Universität - Campus Riedberg, Institute for Cell Biology and Neuroscience, Department of Developmental Biology of Vertebrates, Max-von-Laue-Straße 13, D-60438 Frankfurt am Main.

[*]Correspondence to: patrick.blader@univ-tlse3.fr; julie.batut@univ-tlse3.fr

One Sentence Summary: Neurog1 controls olfactory placode morphogenesis via *cxcr4b*

Abstract

Development of the vertebrate nervous system requires that neural progenitors differentiate at the correct times and in the correct numbers, that they migrate to appropriate sites, and ultimately that they establish connections with suitable partners. While much progress has made into the mechanisms controlling these individual processes, how they are coordinated remains relatively unknown. We have previously shown that neurogenesis in the zebrafish olfactory placode requires the bHLH proneural transcription factor Neurogenin1 (Neurog1). Concomitant with the earliest wave of olfactory neurogenesis, morphogenetic movements shape the placode into a rudimentary cup. To address whether Neurog1 couples neurogenesis and morphogenesis in this system, we analysed the morphogenetic behaviour of early olfactory neural progenitors. Our results indicate that the oriented cell movements required for proper morphogenesis of the placode are affected in *neurog1* mutants. Morphogenesis is similarly affected by mutations in the chemokine receptor, *cxcr4b*, suggesting that it could be a Neurog1 target gene. Using a combination of classical approaches (promoter analysis and Chromatin IP) and Crispr/Cas9 genome editing we show that Neurog1 directly regulates *cxcr4b* transcription through a cluster of E-boxes located immediately upstream of the *cxcr4b* transcription start site. Our results suggest that proneural transcription factors, such as Neurog1, directly couple distinct aspects of nervous system development.

Main Text

The morphology of peripheral sensory organs is exquisitely adapted for detecting specific stimuli. Concomitant with the morphogenetic movements that shape these organs during development, cell types are specified that will participate in the transmission of sensory information they receive to the brain. There is a growing understanding of the molecular mechanisms controlling morphogenesis and specification of different cell types in sensory organs. How morphogenesis and fate specification are coupled molecularly during their development, on the other hand, remains largely unexplored.

We have shown that neurogenesis in the developing zebrafish olfactory placode requires the proneural gene *neurog1*, which encodes a bHLH transcription factor (Blader et al., 1997; Madelaine et al., 2011). Concomitant with the earliest

wave of neurogenesis in the developing olfactory placode, morphogenetic movements shape placodal progenitors and newly born neurons into a rudimentary cup (Whitlock and Westerfield, 2000; Miyasaka et al., 2007; Breau et al., 2017). We hypothesised that, in parallel to its role in olfactory neurogenesis, Neurog1 is ideally placed to control the cell movements that underlie morphogenesis of the olfactory cup, thus coupling morphogenesis and neurogenesis. To address this possibility, we analysed morphogenesis of the olfactory cup by time-lapse imaging *neurog1* mutant or wildtype embryos carrying a *Tg(-8.4neurog1:gfp)* transgene (fig. S1 and Movie S1; (Golling et al., 2002; Blader et al., 2003)); this transgenes recapitulates the expression of endogenous *neurog1* in the developing placode/cup and can be used as a short-term lineage label for the progenitors of early olfactory neurons, referred to hereafter as EON (Madelaine et al., 2011; Breau et al., 2017). As recently described, we found that EON reach their final position in wildtype embryos by converging towards a point close to the centre of the future cup (Fig. 1A;(Breau et al., 2017)). Considering overall antero-posterior (AP) length of the placode, this convergence appears to happen quickly between 12 and 18 hours post-fertilization (hpf), after which it slows (Fig. 1B). In *neurog1*^{hi1059} mutants, we observed a delay in convergence, which translates into a relatively longer AP spread of EON than seen in wildtype embryos (Fig. 1 A,B and Movie S2). This delay is overcome, however, with the final placode in *neurog1*^{hi1059} mutant embryos attaining wildtype AP length around 27 hpf (Fig. 1A,B); ultimately, the placode in *neurog1*^{hi1059} mutant embryos is smaller than in siblings as it contains half the wildtype complement of neurons on average (Madelaine et al., 2011).

To assess the morphogenetic phenotype of *neurog1*^{hi1059} mutant embryos at cellular resolution, we injected synthetic mRNAs encoding Histone2B-RFP (H2B-RFP) into *Tg(-8.4neurog1:gfp)* transgenic embryos, which were again imaged from 12 to 27 hpf. Morphogenetic parameters of individual EON located in the anterior, middle and posterior thirds of the neurog1:GFP+ population were then extracted from datasets generated by manually tracking H2B-RFP positive nuclei using Imaris software (Fig. 1C and fig S1 and Movie S3). Again, the cell behaviour we observe in wildtype embryos largely recapitulates those already reported by Breau and colleagues (Fig. 1 D and data not shown;(Breau et al., 2017)). Comparing the behaviour of EON in *neurog1*^{hi1059} mutants and siblings, we found that whereas EON in the middle and posterior regions of mutant placodes migrate similarly to their

wildtype counterparts, the migratory behaviour of anterior EON appears profoundly affected in *neurog1*^{hi1059} mutant embryos (Fig. 1D); morphogenetic movements of individual skin cells showed no obvious differences in control versus *neurog1* mutants suggesting that the effect is specific to EON (fig. S2A). Principal component analysis (PCA) of the morphometric datasets confirmed that the major difference between olfactory placode morphogenesis in wildtype and *neurog1*^{hi1059} mutant embryos (PC1) lies in the migratory behaviour of anterior EON in the AP axis, but also highlighted differences in migration of the middle and posterior EON population of mutant versus siblings along the same axis (Fig. 1E). These migratory defects are not due to a decrease in cell mobility as EON in *neurog1* mutants displayed increase displacement over time compare to controls (fig. S2B). Intriguingly, the defect in migration of the EON population is only detected until 18 hpf (Fig. 1D). This suggests that the recovery of convergence of the placode in the *neurog1*^{hi1059} mutant is achieved via the restoration of wildtype-like migration from this stage. Taken together, our results suggest that Neurog1 plays a role during the early phase of olfactory placode morphogenesis.

We have shown that oriented migration of the anterior EON cohort is severely affected in *neurog1*^{hi1059} mutant embryos, and to a lesser extent the middle and posterior cohorts. While we cannot rule out that this phenotype is indirectly due to the effect of the *neurog1*^{hi1059} mutant on neurogenesis, our observations hint that the activity of a guidance factor or its receptor is affected in *neurog1*^{hi1059} mutant embryos. The chemokine receptor Cxcr4b and its ligand Cxcl12a (also known as Sdf1a) have been implicated in olfactory placode morphogenesis in the zebrafish (Miyasaka et al., 2007). To address whether the behaviour of EON in *neurog1*^{hi1059} mutants resembles that caused when the activity of this guidance receptor/ligand pair is abrogated, we analysed the morphogenetic parameters of EON migration in *cxcr4b*^{t26035} and *cxcl12a*^{t30516} mutants (Knaut et al., 2003; Valentin et al., 2007). As previously reported, olfactory placodes of embryos lacking Cxcr4b or Cxcl12a function display convergence defects (Fig. 2 A and B, and Movies S4 and S5). Analysis of the behaviour of individual cells in *cxcr4b*^{t26035} and *cxcl12a*^{t30516} mutant embryos indicates that defects in EON migration are largely restricted to the anterior cohort of EON (Fig. 2C); in both *cxcr4b*^{t26035} and *cxcl12a*^{t30516} mutants, EON show increased displacement over time (fig. S3A) and no difference is seen in skin cells (fig. S3B). Pairwise PCA between *cxcr4b*^{t26035} or *cxcl12a*^{t30516} mutants and wildtype

embryos showed that, similar to the *neurog1*^{hi1059} mutant context, the major difference in migratory parameters concerns EON migration in the AP axis (PC1; Fig. 2D). Finally, a combined PCA of morphometric datasets from *neurog1*^{hi1059}, *cxcr4b*^{t26035} and *cxcl12a*^{t30516} mutants confirms that the major difference of the behaviour of anterior, middle and posterior EON lies in their displacement along the AP axis (PC1; Fig. 2E). Indeed, clustering of the PCA analysis reveals that there is more similarity in the behaviour of anterior EON between the three mutants than between any single mutant and wildtype (fig. S4A-C); no distinction can be detected between mutants and wildtype when PCA clusters are generated for the skin (fig. S4D-F).

The similarity between the migration phenotype of EON in *neurog1*^{hi1059}, *cxcr4b*^{t26035} and *cxcl12a*^{t30516} mutant embryos suggests that the proneural transcription factor and the receptor/ligand couple act in the same pathway. To determine if the expression of either the receptor or its ligand are affected in the absence of Neurog1, we assessed their expression in *neurog1*^{hi1059} mutant embryos. We found that *cxcr4b* expression is dramatically reduced or absent in EON progenitors at 11, 13 and 15 hpf in this context (Fig. 3A). Intriguingly, however, the expression of *cxcr4b* recovers in *neurog1*^{hi1059} mutant embryos from 17-18 hpf, at which stage the migratory behaviour of *neurog1*^{hi1059} mutant EON becomes more like wildtype (Fig. 1B and Fig. 3A). The expression of *cxcl12a* is unaffected in *neurog1*^{hi1059} mutant embryos at all stages analysed (Fig. 3B To be added). Taken together, these results suggest that the EON migration phenotype in *neurog1*^{hi1059} mutant embryos is cause by a lack of Cxcr4b between 12-18 hpf.

Our data suggests that *cxcr4b* is a direct transcriptional target of Neurog1. As such, we searched for potential Neurog1-dependent cis-regulatory modules (CRM) at the *cxcr4b* locus. Proneural transcription factors bind CANNTG sequences known as E-boxes, which are often found in clusters (Bertrand et al., 2002). We identified 18 E-boxes clusters in the sequences from -100 to +100 kb of the *cxcr4b* initiation codon, but only 2 of these clusters contain at least one of the CA^{A}/$_{G}$ATG E-box sequence preferred by Neurog1 (Fig. 4A, cluster 7 and 8; (Madelaine and Blader, 2011)). Coherent with a possible role for these clusters in the regulation of *cxcr4b* expression, a transgenic line generated using a 35kb fosmid clone that contains only clusters 7 and 8, *TgFOS (cxcr4b:eGFP)*, recapitulates the expression of *cxcr4b* in the

olfactory cup (Fig. 4A). To investigate whether these clusters act as *bona fide* Neurog1-dependent CRM, we first performed chromatin immunoprecipitation (ChIP) experiments to see if Neurog1 binds them *in vivo*. In the absence of a ChIP compatible antibody against endogenous Neurog1, we chose a strategy based on misexpression of a Ty1-tagged form of Neurog1. As we previously showed with a Myc-tagged form of Neurog1, misexpression of Neurog1-Ty1 efficiently induces the known Neurog1 target *deltaA* (Fig. 4B; (Madelaine and Blader, 2011). We found that ChIP against Neurog1-Ty1 after misexpression effectively discriminates between the proneural-regulated HI and HII CRM at the *deltaA* locus (Fig. 4C); whereas HI is a known Neurog1-dependent CRM and is efficiently precipitated, HII underlies regulation of *deltaA* by members of the Ascl1 family of bHLH proneural factors and does not appear to bind Neurog1-Ty1 despite the presence of 2 E-boxes (Hans and Campos-Ortega, 2002; Madelaine and Blader, 2011). Misexpression of Neurog1-Ty1 leads to an increase of expression of *cxcr4b* comparable to that seen for *deltaA* (Fig.4B). However, despite both cluster 7 and 8 at the *cxcr4b* locus containing at least one Neurog1 preferred E-box, however, ChIP experiments indicated that only the first of these two potential CRM is bound significantly by Neurog1-Ty1 (Fig.4C).

To address whether the potential CRM containing E-box cluster 7 is sufficient to drive expression in the developing olfactory placode, we employed a classical transgenesis approach. For this, we constructed eGFP transgenes carrying either a 1.8kb genomic fragment flanking the *cxcr4b* start codon and containing the potential CRM or 1.65kb fragment lacking with CRM; a transgene was also constructed that contains mutations in the 2 E-boxes of the putative CRM in the 1.8kb fragment context. Embryos were injected with the transgenes, raised to adulthood and screened for transmission by PCR and eGFP expression in progeny. We found that while eGFP expression was detected in the olfactory placode of embryos from 6 of 9 carriers transmitting the *Tg(-1.8cxcr4b:eGFP)* transgene, embryos of only 3 of 12 carriers of the *Tg(-1.65cxcr4b:eGFP)* showed reporter expression in the olfactory placode (Fig.4D). These results suggest that the CRM containing E-box cluster 7 enhances expression of the transgene in the olfactory placode. No embryos from the 5 carriers of the *Tg(-1.8^{mut}cxcr4b:eGFP)* transgene showed expression of the reporter in the olfactory placode, indicating that the E-boxes are necessary for this activity (Fig.4D). To confirm the importance of the E-box cluster 7 CRM in the regulation of *cxcr4b* expression, we employed a Crispr/Cas9 approach to delete this

CRM using a pair of sgRNAs flanking the CRM; a similar deletion strategy was designed against cluster 8 as a control. Both the cluster 7 and cluster 8 sgRNA pairs efficiently induce deletions in the targeted sequence, as judged by PCR on genomic DNA extracted from embryos injected with either sgRNA pair and Cas9 protein (fig. S4). Only the cluster 7 sgRNA pair, however, caused mosaic disruption of the eGFP expression pattern in the olfactory placode when injected into *TgFOS (cxcr4b:eGFP)* transgenic embryos (Fig.4E). Loss of *TgFOS (cxcr4b:eGFP)* transgene expression is not due to cell death as eGFP-negative cells maintain the expression of the early neuronal marker HuC/D (Fig.4E). Our results strongly suggest that *cxcr4b* is a direct transcriptional target gene of Neurog1.

In zebrafish, the proneural transcription factor Neurog1 directly regulates the expression of the neurogenic genes *deltaA* and *deltaD* (Hans and Campos-Ortega, 2002; Madelaine and Blader, 2011). We have shown that Neurog1 is required for the development of an early wave of neurons in the olfactory placode (Madelaine et al., 2011). The data presented here are consistent with the idea that Neurog1 controls an early phase of morphogenesis of the zebrafish peripheral olfactory sensory organ via its target gene *cxcr4b*. We propose that Neurog1 couples neurogenesis with morphogenesis in this organ via the transcriptional regulation of distinct sets of targets. That members of the Neurog family regulate *Delta1* and *Cxcr4* expression, as well as development the olfactory epithelium in mouse suggests that this role may be conserved (Beckers et al., 2000; Mattar et al., 2004; Shaker et al., 2012).

Acknowledgments

This work was supported by the Centre National de la Recherche Scientifique (CNRS); the Institut National de la Santé et de la Recherche Médicale (INSERM); Université de Toulouse III (UPS); Fondation pour la Recherche Médicale (FRM; DEQ20131029166); Fédération pour la Recherche sur le Cerveau (FRC); and the Ministère de la Recherche. We would like to thank Stéphanie Bosch and the Toulouse RIO Imaging platform, and Aurore Laire and Richard Brimicombe for taking care of the fish. We also thank Marie Breau, Magali Suzanne, Christian Mosimann and members of the Blader and Knaut labs for advice on experiments and comments on the manuscript.

Materials and Methods

Fish Husbandry and lines

Ethics Statement and Embryos All embryos were handled according to relevant national and international guidelines. French veterinary service and national ethical committee approved the protocols in this study, with approval ID: A-31-555-01 and APAPHIS #3653-2016011512005922v6.

Fish were maintained at the CBD zebrafish facility in accordance with the rules and protocols in place. The *neurog1*^{hi1059Tg}, *cxcr4b*^{t26035} and *cxcl12a*^{t30516} mutant lines have previously been described (Golling et al., 2002; Knaut et al., 2003; Valentin et al., 2007), as was the *Tg(-8.4neurog1:gfp)*^{sb1} (Blader et al., 2003). Embryos were obtained through natural crosses and staged according to (Kimmel et al., 1995).

Establishment of transgenic lines

The *TgFOS (cxcr4b:eGFP)* transgenic line was generated by To be added. The *Tg(8.4neurog1:cxcr4b-mCherry)* line was generated by cloning To be added.

In situ Hybridisation, Immunostaining and Microscopy

In situ hybridisation was performed as previously described (Oxtoby and Jowett, 1993). Antisense DIG-labelled probes for *cxcr4b* and *cxcl12a* (David et al., 2002) were generated using standard procedures. In situ hybridisations were visualised using BCIP and NBT (Roche) as substrates.

Embryos were immunostained as previously described (Madelaine et al., 2011); primary antibody used was rabbit anti-GFP (1:1000; TP-401, Torrey Pines Biolabs, USA), which was detected using Alexa Fluor 488 conjugated goat anti-rabbit IgG diluted 1/1000: (A-11034, Molecular Probes, USA). Immunolabellings were counterstained with Topro3 (T3605, Molecular Probes, USA). Labelled embryos were imaged using an upright SP8 Leica confocal and analysed using ImageJ and Imaris 8.3 (Bitplane, Switzerland) software.

Cell tracking in time-lapse confocal datasets

Embryos from the *Tg(-8.4neurog1:gfp)* (Blader et al., 2003) transgenic line were injected with synthetic mRNA encoding an H2B-RFP fusion protein; for analysis of the global behaviour of olfactory placode morphogenesis, uninjected embryos were used. Resulting embryos were then grown to 12 hpf at which point they were

dechorionated and embedded for imaging in 0.7% low-melting point agarose in embryos medium. A time-lapse series of confocal stacks (1 µm slice/180 µm deep) was generated of the anterior neural plate and flanking non-neural ectoderm on an upright Leica SP8 Confocal microscope using a 25x HC Fluotar water-immersion objective. Acquisitions each 7 min were stopped at 27 hpf, when the olfactory rosette was clearly visible. The lineage of anterior, midline and posterior early olfactory neuron cohorts were subsequently constructed semi-automatically following H2B-RFP of neurog1:GFP+ EON using Imaris 8.3 analysis software (Bitplane, Switzerland); two cells from the left and right EON populations were tracked for each cohort per embryo. A schematic outline of the approach is presented in fig. S1.

Track analysis

Track parameters were extracted from Imaris as Excel files and analysed using a custom script generated in R (The R Project for Statistical Computing, www.r-project.org). First, tracks were rendered symmetric across the left-right axis for ease of interpretation. Tracks were then colour coded according to their genotype and to the phase of migration (early from 12-18 hpf; late from 18-27 hpf). Tracks were then plotted. Finally, the mean for each set of tracks was generated using the "RowMeans" function and a plot was generated.

Principal component analysis (PCA) and clustering were performed using the built-in R function "prcomp" from the "FactoMineR" package and the "kmeans" function, from the "stats" package, respectively. Finally, the "barplot" function ("graphics" package) was used to represent either the EON cluster composition or the Skin cluster composition.

Chromatin Immunoprecipitation and qPCR

ChIP experiments were performed as previously described using approximately 300 embryos (12 to 15 hpf) per immunoprecipitation (Wardle et al., 2006). Two to four separate ChIP experiments were carried out with corresponding independent batches of either control un-injected embryos or embryos injected with a synthetic mRNA encoding Neurog1-Ty1; ChIP-grade anti-Ty1 (Sigma) was used. Primers used for qPCR on ChIPs were: *cxcr4b* cluster 7 fw 5'- CTACATCTAAAAATTGAAAGA-3', *cxcr4b* cluster 7 rev 5'- CAAACCCAACACCCCTACTG-3', *cxcr4b* cluster 8 fw 5'-TTCCCATTGGTGCTTGAAAC-3', *cxcr4b* cluster 8 rev 5'-

AACTACAGCAGTCGCGATCA-3', *deltaA* HI fw 5'- GCGGAATGAACCACCAACTT-3', *deltaA* HI rev 5'- GTGTGACTAAAGGTGTATGGGTG-3', *deltaA* HII fw 5'-TATTGTGTGCAGGCGGAATA-3', *deltaA* HII rev 5'-GTTTGAATGGGCTCCTGAGA-3'. Reactions were carried out in triplicates on a MyIQ device (Bio-Rad). The specific signals were calculated as the ratio between the signals from the specific Ty1 antibody and from the beads alone and were expressed as percentage of chromatin input.

For qPCR experiments to determine expression levels of *cxcr4b* and *deltaA* after misexpression of Neurog1-Ty1, total RNAs were extracted from 20 injected embryos at 15 hpf with the RNeasy Mini Kit (QIAGEN), and reverse-transcribed with the PrimeScript RT reagent kit (Ozyme) according to the supplier's instructions. Q-PCR analyzes were performed on MyIQ device (Bio-Rad) with the SsoFast EvaGreen Supermix (Bio-Rad), according to the manufacturer's instructions. All experiments include a standard curve. Samples from fish were normalized to the number of *ef1a* mRNA copies. Primers for qPCR to determine the expression levels of *cxcr4b* and *deltaA* after misexpression of Neurog1-Ty1 normalised to the expression of *ef1a* were: *cxcr4b* coding fw 5'- GCTGGCATATTTCCACTGCT-3', *cxcr4b* coding rev 5'- AGTGCACTGGACGACTCTGA-3', *deltaA coding* fw 5'-CGGGTTTACAGGCATGAACT-3', *deltaA coding* rev 5'-ATTGTTCCTTTCGTGGCAAG-3', *ef1a* fw 5'-GCATACATCAAGAAGATCGGC, *ef1a* rev 5'-GCAGCCTTCTGTGCAGACTTTG-3'.

Crispr/Cas9 editing of potential CRM at the cxcr4b locus

sgRNA sequences flanking the E-box clusters 7 and 8 at the cxcr4b locus were designed using the web-based CRIPSRscan programme ((Moreno-Mateos et al., 2015); http://www.crisprscan.org). Templates for the transcription of sgRNAs were generated by PCR following previously described protocols (Nakayama et al., 2014). Injection of sgRNAs was performed as described by Burger and colleagues using a commercially available Cas9 protein (New England Biolabs) instead of preparing our homemade Cas9 (Burger et al., 2016).

Figure Legends

Fig. 1. Morphogenesis of the olfactory placode is affected in *neurog1*^{hi1059} mutant embryos.

(**A**) Confocal projections extracted from time-lapse series' showing the morphogenesis of the olfactory placode in wildtype and *neurog1*^{hi1059} mutant embryos carrying the *Tg(-8.4neurog1:gfp)* transgene. Embryos are viewed dorsally and the developmental stage is indicated for each frame. Scalebars represent 30 μm.

(**B**) Graph showing antero-posterior length of the developing olfactory placode in *neurog1*^{hi1059} mutant (Red) and wildtype embryos (Blue) over time. Lengths are normalized relative to the 12 hpf time point. The mean ± s.e.m of 12 tracks are represented (2 cells each from the left and right placodes from 3 embryos for each of the anterior, middle and posterior domains of the developing placode) per condition.

(**C**) Graphic representation of the morphogenesis of olfactory placodes indicating the anterior (A^{nt}), middle (M^{id}) and posterior (Pst) regions of the -8.4neurog1:GFP+ placodal domain. The early (12-18 hpf; Blue) and late (18-27 hpf; Grey) phases of this process are noted in the time line by arrows.

(**D**) Tracks showing migration of olfactory placode progenitors of wildtype (blue) or *neurog1*^{hi1059} mutant (red) embryos. 12 tracks are represented (2 cells each from the left and right placodes from 3 embryos) for each of the anterior, middle and posterior domains of the developing placode indicated in (**C**). The mean for each set of 12 tracks is also shown. The origin of the tracks has been arbitrarily set to the intersection of the X/Y axis and the early (coloured) and late (Grey) phases of migration have been highlighted.

(**E**) Pairwise principal component analysis scatterplots of morphogenetic parameters extracted from the datasets corresponding to the tracks in (**D**). For each of the anterior, middle and posterior datasets, the major difference between wildtype and *neurog1*^{hi1059} mutant embryos (PC1) corresponds to the antero-posterior axis.

Fig. 2. Morphogeneic defects in *neurog1*^{hi1059} mutant embryos resemble those of *cxcr4b*^{t26035} and *cxcl12a*^{t30516}.

(**A**) Confocal projections extracted from a time-lapse series showing the morphogenesis of the olfactory placode in wildtype, *cxcr4b*^{t26035} and *cxcl12a*^{t30516} mutant embryos carrying the *Tg(-8.4neurog1:gfp)* transgene. Embryos are viewed

dorsally and the developmental stage is indicated for each frame. Scalebars represent 30 μm.

(**B**) Graph showing antero-posterior length of the developing olfactory placode in *cxcr4b*^{t26035} (Orange) and *cxcl12a*^{t30516} (Green) mutant relative to wildtype embryos (Blue) over time. Lengths are normalized relative to the 12hpf time point. The mean ± s.e.m of 12 tracks are represented (2 cells each from the left and right placodes from 3 embryos for each of the anterior, middle and posterior domains of the developing placode) per condition.

(**C**) Tracks showing migration of olfactory placode progenitors of wildtype, *cxcr4b*^{t26035} and *cxcl12a*^{t30516} mutant embryos. 12 tracks are represented (2 cells each from the left and right placodes from 3 embryos) for each of the anterior, middle and posterior domains of the developing placode. The mean for each set of 12 tracks is also shown. The origin of the tracks has been arbitrarily set to the intersection of the X/Y axis and the early (coloured) and late (Grey) phases of migration have been highlighted.

(**D**) Pairwise principal component analysis scatterplots of morphogenetic parameters extracted from the datasets corresponding the tracks in (**C**). For each of the anterior, middle and posterior datasets, the major difference between wildtype, *cxcr4b*^{t26035} and *cxcl12a*^{t30516} mutant embryos (PC1) corresponds to the antero-posterior axis.

(**E**) Global principal component analysis scatterplots of morphogenetic parameters extracted from the dataset for *neurog1*^{hi1059}, *cxcr4b*^{t26035} and *cxcl12a*^{t30516} mutant relative to wildtype embryos. The major difference between wildtype and mutant embryos (PC1) corresponds to the antero-posterior axis.

Fig. 3. The expression of *cxcr4b* required Neurog1.

(**A**) *cxcr4b* whole mount *in situ* hybridization during early olfactory cup formation at 11, 13, 15 and 17 hpf in wildtype and *neurog1*^{hi1059} mutant embryos. *cxcr4b* expression is dramatically reduced or absent in EON progenitors at 12 and 15 hpf in *neurog1*^{hi1059} mutant embryos. From 17 hpf the expression of *cxcr4b* recovers in *neurog1*^{hi1059} mutant embryos.

(**B**) (To Be added).

Fig. 4. Neurog1 directly controls *cxcr4b* expression via an upstream Cis-regulatory module containing E-boxes

(**A**) Schematic representation of the *cxcr4b* locus indicating the position of exons of the *cxcr4b* gene (orange) and E-box clusters, which are colour coded depending on the nature of the E-box sequences. Also presented is the relative position of the genomic sequences found in the *TgFOS(cxcr4b:eGFP)* transgene. The sequences of the potential *cxcr4b* cis-regulatory modules containing E-box clusters 7 and 8 are indicated.

(**B**) qPCR analysis of the effect of misexpression of Neurog1-Ty1 on the relative mRNA levels of the known Neurog1 target *deltaA* and *cxcr4b*. A significant increase in expression is detected for both genes. Shown are mean ± s.e.m, p values are calculated using a two-tailed Student's t-test, *p=0.01, ***p=0.0001.

(**C**) Chromatin immunoprecipitation (ChIP) using an antibody against Ty1 and chromatin prepared from 15 hpf embryos misexpressing Neurog1-Ty1. Controls represent ChIP with an IgG alone. Shown are mean ± s.e.m, p values are calculated using a two-tailed Student's t-test, n.s. not significant, *p=0.01.

(**D**) Single confocal sections of 24 hpf embryonic heads showing representative eGFP expression patterns for transgenic lines generated using the *Tg(-1.8cxcr4b:eGFP)*, *Tg(-1.65cxcr4b:eGFP)* and *Tg(-1.8^{mut}cxcr4b:eGFP)* transgenes. The number of distinct lines showing these patterns relative to the total number of lines generated for each transgene is included.

(**E**) Single confocal sections of *TgFOS(cxcr4b:eGFP)* embryos at 24 hpf showing eGFP expression in the olfactory placodes, and either HuC/D expression of nuclear labelling (TOPRO). Embryos were injected with sgRNA pairs that create targeted deletions of either the E-box cluster 7 or cluster 8 containing CRM at the *cxcr4b* locus (indicated in **A**).

References

Beckers, J., Caron, A., Hrabe de Angelis, M., Hans, S., Campos-Ortega, J. A. and Gossler, A. (2000) Distinct regulatory elements direct delta1 expression in the nervous system and paraxial mesoderm of transgenic mice, *Mech Dev* 95(1-2): 23-34.

Bertrand, N., Castro, D. S. and Guillemot, F. (2002) Proneural genes and the specification of neural cell types, *Nat Rev Neurosci* 3(7): 517-30.

Blader, P., Fischer, N., Gradwohl, G., Guillemot, F. and Strahle, U. (1997) The activity of neurogenin1 is controlled by local cues in the zebrafish embryo, *Development* 124(22): 4557-69.

Blader, P., Plessy, C. and Strahle, U. (2003) Multiple regulatory elements with spatially and temporally distinct activities control neurogenin1 expression in primary neurons of the zebrafish embryo, *Mech Dev* 120(2): 211-8.

Breau, M. A., Bonnet, I., Stoufflet, J., Xie, J., De Castro, S. and Schneider-Maunoury, S. (2017) Extrinsic mechanical forces mediate retrograde axon extension in a developing neuronal circuit, *Nat Commun* 8(1): 282.

Burger, A., Lindsay, H., Felker, A., Hess, C., Anders, C., Chiavacci, E., Zaugg, J., Weber, L. M., Catena, R., Jinek, M. et al. (2016) Maximizing mutagenesis with solubilized CRISPR-Cas9 ribonucleoprotein complexes, *Development* 143(11): 2025-37.

David, N. B., Sapede, D., Saint-Etienne, L., Thisse, C., Thisse, B., Dambly-Chaudiere, C., Rosa, F. M. and Ghysen, A. (2002) Molecular basis of cell migration in the fish lateral line: role of the chemokine receptor CXCR4 and of its ligand, SDF1, *Proc Natl Acad Sci U S A* 99(25): 16297-302.

Golling, G., Amsterdam, A., Sun, Z., Antonelli, M., Maldonado, E., Chen, W., Burgess, S., Haldi, M., Artzt, K., Farrington, S. et al. (2002) Insertional mutagenesis in zebrafish rapidly identifies genes essential for early vertebrate development, *Nat Genet* 31(2): 135-40.

Hans, S. and Campos-Ortega, J. A. (2002) On the organisation of the regulatory region of the zebrafish deltaD gene, *Development* 129(20): 4773-84.

Kimmel, C. B., Ballard, W. W., Kimmel, S. R., Ullmann, B. and Schilling, T. F. (1995) Stages of embryonic development of the zebrafish, *Dev Dyn* 203(3): 253-310.

Knaut, H., Werz, C., Geisler, R., Nusslein-Volhard, C. and Tubingen Screen, C. (2003) A zebrafish homologue of the chemokine receptor Cxcr4 is a germ-cell guidance receptor, *Nature* 421(6920): 279-82.

Madelaine, R. and Blader, P. (2011) A cluster of non-redundant Ngn1 binding sites is required for regulation of deltaA expression in zebrafish, *Dev Biol* 350(1): 198-207.

Madelaine, R., Garric, L. and Blader, P. (2011) Partially redundant proneural function reveals the importance of timing during zebrafish olfactory neurogenesis, *Development* 138(21): 4753-62.

Mattar, P., Britz, O., Johannes, C., Nieto, M., Ma, L., Rebeyka, A., Klenin, N., Polleux, F., Guillemot, F. and Schuurmans, C. (2004) A screen for downstream effectors of Neurogenin2 in the embryonic neocortex, *Dev Biol* 273(2): 373-89.

Miyasaka, N., Knaut, H. and Yoshihara, Y. (2007) Cxcl12/Cxcr4 chemokine signaling is required for placode assembly and sensory axon pathfinding in the zebrafish olfactory system, *Development* 134(13): 2459-68.

Moreno-Mateos, M. A., Vejnar, C. E., Beaudoin, J. D., Fernandez, J. P., Mis, E. K., Khokha, M. K. and Giraldez, A. J. (2015) CRISPRscan: designing highly efficient sgRNAs for CRISPR-Cas9 targeting in vivo, *Nat Methods* 12(10): 982-8.

Nakayama, T., Blitz, I. L., Fish, M. B., Odeleye, A. O., Manohar, S., Cho, K. W. and Grainger, R. M. (2014) Cas9-based genome editing in Xenopus tropicalis, *Methods Enzymol* 546: 355-75.

Oxtoby, E. and Jowett, T. (1993) Cloning of the zebrafish krox-20 gene (krx-20) and its expression during hindbrain development, *Nucleic Acids Res* 21(5): 1087-95.

Shaker, T., Dennis, D., Kurrasch, D. M. and Schuurmans, C. (2012) Neurog1 and Neurog2 coordinately regulate development of the olfactory system, *Neural Dev* 7: 28.

Valentin, G., Haas, P. and Gilmour, D. (2007) The chemokine SDF1a coordinates tissue migration through the spatially restricted activation of Cxcr7 and Cxcr4b, *Curr Biol* 17(12): 1026-31.

Wardle, F. C., Odom, D. T., Bell, G. W., Yuan, B., Danford, T. W., Wiellette, E. L., Herbolsheimer, E., Sive, H. L., Young, R. A. and Smith, J. C. (2006) Zebrafish promoter microarrays identify actively transcribed embryonic genes, *Genome Biol* 7(8): R71.

Whitlock, K. E. and Westerfield, M. (2000) The olfactory placodes of the zebrafish form by convergence of cellular fields at the edge of the neural plate, *Development* 127(17): 3645-53.

Supplemental Movies

Movie S1. Shaping of the olfactory cup reveals a convergence migration towards the centre of the future cup.

Movie showing an acquisition series of *Tg(-8.4neurog1:gfp)* labeled EON in a control embryo. The movie shows the whole acquisition from 12 hpf to 27 hpf every 10 min.

Movie S2. *neurog1* mutated olfactory placodes exhibit a delayed in convergence.

Movie showing an acquisition series displaying EON migration in transgenic *Tg(-8.4neurog1:gfp) neurog1*^{hi1059} mutant embryo. The movie shows the whole acquisition from 12 hpf to 27 hpf every 10 min.

Movie S3. EON lineages tracking along the AP axis are manually generated.

Lineage of EON located in the anterior, middle and posterior thirds of the neurog1:GFP+ population were established by manually tracking H2B-RFP positive nucleus. The movie is divided into 5 parts representing: anterior EON tracks, middle EON tracks, posterior EON tracks and a final part with all anterior, middle and posterior tracks. The movie finishes with anterior, middle and posterior Skin tracks from 12 hpf to 27 hpf. During the movie, EON/spots and Skin/spots being followed are respectively labeled with a white and a pink square. When the 12 tracks are represented the tracks are color code according to their AP displacement.

Movie S4. Behaviour of EONs in *cxcr4b*^{t26035} mutant embryo are mostly affected in the anterior compartment.

Movie showing an acquisition series displaying EON migration in transgenic *Tg(-8.4neurog1:gfp) cxcr4b*^{t26035} mutant embryo. The movie shows the whole acquisition from 12 hpf to 27 hpf every 10 min.

Movie S5. Behaviour of EONs in *cxcl12a*^{t30516} mutant embryo display severe migration defect and seem mostly affected in the anterior compartment.

Movie showing an acquisition series displaying EON migration in transgenic *Tg(-8.4neurog1:gfp) cxcl12a*^{t30516} mutant embryo. The movie shows the whole acquisition from 12 hpf to 27 hpf every 10 min.

Supplemental Figures

Fig. S1. Set up to produce 4D confocal EON migration datasets to generate EON tracks and to extract morphogenetic parameters.

(A) Schematic representation of *Tg(-8.4neurog1:gfp)* transgenic embryo mounting for time-lapse imaging. Transgenic embryos are embedded in low melting agarose and imaged every 10 min from 12 hpf to 27 hpf to generate 4D confocal dataset (every 1μm).

(B) EON lineage generation using *Tg(-8.4neurog1:gfp)* transgenic embryo loaded with H2B-RFP. EON track is generate by manually following individual red nucleus of neurog1:GFP+ cell from 12 hpf (blue star) to 27 hpf (white star). Scalebars represent 7 μm.

(C) Extraction of EON morphogenetic parameters using Imaris software.

Fig. S2. Morphogenetic EON movements seem specifically affected in *neurog1*^{hi1059} mutant embryos.

(A) Morphogenetic movements of individual skin cells showed no obvious differences in control versus *neurog1* mutants. Tracks showing migration of skin cells of wildtype (blue) or *neurog1*^{hi1059} mutant (red) embryos. 12 tracks are represented (2 cells each from the left and right placodes from 3 embryos) for each of the anterior, middle and posterior domains of the developing placode. The mean for each set of 12 tracks is also shown. The origin of the tracks has been arbitrarily set to the intersection of the X/Y axis and the early (coloured) and late (Grey) phases of migration have been highlighted.

(B) Graph showing the global displacement (along both X, medio-lateral axis and Y, antero-posterior axis) of wildtype (blue) or *neurog1*^{hi1059} mutant (red) EON at five indicated time periods. The mean ± s.e.m of 36 tracks are represented (12 tracks per embryo and 3 embryos per genotype) per condition.

Fig. S3. Morphogenetic EON movements seem specifically affected in *cxcr4b*^{t26035} and *cxcl12a*^{t30516} mutant embryos and phenocopy neurog1 mutated EON behaviour.

(A-B) Graph showing the global displacement (along both X, medio-lateral axis and Y, antero-posterior axis) of wildtype (blue), *neurog1*^{hi1059} mutant (red), *cxcr4b*^{t26035} (orange) and *cxcl12a*^{t30516} (green) mutants EON **(A)** or Skin cells **(B)** at five indicated

time periods. The mean ± s.e.m of 36 tracks are represented per condition (12 tracks per embryo and 3 embryos per genotype).

(C) Morphogenetic movements of individual skin cells showed no major differences in control versus *cxcr4b*^{t26035} and *cxcl12a*^{t30516} mutants. Tracks showing migration of skin cells of wildtype (blue), *cxcr4b*^{t26035} mutant (orange) or *cxcl12a*^{t30516} (green) mutant embryos. 12 tracks are represented (2 cells each from the left and right placodes from 3 embryos) for each of the anterior, middle and posterior domains of the developing placode. The mean for each set of 12 tracks is also shown. The origin of the tracks has been arbitrarily set to the intersection of the X/Y axis and the early (coloured) and late (Grey) phases of migration have been highlighted.

Fig. S4. Anterior mutated EON seem to behave similarly.

(A-C) PCA clustering of anterior early EONs (from 12 to 18 hpf) from control, *neurog1*^{hi1059}, *cxcr4b*^{t26035} and *cxcl12a*^{t30516} mutants indicate that only control EON can segregate alone. **(A)** Clustering analysis (k=4) of the PCA represents 4 groups of EONs from light to dark grey. **(B)** Cluster composition according to EON genotype: control (blue), *neurog1*^{hi1059} mutants (red), *cxcr4b*^{t26035} mutants (orange) and *cxcl12a*^{t30516} mutants (green). **(C)** PCA of anterior early EONs colour code according to their corresponding genotype either control, *neurog1*^{hi1059}, *cxcr4b*^{t26035} or *cxcl12a*^{t30516} mutated.

(D-F) PCA clustering of anterior early skin cells (from 12 to 18 hpf) from control, *neurog1*^{hi1059}, *cxcr4b*^{t26035} and *cxcl12a*^{t30516} mutants shows that no major distinction can be detected between mutants and wildtype. **(D)** Clustering analysis (k=4) of the PCA represents 4 groups of skin cells from light to dark grey. **(E)** Cluster composition according to skin cells genotype: control (blue), *neurog1*^{hi1059} mutants (red), *cxcr4b*^{t26035} mutants (orange) and *cxcl12a*^{t30516} mutants (green). **(F)** PCA of anterior early skin cells colour code according to their corresponding genotype either control, *neurog1*^{hi1059}, *cxcr4b*^{t26035} or *cxcl12a*^{t30516} mutants.

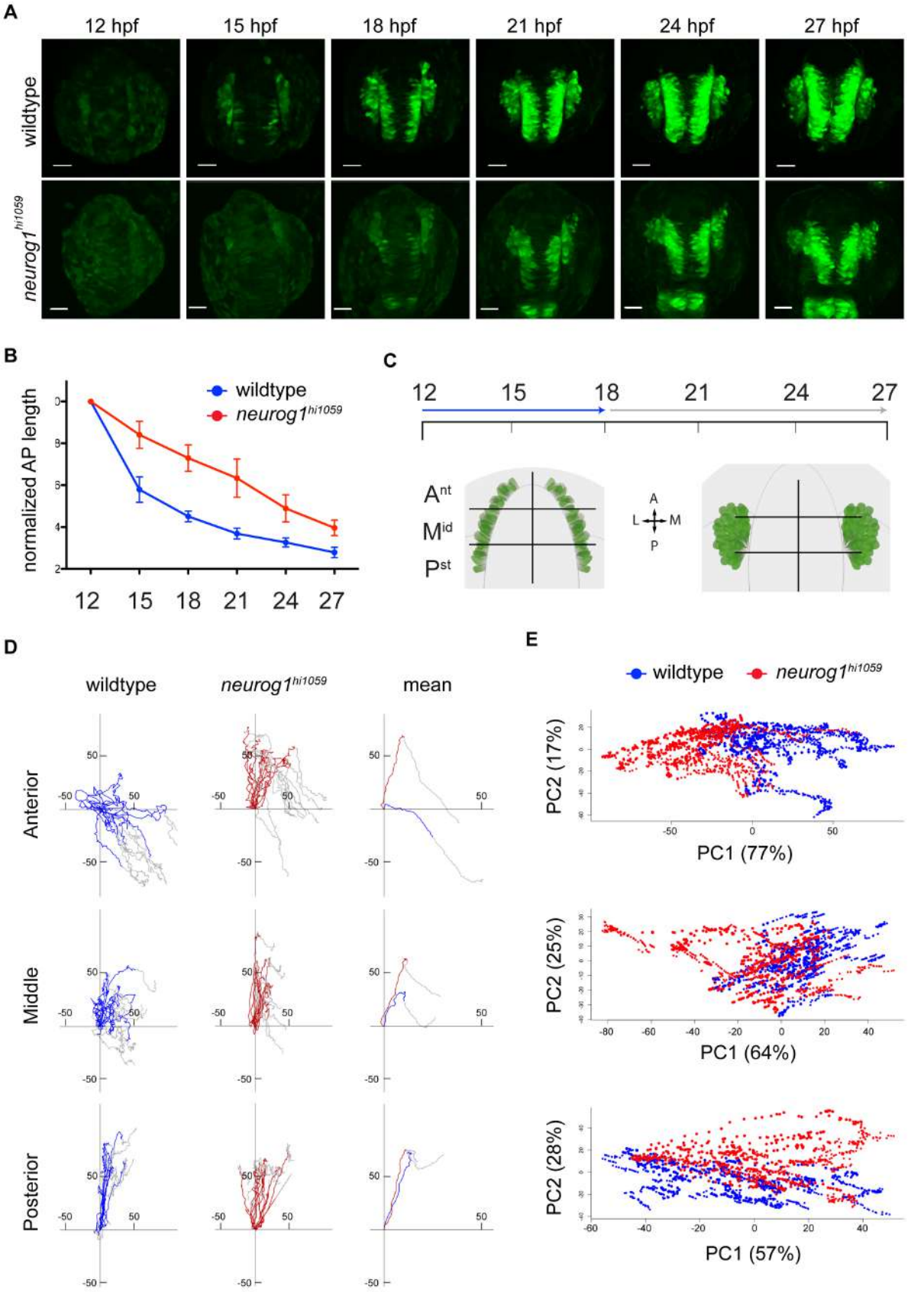

Aguillon et al, Figure 1

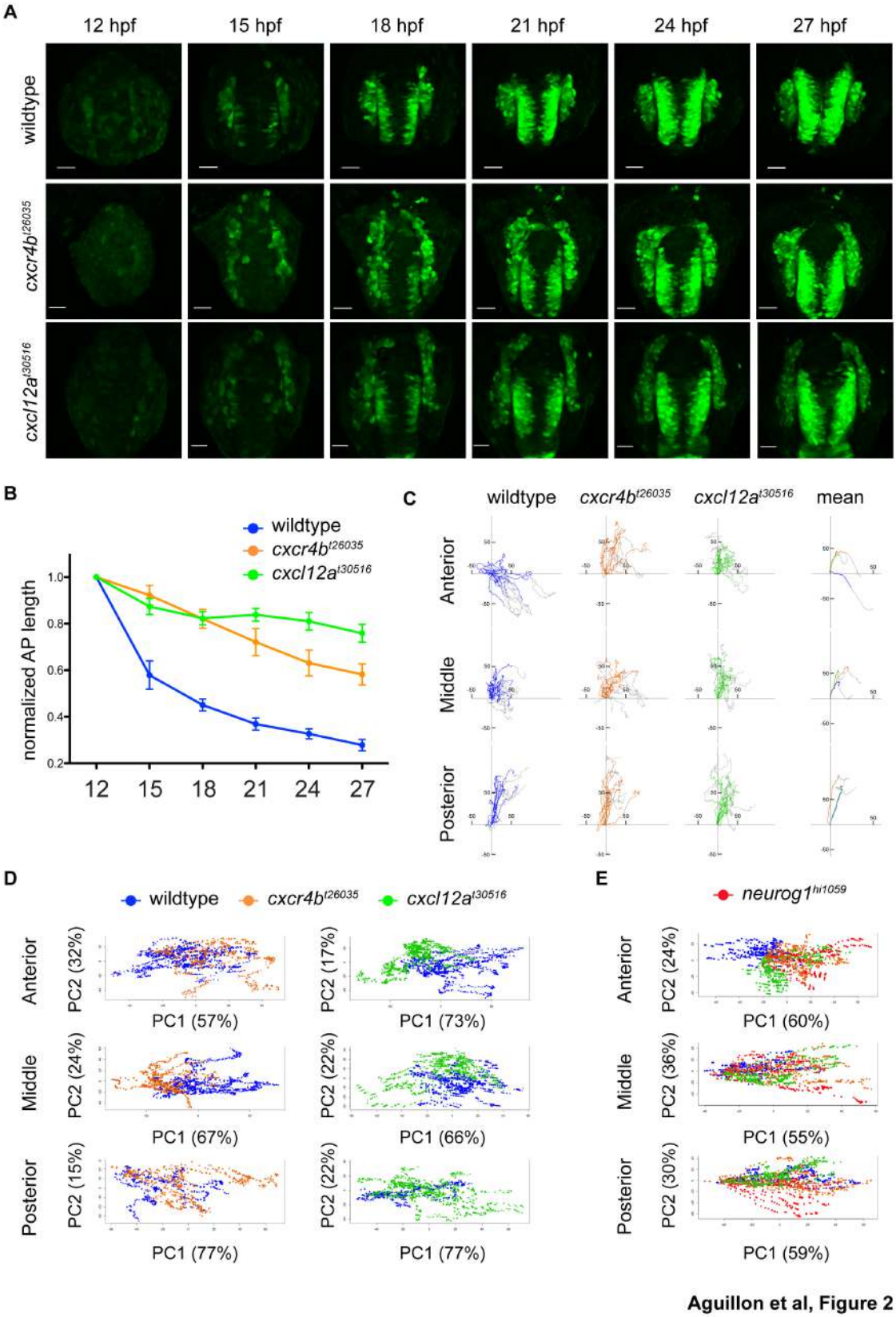

Aguillon et al, Figure 2

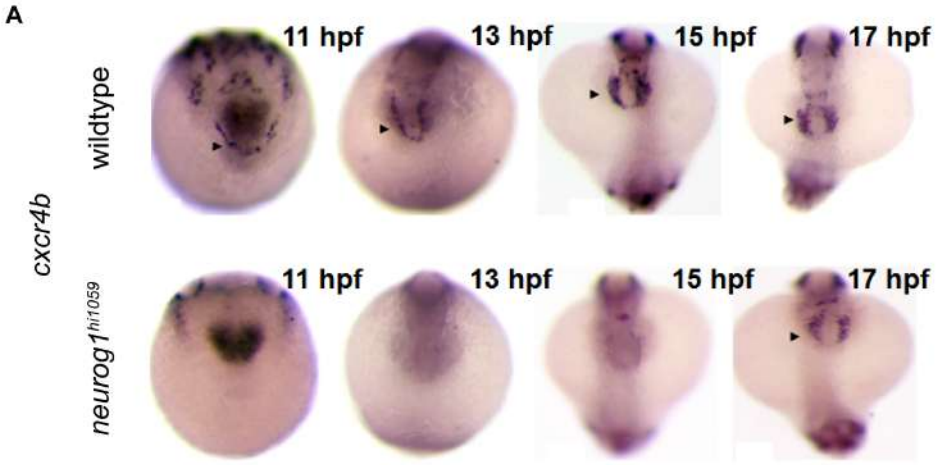

Aguillon et al, Figure 3

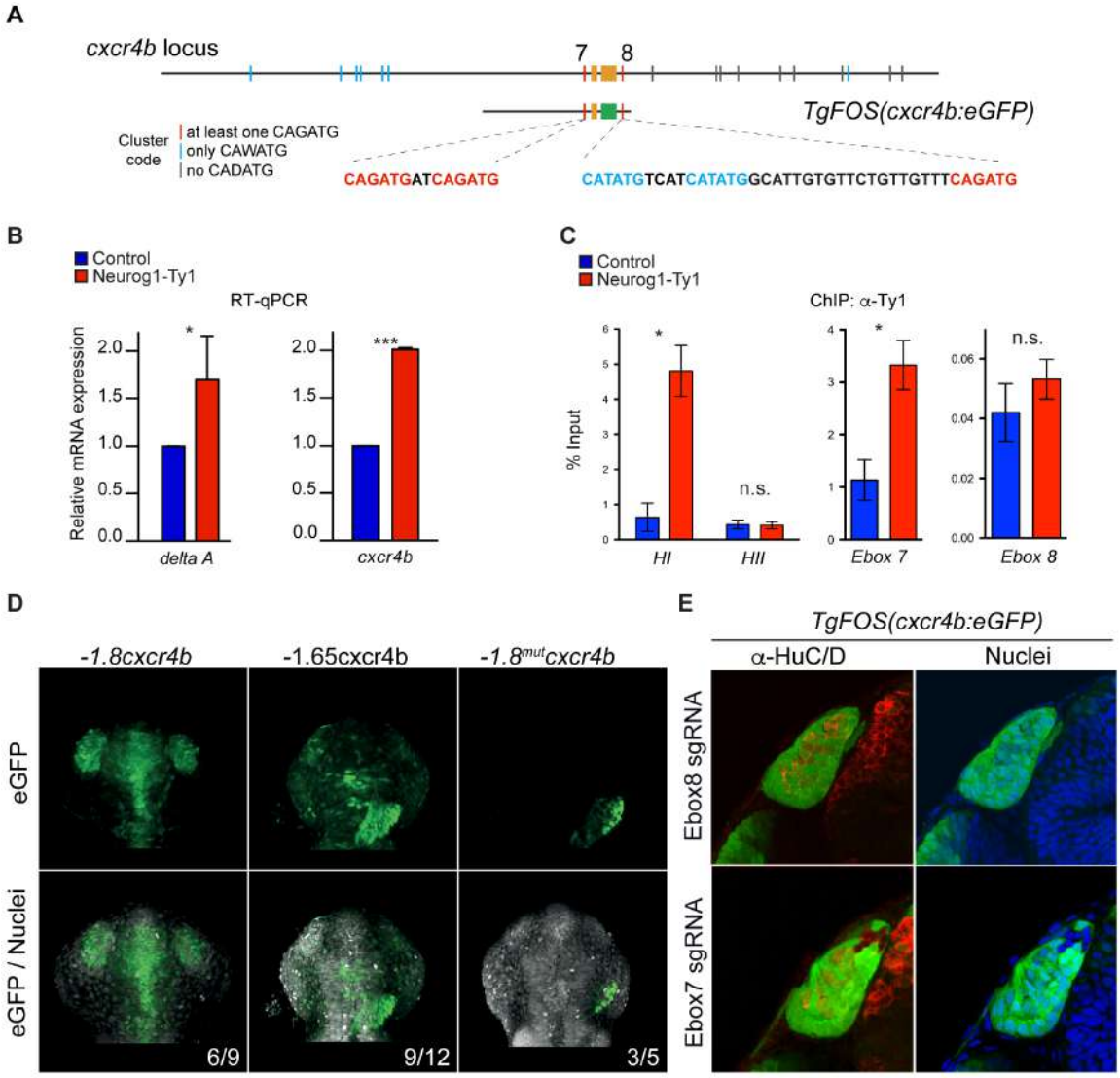

Aguillon et al, Figure 4

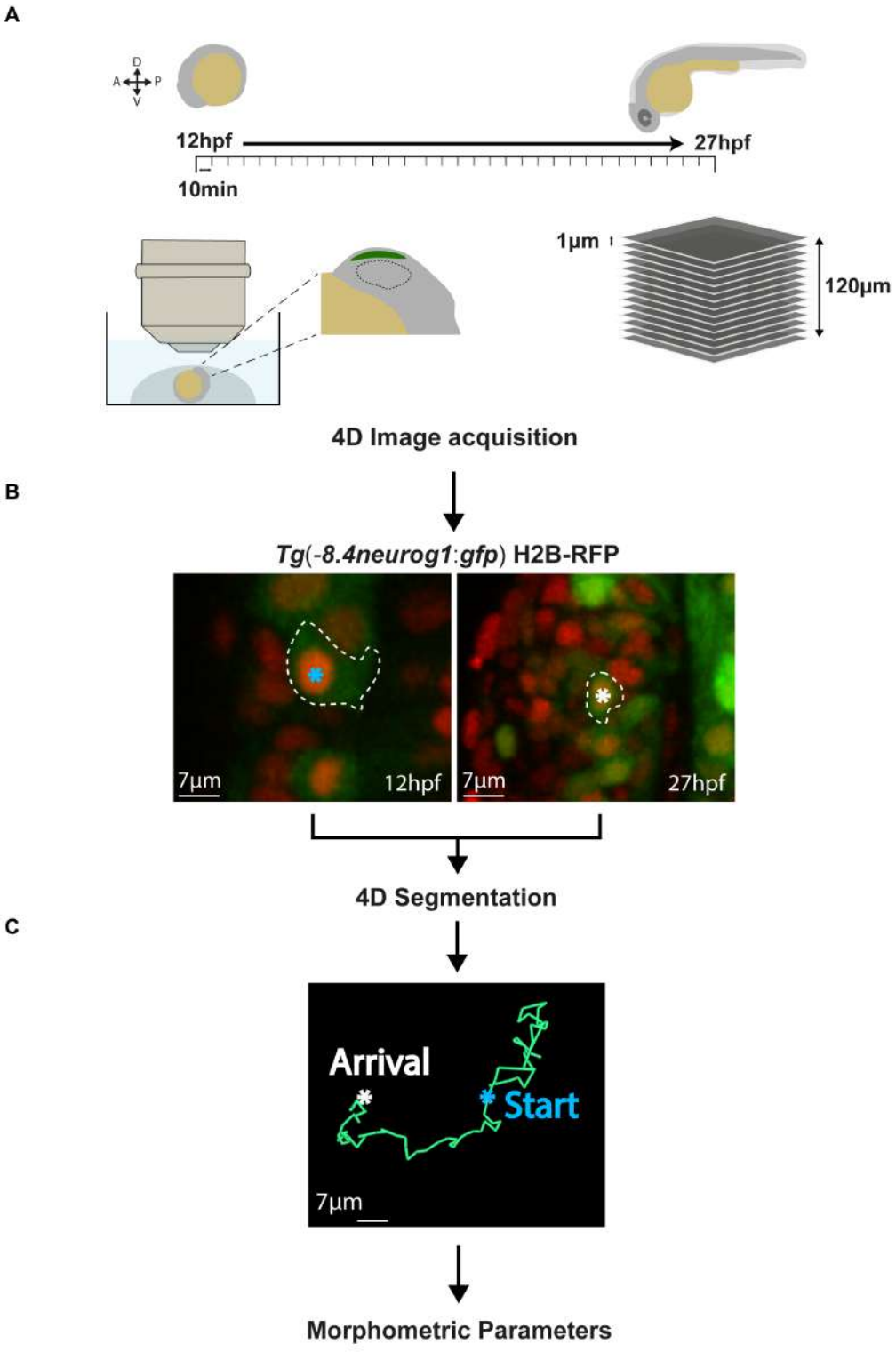

Aguillon et al, Figure S1

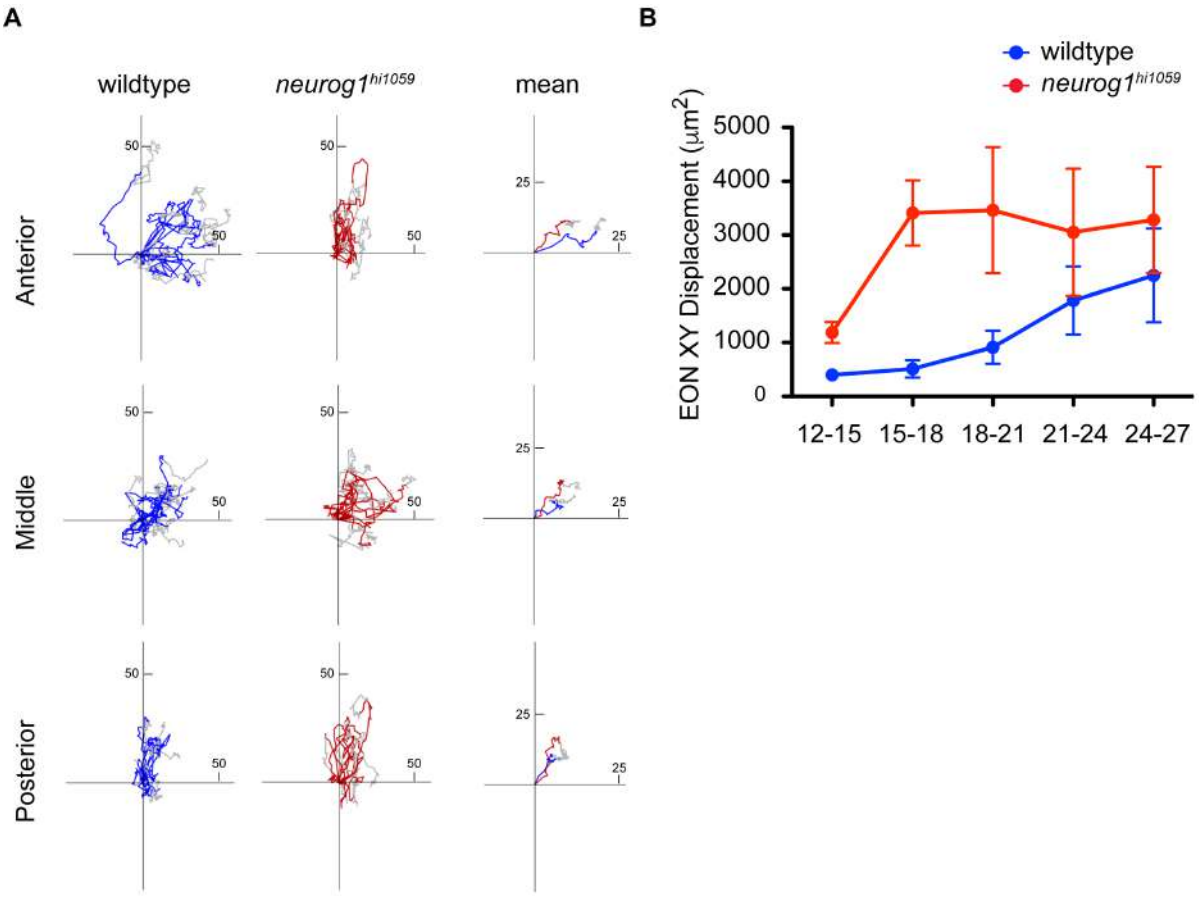

Aguillon et al, Figure S2

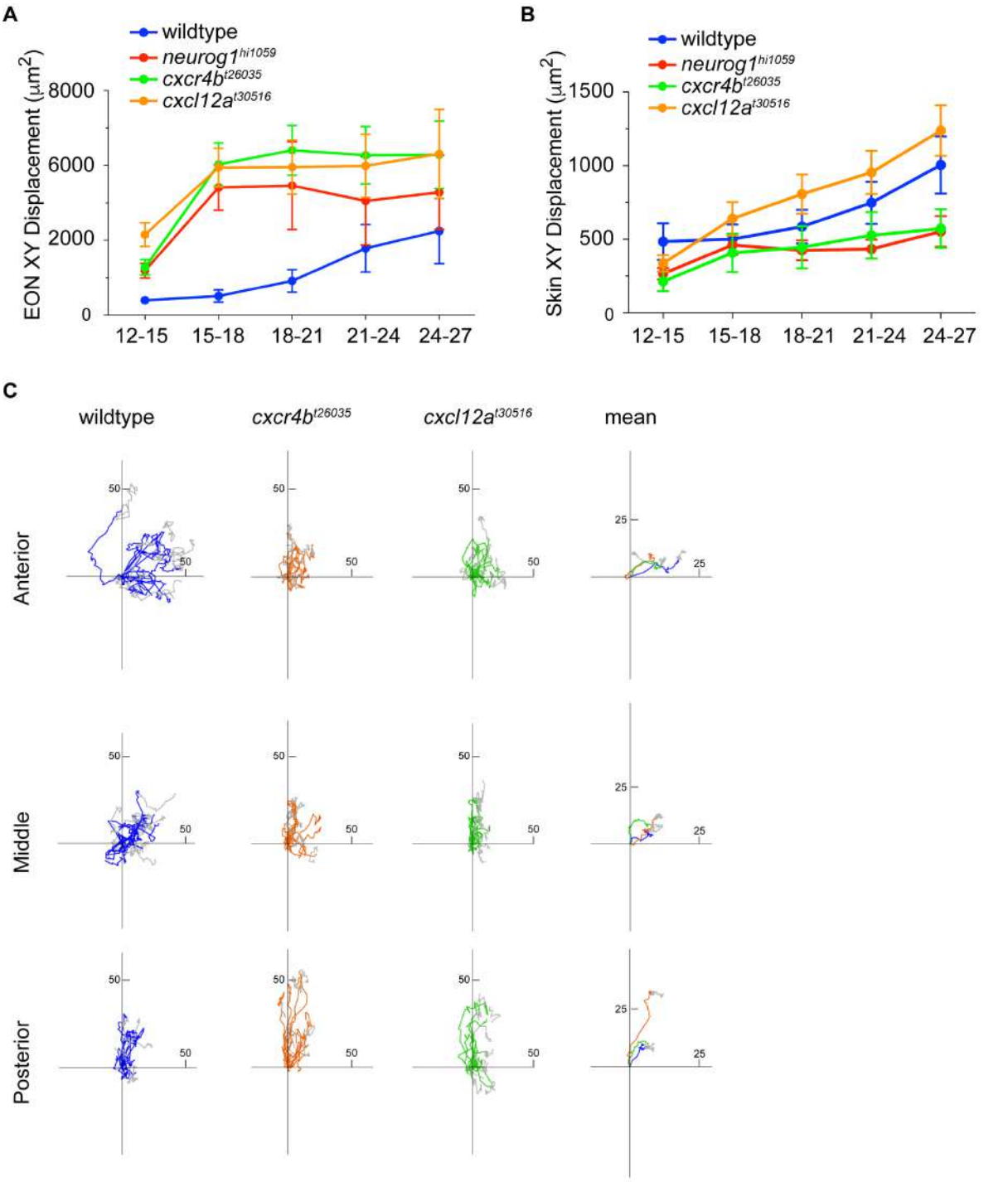

Aguillon et al, Figure S3

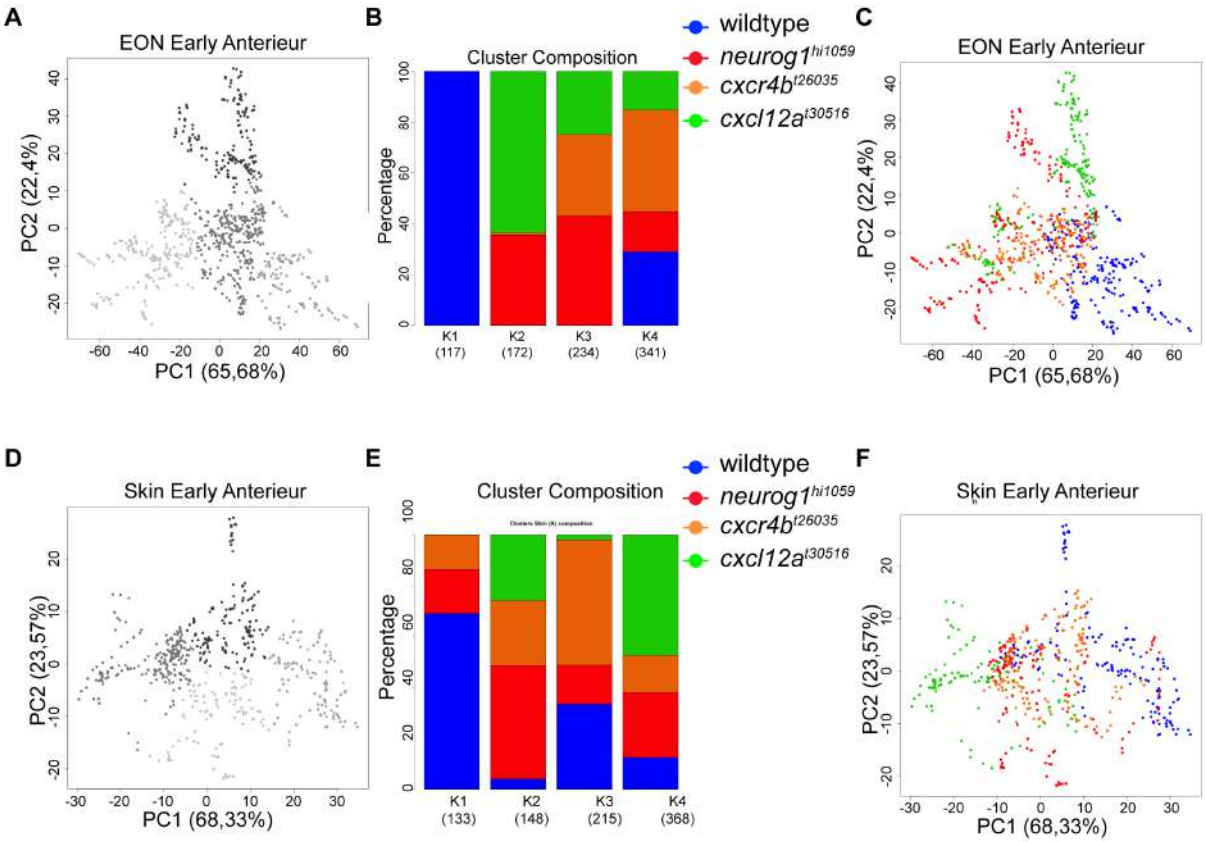

Aguillon et al, Figure S4

III. Discussion

3.1. Cranial neural crest does not contribute significantly to cell-type heterogeneity in the zebrafish olfactory placode

3.1.1 Islet1/2 est un nouveau marqueur des neurones à GnRH3

Le point de départ de ces travaux repose sur l'identification des facteurs de transcription Islet1 et Islet2b (l'anticorps utilisé ne permet pas de les discriminer) comme nouveaux marqueurs spécifiques des neurones à GnRH3 au sein de l'épithélium olfactif dans l'embryon. Ces deux gènes semblent effectivement exprimés dans la population (fig.12A), cependant l'analyse avec une résolution cellulaire de l'expression de cet anticorps dans la lignée *Tg(-17.6islet2b :eGFP)*^{zf7Tg} suggère qu'ils ne sont pas co-exprimés dans tous les neurones à GnRH3 (fig.12B). Hormis l'intérêt de disposer d'un nouveau marqueur pour ces neurones, la découverte de l'expression de ces facteurs soulèvent de nombreuses questions quant à leurs fonctions.

La fonction des neurones à GnRH ainsi que leur projectome diffèrent complétement des ORN (Abraham *et al,* 2008; Abraham *et al,* 2009; Abraham *et al*, 2010) (fig.12C). Chez la souris la combinatoire des facteurs Islet associée à des facteurs de transcription de type bHLH comme Neurod4 assurent la spécification et l'axogenèse de sous-types neuronaux dans la moelle épinière (Thaler *et al,* 2002; Kim *et al,* 2016; Soo-Kyung & Pfaff, 2003). Il est donc probable qu'une telle combinaison opère de façon similaire pour le développement des neurones à GnRH. En effet, les facteurs Islet sont essentiels au développement d'organes endocriniens comme le pancréas chez les vertébrés (Bramswig & Kaestner, 2011). De plus, ils sont exprimés par les cellules gonadotropes (LH et FSH) chez le poulet et le mouton et sont requis pour l'expression du récepteur au GnRH chez le rat par ces mêmes cellules (Liu *et al*, 2005; Liu *et al*, 2005 ; Granger *et al,* 2006).

Finalement, ces facteurs pourraient être un module de spécification neuroendocrinien assurant le développement du réseau GnRH-LH/FSH élément

A

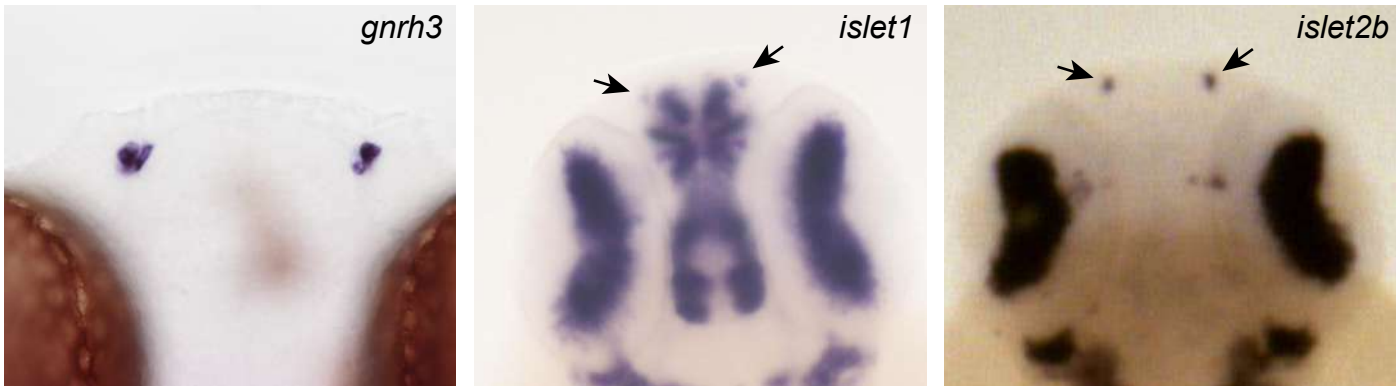

(RA,JB,PB, non publié) (Thisse et al, 2005) (Thisse et al, 2005)

B

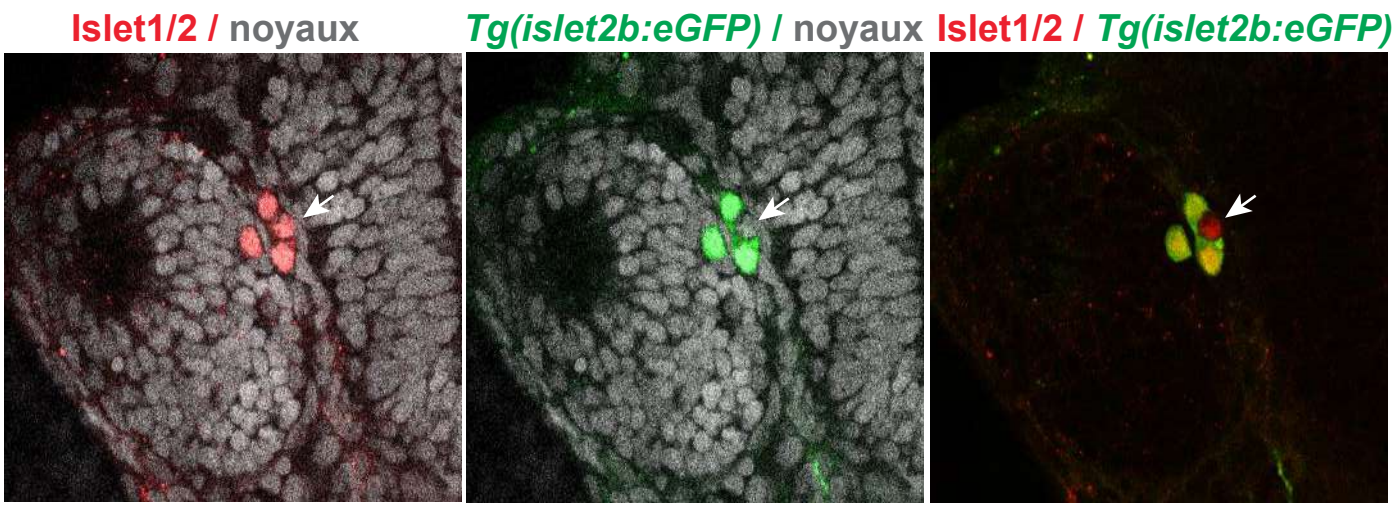

(RA,JB,PB, non publié)

C

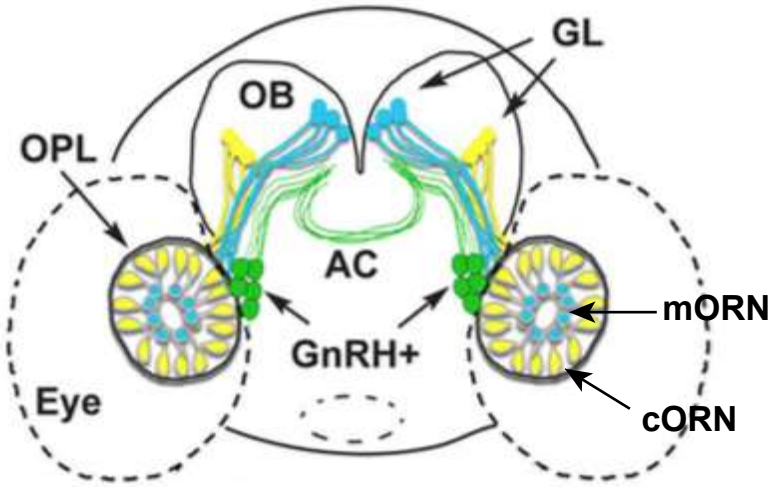

(Garaffo et al, 2013)

D

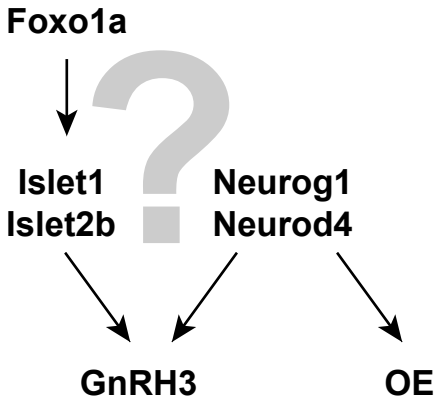

Figure 12: Islet1/2 est un nouveau marqueur des neurones à GnRH3.
En **A**, les gènes *islet1* et *islet2b* sont exprimés dans un territoire similaire à celui des neurones à GnRH3. En **B**, l'expression du transgène *Tg(islet2b:eGFP)* suggère que l'expression des facteurs Islet est hétérogène dans les neurones à GnRH3. En **C**, les neurones à GnRH3 ont un patron de projection axonal différents des ORN. En **D**, le développement des neurones à GnRH3 serait sous le contrôle des facteurs Islets.
OP: Placode olfactif, **OB**: Bulbe olfactif, **AC**: Commissure antérieure, **GL**: couche glomérulaire, **mORN**: neurones olfactifs à microvillosités, **cORN**: neurones olfactifs ciliés.

essentiel de l'axe hypothalamus-hypophyse-gonade gouvernant la reproduction des vertébrés.

- L'expression des facteurs Islet1 et Islet2b est-elle conservée dans les cellules gonadotropes à LH et FSH chez le poisson zèbre ?

- Quelle serait la fonction de ces deux gènes pour le développement du réseau GnRH & LH/FSH ?

Chez la souris, l'expression d'Islet1 dans l'OE de l'embryon est sous contrôle d'élément de régulation lié notamment par le facteur Foxo1 (Kappen *et al*, 2009). L'orthologue *foxo1a* chez le poisson zèbre est exprimé dans l'OE à 48 hpf suggérant une conservation de la régulation. Cependant le patron d'expression de *foxo1a* est plus large que l'anticorps et ne peut expliquer à lui seul cette régulation si spécifique (Berry *et al*, 2008).

- Le facteur de transcription Foxo1a régule-t-il l'expression des gènes *islet1* et *islet2b* ? Si oui, comment réconcilier le patron d'expression très restreint d'*islet1* / *islet2b* avec celui de *foxo1a*, exprimé dans toute la placode (fig.12D) ?

3.1.2 Les neurones à GnRH3 et mORN ne dérivent pas des crêtes neurales céphaliques.

La découverte de ce nouveau marqueur des neurones à GnRH3 nous a conduit à revisiter la contribution des crêtes neurales à la diversité des populations olfactives. Mes travaux révèlent que les neurones à GnRH3 mais aussi les mORN sont issus de la région antérieure de la PPR. Si contribution des CNC il y a, elle n'est pas significative. Les raisons principales ayant conduit à cette confusion sur la contribution des CNC sont :

Proximité physique : Des étapes précoces aux plus tardives, les CNC et progéniteurs olfactifs sont physiquement intimement associées (fig.13Aa) (Torres-Paz & Whitlock, 2014). Il est donc indispensable d'étudier cette interaction avec une résolution cellulaire suffisante pour éviter toute confusion (fig.13Ab).

- **Proximité génétique** : Chez la souris et le poisson zèbre, l'étude de la contribution des CNC aux populations cellulaires olfactives repose notamment sur l'utilisation de lignées transgéniques. Ces lignées permettent de diriger l'expression de rapporteurs sous contrôle d'éléments de régulation sélectionnés. Chez le poisson zèbre, les lignées transgéniques marqueurs des CNC : *Tg(-4.9sox10 :GFP)*^{ba2Tg} et *Tg(-7.2sox10 :mRFP)*^{vu234Tg} sont exprimés dans l'OE pouvant suggérer une origine CNC. Cependant ces deux lignées ne s'expriment pas dans les mêmes cellules de l'OE. Il s'agit très certainement d'une expression ectopique non représentative d'une origine CNC. Les variations constatées sont probablement dues à la différence de taille du promoteur ainsi que du site d'intégration du transgène.

  Chez la souris, l'un des outils phare du lignage NC est la lignée *Tg(Wnt1:CRE)* qui suggère que les CNC contribuent partiellement à presque tous les types cellulaires olfactifs, notamment les neurones à GnRH à hauteur de 30% (Forni *et al,* 2011). Il est alors étonnant que dans le mutant pour *sox10*, contexte où les CNC ne se différencient pas, les neurones à GnRH ne semblent pas être affectés (Barraud et al, 2013). Ici encore, ces résultats contradictoires remettent en cause l'origine CNC mais surtout l'utilisation de cet outil pour étudier la contribution des crêtes au développement.

  Finalement, les CNC et les progéniteurs olfactifs proviennent du même territoire : la bordure neurale (fig.13Ba). On peut supposer que cette parenté soit à l'origine d'un biais pouvant générer des signaux ectopiques dans les contextes transgéniques où les éléments de régulation sont insuffisants pour restreindre l'expression au patron endogène (fig.13Bb).

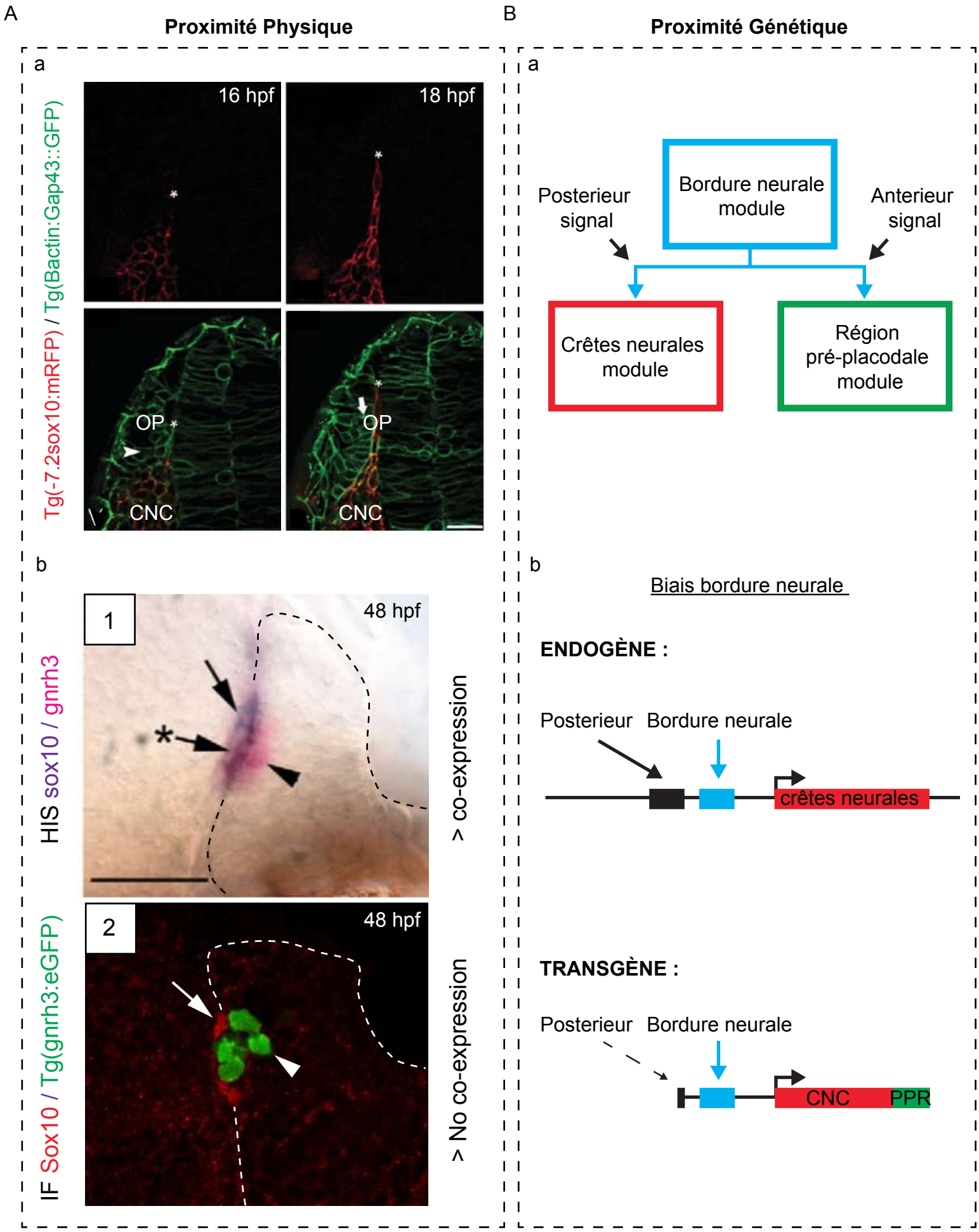

Figure 13: **Proximité physique et génétique des crêtes neurales et des placodes.**
En **A**, les cellules des crêtes neurales céphaliques (CNC) sont physiquement associées aux cellules de l'OE précocement (**a**, Torres-paz & Whitlock, 2014) au plus tardif (**b1**, Whitlock *et al*, 2003 et **b2**, RA, JB, PB non publié). En **B**, Les cellules des placodes et des crêtes neurales sont issus de la bordure neurale (**a**). Cette parenté pourrait être à l'origine d'un biais sur l'expression de transgènes sensés être spécifiques des crêtes neurales (**b**).

Les neurones à GnRH3 proviennent donc de progéniteurs de la région pré-placodale chez le poisson zèbre, comme chez le poulet ou le xénope. L'origine crêtes de ces neurones chez la souris semble d'autant plus étrange considérant ces nouveaux résultats. Bien qu'il existe d'autres lignées transgéniques chez la souris pour l'étude du lignage des CNC (Trainor, 2013), les résultats seront aussi discutables que ceux obtenus avec la lignée *Tg(Wnt1 :CRE)*. Il faut donc que les rapporteurs soient dirigés par des éléments de régulation endogènes via des approches de knock-in (Ackermann *et al*, 2017).

3.1.3 Les neurones à GnRH3 et les mORN sont produits par la région préplacodale.

Mes travaux sur le lignage des neurones à GnRH3 démontrent qu'ils sont issus de la PPR antérieure où se trouve les territoires olfactif et adenohypophysaire (ADH) (Toro & Varga, 2007) (fig.15A). Ce dernier est à l'origine des cellules endocrines de l'ADH mais aussi des neurones à GnRH2 chez le poisson zèbre (Whitlock *et al*, 2003). Les neurones à GnRH2 sont situés dans le mésencéphale et seraient impliqués dans la locomotion et la prise alimentaire (Xia *et al,* 2014). Cependant chez la souris, l'ablation génétique de l'ADH n'affecte pas la production des neurones à GnRH (Metz & Wray, 2010). Lors du développement embryonnaire de l'ascidie, les neurones à GnRH présentent les caractéristiques des neurones olfactifs et sont issus d'un territoire exprimant les marqueurs de la PPR (Abitua *et al*, 2015). Ces études suggèrent que les neurones à GnRH3 seraient bien issus des progéniteurs olfactifs chez les vertébrés.

Les résultats que j'ai obtenus sur l'origine des neurones à GnRH3 nous ont amené à reconsidérer également l'origine CNC des mORN (Saxena *et al,* 2013). C'est par une méthodologie identique que j'ai ainsi pu démontrer que cette population est également issue de la PPR. Chez la souris les cORN et mORN sont majoritairement issus de la placode olfactive, cependant environ 10% des mORN proviendrait des CNC (Suarez *et al,* 2012; Forni *et al,* 2011). Je n'ai pourtant observé aucun mORN provenant du territoire des CNC au cours de mes analyses.

La principale limitation pour étudier l'origine de l'hétérogénéité des cellules olfactives est le manque de marqueurs spécifiques et précoces du territoire olfactif, mais également des territoires adjacents ADH et CNC.

1) L'une des approches possibles est de réaliser un crible type « *enhancer-trap* » (Trinh & fraser, 2013). Le principe est d'intégrer de façon aléatoire dans le génome un rapporteur sous contrôle d'un promoteur minimal. En fonction du site d'intégration, l'expression de cette construction sera influencée par l'environnement génomique. Parmi les intégrations générées, il suffit de sélectionner les patrons d'expressions d'intérêt, de déterminer le site d'intégration et d'identifier les gènes candidats à proximité.

2) Une autre façon d'étudier le lignage de façon non biaisée est d'utiliser la technique GESTALT (genome editing of synthetic target arrays for lineage tracing) (McKenna et al, 2016). Cette technique repose sur la réparation imparfaite d'une séquence ADN suite à l'activité du système CrispR-Cas9. Cette activité étant continue au cours du développement cela génère des modifications successives. On obtient donc au stade d'intérêt un embryon dont les cellules contiennent des modifications propres à leur lignage. On peut ainsi établir théoriquement la généalogie de n'importe quelle cellule. En utilisant une lignée transgénique marquant spécifiquement l'OE il est alors possible d'extraire les cellules olfactives et d'identifier leur parenté.

La combinaison de l'enhancer-trap pour identifier de nouveaux facteurs précoces associés au GESTALT pour l'étude extensive du lignage olfactif permettra de fournir une connaissance sans précédent sur l'origine de cette hétérogénéité.

3.1.4 A l'origine de l'hétérogénéité olfactive : code bHLH

Mes travaux révèlent que le territoire olfactif est à l'origine des mORN et des neurones à GnRH3 dont sont également issus les cORN et les EONs (Madelaine *et al*, 2011). Je ne prends pas en compte les autres types cellulaires olfactifs dont l'origine placodale reste à démontrer. Nous avons précédemment vu comment

déterminer quelle est l'origine anatomique de cette hétérogénéité. Maintenant il nous faudrait déterminer **les bases génétiques** de cette hétérogénéité.
La neurogenèse olfactive est gouvernée par le couple de bHLH Neurog1-Neurod4 (Madelaine *et al*, 2011). Les bHLH forment des dimères avec les protéines HLH pour lier l'ADN et réguler l'activité transcriptionnelle (Huand *et al*, 2014). Dans le territoire olfactif le facteur HLH *Coe2* (Collier/Olf1/EBF) est également exprimé (Bally-Cuif *et al*, 1998). Chez le nématode, le dimorphisme sexuel des gonades est sous contrôle d'un trio composé d'un bHLH et de deux HLH. Selon l'association du bHLH avec un des deux HLH, l'identité de la gonade sera mâle ou femelle (Sallee *et al*, 2017).

L'identité peut donc être codée par l'association de ces facteurs bHLH/HLH et pourrait être l'un des mécanismes à l'origine de l'hétérogénéité cellulaire olfactive.

- Analyser les patrons d'expression de *neurog1*, *neurod4* et *coe2* avec une résolution cellulaire au cours de la formation de la placode. Ceci permettra de savoir s'il y a des associations particulières entre ces facteurs dans les progéniteurs.

- La perte de fonction de ces facteurs entraine-t-elle des variations dans cette hétérogénéité?

- Peut-on prédire la descendance d'un progéniteur en fonction du couple de bHLH/HLH exprimé ?

  Il faudrait identifier le lignage issu de l'association de ces facteurs. L'approche par lignage génétique intersectionnel permet de répondre à cette question (Seidi *et al,* 2007). Cela repose sur la reconstitution d'une protéine rapportrice divisée en deux fragments dont chacun est exprimé sous le contrôle d'éléments de régulation d'un des deux facteurs d'intérêt. Le rapporteur ne sera actif que dans les cellules co-exprimant les gènes d'intérêt.

- Peut-on faire varier l'hétérogénéité olfactive en remplaçant un facteur bHLH/HLH par un autre ?

3.2 Neurog1 couples neurogenesis with morphogenetic movements during olfactory placode development

3.2.1 Neurog1, l'architecte de la placode olfactive

Au cours de la formation de la placode olfactive, la neurogenèse et la convergence se déroulent en même temps. La neurogenèse olfactive embryonnaire est dépendante des proneuraux Neurog1 et Neurod4 (Madelaine *et al*, 2011). J'ai extrait et quantifié le déplacement des progéniteurs olfactifs lors de la convergence dans un contexte de perte-de-fonction de *neurog1*. Le déplacement et l'orientation des cellules antérieures sont initialement affectés. Les seuls facteurs connus pour être impliqué dans le processus de convergence sont le récepteur aux chimiokines Cxcr4b et son ligand Cxcl12a (Miyasaka *et al,* 2007). En appliquant la même méthodologie d'analyse j'ai pu montrer que le mouvement des cellules est affecté de façon similaire dans les mutants pour *neurog1*, *cxcr4b* et *cxcl12a*, suggérant une interaction entre ces facteurs. En effet, l'expression précoce du récepteur *cxcr4b* par les progéniteurs olfactifs est dépendante de Neurog1. J'ai démontré que cette régulation transcriptionnelle est dépendante de la liaison de Neurog1 au promoteur de *cxcr4b*. Ainsi le proneural Neurog1 dirige à la fois la neurogenèse et la convergence des progéniteurs olfactifs au cours de la formation de la placode (fig.14).

3.2.1.1 Neurog1, via Cxcr4b, permet aux progéniteurs d'orienter leur migration et d'être positionnés au bon endroit à la fin de la convergence.

- **Comment ces cellules s'orientent au cours de la convergence ?**

- Cxcr4b est requis pour l'orientation des cellules germinales (PGC) lors du développement précoce chez le poisson zèbre (Knaut *et al*, 2003). Au cours de leur migration les PGC déploient des protrusions membranaires

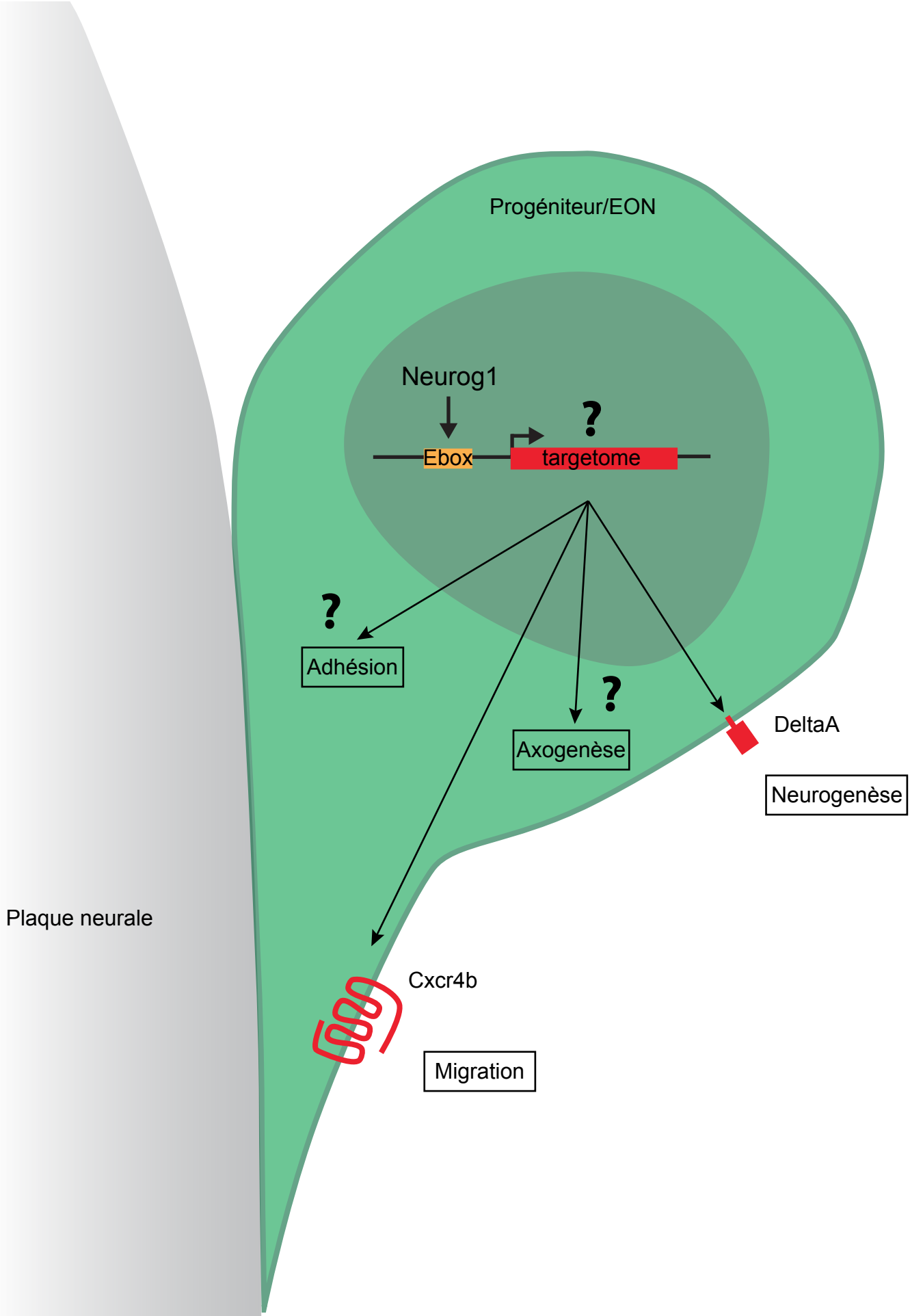

Figure 14: Neurog1 controle le développement de l'OE via ses cibles transcriptionnelles.
Neurog controle la morphogenèse et la neurogenèse de l'épithélium olfactif via des cibles transcriptionnelles différentes.

- qui contiennent le récepteur en direction de la plus forte concentration de ligand Cxcl12a et migrent dans cette direction (Meyen *et al*, 2015). Le déplacement des progéniteurs olfactifs repose sur les mêmes acteurs (Miyasaka *et al*, 2007 ; Bréau *et al*, 2017). Cependant dans ce contexte, le ligand *cxcl12a* est exprimé par le télencéphale selon un patron bien plus large que la placode suggérant une régulation de la localisation de la protéine. Le transgène *TgBAC(cxcl12a:cxcl12a-EGFP)*^{sk82Tg} a été développé pour pouvoir visualiser Cxcl12a en contexte *in vivo* (Venkiteswaran *et al*, 2013). Cet outil permettrait de visualiser la répartition du ligand dans l'environnement au cours de la convergence.

➢ **Comment est définie la position finale des cellules ?**

- Lorsqu'un navire arrive à quai, celui-ci doit couper les moteurs et s'amarrer au pont pour se maintenir sur place. Il en est de même pour les progéniteurs olfactifs. Dans leur environnement, les cellules se déplacent grâce à leur interaction avec les composants de la matrice extra-cellulaire (ECM). La composition de l'ECM sur le trajet des progéniteurs n'est pas encore explorée. Chez la souris, la composition en laminine de la matrice sur laquelle reposent les entérocytes change entre la base et l'apex de la villosité intestinale. Il est intéressant de constater que les fibroblastes naviguant dans l'ECM au niveau de l'apex présentent un comportement migratoire plus intense (Glensis *et al*, 2014). Outre le type de laminine, la quantité de laminine peut également influencer la vitesse de migration des cellules folliculaires lors de l'ovogenèse chez la drosophile (Diaz de la loza *et al*, 2017).
-
    - Quelle est la composition de l'ECM sur laquelle évoluent les progéniteurs olfactifs ? Varie-t-elle au cours du temps ?

Neurog1 coordonne la neurogenèse et la morphogenèse de la placode olfactive via ses cibles transcriptionnelles.

J'ai démontré que Neurog1 contrôle le positionnement des progéniteurs olfactifs par l'une de ses cibles transcriptionnelles. Chez différents organismes modèles, il a été montré que les facteurs proneuraux régulent l'expression de facteurs dans des neurones post-mitotiques requis pour la migration ou l'axogenèse (Heng *et al*, 2008 ; Madelaine *et al,* 2011 ; Yuan *et al,* 2016 ; Klish *et al,* 2011). Chez la souris, le développement du cervelet dépend du proneural Atoh1 (Atonal homologue 1). La réalisation du « targetome » (RNA-seq/ChIP-seq/Histone-seq) d'Atoh1 révèle que les gènes régulés sont impliqués dans de nombreux processus comme la neurogenèse, la différenciation, le métabolisme, l'adhésion ou encore la migration (CXCR4, par exemple). Bien loin donc de la seule fonction neurogénique proposée initialement (Gysen & Dambly-Chaudière, 1988 ; Jarman *et al*, 1993), les facteurs proneuraux semblent être des coordinateurs de processus développementaux des structures neurales sensorielles. Les approches par gènes candidats (patron d'expression, dépendance de l'activité à Neurog1, éléments de régulation identifiés dans le locus) peuvent s'avérer fructueuse comme cela a été le cas avec son gène cible *cxcr4b* (Aguillon *et al.,* en préparation). Cependant les approches génomiques offrent un angle de vue incomparable et la réalisation du « targetome » de Neurog1 dans la placode olfactive fournirait une vue d'ensemble de tous les processus gouvernés par ce proneural via l'identification pan-génomique de ses gènes cibles (fig.14).

-

3.2.2 Neurog1-Cxcr4b : un module pan-placodale.

Au cours du développement embryonnaire du poisson zèbre, le proneural Neurog1 est exprimé par la placode olfactive mais aussi par les placodes à l'origine du ganglion trijumeau (Tg), du ganglion stato-accoustique (SAg), du ganglion postérieur de la ligne latérale (Pllg) et enfin des ganglions épibranchiaux (EBg)

(fig.15A). Ces structures neurales périphériques sont toutes générées à partir de la PPR et sont liées à des modalités sensorielles (odorat, ouïe et toucher) ou viscerosensorielles (Andermann et al, 2002 *; Schlosser, 2014*). La perte de fonction de *neurog1* entraine une perte des marqueurs de différenciation neuronale dans toutes ces structures à 24 hpf *(*Andermann et al, 2002 *; Madelaine* et al*, 2011).* L'expression et la fonction des orthologues (Neurog1 et Neurog2) chez la souris sont conservées dans ces structures (*Cau et al, 2002 ; Takano-Maruyama et al, 2012 ;* Ma *et al*, 2014) Chez les vertébrés, Neurog1 est donc essentiel au développement des structures nerveuses périphériques qui font le lien entre l'environnement (externe : OP, Tg, SAg, Pllg et aussi interne : EBg) et le système nerveux central.

Mes travaux révèlent que Neurog1, via *cxcr4b* contribue à la fois à la formation de la placode olfactive via le positionnement de ces progéniteurs et leur axogenèse (fig.15B). Chez le poisson zèbre, la convergence de l'OE mais aussi du Tg est dépendante de Cxcr4b (Miyasaka et al, 2007 ; Knaut et al, 2007).

- La fonction du couple Neurog1-Cxcr4b est-elle conservée entre la placode olfactive et la placode trigéminale? Dans toutes les structures neurales sensorielles issues de la PPR?

3.3 Le syndrome de Kallmann : une pathologie de la bordure neurale ?

Les pathologies du développement sont par nature complexes. Contrairement à d'autres pathologies congénitales comme la mucoviscidose (mutation affectant la fonction du canal ionique CFTR), ici ce n'est pas tant la fonction du gène mais plutôt le processus dans lequel il agit qui compte.

Le système olfactif et le système reproducteur interagissent précocement au cours du développement et c'est l'altération de cette interaction qui est à l'origine du syndrome de Kallmann.

Les patients KS, en plus des troubles olfactifs et de l'HH, peuvent présenter des signes cliniques très variés. Il peut arriver même dans certains cas que le KS soit associé à d'autres pathologies du développement comme le syndrome de CHARGE

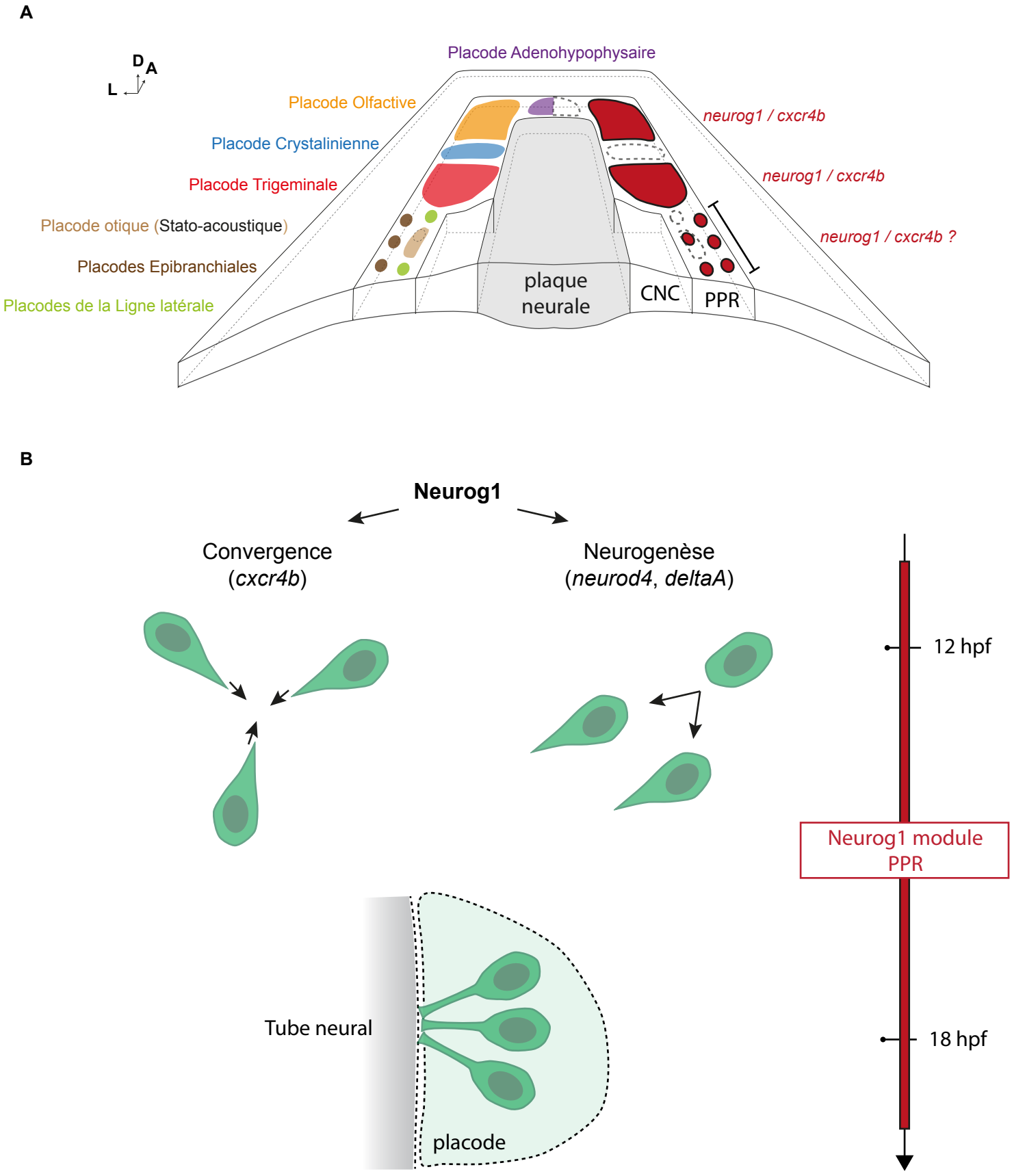

Figure 15: Neurog1 dirige la formation des placodes neurales sensorielles.
En **A**, localisation des territoires des placodes dans la région pré-placodale à la fin de la gastrulation. Les placodes dans lesquelles sont exprimés *neurog1* et *cxcr4b* sont colorées en rouge sur le côté droit du schéma. (adapté de Aguillon *et al*, 2016). En **B**, Neurog1 et ses cibles seraient un module d'assemblage des structures neurales sensorielles issus de la PPR.

ou de Diegorges. Cette complexité apparente trouve son origine dans les nombreux facteurs impliqués dans le développement du système olfactif et reproducteur. A travers cette thèse, je vous ai donné une vision globale des phases préalables et nécessaires à ce processus ainsi que des acteurs actuellement connus. Il devient alors plus simple d'appréhender la complexité des bases génétiques du KS qui ne sont finalement que le reflet de cette interaction. Ce processus développemental repose donc sur la formation correcte de la placode olfactive ou des crêtes neurales qui sont issues de la bordure neurale. A l'image des neurocristopathies qui sont des pathologies dues au défaut de développement des crêtes neurales, le syndrome de Kallmann pourrait donc être qualifié de pathologie de la bordure neurale ectodermique ou ectopathie de la bordure neurale.

Références bibliographiques

Abraham, E., Palevitch, O., Ijiri, S., Du, S.J., Gothilf, Y., and Zohar, Y. (2008). Early development of forebrain gonadotrophin-releasing hormone (GnRH) neurones and the role of GnRH as an autocrine migration factor. J. Neuroendocrinol. *20*, 394–405.

Abraham, E., Palevitch, O., Gothilf, Y., and Zohar, Y. (2009). The zebrafish as a model system for forebrain GnRH neuronal development. Gen. Comp. Endocrinol. *164*, 151–160.

Abraham, E., Palevitch, O., Gothilf, Y., and Zohar, Y. (2010). Targeted gonadotropin-releasing hormone-3 neuron ablation in zebrafish: effects on neurogenesis, neuronal migration, and reproduction. Endocrinology *151*, 332–340.

Ackermann, A.M., Zhang, J., Heller, A., Briker, A., and Kaestner, K.H. (2017). High-fidelity Glucagon-CreER mouse line generated by CRISPR-Cas9 assisted gene targeting. Mol Metab *6*, 236–244.

Aguillon, R., Blader, P., and Batut, J. (2016). Patterning, morphogenesis, and neurogenesis of zebrafish cranial sensory placodes. Methods in Cell Biology *134*, 33–67.

Ahrens, K., and Schlosser, G. (2005). Tissues and signals involved in the induction of placodal Six1 expression in Xenopus laevis. Dev. Biol. *288*, 40–59.

Ahuja, G., and Korsching, S. (2014). Zebrafish olfactory receptor ORA1 recognizes a putative reproductive pheromone. Commun Integr Biol *7*.

Ahuja, G., Bozorg Nia, S., Zapilko, V., Shiriagin, V., Kowatschew, D., Oka, Y., and Korsching, S.I. (2014). Kappe neurons, a novel population of olfactory sensory neurons. Sci Rep *4*, 4037.

Akimenko, M.A., Ekker, M., Wegner, J., Lin, W., and Westerfield, M. (1994). Combinatorial expression of three zebrafish genes related to distal-less: part of a homeobox gene code for the head. J. Neurosci. *14*, 3475–3486.

Andermann, P., Ungos, J., and Raible, D.W. (2002). Neurogenin1 defines zebrafish cranial sensory ganglia precursors. Dev. Biol. *251*, 45–58.

Ardouin, O., Legouis, R., Fasano, L., David-Watine, B., Korn, H., Hardelin, J., and Petit, C. (2000). Characterization of the two zebrafish orthologues of the KAL-1 gene underlying X chromosome-linked Kallmann syndrome. Mech. Dev. *90*, 89–94.

Azzarelli, R., Guillemot, F., and Pacary, E. (2015). Function and regulation of Rnd proteins in cortical projection neuron migration. Front Neurosci *9*, 19.

Bally-Cuif, L., Dubois, L., and Vincent, A. (1998). Molecular cloning of Zcoe2, the zebrafish homolog of Xenopus Xcoe2 and mouse EBF-2, and its expression during primary neurogenesis. Mech. Dev. *77*, 85–90.

Barrallo-Gimeno, A., Holzschuh, J., Driever, W., and Knapik, E.W. (2004). Neural crest survival and differentiation in zebrafish depends on mont blanc/tfap2a gene function. Development *131*, 1463–1477.

Barraud, P., St John, J.A., Stolt, C.C., Wegner, M., and Baker, C.V.H. (2013). Olfactory ensheathing glia are required for embryonic olfactory axon targeting and the migration of gonadotropin-releasing hormone neurons. Biol Open *2*, 750–759.

Berry, F.B., Skarie, J.M., Mirzayans, F., Fortin, Y., Hudson, T.J., Raymond, V., Link, B.A., and Walter, M.A. (2008). FOXC1 is required for cell viability and resistance to oxidative stress in the eye through the transcriptional regulation of FOXO1A. Hum Mol Genet *17*, 490–505.

Bhat, N., Kwon, H.-J., and Riley, B.B. (2013). A gene network that coordinates preplacodal competence and neural crest specification in zebrafish. Dev. Biol. *373*, 107–117.

Bhatnagar, K.P., and Smith, T.D. (2001). The human vomeronasal organ. III. Postnatal development from infancy to the ninth decade. J. Anat. *199*, 289–302.

Bhattacharyya, S., and Bronner-Fraser, M. (2004). Hierarchy of regulatory events in sensory placode development. Curr. Opin. Genet. Dev. *14*, 520–526.

Bhattacharyya, S., Bailey, A.P., Bronner-Fraser, M., and Streit, A. (2004). Segregation of lens and olfactory precursors from a common territory: cell sorting and reciprocity of Dlx5 and Pax6 expression. Dev. Biol. *271*, 403–414.

Biechl, D., Tietje, K., Gerlach, G., and Wullimann, M.F. (2016). Crypt cells are involved in kin recognition in larval zebrafish. Sci Rep *6*, 24590.

Blader, P., Lam, C.S., Rastegar, S., Scardigli, R., Nicod, J.-C., Simplicio, N., Plessy, C., Fischer, N., Schuurmans, C., Guillemot, F., et al. (2004). Conserved and acquired features of neurogenin1 regulation. Development *131*, 5627–5637.

Boehm, U., Bouloux, P.-M., Dattani, M.T., Roux, N. de, Dodé, C., Dunkel, L., Dwyer, A.A., Giacobini, P., Hardelin, J.-P., Juul, A., et al. (2015). Expert consensus document: European Consensus Statement on congenital hypogonadotropic hypogonadism—pathogenesis, diagnosis and treatment. Nature Reviews Endocrinology *11*, nrendo.2015.112.

Breau, M.A., and Schneider-Maunoury, S. (2015). Cranial placodes: models for exploring the multi-facets of cell adhesion in epithelial rearrangement, collective migration and neuronal movements. Dev. Biol. *401*, 25–36.

Breau, M.A., Bonnet, I., Stoufflet, J., Xie, J., De Castro, S., and Schneider-Maunoury, S. (2017). Extrinsic mechanical forces mediate retrograde axon extension in a developing neuronal circuit. Nat Commun *8*, 282.

Bricaud, O., and Collazo, A. (2006). The transcription factor six1 inhibits neuronal and promotes hair cell fate in the developing zebrafish (Danio rerio) inner ear. J. Neurosci. *26*, 10438–10451.

Brignall, A.C., and Cloutier, J.-F. (2015). Neural map formation and sensory coding in the vomeronasal system. Cell. Mol. Life Sci. *72*, 4697–4709.

Burns, C.J., and Vetter, M.L. (2002). Xath5 regulates neurogenesis in the Xenopus olfactory placode. Dev. Dyn. *225*, 536–543.

Bussmann, J., and Raz, E. (2015). Chemokine-guided cell migration and motility in zebrafish development. EMBO J. *34*, 1309–1318.

Cai, C.-L., Liang, X., Shi, Y., Chu, P.-H., Pfaff, S.L., Chen, J., and Evans, S. (2003). Isl1 identifies a cardiac progenitor population that proliferates prior to differentiation and contributes a majority of cells to the heart. Dev. Cell *5*, 877–889.

Casoni, F., Malone, S.A., Belle, M., Luzzati, F., Collier, F., Allet, C., Hrabovszky, E., Rasika, S., Prevot, V., Chédotal, A., et al. (2016). Development of the neurons controlling fertility in humans: new insights from 3D imaging and transparent fetal brains. Development *143*, 3969–3981.

Castro, D.S., and Guillemot, F. (2011). Old and new functions of proneural factors revealed by the genome-wide characterization of their transcriptional targets. Cell Cycle *10*, 4026–4031.

Cau, E., Gradwohl, G., Fode, C., and Guillemot, F. (1997). Mash1 activates a cascade of bHLH regulators in olfactory neuron progenitors. Development *124*, 1611–1621.

Cau, E., Casarosa, S., and Guillemot, F. (2002). Mash1 and Ngn1 control distinct steps of determination and differentiation in the olfactory sensory neuron lineage. Development *129*, 1871–1880.

Cavodeassi, F. (2014). Integration of anterior neural plate patterning and morphogenesis by the Wnt signaling pathway. Dev Neurobiol *74*, 759–771.

Chen, C.R., Kachramanoglou, C., Li, D., Andrews, P., and Choi, D. (2014). Anatomy and cellular constituents of the human olfactory mucosa: a review. J Neurol Surg B Skull Base *75*, 293–300.

Creppe, C., Malinouskaya, L., Volvert, M.-L., Gillard, M., Close, P., Malaise, O., Laguesse, S., Cornez, I., Rahmouni, S., Ormenese, S., et al. (2009). Elongator controls the migration and differentiation of cortical neurons through acetylation of alpha-tubulin. Cell *136*, 551–564.

Croy, I., Nordin, S., and Hummel, T. (2014). Olfactory Disorders and Quality of Life—An Updated Review. Chem Senses *39*, 185–194.

D'Aniello, B., Semin, G.R., Scandurra, A., and Pinelli, C. (2017). The Vomeronasal Organ: A Neglected Organ. Front Neuroanat *11*, 70.

Devos, N., Deflorian, G., Biemar, F., Bortolussi, M., Martial, J.A., Peers, B., and Argenton, F. (2002). Differential expression of two somatostatin genes during zebrafish embryonic development. Mech. Dev. *115*, 133–137.

Di Schiavi, E., and Andrenacci, D. (2013). Invertebrate models of kallmann syndrome: molecular pathogenesis and new disease genes. Curr. Genomics *14*, 2–10.

Distel, M., Hocking, J.C., Volkmann, K., and Köster, R.W. (2010). The centrosome neither persistently leads migration nor determines the site of axonogenesis in migrating neurons in vivo. The Journal of Cell Biology *191*, 875–890.

Dupin, E., and Le Douarin, N.M. (2014). The neural crest, a multifaceted structure of the vertebrates. Birth Defects Res. C Embryo Today *102*, 187–209.

Dyballa, S., Savy, T., Germann, P., Mikula, K., Remesikova, M., Špir, R., Zecca, A., Peyriéras, N., and Pujades, C. (2017). Distribution of neurosensory progenitor pools during inner ear morphogenesis unveiled by cell lineage reconstruction. Elife *6*.

Dynes, J.L., and Ngai, J. (1998). Pathfinding of olfactory neuron axons to stereotyped glomerular targets revealed by dynamic imaging in living zebrafish embryos. Neuron *20*, 1081–1091.

Echelard, Y., Vassileva, G., and McMahon, A.P. (1994). Cis-acting regulatory sequences governing Wnt-1 expression in the developing mouse CNS. Development *120*, 2213–2224.

Ekberg, J.A.K., Amaya, D., Mackay-Sim, A., and St John, J.A. (2012). The migration of olfactory ensheathing cells during development and regeneration. Neurosignals *20*, 147–158.

Esterberg, R., and Fritz, A. (2009). dlx3b/4b are required for the formation of the preplacodal region and otic placode through local modulation of BMP activity. Dev. Biol. *325*, 189–199.

Forni, P.E., and Wray, S. (2015). GnRH, anosmia and hypogonadotropic hypogonadism--where are we? Front Neuroendocrinol *36*, 165–177.

Forni, P.E., Taylor-Burds, C., Melvin, V.S., Williams, T., Williams, T., and Wray, S. (2011). Neural crest and ectodermal cells intermix in the nasal placode to give rise to GnRH-1 neurons, sensory neurons, and olfactory ensheathing cells. J. Neurosci. *31*, 6915–6927.

Friedrich, R.W., and Korsching, S.I. (1997). Combinatorial and Chemotopic Odorant Coding in the Zebrafish Olfactory Bulb Visualized by Optical Imaging. Neuron *18*, 737–752.

Garnett, A.T., Square, T.A., and Medeiros, D.M. (2012). BMP, Wnt and FGF signals are integrated through evolutionarily conserved enhancers to achieve robust expression of Pax3 and Zic genes at the zebrafish neural plate border. Development *139*, 4220–4231.

Ghysen, A., and Dambly-Chaudière, C. (1988). From DNA to form: the achaete-scute complex. Genes Dev. *2*, 495–501.

Glavic, A., Silva, F., Aybar, M.J., Bastidas, F., and Mayor, R. (2004). Interplay between Notch signaling and the homeoprotein Xiro1 is required for neural crest induction in Xenopus embryos. Development *131*, 347–359.

Glentis, A., Gurchenkov, V., and Matic Vignjevic, D. (2014). Assembly, heterogeneity, and breaching of the basement membranes. Cell Adh Migr *8*, 236–245.

Granger, A., Bleux, C., Kottler, M.-L., Rhodes, S.J., Counis, R., and Laverrière, J.-N. (2006). The LIM-Homeodomain Proteins Isl-1 and Lhx3 Act with Steroidogenic Factor 1 to Enhance Gonadotrope-Specific Activity of the Gonadotropin-Releasing Hormone Receptor Gene Promoter. Mol Endocrinol *20*, 2093–2108.

Grosmaitre, X., Fuss, S.H., Lee, A.C., Adipietro, K.A., Matsunami, H., Mombaerts, P., and Ma, M. (2009). SR1, a Mouse Odorant Receptor with an Unusually Broad Response Profile. J Neurosci *29*, 14545.

Groves, A.K., and LaBonne, C. (2014). Setting appropriate boundaries: Fate, patterning and competence at the neural plate border. Developmental Biology *389*, 2–12.

Grus, W.E., and Zhang, J. (2009). Origin of the Genetic Components of the Vomeronasal System in the Common Ancestor of all Extant Vertebrates. Mol Biol Evol *26*, 407–419.

Gyoja, F. (2017). Basic helix-loop-helix transcription factors in evolution: Roles in development of mesoderm and neural tissues. Genesis *55*.

Haberly, L.B. (2001). Parallel-distributed processing in olfactory cortex: new insights from morphological and physiological analysis of neuronal circuitry. Chem. Senses *26*, 551–576.

Hahn, C.-G., Han, L.-Y., Rawson, N.E., Mirza, N., Borgmann-Winter, K., Lenox, R.H., and Arnold, S.E. (2005). In vivo and in vitro neurogenesis in human olfactory epithelium. J. Comp. Neurol. *483*, 154–163.

Hansen, A., and Zeiske, E. (1993). Development of the olfactory organ in the zebrafish, Brachydanio rerio. J. Comp. Neurol. *333*, 289–300.

Hardelin, J.P., Levilliers, J., del Castillo, I., Cohen-Salmon, M., Legouis, R., Blanchard, S., Compain, S., Bouloux, P., Kirk, J., and Moraine, C. (1992). X chromosome-linked Kallmann syndrome: stop mutations validate the candidate gene. Proc. Natl. Acad. Sci. U.S.A. *89*, 8190–8194.

Harden, M.V., Pereiro, L., Ramialison, M., Wittbrodt, J., Prasad, M.K., McCallion, A.S., and Whitlock, K.E. (2012). Close association of olfactory placode precursors and cranial neural crest cells does not predestine cell mixing. Dev. Dyn. *241*, 1143–1154.

Hatt, H. (2004). Molecular and cellular basis of human olfaction. Chem. Biodivers. *1*, 1857–1869.

Heng, J.I.-T., Nguyen, L., Castro, D.S., Zimmer, C., Wildner, H., Armant, O., Skowronska-Krawczyk, D., Bedogni, F., Matter, J.-M., Hevner, R., et al. (2008). Neurogenin 2 controls cortical neuron migration through regulation of Rnd2. Nature *455*, 114–118.

Herzog, W., Zeng, X., Lele, Z., Sonntag, C., Ting, J.-W., Chang, C.-Y., and Hammerschmidt, M. (2003). Adenohypophysis formation in the zebrafish and its dependence on sonic hedgehog. Developmental Biology *254*, 36–49.

Holbrook, E.H., Wu, E., Curry, W.T., Lin, D.T., and Schwob, J.E. (2011). Immunohistochemical characterization of human olfactory tissue. Laryngoscope *121*, 1687–1701.

Housden, B.E., Muhar, M., Gemberling, M., Gersbach, C.A., Stainier, D.Y.R., Seydoux, G., Mohr, S.E., Zuber, J., and Perrimon, N. (2017). Loss-of-function genetic tools for animal models: cross-species and cross-platform differences. Nat. Rev. Genet. *18*, 24–40.

Huang, S., and Sato, S. (1998). Progenitor cells in the adult zebrafish nervous system express a Brn-1-related POU gene, tai-ji1`Tai-ji' is a Chinese philosophical term meaning `the source of generation and change'.1. Mechanisms of Development *71*, 23–35.

Huang, X., Hong, C.-S., O'Donnell, M., and Saint-Jeannet, J.-P. (2005). The doublesex-related gene, XDmrt4, is required for neurogenesis in the olfactory system. Proc. Natl. Acad. Sci. U.S.A. *102*, 11349–11354.

Ikeda, K., Watanabe, Y., Ohto, H., and Kawakami, K. (2002). Molecular interaction and synergistic activation of a promoter by Six, Eya, and Dach proteins mediated through CREB binding protein. Mol. Cell. Biol. *22*, 6759–6766.

Iqbal, T., and Byrd-Jacobs, C. (2010). Rapid degeneration and regeneration of the zebrafish olfactory epithelium after triton X-100 application. Chem. Senses *35*, 351–361.

Itoh, M., Kudoh, T., Dedekian, M., Kim, C.-H., and Chitnis, A.B. (2002). A role for iro1 and iro7 in the establishment of an anteroposterior compartment of the ectoderm adjacent to the midbrain-hindbrain boundary. Development *129*, 2317–2327.

Itoh, Y., Tyssowski, K., and Gotoh, Y. (2013). Transcriptional coupling of neuronal fate commitment and the onset of migration. Curr. Opin. Neurobiol. *23*, 957–964.

Jarman, A.P., Grau, Y., Jan, L.Y., and Jan, Y.N. (1993). atonal is a proneural gene that directs chordotonal organ formation in the Drosophila peripheral nervous system. Cell *73*, 1307–1321.

Joris, M., Schloesser, M., Baurain, D., Hanikenne, M., Muller, M., and Motte, P. (2017). Number of inadvertent RNA targets for morpholino knockdown in Danio rerio is largely underestimated: evidence from the study of Ser/Arg-rich splicing factors. Nucleic Acids Res. *45*, 9547–9557.

Kaji, T., and Artinger, K.B. (2004). dlx3b and dlx4b function in the development of Rohon-Beard sensory neurons and trigeminal placode in the zebrafish neurula. Dev. Biol. *276*, 523–540.

Kappen, C., and Salbaum, J.M. (2009). Identification of regulatory elements in the Isl1 gene locus. Int. J. Dev. Biol. *53*, 935–946.

Kim, K.-T., Kim, N., Kim, H.-K., Lee, H., Gruner, H.N., Gergics, P., Park, C., Mastick, G.S., Park, H.-C., and Song, M.-R. (2016). ISL1-based LIM complexes control Slit2 transcription in developing cranial motor neurons. Sci Rep *6*, 36491.

Kimmel, C.B., Ballard, W.W., Kimmel, S.R., Ullmann, B., and Schilling, T.F. (1995). Stages of embryonic development of the zebrafish. Dev. Dyn. *203*, 253–310.

Klisch, T.J., Xi, Y., Flora, A., Wang, L., Li, W., and Zoghbi, H.Y. (2011). In vivo Atoh1 targetome reveals how a proneural transcription factor regulates cerebellar development. Proceedings of the National Academy of Sciences *108*, 3288–3293.

Klymkowsky, M.W., Rossi, C.C., and Artinger, K.B. (2010). Mechanisms driving neural crest induction and migration in the zebrafish and Xenopus laevis. Cell Adh Migr *4*, 595–608.

Kohli, P., Soler, Z.M., Nguyen, S.A., Muus, J.S., and Schlosser, R.J. (2016). The Association Between Olfaction and Depression: A Systematic Review. Chem. Senses *41*, 479–486.

Korsching, S. (2009). The molecular evolution of teleost olfactory receptor gene families. Results Probl Cell Differ *47*, 37–55.

Korsensky, L., and Ron, D. (2016). Regulation of FGF signaling: Recent insights from studying positive and negative modulators. Semin. Cell Dev. Biol. *53*, 101–114.

Kozlowski, D.J., Whitfield, T.T., Hukriede, N.A., Lam, W.K., and Weinberg, E.S. (2005). The zebrafish dog-eared mutation disrupts eya1, a gene required for cell survival and differentiation in the inner ear and lateral line. Dev. Biol. *277*, 27–41.

Kuo, M.-W., Lou, S.-W., and Chung, B. (2014). Hedgehog-PKA signaling and gnrh3 regulate the development of zebrafish gnrh3 neurons. PLoS ONE *9*, e95545.

Kwon, H.-J., Bhat, N., Sweet, E.M., Cornell, R.A., and Riley, B.B. (2010). Identification of early requirements for preplacodal ectoderm and sensory organ development. PLoS Genet. *6*, e1001133.

Laclef, C., Souil, E., Demignon, J., and Maire, P. (2003). Thymus, kidney and craniofacial abnormalities in Six 1 deficient mice. Mech. Dev. *120*, 669–679.

Lakhina, V., Marcaccio, C.L., Shao, X., Lush, M.E., Jain, R.A., Fujimoto, E., Bonkowsky, J.L., Granato, M., and Raper, J.A. (2012). Netrin/DCC signaling guides olfactory sensory axons to their correct location in the olfactory bulb. J. Neurosci. *32*, 4440–4456.

Lazzari, M., Bettini, S., and Franceschini, V. (2014). Immunocytochemical characterisation of olfactory ensheathing cells of zebrafish. J. Anat. *224*, 192–206.

Lecaudey, V., Anselme, I., Dildrop, R., Rüther, U., and Schneider-Maunoury, S. (2005). Expression of the zebrafish Iroquois genes during early nervous system formation and patterning. J. Comp. Neurol. *492*, 289–302.

Lee, S.-K., and Pfaff, S.L. (2003). Synchronization of Neurogenesis and Motor Neuron Specification by Direct Coupling of bHLH and Homeodomain Transcription Factors. Neuron *38*, 731–745.

Leopold, D. (2002). Distortion of olfactory perception: diagnosis and treatment. Chem. Senses *27*, 611–615.

Li, X., Oghi, K.A., Zhang, J., Krones, A., Bush, K.T., Glass, C.K., Nigam, S.K., Aggarwal, A.K., Maas, R., Rose, D.W., et al. (2003). Eya protein phosphatase activity regulates Six1-Dach-Eya transcriptional effects in mammalian organogenesis. Nature *426*, 247–254.

Litsiou, A., Hanson, S., and Streit, A. (2005). A balance of FGF, BMP and WNT signalling positions the future placode territory in the head. Development *132*, 4051–4062.

Liu, J., He, Y., Wang, X., Zheng, X., and Cui, S. (2005a). Developmental changes of Islet-1 and its co-localization with pituitary hormones in the pituitary gland of chick embryo by immunohistochemistry. Cell Tissue Res. *322*, 279–287.

Liu, J., Liu, Z., Yi, S., and Cui, S. (2005b). Islet-1 expression and its colocalization with luteinising hormone, thyroid-stimulating hormone and oestrogen receptor alpha in the developing pituitary gland of the sheep foetus. J. Neuroendocrinol. *17*, 773–780.

Liu, Q., Marrs, J.A., Azodi, E., Kerstetter, A.E., Babb, S.G., and Hashmi, L. (2004). Differential expression of cadherins in the developing and adult zebrafish olfactory system. J. Comp. Neurol. *478*, 269–281.

Lleras-Forero, L., Tambalo, M., Christophorou, N., Chambers, D., Houart, C., and Streit, A. (2013). Neuropeptides: developmental signals in placode progenitor formation. Dev. Cell *26*, 195–203.

Lowery, L.A., and Sive, H. (2005). Initial formation of zebrafish brain ventricles occurs independently of circulation and requires the nagie oko and snakehead/atp1a1a.1 gene products. Development *132*, 2057–2067.

Ma, Q., Chen, Z., Barrantes, I. del B., Pompa, J.L. de la, and Anderson, D.J. (1998). neurogenin1 Is Essential for the Determination of Neuronal Precursors for Proximal Cranial Sensory Ganglia. Neuron *20*, 469–482.

Madelaine, R., Garric, L., and Blader, P. (2011). Partially redundant proneural function reveals the importance of timing during zebrafish olfactory neurogenesis. Development *138*, 4753–4762.

Mainland, J.D., Lundström, J.N., Reisert, J., and Lowe, G. (2014). From Molecule to Mind: an Integrative Perspective on Odor Intensity. Trends Neurosci *37*, 443–454.

McHugh, B., Krause, S.A., Yu, B., Deans, A.-M., Heasman, S., McLaughlin, P., and Heck, M.M.S. (2004). Invadolysin: a novel, conserved metalloprotease links mitotic structural rearrangements with cell migration. J Cell Biol *167*, 673–686.

McKenna, A., Findlay, G.M., Gagnon, J.A., Horwitz, M.S., Schier, A.F., and Shendure, J. (2016). Whole organism lineage tracing by combinatorial and cumulative genome editing. Science *353*, aaf7907.

Metz, H., and Wray, S. (2010). Use of mutant mouse lines to investigate origin of gonadotropin-releasing hormone-1 neurons: lineage independent of the adenohypophysis. Endocrinology *151*, 766–773.

Meyen, D., Tarbashevich, K., Banisch, T.U., Wittwer, C., Reichman-Fried, M., Maugis, B., Grimaldi, C., Messerschmidt, E.-M., and Raz, E. (2015). Dynamic filopodia are required for chemokine-dependent intracellular polarization during guided cell migration in vivo. Elife *4*.

Mitchell, A.L., Dwyer, A., Pitteloud, N., and Quinton, R. (2011). Genetic basis and variable phenotypic expression of Kallmann syndrome: towards a unifying theory. Trends Endocrinol. Metab. *22*, 249–258.

Miyasaka, N., Sato, Y., Yeo, S.-Y., Hutson, L.D., Chien, C.-B., Okamoto, H., and Yoshihara, Y. (2005). Robo2 is required for establishment of a precise glomerular map in the zebrafish olfactory system. Development *132*, 1283–1293.

Miyasaka, N., Knaut, H., and Yoshihara, Y. (2007). Cxcl12/Cxcr4 chemokine signaling is required for placode assembly and sensory axon pathfinding in the zebrafish olfactory system. Development *134*, 2459–2468.

Miyasaka, N., Morimoto, K., Tsubokawa, T., Higashijima, S., Okamoto, H., and Yoshihara, Y. (2009). From the Olfactory Bulb to Higher Brain Centers: Genetic Visualization of Secondary Olfactory Pathways in Zebrafish. J. Neurosci. *29*, 4756–4767.

Monti-Bloch, L., Jennings-White, C., and Berliner, D.L. (1998). The human vomeronasal system. A review. Ann. N. Y. Acad. Sci. *855*, 373–389.

Mork, L., and Crump, G. (2015). Zebrafish Craniofacial Development: A Window into Early Patterning. Curr. Top. Dev. Biol. *115*, 235–269.

Nair, S., and Schilling, T.F. (2008). Chemokine signaling controls endodermal migration during zebrafish gastrulation. Science *322*, 89–92.

Neave, B., Holder, N., and Patient, R. (1997). A graded response to BMP-4 spatially coordinates patterning of the mesoderm and ectoderm in the zebrafish. Mech. Dev. *62*, 183–195.

Nguyen, V.H., Schmid, B., Trout, J., Connors, S.A., Ekker, M., and Mullins, M.C. (1998). Ventral and lateral regions of the zebrafish gastrula, including the neural crest progenitors, are established by a bmp2b/swirl pathway of genes. Dev. Biol. *199*, 93–110.

Nica, G., Herzog, W., Sonntag, C., Nowak, M., Schwarz, H., Zapata, A.G., and Hammerschmidt, M. (2006). Eya1 is required for lineage-specific differentiation, but not for cell survival in the zebrafish adenohypophysis. Dev. Biol. *292*, 189–204.

Oka, Y., Saraiva, L.R., and Korsching, S.I. (2012). Crypt neurons express a single V1R-related ora gene. Chem. Senses *37*, 219–227.

Ozaki, H., Watanabe, Y., Ikeda, K., and Kawakami, K. (2002). Impaired interactions between mouse Eyal harboring mutations found in patients with branchio-oto-renal syndrome and Six, Dach, and G proteins. J. Hum. Genet. *47*, 107–116.

Palevitch, O., Abraham, E., Borodovsky, N., Levkowitz, G., Zohar, Y., and Gothilf, Y. (2010). Cxcl12a-Cxcr4b signaling is important for proper development of the forebrain GnRH system in zebrafish. Gen. Comp. Endocrinol. *165*, 262–268.

Pascarella, G., Lazarevic, D., Plessy, C., Bertin, N., Akalin, A., Vlachouli, C., Simone, R., Faulkner, G.J., Zucchelli, S., Kawai, J., et al. (2014). NanoCAGE analysis of the mouse olfactory epithelium identifies the expression of vomeronasal receptors and of proximal LINE elements. Front Cell Neurosci *8*, 41.

Pérez-Gómez, A., Stein, B., Leinders-Zufall, T., and Chamero, P. (2014). Signaling mechanisms and behavioral function of the mouse basal vomeronasal neuroepithelium. Front Neuroanat *8*, 135.

Quaynor, S.D., Bosley, M.E., Duckworth, C.G., Porter, K.R., Kim, S.-H., Kim, H.-G., Chorich, L.P., Sullivan, M.E., Choi, J.-H., Cameron, R.S., et al. (2016). Targeted next generation sequencing approach identifies eighteen new candidate genes in normosmic hypogonadotropic hypogonadism and Kallmann syndrome. Mol. Cell. Endocrinol. *437*, 86–96.

Ramel, M.-C., and Hill, C.S. (2012). Spatial regulation of BMP activity. FEBS Lett. *586*, 1929–1941.

Reichert, S., Randall, R.A., and Hill, C.S. (2013). A BMP regulatory network controls ectodermal cell fate decisions at the neural plate border. Development *140*, 4435–4444.

Riddiford, N., and Schlosser, G. (2017). Six1 and Eya1 both promote and arrest neuronal differentiation by activating multiple Notch pathway genes. Dev. Biol.

Rossi, A., Kontarakis, Z., Gerri, C., Nolte, H., Hölper, S., Krüger, M., and Stainier, D.Y.R. (2015). Genetic compensation induced by deleterious mutations but not gene knockdowns. Nature *524*, 230–233.

Rossi, C.C., Kaji, T., and Artinger, K.B. (2009). Transcriptional control of Rohon-Beard sensory neuron development at the neural plate border. Dev. Dyn. *238*, 931–943.

Sabado, V., Barraud, P., Baker, C.V.H., and Streit, A. (2012). Specification of GnRH-1 neurons by antagonistic FGF and retinoic acid signaling. Dev. Biol. *362*, 254–262.

Sallee, M.D., Littleford, H.E., and Greenwald, I. (2017). A bHLH Code for Sexually Dimorphic Form and Function of the C. elegans Somatic Gonad. Current Biology *27*, 1853–1860.e5.

Sánchez-Arrones, L., Ferrán, J.L., Hidalgo-Sanchez, M., and Puelles, L. (2015). Origin and early development of the chicken adenohypophysis. Front Neuroanat *9*, 7.

Sanchez-Arrones, L., Sandonís, Á., Cardozo, M.J., and Bovolenta, P. (2017). Adenohypophysis placodal precursors exhibit distinctive features within the rostral preplacodal ectoderm. Development *144*, 3521–3532.

Saraiva, L.R., Ahuja, G., Ivandic, I., Syed, A.S., Marioni, J.C., Korsching, S.I., and Logan, D.W. (2015). Molecular and neuronal homology between the olfactory systems of zebrafish and mouse. Sci Rep *5*, 11487.

Sato, Y., Miyasaka, N., and Yoshihara, Y. (2005). Mutually Exclusive Glomerular Innervation by Two Distinct Types of Olfactory Sensory Neurons Revealed in Transgenic Zebrafish. J. Neurosci. *25*, 4889–4897.

Sato, Y., Miyasaka, N., and Yoshihara, Y. (2007). Hierarchical regulation of odorant receptor gene choice and subsequent axonal projection of olfactory sensory neurons in zebrafish. J. Neurosci. *27*, 1606–1615.

Saxena, A., Peng, B.N., and Bronner, M.E. (2013). Sox10-dependent neural crest origin of olfactory microvillous neurons in zebrafish. Elife *2*, e00336.

Sbrogna, J.L., Barresi, M.J.F., and Karlstrom, R.O. (2003). Multiple roles for Hedgehog signaling in zebrafish pituitary development. Developmental Biology *254*, 19–35.

Schild, D., and Restrepo, D. (1998). Transduction Mechanisms in Vertebrate Olfactory Receptor Cells. Physiological Reviews *78*, 429–466.

Schille, C., and Schambony, A. (2017). Signaling pathways and tissue interactions in neural plate border formation. Neurogenesis.

Schlosser, G. (2014). Early embryonic specification of vertebrate cranial placodes. Wiley Interdiscip Rev Dev Biol *3*, 349–363.

Schumacher, J.A., Hashiguchi, M., Nguyen, V.H., and Mullins, M.C. (2011). An intermediate level of BMP signaling directly specifies cranial neural crest progenitor cells in zebrafish. PLoS ONE *6*, e27403.

Schwanzel-Fukuda, M., and Pfaff, D.W. (1989). Origin of luteinizing hormone-releasing hormone neurons. Nature *338*, 161–164.

Schwarting, G.A., Henion, T.R., Nugent, J.D., Caplan, B., and Tobet, S. (2006). Stromal cell-derived factor-1 (chemokine C-X-C motif ligand 12) and chemokine C-X-

C motif receptor 4 are required for migration of gonadotropin-releasing hormone neurons to the forebrain. J. Neurosci. *26*, 6834–6840.

Seidi, A., Mie, M., and Kobatake, E. (2007). Novel recombination system using Cre recombinase alpha complementation. Biotechnol Lett *29*, 1315–1322.

Sétáló, G. (1996). Gonadotropin-releasing hormone neuroblasts from one olfactory placode can be present in both hemispheres in the clawed toad Xenopus laevis. Neuroendocrinology *63*, 408–414.

Shao, X., Lakhina, V., Dang, P., Cheng, R.P., Marcaccio, C.L., and Raper, J.A. (2017). Olfactory sensory axons target specific protoglomeruli in the olfactory bulb of zebrafish. Neural Dev *12*, 18.

Shi, X., Bosenko, D.V., Zinkevich, N.S., Foley, S., Hyde, D.R., Semina, E.V., and Vihtelic, T.S. (2005). Zebrafish pitx3 is necessary for normal lens and retinal development. Mech. Dev. *122*, 513–527.

Shiotsugu, J., Katsuyama, Y., Arima, K., Baxter, A., Koide, T., Song, J., Chandraratna, R.A.S., and Blumberg, B. (2004). Multiple points of interaction between retinoic acid and FGF signaling during embryonic axis formation. Development *131*, 2653–2667.

Smith, T.D., and Bhatnagar, K.P. (2000). The human vomeronasal organ. Part II: prenatal development. J. Anat. *197 Pt 3*, 421–436.

Solomon, K.S., and Fritz, A. (2002). Concerted action of two dlx paralogs in sensory placode formation. Development *129*, 3127–3136.

Steventon, B., Mayor, R., and Streit, A. (2014). Neural crest and placode interaction during the development of the cranial sensory system. Dev. Biol. *389*, 28–38.

Storan, M.J., and Key, B. (2006). Septal organ of Grüneberg is part of the olfactory system. J. Comp. Neurol. *494*, 834–844.

Streit, A. (2008). The cranial sensory nervous system: specification of sensory progenitors and placodes. In StemBook, (Cambridge (MA): Harvard Stem Cell Institute), p.

Stuhlmiller, T.J., and García-Castro, M.I. (2012). Current perspectives of the signaling pathways directing neural crest induction. Cell. Mol. Life Sci. *69*, 3715–3737.

Suárez, R., García-González, D., and de Castro, F. (2012). Mutual influences between the main olfactory and vomeronasal systems in development and evolution. Front Neuroanat *6*.

Suzuki, J., and Osumi, N. (2015). Neural crest and placode contributions to olfactory development. Curr. Top. Dev. Biol. *111*, 351–374.

Takano-Maruyama, M., Chen, Y., and Gaufo, G.O. (2012). Differential contribution of Neurog1 and Neurog2 on the formation of cranial ganglia along the anterior-posterior axis. Dev. Dyn. *241*, 229–241.

Taku, A.A., Marcaccio, C.L., Ye, W., Krause, G.J., and Raper, J.A. (2016). Attractant and repellent cues cooperate in guiding a subset of olfactory sensory axons to a well-defined protoglomerular target. Development *143*, 123–132.

Thaler, J.P., Lee, S.-K., Jurata, L.W., Gill, G.N., and Pfaff, S.L. (2002). LIM factor Lhx3 contributes to the specification of motor neuron and interneuron identity through cell-type-specific protein-protein interactions. Cell *110*, 237–249.

Tian, H., and Ma, M. (2004). Molecular organization of the olfactory septal organ. J. Neurosci. *24*, 8383–8390.

Tirindelli, R., Dibattista, M., Pifferi, S., and Menini, A. (2009). From Pheromones to Behavior. Physiological Reviews *89*, 921–956.

Tissir, F., Wang, C.-E., and Goffinet, A.M. (2004). Expression of the chemokine receptor Cxcr4 mRNA during mouse brain development. Brain Res. Dev. Brain Res. *149*, 63–71.

Toba, Y., Tiong, J.D., Ma, Q., and Wray, S. (2008). CXCR4/SDF-1 system modulates development of GnRH-1 neurons and the olfactory system. Dev Neurobiol *68*, 487–503.

Toro, S., and Varga, Z.M. (2007). Equivalent progenitor cells in the zebrafish anterior preplacodal field give rise to adenohypophysis, lens, and olfactory placodes. Semin. Cell Dev. Biol. *18*, 534–542.

Torres-Paz, J., and Whitlock, K.E. (2014). Olfactory sensory system develops from coordinated movements within the neural plate. Dev. Dyn. *243*, 1619–1631.

Trainor, P. (2013). Neural Crest Cells: Evolution, Development and Disease (Academic Press).

Trinh, L.A., and Fraser, S.E. (2013). Enhancer and gene traps for molecular imaging and genetic analysis in zebrafish. Dev. Growth Differ. *55*, 434–445.

Tucker, J.A., Mintzer, K.A., and Mullins, M.C. (2008). The BMP signaling gradient patterns dorsoventral tissues in a temporally progressive manner along the anteroposterior axis. Dev. Cell *14*, 108–119.

von Uexküll, J. A Foray into the Worlds of Animals and Humans (1934).

Vassar, R., Chao, S.K., Sitcheran, R., Nuñez, J.M., Vosshall, L.B., and Axel, R. (1994). Topographic organization of sensory projections to the olfactory bulb. Cell *79*, 981–991.

Viktorin, G., Chiuchitu, C., Rissler, M., Varga, Z.M., and Westerfield, M. (2009). Emx3 is required for the differentiation of dorsal telencephalic neurons. Dev. Dyn. *238*, 1984–1998.

Villanueva, S., Glavic, A., Ruiz, P., and Mayor, R. (2002). Posteriorization by FGF, Wnt, and retinoic acid is required for neural crest induction. Dev. Biol. *241*, 289–301.

Von Niederhäusern, V., Kastenhuber, E., Stäuble, A., Gesemann, M., and Neuhauss, S.C.F. (2013). Phylogeny and expression of canonical transient receptor potential (TRPC) genes in developing zebrafish. Dev. Dyn. *242*, 1427–1441.

Wang, F., Nemes, A., Mendelsohn, M., and Axel, R. (1998). Odorant receptors govern the formation of a precise topographic map. Cell *93*, 47–60.

Wessels, Q., Hoogland, P.V.J.M., and Vorster, W. (2014). Anatomical evidence for an endocrine activity of the vomeronasal organ in humans. Clin Anat *27*, 856–860.

Whitlock, K.E., and Westerfield, M. (1998). A transient population of neurons pioneers the olfactory pathway in the zebrafish. J. Neurosci. *18*, 8919–8927.

Whitlock, K.E., and Westerfield, M. (2000). The olfactory placodes of the zebrafish form by convergence of cellular fields at the edge of the neural plate. Development *127*, 3645–3653.

Whitlock, K.E., Wolf, C.D., and Boyce, M.L. (2003). Gonadotropin-releasing hormone (GnRH) cells arise from cranial neural crest and adenohypophyseal regions of the neural plate in the zebrafish, Danio rerio. Dev. Biol. *257*, 140–152.

Whitlock, K.E., Smith, K.M., Kim, H., and Harden, M.V. (2005). A role for foxd3 and sox10 in the differentiation of gonadotropin-releasing hormone (GnRH) cells in the zebrafish Danio rerio. Development *132*, 5491–5502.

Wilson, R.I., and Mainen, Z.F. (2006). Early events in olfactory processing. Annu. Rev. Neurosci. *29*, 163–201.

Wilson, S.W., Ross, L.S., Parrett, T., and Easter, S.S. (1990). The development of a simple scaffold of axon tracts in the brain of the embryonic zebrafish, Brachydanio rerio. Development *108*, 121–145.

Winkler, C., Hornung, U., Kondo, M., Neuner, C., Duschl, J., Shima, A., and Schartl, M. (2004). Developmentally regulated and non-sex-specific expression of autosomal dmrt genes in embryos of the Medaka fish (Oryzias latipes). Mech. Dev. *121*, 997–1005.

Woda, J.M., Pastagia, J., Mercola, M., and Artinger, K.B. (2003). Dlx proteins position the neural plate border and determine adjacent cell fates. Development *130*, 331–342.

Wray, S., Grant, P., and Gainer, H. (1989). Evidence that cells expressing luteinizing hormone-releasing hormone mRNA in the mouse are derived from progenitor cells in the olfactory placode. Proc Natl Acad Sci U S A *86*, 8132–8136.

Wurtzel, O., Oderberg, I.M., and Reddien, P.W. (2017). Planarian Epidermal Stem Cells Respond to Positional Cues to Promote Cell-Type Diversity. Developmental Cell *40*, 491–504.e5.

Xu, P.X., Adams, J., Peters, H., Brown, M.C., Heaney, S., and Maas, R. (1999). Eya1-deficient mice lack ears and kidneys and show abnormal apoptosis of organ primordia. Nat. Genet. *23*, 113–117.

Yamaguchi, T., Yamashita, J., Ohmoto, M., Aoudé, I., Ogura, T., Luo, W., Bachmanov, A.A., Lin, W., Matsumoto, I., and Hirota, J. (2014). Skn-1a/Pou2f3 is required for the generation of Trpm5-expressing microvillous cells in the mouse main olfactory epithelium. BMC Neurosci *15*, 13.

Yanicostas, C., Herbomel, E., Dipietromaria, A., and Soussi-Yanicostas, N. (2009). Anosmin-1a is required for fasciculation and terminal targeting of olfactory sensory neuron axons in the zebrafish olfactory system. Mol. Cell. Endocrinol. *312*, 53–60.

Yao, D., Zhao, F., Wu, Y., Wang, J., Dong, W., Zhao, J., Zhu, Z., and Liu, D. (2014). Dissecting the differentiation process of the preplacodal ectoderm in zebrafish. Dev. Dyn. *243*, 1338–1351.

Yoshida, T., Ito, A., Matsuda, N., and Mishina, M. (2002). Regulation by protein kinase A switching of axonal pathfinding of zebrafish olfactory sensory neurons through the olfactory placode-olfactory bulb boundary. J. Neurosci. *22*, 4964–4972.

Yuan, L., Hu, S., Okray, Z., Ren, X., De Geest, N., Claeys, A., Yan, J., Bellefroid, E., Hassan, B.A., and Quan, X.-J. (2016). The Drosophila neurogenin Tap functionally interacts with the Wnt-PCP pathway to regulate neuronal extension and guidance. Development *143*, 2760–2766.

Zecca, A., Dyballa, S., Voltes, A., Bradley, R., and Pujades, C. (2015). The Order and Place of Neuronal Differentiation Establish the Topography of Sensory Projections and the Entry Points within the Hindbrain. J. Neurosci. *35*, 7475–7486.

Zheng, W., Huang, L., Wei, Z.-B., Silvius, D., Tang, B., and Xu, P.-X. (2003). The role of Six1 in mammalian auditory system development. Development *130*, 3989–4000.

Zilinski, C.A., Shah, R., Lane, M.E., and Jamrich, M. (2005). Modulation of zebrafish pitx3 expression in the primordia of the pituitary, lens, olfactory epithelium and cranial ganglia by hedgehog and nodal signaling. Genesis *41*, 33–40.

Zou, D., Silvius, D., Fritzsch, B., and Xu, P.-X. (2004). Eya1 and Six1 are essential for early steps of sensory neurogenesis in mammalian cranial placodes. Development *131*, 5561–5572.

V. Annexes

CHAPTER

2

Patterning, morphogenesis, and neurogenesis of zebrafish cranial sensory placodes

R. Aguillon, P. Blader[1], J. Batut[1]

Centre de Biologie du Développement (CBD, UMR5547), Centre de Biologie Intégrative (CBI), Université de Toulouse, CNRS, UPS, Toulouse, France

[1]*Corresponding authors: E-mail: julie.batut@univ-tlse3.fr; patrick.blader@univ-tlse3.fr*

CHAPTER OUTLINE

Abstract

Peripheral sensory organs and ganglia found in the vertebrate head arise during embryonic development from distinct ectodermal thickenings, called cranial sensory placodes (adenohypophyseal, olfactory, lens, trigeminal, epibranchial, and otic). A series of patterning events leads to the establishment of these placodes. Subsequently, these placodes undergo specific morphogenetic movements and cell-type specification in order to shape the final placodal derivatives and to produce differentiated cell types necessary for their function. In this

Methods in Cell Biology, Volume 134, ISSN 0091-679X, http://dx.doi.org/10.1016/bs.mcb.2016.01.002

chapter, we will focus on recent studies in the zebrafish that have advanced our understanding of cranial sensory placode development. We will summarize the signaling events and their molecular effectors guiding the formation of the so-called preplacodal region, and the subsequent subdivision of this region along the anteroposterior axis that gives rise to specific placode identities as well as those controlling morphogenesis and neurogenesis. Finally, we will highlight the approaches used in zebrafish that have been established to precisely label cell populations, to follow their development, and/or to characterize cell fates within a specific placode.

INTRODUCTION

Cranial placodes arise from the embryonic ectoderm immediately adjacent to the anterior neural plate (recently reviewed by Moody & LaMantia, 2015; Patthey, Schlosser, & Shimeld, 2014; Saint-Jeannet & Moody, 2014; Schlosser, 2005, 2007, 2010, 2014, 2015). While anteriorly, these placodes will ultimately give rise to the adenohypophysis, the olfactory epithelium, and the lens of the eye; more posteriorly the otic placode will generate the inner ear and the statoacoustic ganglion (SAG), and the trigeminal and epibranchial placodes will provide sensory neurons that innervate the skin as well as internal organs in order to transmit information such as heart rate, blood pressure, and visceral distension from the periphery to the brain (Fig. 1). Finally, in aquatic vertebrates, additional placodes have arisen that develop into the anterior and posterior lateral line ganglia and mechanosensory neuromasts of the head and flank that sense water flow.

Cranial placodes give rise to a plethora of different cell types including neuroendocrine cells, sensory neurons, lens fibers, and self-renewing stem cells that will generate the peripheral nervous system of the vertebrate head. As such, cranial placode development provides an attractive model to explore how cell fate is established, and gene regulatory networks controlling cranial placode patterning and specification are beginning to be unraveled. The distinct morphologies of the final placodal derivatives also provide a paradigm for dissecting genetic networks involved in their morphogenesis, including the regulation of epithelial rearrangement, cell adhesion, and migration (Breau & Schneider-Maunoury, 2014, 2015; Grocott, Tambalo, & Streit, 2012; Moody & LaMantia, 2015). Finally, cranial placodes originate adjacent to the neural crest at the neural plate border. As both placodal and crest cells contribute to cranial sensory ganglia, this system also provides a paradigm for understanding how the development of different tissues is coordinated.

At the end of gastrulation, cranial placodes are born from a common ectodermal domain of multipotent progenitors, known as the preplacodal region (PPR) (Fig. 2) (Bailey & Streit, 2006; Bhattacharyya & Bronner-Fraser, 2008; Kwon, Bhat, Sweet, Cornell, & Riley, 2010; Martin & Groves, 2006; Schlosser, 2005, 2010). Using explant cultures in chick embryos, it was demonstrated that placode precursors initially share a common "lenslike" ground state (Bailey,

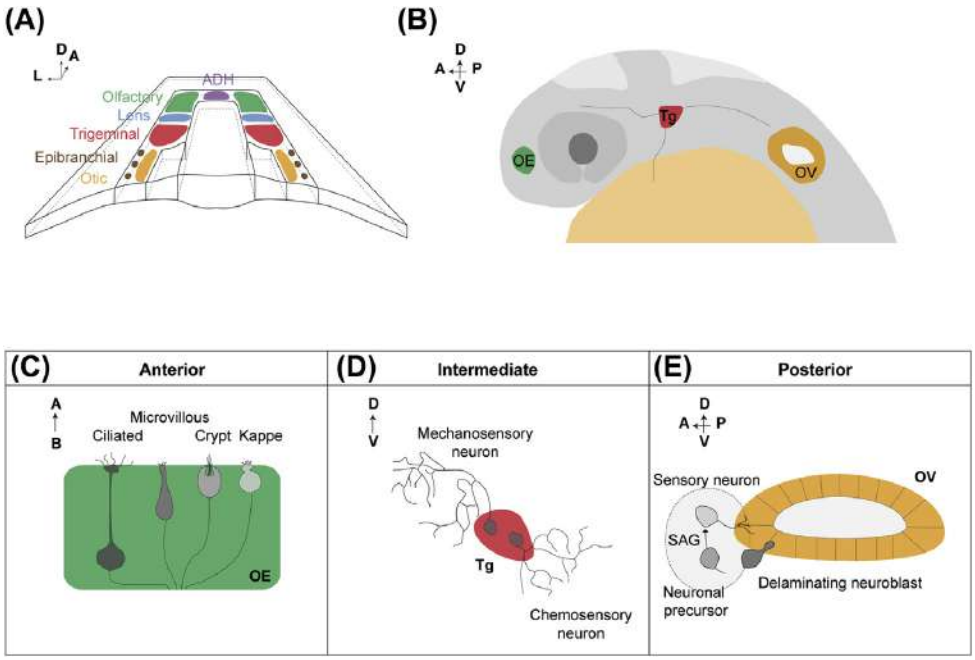

FIGURE 1 Cranial sensory placode development.

(A) Schematic representation of individualized cranial sensory placodes occupying specific positions along the anteroposterior axis during somitogenesis (dorsal view, anterior to the top). (B) Schematic positioning of the anterior olfactory placode (green (gray in print versions)), the intermediate trigeminal placode (red (dark gray in print versions)), and the posterior otic placode (orange (light gray in print versions)) at 24 hpf (hours postfertilization) (lateral view, anterior to the left). *OE*, olfactory epithelium; *Tg*, trigeminal placode, and *OV*, otic vesicle. (C–E) Schemes illustrating olfactory, trigeminal and otic neuronal subtypes. (C) Anterior olfactory sensory neuron (OSN) types. Schematic representation of the four classes of OSNs in the olfactory epithelium: while the cell bodies of ciliated OSNs are located basally, those of microvillous OSNs are positioned at intermediate position and those of crypt and kappe neurons more apically. (D) Intermediate trigeminal mechanosensory and chemosensory neurons. (E) Posterior otic neurogenesis. After specification, neuronal precursors delaminate as neuroblasts from an anterior–ventral position in the otic vesicle and give rise to the eighth cranial or statoacoustic ganglion (SAG).

Bhattacharyya, Bronner-Fraser, & Streit, 2006). During early neurulation, the PPR is subdivided into specialized domains that prefigure the full range of cranial placodes (Breau & Schneider-Maunoury, 2014; Schlosser, 2014). Subsequently, coordinated morphogenetic movements and cell-type specification sculpt the final form of the placodal derivatives and produce differentiated cell types necessary for their function.

Here, we will summarize recently published data primarily concerning the development of a subset of so-called "neurogenic" placodes, focusing on their patterning, morphogenesis, and neurogenesis. We will highlight advances made using the

zebrafish as a model, but will also mention work performed in chick, *Xenopus*, and mouse. Where it might be of particular interest, we will mention specific techniques used to make these advances (schematically depicted in Fig. 4). Finally, we provide two tables summarizing the transgenic zebrafish lines generated (Table 1) and the mutants established (Table 2) to study these processes.

1. SPECIFICATION OF THE PPR AND PATTERNING THE PPR INTO SPECIFIC PLACODES (FIG. 2)

1.1 SIGNALING PATHWAYS ORCHESTRATING PPR SPECIFICATION

Since the beginning of the 20th century, studies have identified a common ectodermal precursor field, the so-called preplacodal region (PPR; also referred to as preplacodal ectoderm or the panplacodal region), which gives rise to the cranial placodes (reviewed elsewhere in Moody & LaMantia, 2015; Patthey et al., 2014; Saint-Jeannet & Moody, 2014; Schlosser, 2005, 2007, 2010, 2014, 2015; Stark, 2014). Initial fate maps and more recent lineage tracing in zebrafish (Dutta et al., 2005; Kozlowski, Murakami, Ho, & Weinberg, 1997; Whitlock & Westerfield, 2000), amphibian and chick (Bhattacharyya, Bailey, Bronner-Fraser, & Streit, 2004; Bhattacharyya & Bronner, 2013; Couly & Le Douarin, 1990, 1987; Pieper, Ahrens, Rink, Peter, & Schlosser, 2012; Streit, 2002; Xu, Dude, & Baker, 2008) embryos have shown that all cranial placodes originate from this domain (Fig. 2). These experiments also illustrate that cells destined to give rise to specific placodes are to some extent intermingled at late gastrula stages, indicating that different cranial placodes arise from partially overlapping domains in the PPR (Bhattacharyya et al., 2004; Dutta et al., 2005; Kozlowski et al., 1997; Whitlock & Westerfield, 2000).

The PPR possesses a molecular signature that includes the expression of genes of the Dlx, Six, and Eya transcription factor families during neurulation (Lleras-Forero & Streit, 2012; Pieper, Eagleson, Wosniok, & Schlosser, 2011; Sato, Miyasaka, & Yoshihara, 2005; Schlosser, 2010). Intriguingly, some genes expressed in the PPR are also expressed in the neural crest cells, raising the question of how these two cell populations become distinct from one another and from the surrounding neural and nonneural tissues (recently reviewed by Groves & LaBonne, 2013). It is now known that during gastrulation, interactions between neural and nonneural ectoderm, as well as signals emanating from underlying mesoderm and endoderm induce the formation of an intermediary ectodermal domain, the neural border or NB, that has the competence to give rise to both neural crest cells and PPR (Fig. 2A). The neural border expresses a combination of specific transcription factors that primes the neural border to respond to lineage-specific signals that induce neural crest cell or placode cell fate (reviewed by Groves & LaBonne, 2013; Moody & LaMantia, 2015). We will first focus our attention on the signaling pathways that operate at the neural border.

Table 1 Summary of Transgenic Zebrafish Lines Used to Study Cranial Placode Development

Transgenic Lines	Domain Labeled/Function	References
Tg(BRE:mRFP)	Anterior neural border	Reichert et al. (2013), Wu et al. (2011)
1. *Tg(−4.9sox10:egfp)*^{ba}	**1.** CNC cells give rise to microvillous olfactory neurons. Otic placode	**1.** Saxena et al. (2013)
2. *Tg(sox10(7.2):mrfp)*^{vu234}	**2.** Olfactory sensory precursors do not incorporate CNC lineages in the OPs. *sox10* gene expression is never observed in microvillous olfactory neurons.	**2.** Harden et al. (2012), Torres-Paz and Whitlock (2014)
Tg(six4b:mCherry)=Tg(pTol2six4.1A:mCherry)^{uv87}	Olfactory placode progenitors	Harden et al. (2012)
Tg(pax2a:GFP)^{e1}	Posterior PPR	McCarroll et al. (2012)
Tg(pax2a:CreER^{T2}*)*$^{\#31}$	Recapitulates *pax2a* expression during OEPD development	Hans et al. (2013)
Tg(hsp70l:loxP-DsRed2-loxP-eGFP)	Conditional red to green reporter for PioTrack	Hans et al. (2013)
Tg(hs:gata3(eGFP))	PPR differentiation	Yao et al. (2014)
Tg((hs:foxi1(eGFP))	PPR differentiation	Yao et al. (2014)
Tg(hsp70:tcfΔC-EGFP)	Inhibition Wnt signalling/reduction otic placode	McCarroll et al. (2012)
Tg(hsp70:dkk1-GFP)^{w32}	Wnt antagonist/reduction otic placode	McCarroll et al. (2012)
Tg(hsp70l-dkk1-mCherry)	Proper level of NPB genes (*pax3a* and *zic3*)	Garnett et al. (2012)
Tg(hsp70l-bmp2b)	Proper positioning in NPB of *pax3a* and *zic3*	Garnett et al. (2012)
Tg(hsp70:fgf8a)^{x17}	**1.** Activation PPR competence factor (with bmp antagonist) **2.** Otic neurogenesis	**1.** Kwon et al. (2010) **2.** Kantarci et al. (2015); Vemaraju et al. (2012)
Tg(hsp70:ca-fgfr1)^{pd3}	*pax2a* induction in posterior PPR	McCarroll et al. (2012)
Tg(hsp70l:dnfgfr1-EGFP)^{pd1}	**1.** Otic neurogenesis	**1.** Kantarci et al. (2015), Vemaraju et al. (2012)
	2. Control *pax2a* induction in posterior PPR	**2.** McCarroll et al. (2012)
Tg(hsp70l:dnBmpr-GFP)	Activation PPR competence factor (with *fgf8*)	Kwon et al. (2010)
Tg(hsp70:chordin)	Activation PPR competence factor (with *fgf8*)	Kwon et al. (2010)
Tg(UAS:myc-Notch1a-intra)^{kca3}	Otic neurogenesis	Kantarci et al. (2015)
Tg(hsp70l:gal41.5)^{kca4}	Otic neurogenesis	Kantarci et al. (2015)

Continued

Table 1 Summary of Transgenic Zebrafish Lines Used to Study Cranial Placode Development—cont'd

Transgenic Lines	Domain Labeled/Function	References
Tg(hsp70:fgf8a)^{x17}	**1.** Nonneural ectoderm is competent to express PPR genes in response to FGF plus inhibition of Bmp.	**1.** Kwon et al. (2010)
	2. *sox3* shows two distinct responses to FGF signaling	**2.** Padanad and Riley (2011)
Tg(hsp70:fgf3)^{x18}	Nonneural ectoderm is competent to express PPR genes in response to FGF plus inhibition of Bmp.	Kwon et al. (2010)
Tg(hsp70:foxi1)^{x19}	**1.** PPR competence factor. **2.** Maintaining *foxi1* expression after 11 hpf impairs completion of otic development in a cell-autonomous manner.	**1.** Bhat et al. (2013), Kwon et al. (2010) **2.** Padanad et al. (2012)
Tg(hsp70:tfap2a)^{x24}	**1.** PPR specification **2.** Otic neurogenesis	**1.** Bhat et al. (2013) **2.** Kantarci et al. (2015)
Tg(hsp70:gata3)^{x25}	PPR specification	Bhat et al. (2013)
Tg(8.4neurog1:GFP)	EON	Madelaine et al. (2011)
Tg(8.4neurog1:nRFP)	Olfactory neurons	Saxena et al. (2013)
Tg(neurod:EGFP)^{nl1}	Morphogenesis of the trigeminal placode	Bhat and Riley (2011)
Tg(her4:EGFP)^{y83}	Otic neurogenesis	Radosevic, Fargas, and Alsina (2014)
Tg(hsp:cxcl12a)	**1.** Ubiquitous heat-induced misexpression of Cxcl12a/Sdf1 **2.** Trigeminal sensory neurons positioning	**1.** Miyasaka et al. (2007) **2.** Knaut et al. (2005)
Tg(hsp70:slit2-GFP)^{rw015d}	Mimic *robo2* mutant (*ast*): impaired OSN axon pathfinding	Miyasaka et al. (2005)
Tg(OMP^{2k}*:lyn-mRFP)*^{rw035}	Ciliated OSNs	Saxena et al. (2013)
Tg(OMP^{2k}*:gap-YFP)*^{rw032a}	Dynamic of OSN axon projections	Miyasaka et al. (2005)
Tg(OMP^{6k}*:gap-YFP)*^{rw031a}	Dynamic of OSN axon projections	Miyasaka et al. (2005)
Tg(TRPC2$^{4.5k}$*:gap—Venus)*^{rw037}	Microvillar OSNs	Harden et al. (2012), Saxena et al. (2013)
Tg(huc:kaede;p2x3:egfp)	BAPTISM: pan neuronal marker; subset of trigeminal sensory neurons	Caron et al. (2008)
Tg(trpa1b:egfp; huc:kaede)	BAPTISM: pan neuronal marker; subset of trigeminal sensory neurons	Caron et al. (2008)
Tg(brn3c:gap43-GFP)^{s356t}	Otic hair cells	Kantarci et al. (2015)
Tg(bactin2:memb-Cerulean-2A-H2B-Dendra2)^{pw1}	PhOTO-N	Saxena et al. (2013)

CNC, *cranial neural crest;* EON, *early olfactory neurons;* OEPD, *otic-epibranchial progenitor domain;* OP, *olfactory placode;* OSNs, *olfactory sensory neurons;* PPR, *preplacodal region.*

Table 2 Summary of Zebrafish Mutants Used to Study Cranial Placode Development

Gene	Mutants	Effect/Phenotypes	References
foxi1	**1.** *foxi1*^{em1} *and foxi1*^{hi3747tg} **2.** *foxi1*^{em1}	**1.** PPR differentiation **2.** Loss of all neuronal OEPD derivatives	**1.** Yao et al. (2014) **2.** Hans et al. (2013)
tfap2a	*mont blanc* *mob*^{m819}	Otic neurogenesis	Kantarci et al. (2015)
pax2a	*pax2a*$^{b593/+}$	Posterior PPR Otic differentiation	McCarroll et al. (2012)
dlx3b, dlx4b	*Df(Chr12:dlx3b,dlx4b,tbx6)* ^{b380}	**1.** *msx1b*, *msx3*, *msx1a* and *dlx3b*, *dlx4b* antagonism at the NB. **2.** Otic and olfactory placodes formation **3.** Trigeminal placode formation **4.** Otic epithelial fates	**1.** Phillips et al. (2006) **2.** Solomon and Fritz (2002) **3.** Kaji and Artinger (2004) **4.** Hans et al. (2013)
msx1b	*Df(Chr01:lef1,msxb)*^{x8}	Reduced size of posterior placodes derivatives	Phillips et al. (2006)
neurog1	*neurog1*^{hi1059Tg}	**1.** Trigeminal sensory ganglia absent at 24 hpf but few neurons at 48 hpf (late born neurons) restricted in their fate. **2.** Delayed EON (reduced number) **3.** Neurog1 controls *her4* expression in otic neurogenic domain	**1.** Caron et al. (2008) **2.** Madelaine et al. (2011) **3.** Radosevic et al. (2014)
eya1	*dog-eared*	Inner ear and lateral line sensory systems	Kozlowski et al. (2005)
cxcr4b	*odysseus*; *cxcr4b*^{t26035} = ody^{JI0049}	**1.** Olfactory placode assembly and sensory axons pathfinding **2.** Trigeminal sensory ganglion assembly	**1.** Miyasaka et al. (2007) **2.** Knaut et al. (2005)
robo2	*astray*, *ast*^{ti272z}	OSNs axons fasciculation	Miyasaka et al. (2005)
n-cadherin, cdh2	*parachute* (*pac*) *glass onion* (*glo*) *pac, glo, ncad, cdh2* *pac*^{tm101B}, *pac*^{fr7} and *pac*$^{paR2.10}$	Morphogenesis Neural tube integrity	Lele et al. (2002)
Integrin-α5	*itga5*^{b926}	Development of posterior placodes	Bhat and Riley (2011)

EON, *early olfactory neurons;* OEPD, *otic-epibranchial progenitor domain;* OSNs, *olfactory sensory neurons;* PPR, *preplacodal region.*

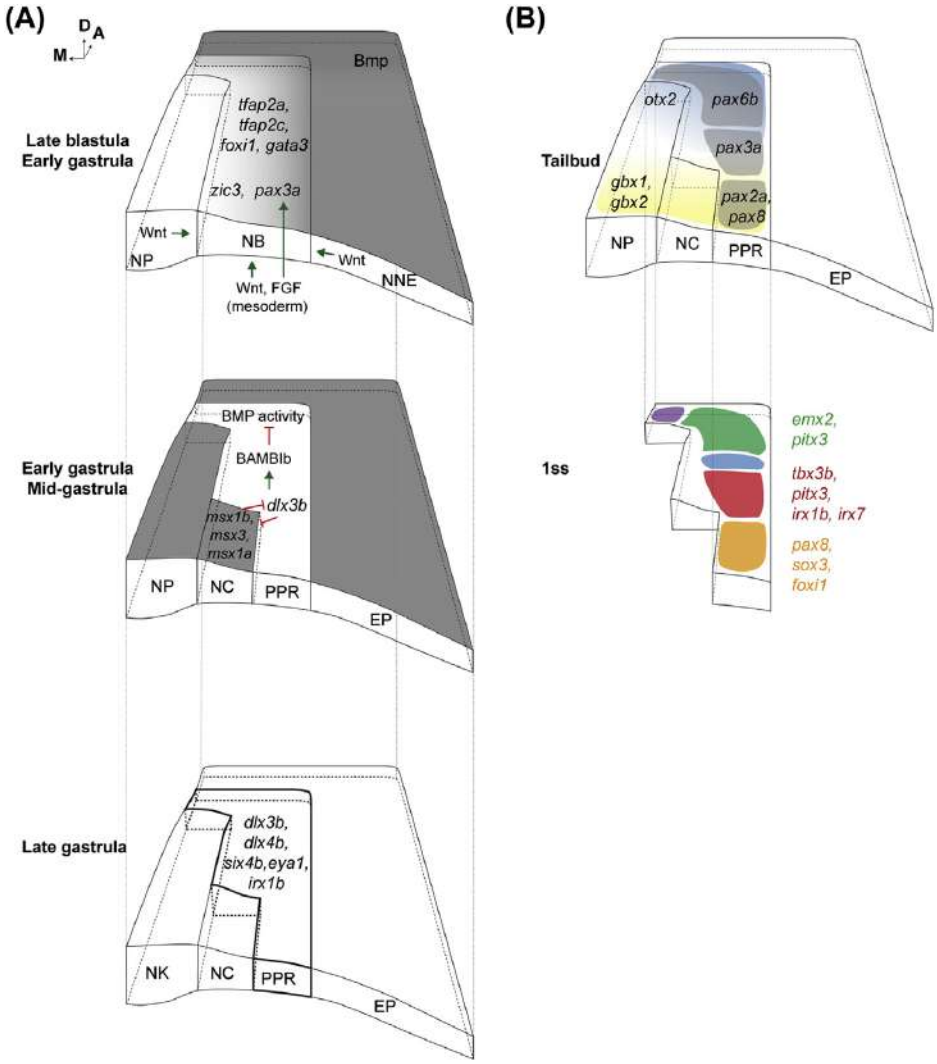

FIGURE 2 Genetic network and key signaling pathways controlling PPR formation and subdivision along the anteroposterior axis.

(A) A gene regulatory network controlling PPR specification during gastrulation. At the late blastula—early gastrula stage, a combined transient activation of FGF signaling with low BMP and Wnt activity are required to induce the expression of the PPR competence factors; *tfap2a*, *tfap2c*, *foxi1*, and *gata3* in the NB. *Zic3* and *pax3a* are expressed in the NB at this stage and are under the control of Wnt and Wnt and FGF, respectively. At the mid-gastrula stage the mutual inhibition between *msx1b*, *msx3*, *msx1a*, and *dlx3b* set up the border between the neural crest domain and the PPR within the NB. Then, *dlx3b* blocks BMP activity through *BAMBIb* to maintain the PPR identity. Finally, at late gastrula stages the PPR signature genes, *dlx3b* and *dlx4b*, *six4b*, *eya1* and *irx1b*, specify this domain (B) Gene network controlling anteroposterior PPR regionalization. At the tailbud stage, the mutual inhibition between rostral *otx2* and caudal *gbx1*, *gbx2* regionalizes the cranial sensory placodes along the anteroposterior axis. Genes specific of the olfactory (green), trigeminal (red), and otic (orange) placode are color coded. *NP*, neural plate; *NB*, neural border; *NNE*, nonneural ectoderm; *EP*, epidermis; *NC*, neural crest cells; *PPR*, preplacodal region; *NK*, neural keel; *1ss*, 1 somite stage; *BMP*, bone morphogenetic protein; *FGF*, fibroblast growth factor. (See color plate)

1.1.1 Fine regulation of bone morphogenetic protein activity during gastrulation defines the neural border

During gastrulation, a gradient of bone morphogenetic protein (BMP) signaling is found across the ectoderm, with the neural border receiving intermediate levels of BMP signaling (Neave, Holder, & Patient, 1997; Nguyen et al., 1998; Schumacher, Hashiguchi, Nguyen, & Mullins, 2011; Tucker, Mintzer, & Mullins, 2008) (Fig. 2A). Recent advances in live imaging have made it possible to visualize the dynamic temporal and spatial regulation of BMP signaling at the NB during ectodermal patterning. Using a BMP reporter *Tg(BMPRE:mRFP)* transgenic zebrafish line that expresses monomeric red fluorescent protein under the control of a BMP response element (Ramel & Hill, 2012; Wu, Ramel, Howell, & Hill, 2011), it was elegantly shown that BMP activity is concentrated in a horseshoe-shaped domain at the NB at the end of gastrulation, which then resolves into two distinct domains, an outer domain abutting the epidermis and an inner domain that corresponds to the PPR and the neural crest, respectively (Reichert, Randall, & Hill, 2013) (Fig. 4A). Bmp2b and Bmp7a are required for establishing the initial BMP^{ON} domain at the NB (Reichert et al., 2013) and have been implicated in promoting neural crest cell fate in several model organisms (reviewed in Stuhlmiller & García-Castro, 2012). Subsequently, PPR specification requires attenuation of BMP signaling (Kwon et al., 2010). This is achieved at least in part via the induction of the BMP antagonist, BMP and activin membrane-bound inhibitor b (BAMBIb), by the PPR-specific transcription factor Dlx3b (Reichert et al., 2013). In parallel, enhanced BMP activity domains in the epidermis and the neural crest are promoted though the BMP-dependent expression of the secreted BMP-binding protein, *crossveinless 2* (*cvl2*, *cv2* or *bmper*, *BMP binding endothelial regulator*) (Reichert et al., 2013). The role of Cvl2 at the NB is controversial, however, because although this factor has been shown to act as a positive regulator of BMP signaling in certain studies (Reichert et al., 2013), its function has also been described as antagonistic to BMP signaling during PPR specification (Esterberg & Fritz, 2009); in the latter example the authors provide evidence that, as for BAMBIb, the transcription factors Dlx3b and Dlx4b regulate *cvl2* expression. The secretion of regulators of BMP signaling from the PPR provides insights into how Dlx factors autonomously establish PPR identity while exerting nonautonomous influence on adjacent neural crest cells. Intriguingly, *dlx3b* and *cvl2* expressions are initially detected in an overlapping domain during gastrulation, but the domains segregate as somitogenesis progress (Reichert et al., 2013). Two possibilities exist for this observation: either one population of cell initially coexpresses these two factors, or they are expressed in specific cell types in a salt-and-pepper manner from the start. It will be of interest in the future to characterize *dlx3b*+ and *cvl2*+ cell sorting during gastrulation as this might shed more light on the specification of the PPR versus the neural crest cell fates.

1.1.2 Fibroblast growth factor signaling promotes PPR identity

PPR formation requires fine-tuning of BMP activity levels but also high levels of fibroblast growth factor (FGF) signaling (Ahrens & Schlosser, 2005; Glavic

et al., 2003; Litsiou, Hanson, & Streit, 2005). Remarkably, *cvl2* induced by Dlx3b and Dlx4b promotes competence to respond to FGF signaling in the PRR, mainly through the regulation of expression of FGF receptors and the FGF targets *erm* and *spry4 specification* (Esterberg & Fritz, 2009). Using heat-shock-inducible transgenes and a pharmacological inhibitor to modulate signaling, Kwon et al. (2010) found that FGF combined with BMP attenuation is sufficient to induce PPR markers throughout the nonneural ectoderm in a manner similar to that previously shown in frog and chick embryos (Ahrens & Schlosser, 2005; Litsiou et al., 2005) (Fig. 2A). Finally, FGF and platelet-derived growth factor A (PDGFa), which is expressed dorsally during gastrulation (Kudoh, Concha, Houart, Dawid, & Wilson, 2004; Liu, Korzh, Balasubramaniyan, Ekker, & Ge, 2002), appear to act in a partially redundant manner during PPR specification (Kwon et al., 2010).

1.1.3 Wnt and retinoic acid signaling and the PPR domain

The Wingless integrated protein (Wnt) signaling pathway has been proposed to antagonize PPR specification. Elevated Wnt signaling in chick and *Xenopus* represses PPR markers, whereas secreted anti-Wnt factors expand them (Hong & Saint-Jeannet, 2007; Litsiou et al., 2005). In zebrafish, Wnts and their antagonists are expressed in the anterior neural plate and the underlying mesoendoderm leading to a proposed "low anterior to high posterior" Wnt activity gradient (Cavodeassi, 2014). It has been demonstrated that sets of regulatory elements at two genes required for NB specification (*pax3a* and *zic3*) integrate the activities of Wnt, FGF, and BMP signaling (Garnett, Square, & Medeiros, 2012). Interestingly, however, while these elements drive expression in largely overlapping domains at the NB, they respond to different combinations of BMP, Wnt, and FGF signals; while BMP and Wnt are required for expression of both *pax3a* and *zic3*, FGF signaling is specifically required for proper expression of *pax3a* but not *zic3* (Fig. 2A) (Garnett et al., 2012).

Finally, the signaling cocktail required to induce PPR markers also appears to include retinoic acid (RA). In *Xenopus*, the RA synthesizing enzyme Raldh2 is expressed in the PPR (Chen, Pollet, Niehrs, & Pieler, 2001; Shiotsugu et al., 2004) and RA signaling limits PPR development to the head (Shiotsugu et al., 2004). It, however, remains to be investigated whether these mechanisms are conserved in zebrafish. On the other hand, epistatic analysis of the function of FGF, Wnt, and RA has been performed concerning the patterning of the neural ectoderm in zebrafish along the anteroposterior axis (Kudoh, Wilson, & Dawid, 2002). It would be interesting to use the same tools to determine the epistatic relationship of these signals during neural border formation and PPR and/or neural crest cell fates choice. Furthermore, it is now possible to generate detailed and dynamic spatiotemporal maps of BMP, FGF, Wnt, and RA activity at cellular resolution during early development using transgenic reporter lines and time lapse (for review see Mandal et al., 2013; Moro et al., 2013). These maps should provide precious tools for understanding how signaling pathway activity is integrated at the neural border to induce the PPR fate.

1.2 A GENE REGULATORY NETWORK UNDERLYING PPR SPECIFICATION (FIG. 2A)

The combination of reduced BMP and Wnt signaling and high FGF activity ultimately leads to the expression of specific PPR markers flanking the anterior neural plate. A pair of recent studies has shown that the expression of these PPR markers requires the activity of Tfap2a, Tfap2c, Gata3, and Foxi1, which collectively establish preplacodal competence in the nonneural ectoderm (Bhat, Kwon, & Riley, 2013; Kwon et al., 2010). The combined abrogation of these PPR competence factors using morpholinos results in complete loss of later PPR markers and subsequent defects in the development of all cranial placodes (Kwon et al., 2010). Chemical inhibition of BMP signaling was used to show that the pathway is required only transiently at blastula stages to induce the expression of these competence factors, which then become independent of BMP signaling (Kwon et al., 2010). Using inducible heat-shock transgenes together with transient loss of function of BMP signaling, it was shown that *tfap2a*, *tfap2c*, *gata3*, and *foxi1* form a self-maintaining gene regulatory network, with robustness in this PPR competence network being achieved through mutual cross-activation (Bhat et al., 2013). These factors not only maintain their own expression but also feed back onto the signaling pathways that induced their expression. For instance, both Gata3 and Foxi1 inhibit BMP signaling (Yao et al., 2014).

Genes specifically expressed in the PPR downstream of the competence factors mentioned in the previous paragraph include members of the *Eyes absent* (*Eya*)/*Sine oculis* (*Six*)/*Dachshund* (*Dach*), Distalless (*Dlx*), and *Iroquois* (*Irx*) gene families (Ahrens & Schlosser, 2005; Bhat et al., 2013; Brugmann, Pandur, Kenyon, Pignoni, & Moody, 2004; Glavic et al., 2003; Kwon et al., 2010; Litsiou et al., 2005; Nguyen et al., 1998). In zebrafish, *dlx3b* is the earliest specific marker of the PPR, starting around 8 h postfertilization (hpf) in the nonneural ectoderm and increasing until late gastrulation (Akimenko, Ekker, Wegner, Lin, & Westerfield, 1994; Esterberg & Fritz, 2009; Solomon & Fritz, 2002; Woda, Pastagia, Mercola, & Artinger, 2003). By 10 hpf, *six4b* (Bhattacharyya et al., 2004; Kobayashi, Osanai, Kawakami, & Yamamoto, 2000) and *eya1* are detected in the PPR. Finally, a member of the Iroquois (Irx) homeobox transcription factor family, *irx1b*, is also expressed in the PPR starting around 10 hpf (Lecaudey, Anselme, Dildrop, Rüther, & Schneider-Maunoury, 2005). Using cell transplantation and constitutively active and dominant negative forms of Irx1b both in zebrafish and *Xenopus*, it was shown that this factor is required for PPR specification (Glavic et al., 2003). Likewise, the analyses of *six1b* and *eya1* mutants and morphants in mouse and zebrafish have confirmed their role in the development of cranial placode derivatives. Indeed, the abrogation of the function of these factors leads to defects in multiple sensory organs, and particularly in zebrafish to inner ear malformations (Bricaud & Collazo, 2006; Nica et al., 2006); in the zebrafish *eya1* mutant, defects are found in the inner ear and the lateral line sensory systems (Kozlowski, Whitfield, Hukriede, Lam, & Weinberg, 2005). In mouse, these genes are involved in the formation of many sensory organs, the

adenohypophysis, olfactory epithelium, trigeminal ganglion, inner ear, and epibranchial ganglia (Ikeda, Watanabe, Ohto, & Kawakami, 2002; Laclef, Souil, Demignon, & Maire, 2003; Li et al., 2003; Ozaki, Watanabe, Ikeda, & Kawakami, 2002; Xu et al., 1999; Zheng et al., 2003; Zou, Silvius, Fritzsch, & Xu, 2004).

Other genes expressed in partially overlapping domains in the neural crest and PPR at the neural border include the muscle segment homeobox genes *msx1b*, *msx3*, and *msx1a*. Combined loss of function of these genes blocks neural crest differentiation, whereas the PPR-derived placodes show elevated levels of apoptosis and are reduced in size (Phillips et al., 2006). As for *dlx* genes, *msx* genes are well-known Bmp targets in vertebrate (Esteves et al., 2014; Feledy et al., 1999; Tribulo, Aybar, Nguyen, Mullins, & Mayor, 2003; Yamamoto, Takagi, & Ueno, 2000). While it remains unclear how *dlx* and *msx* expressing domains segregate after their induction by BMP signaling, it is tempting to speculate that this is achieved through reciprocal inhibition. Indeed, Msx proteins have been described as antagonists of *dlx* genes during development (Suzuki, Ueno, & Hemmati-Brivanlou, 1997, reviewed in Bendall & Abate-Shen, 2000). Furthermore, the loss of function of *msx* genes is able to restore expression of the PPR marker *six4b* in embryos harboring a deletion containing *dlx3b* and *dlx4b* (Solomon & Fritz, 2002), again suggesting an interaction between these two gene families.

Finally, members of the Pax (Krauss, Johansen, Korzh, & Fjose, 1991) and Zic families, in particular *pax3a* and *zic3*, are also expressed during gastrulation at the neural border. As mentioned above, evolutionarily conserved neural borders enhancers associated with these two genes have been characterized that integrate different combinations of FGF, BMP, and Wnt signaling (Garnett et al., 2012).

1.3 ANTEROPOSTERIOR REGIONALIZATION OF THE PPR (FIG. 2B)

Shortly after the establishment of the PPR, gene expression analysis and fate mapping data show that distinct placodal primordia become apparent. This is exemplified by the broad expression of *pax6b*, *pax3a* and *pax2, pax8* in specific domains within the PPR (Pieper et al., 2011). In this section, we will touch on what is known concerning the molecular mechanisms that control anteroposterior patterning within the PPR and mention factors linked with the development of specific placodes.

After gastrulation, *pax* gene expression distinguishes three large placodal primordia along the anteroposterior axis: a large anterior primordium (adenohypophyseal, olfactory, lens), a smaller intermediate primordium (trigeminal placode), and a large posterior primordium (otic, epibranchial, and lateral line). As for the formation of the PPR itself, the establishment of these primordia requires the input of signaling cascades and regional expression of sets of transcription factors but currently less is known about this process in the fish. It is known, however, that subdivision of the PPR happens synchronously with anteroposterior regionalization in the adjacent neural plate, which is characterized by positioning the midbrain–hindbrain boundary (MHB). Toward the end of gastrulation the future MHB is manifested by the border

between the expression of two transcription factors: *otx* (*orthodenticle homeobox*) anteriorly and *gbx* (*gastrulation brain homeobox*) posteriorly (Hibi & Shimizu, 2012; Kiecker & Lumsden, 2012; Raible & Brand, 2004; Rhinn, Lun, Luz, Werner, & Brand, 2005). In the zebrafish, the mutually exclusive expression of *otx2* and *gbx1* is achieved by reciprocal inhibition between these two factors, and with the control of *gbx1* expression requiring the posteriorizing activity of Wnt signaling (Rhinn, Lun, Ahrendt, Geffarth, & Brand, 2009). Interestingly, in chick and *Xenopus*, mutual repression between Gbx and Otx family members not only patterns the neural plate but also the adjacent placodal territory, leading to segregation of otic and trigeminal progenitors (Steventon, Mayor, & Streit, 2012). Similarly in the mouse, Gbx2 is necessary posteriorly for otic vesicle morphogenesis after placode formation (Lin, Cantos, Patente, & Wu, 2005); anteriorly, Otx2 cooperates with Notch signaling to induce lens fate (Ogino, Fisher, & Grainger, 2008). It remains to be addressed whether the Gbx−Otx couple regulates the segregation of the PPR in the zebrafish.

In *Xenopus*, *Gbx2* is among the earliest factors to promote posterior PPR identity and appears to play a dual role (Steventon et al., 2012)—it first represses *otx2* expression and later drives *pax8* and *pax2* expression. These latter factors are critical for normal ear development in zebrafish, chick, and mice (Bouchard, de Caprona, Busslinger, Xu, & Fritzsch, 2010; Burton, Cole, Mulheisen, Chang, & Wu, 2004; Christophorou, Mende, Lleras-Forero, Grocott, & Streit, 2010; Mackereth, Kwak, Fritz, & Riley, 2005; Torres, Gómez-Pardo, Dressler, & Gruss, 1995); while concomitant abrogation of *pax2a*, *pax2b*, and *pax8* function in zebrafish using morpholinos leads to a small otic placode that will ultimately degenerate (Mackereth et al., 2005), overexpression of *pax2a* favors otic at the expense of epibranchial placode differentiation (McCarroll et al., 2012). Intriguingly, the *pax2a*, *pax2b*, and *pax8* loss of function phenotype is reminiscent of the knockdown of *fgf3* activity in *fgf8* (*acerebellar* or *ace*) mutants, and indeed, posterior PPR cells in *Fgf*-deficient embryos fail to express *pax8* and *pax2a* (Phillips, Bolding, & Riley, 2001). FGF3 and FGF8 from the hindbrain and adjacent mesendoderm induce not only *pax* gene expression but also that of *sox3* in preotic cells. In this context, specific responsiveness to FGF requires the competence factor Foxi1, which has, at these stages, become restricted to the otic and epibranchial regions. By 12 hpf, Pax8 in turn induces expression of *fgf24* and represses otic expression of *foxi1*. FGF24 then downregulates otic expression of *sox3* while inducing it in adjacent epibranchial cells (Padanad, Bhat, Guo, & Riley, 2012); FGF10b also participates in the late phase of otic placode induction (Maulding, Padanad, Dong, & Riley, 2014). Finally, Wnt signaling also plays a role in otic placode patterning via regulation of *pax* gene expression (McCarroll et al., 2012). Here, increasing Wnt activity at early somite stages causes *pax2a* upregulation and an enhanced recruitment of cells into otic placode, and blocking Wnt signaling has the opposite effect.

At an intermediate level in the PPR, the chick PDGF receptor beta is expressed in the cranial ectoderm at the time of trigeminal placode formation, while the corresponding ligand is expressed in the adjacent midbrain neural folds. Antagonizing

PDGF signaling abrogates *pax3* expression and impairs trigeminal placode induction (McCabe & Bronner-Fraser, 2009). The functions of PDGF in trigeminal placode induction remain to be elucidated in zebrafish. Two Iroquois transcription factors, *irx1b* and *irx7*, are expressed in zebrafish trigeminal placode and loss of function analysis reveals that *irx7* is required for correct trigeminal placode development (Itoh, Kudoh, Dedekian, Kim, & Chitnis, 2002). Whether this reflects a role in patterning or neurogenesis is unclear, however, as the trigeminal placode is largely composed of sensory neurons and defects in either patterning or neurogenesis would result in similar phenotypes. Another transcription factor expressed in zebrafish trigeminal progenitors is the *T-cell leukemia, homeobox 3b*, *tlx3b* (Langenau et al., 2002), but here again functional requirements for this gene in trigeminal placode remain to be addressed. Finally, the dynamic expression of pitx3 (*pairedlike homeodomain 3*) in the PPR suggests that this gene marks a common step in patterning of the trigeminal placode as well as the pituitary, lens, and olfactory placodes (Zilinski, Shah, Lane, & Jamrich, 2005).

Anteriorly, signals from the mesendoderm are required for lens and olfactory placode formation in both zebrafish and chick embryos (Devos et al., 2002; Lleras-Forero et al., 2013). For example, somatostatin first regulates and then cooperates with nociceptin to control *pax6b* expression in anterior placodal progenitors. Unlike the *gbx—otx* system, this study shows that nociceptin signaling controls anterior placode development without affecting neural plate development. Conversely, FGF signals emanating from the posterior head mesoderm inhibit anterior placode identity (Lleras-Forero et al., 2013). Here, the interplay between two previously mentioned PPR competence factors, Gata3 and Foxi1, and FGF signaling shapes the activity gradient of the pathway along the anteroposterior axis allowing the development of different anterior versus posterior placodal identities (Yao et al., 2014).

Another marker of the anterior placode domain is *pitx3* (Zilinski et al., 2005). Knockdown analysis using morpholinos revealed a function for this gene in lens and retina development, without affecting olfactory development (Shi et al., 2005). In *Xenopus*, *Dmrt4* (*Doublesex-relate*d 4) also initially labels the anterior placode domain (Huang, Hong, O'Donnell, & Saint-Jeannet, 2005) and it was shown that reducing Dmrt4 function specifically affects neurogenesis in the olfactory placode. In the teleost Medaka, *dmrt4* is also expressed in the developing olfactory system (Winkler et al., 2004); however, its function in olfactory placode patterning has not been addressed yet. Finally, three members of the *emx* (empty spiracles homeobox) transcription factor family are expressed in the anterior placode domain, and more specifically in the olfactory placode but, here again, functional analyses are lacking (Viktorin, Chiuchitu, Rissler, Varga, & Westerfield, 2009); *Emx2*-knockout mice display smaller olfactory bulbs (Bishop, Garel, Nakagawa, Rubenstein, & O'Leary, 2003). In conclusion, makers of the anterior placode domain in the PPR have mainly been identified based on expression and further functional analysis of these genes will be required in order to understand their role in early anterior placode specification.

2. CRANIAL PLACODE MORPHOGENESIS AND NEUROGENESIS (FIG. 3)

After individualization of specific placodes in the PPR domain, distinct morphogenetic processes will sculpt the final forms of the placodal derivatives (reviewed in Breau & Schneider-Maunoury, 2014; Schlosser, 2010, 2014, 2015). Simultaneously, neurogenesis in certain placodes will produce distinct neuronal subtypes characteristic of the mature placode-derived organs. In this section, we will address the mechanisms underlying morphogenesis and neurogenesis, specifically concentrating on the olfactory, trigeminal, and otic placodes and their derivatives (Fig. 3).

2.1 OLFACTORY PLACODE

The olfactory placode arises from an extended cellular field stretching along the lateral edge of the anterior neural plate (Fig. 3A) (Whitlock, 2004, 2008; Whitlock & Westerfield, 2000 and for reviews see Breau & Schneider-Maunoury, 2014, 2015; Maier, Saxena, Alsina, Bronner, & Whitfield, 2014; Miyasaka et al., 2013). Analysis of early olfactory placode morphogenesis in the zebrafish was first reported 15 years ago (Whitlock & Westerfield, 2000). In this study, fate mapping of cells labeled with fluorescent dextrans in the anterior neural plate indicated that the olfactory placodes develop via anterior convergence of progenitor cells (Whitlock & Westerfield, 2000). More recently, using a *Tg(βeta-actin:GAP-43-GFP)* transgenic line combined with the nuclear marker H2B-RFP, the same laboratory demonstrated the existence of coordinated cells movement within the population of olfactory placode progenitors (Torres-Paz & Whitlock, 2014). A similar live imaging approach showed that cranial neural crest cells associate closely with the forming olfactory placode, suggesting coordination between anterior neural crest migration and olfactory placode condensation (Harden et al., 2012). Finally, live imaging studies using a *Tg(sox10:eGFP)* transgenic line have shown that neural crest cells invade the developing olfactory placode and differentiate into a subclass of olfactory sensory neurons (OSNs) (Saxena, Peng, & Bronner, 2013) (Fig. 4B); laser ablation of *sox10:eGFP* positive cells prevents microvillous neurons formation in the olfactory placode.

The molecular mechanisms driving olfactory placode morphogenesis are beginning to be identified. It is known, for instance, that this process requires the chemokine receptor Cxcr4b, and its ligand Cxcl12a (also known as stromal cell-derived factor 1 or Sdf1). Interfering with Cxcl12a or Cxcr4b signaling, either by misexpression of Cxcl12a or in *odysseus* (ody) embryos carrying mutations in *cxcr4b*, affects olfactory placode condensation (Miyasaka, Knaut, & Yoshihara, 2007). Subsequently, while *cxcr4b* expression persists within the olfactory placode, *cxcl12a* is expressed along the placode—telencephalon border prefiguring the projection route of mature OSNs axons. In keeping with a role for chemokine signaling in the targeting of olfactory projections to the brain, OSN axons frequently fail to exit the olfactory placode and accumulate near the placode—telencephalon border in the absence of Cxcr4b-mediated signaling (Miyasaka et al., 2007). Whether this reflects a role of

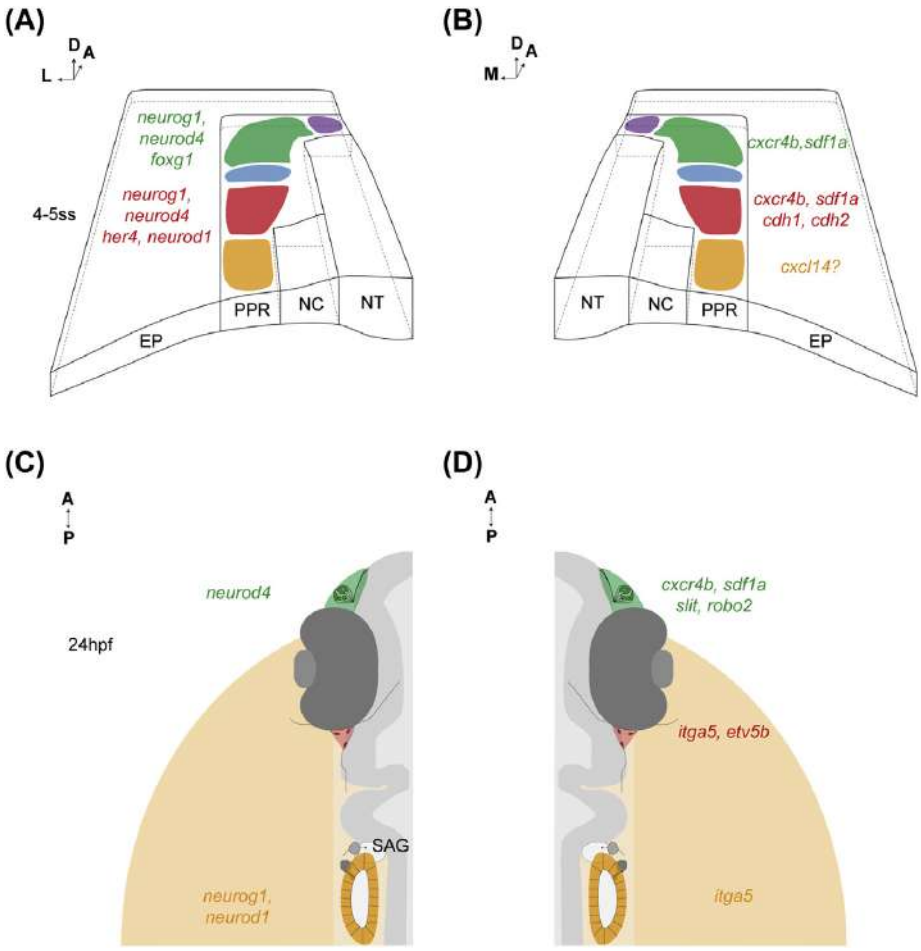

FIGURE 3 Neurogenesis and morphogenesis of olfactory, trigeminal, and otic placodes.

(A, C) Genes essential for neurogenesis of olfactory, trigeminal, and otic placodes at the 4–5 ss (A) and at 24 hpf (C). (B, D) Genes required for morphogenesis of these placodes at the 4–5 ss (B) and at 24 hpf (D). Genes specific of the olfactory (green), trigeminal (red), and otic (orange) placode are color coded. *NT*, neural tube; *EP*, epidermis; *NC*, neural crest cells; *PPR*, preplacodal region; *4–5 ss*, 4–5 somite stages; *hpf*, hours postfertilization. (See color plate)

Cxcr4-Cxcl12 signaling during the guidance of olfactory neuron projects to the olfactory bulb or is a secondary consequence of an earlier morphogenesis defect is not clear. Finally, Robo and Slit, Semaphorin, Ephrin and Netrin signaling have also been implicated in the guidance and fasciculation of olfactory neuron projections (Cutforth et al., 2003; Lakhina et al., 2012; Miyasaka et al., 2005; Schwarting et al., 2000; Taniguchi et al., 2003).

Neurogenesis in the olfactory placodes has been studied in depth in the mouse, and more recently in the zebrafish. In the adult zebrafish, four classes of OSNs have

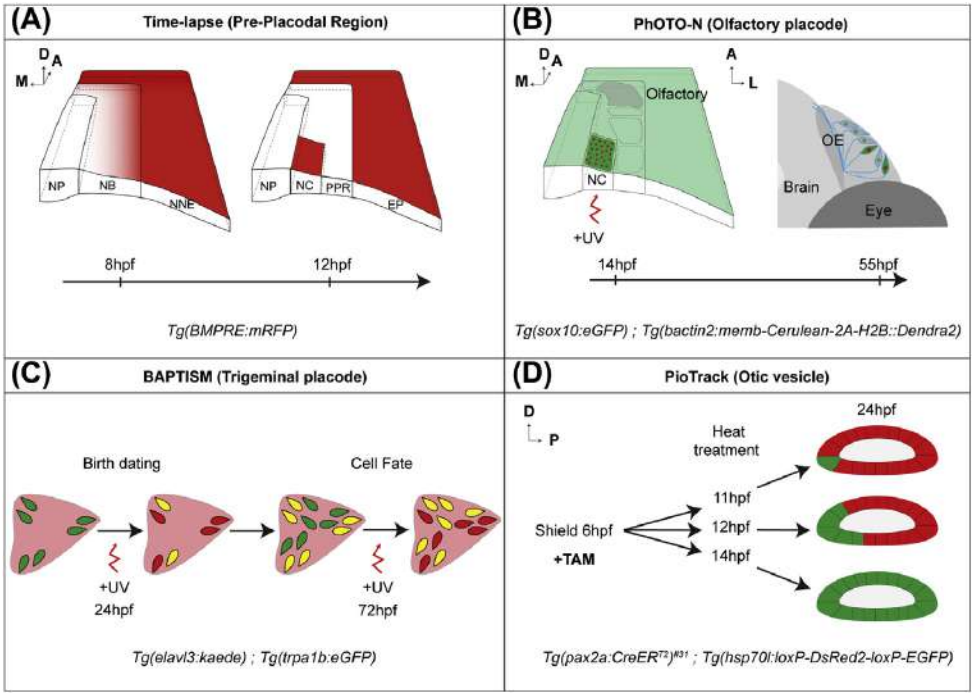

FIGURE 4 Sophisticated methodologies developed in zebrafish to study cranial sensory placodes development.

Examples of cutting of the edge technics elaborated in zebrafish to study cell fate in (A) ectoderm territories, (B) olfactory placode, (C) trigeminal placode, and (D) otic placode. (A) BMP activity reporter during ectodermal patterning (Reichert et al., 2013). (B) Photoconvertible fate mapping with the Photo-N fish (Dempsey, Fraser, & Pantazis, 2012) expressing a nuclear localized version of the highly stable photoconvertible (green to red) protein Dendra2 leading to the intriguing conclusion that NC contribute to olfactory sensory neurons (Saxena et al., 2013). (C) Neuronal birthdate determination using BAPTI (birthdating analysis by photoconverted fluorescent protein tracing in vivo) and neuronal specification using BAPTI combined with subpopulation markers, or BAPTISM, provide evidences that the timing of neurogenesis regulates trigeminal sensory neuron identity (Caron et al., 2008). (D) A Cre-mediated lineage-tracing method called pioneer tracking or PioTrack developed by Hans and collaborators analysing the pax2 positive cells contribution to the otic vesicle during development (Hans et al., 2013). *NP*, neural plate; *NB*, neural border; *NNE*, nonneural ectoderm; *EP*, epidermis; *NC*, neural crest cells; *PPR*, preplacodal region: *OE*, olfactory epithelium; *TAM*, tamoxifen; *UV*, ultraviolet irradiation. (See color plate)

been identified (Ahuja et al., 2014); basally located ciliated and microvillous neurons, and apically located crypt and kappe neurons (Fig. 1C). Each subtype displays specific gene expression profile, and differ both in patterns of innervation and function (Ahuja et al., 2013; Bazáes, Olivares, & Schmachtenberg, 2013; Gayoso,

Castro, Anadón, & Manso, 2012; Hansen & Zielinski, 2005 as a review); the ciliated and microvillous subtypes are predominant and make up at least 85% of the total OSN numbers (Ahuja et al., 2014).

The molecular mechanisms underlying olfactory neurogenesis at embryonic stages are beginning to be unraveled. For instance, it has been shown that a member of the Forkhead family of the winged helix transcription factors, Foxg1 (*forkhead box g1*), is required for patterning, proliferation, differentiation, and cell fate determination of progenitor cells of both the olfactory placodes and the olfactory bulb (Hanashima, Fernandes, Hebert, & Fishell, 2007; Hanashima, Li, Shen, Lai, & Fishell, 2004; Shen, Nam, Song, Moore, & Anderson, 2006); Foxg1 knockout mice ultimately fail to form olfactory structures and a similar phenotype is seen after *foxg1a* knockdown in zebrafish embryos (Duggan, DeMaria, Baudhuin, Stafford, & Ngai, 2008). Studies both in mice and zebrafish suggest that Foxg1 controls olfactory neurogenesis upstream of so-called proneural genes (Duggan et al., 2008), with maintenance of neurogenesis apparently requiring microRNAs of the miR-200 family in both species (Choi et al., 2008). Downstream of Foxg1, genetic analyses in mice have revealed that the sequential activity of members of the Ascl and Atonal families of bHLH proneural transcription factors controls olfactory neurogenesis (Cau, Casarosa, & Guillemot, 2002; Cau, Gradwohl, Fode, & Guillemot, 1997; Guillemot et al., 1993; Nicolay, Doucette, & Nazarali, 2006). Interestingly, while proneural genes are also required in fish, here only Atonal family members appear to be involved. Indeed, we have recently shown that Neurog1 and Neurod4 act in a partially redundant manner during the generation of both early born olfactory neurons (EONs) and mature OSNs (Madelaine, Garric, & Blader, 2011).

Intriguingly, neurogenesis in the olfactory placode in the zebrafish is concomitant with morphogenesis (Madelaine et al., 2011; Whitlock & Westerfield, 1998); early born olfactory neurons leave the cell cycle throughout the period of olfactory placode condensation (Madelaine et al., 2011) and provide the axonal scaffold followed later by OSN projections (Whitlock & Westerfield, 1998). While we now have a growing understanding of the mechanisms controlling either olfactory placode morphogenesis or neurogenesis individually, how these processes are coordinated has yet to be determined.

2.2 TRIGEMINAL PLACODE

The trigeminal placode is composed of neural crest and placodal-derived cells that ultimately form compact ganglia on either side of the head between eye and ear (Fig. 1D) (Davies, 1988; Schlosser, 2014); trigeminal sensory neurons are placodal derived, whereas the glial component of these ganglia is crest derived (Schlosser, 2014). Trigeminal sensory neurons extend peripheral dendrites throughout the skin of the head, to detect mechanical, chemical, and thermal stimuli, and central axons into the hindbrain, to communicate these inputs to the central nervous system (Baker & Bronner-Fraser, 2001; Hamburger, 1961). In zebrafish, by 24 hpf, the trigeminal ganglia are functional and mediate response to mechanical stimulation of the head,

resulting in a highly stereotypic and well-studied escape behavior (Andermann, Ungos, & Raible, 2002; Saint-Amant & Drapeau, 1998).

Studies in zebrafish embryos have shown that trigeminal sensory neurons are born from a dispersed group of progenitors that coalesce into a ganglion during early gastrulation (Knaut, Blader, Strähle, & Schier, 2005). More recently, the dynamics of this process have been studied by live imaging of a *Tg(neurod:eGFP)* transgenic line. In this manner, it was established that *neurod* expressing trigeminal neuronal progenitors were initially scattered at the end of gastrulation but then rapidly converged into a compact placode (Bhat & Riley, 2011). As for the olfactory placode, Knaut et al. (2005) showed that in the trigeminal ganglia, this process requires Cxcr4b and Cxcl12a; *ody* mutant trigeminal ganglia condense poorly and misexpression of the ligand can lead to inappropriate positioning of the ganglia. Interactions between cells and components of the extracellular matrix are involved in these Cxcr4b- and Cxcl12a-dependent morphogenetic movements. For instance, by cell transplantation, it was shown that the adhesion molecules E- and N-cadherin (cdh1 and cdh2, respectively) participate in ganglion assembly (Knaut et al., 2005). Similarly, morpholino knockdown of integrin-α5 leads to trigeminal sensory neuron migration defects (Bhat & Riley, 2011). The same actors described for the trigeminal ganglia morphogenesis have also been implicated in *Xenopus* epibranchial placode coalescence, in a process that requires reciprocal interactions between placodal cells and the neural crest cells (Theveneau et al., 2013). Indeed, neural crest cells chase placodal cells in an Sdf1-dependent manner in a mechanism that also involves Wnt−planar cell polarity and N-cadherin signaling (Theveneau et al., 2013). It will be interesting to determine if Wnt−planar cell polarity is also involved in trigeminal placode morphogenesis in the zebrafish.

Two distinct subpopulations of trigeminal neurons are specifically labeled by the expression of *trpa1b* (*transient receptor potential cation channel, subfamily 1, member 1b)* and *p2x3 receptor* (*p2rx3b*, an ATP sensor), which correspond to neurons responsive to chemical irritants (Bandell et al., 2004; Jordt et al., 2004) and neurons involved in the modulation of nociceptive signals (Chen, Gu, & Huang, 1995), respectively. Using a pair of in vivo birthdating techniques (BAPTI and BAPTISM), the temporal dynamics of trigeminal neurogenesis in living zebrafish embryos has been decoded (Fig. 4C) (Caron, Prober, Choy, & Schier, 2008). In this manner, it was demonstrated that early born neurons are competent to form both *trpa1b* and *p2rx3b* expressing neurons, whereas late-born neurons are restricted in their cell-type specification. Neurogenesis in the trigeminal ganglia is affected in zebrafish embryos carrying mutations in *neurog1* (Andermann et al., 2002; Cornell & Eisen, 2002; Golling et al., 2002). While simultaneous knockdown of *neurog1* and *neurod4* results in a fully penetrant reduction of neural marker gene expression at early stages (So et al., 2009; Yeo, Kim, Kim, Huh, & Chitnis, 2007), at later stages a ganglion is generated with a reduced number of neurons in the absence of Neurog1 function alone (Caron et al., 2008). Intriguingly, the residual trigeminal sensory ganglia of *neurog1*-deficient embryos are composed solely of the late-born neuron subtype. Thus, the timing of neurogenesis appears crucial for orchestrating the specification

of fully functional trigeminal sensory ganglia, and cell fate restriction of late-born trigeminal neurons can occur independently of early born neurons (Caron et al., 2008).

2.3 OTIC PLACODE

As in other vertebrates, the zebrafish inner ear is composed of sensory components involved in controlling balance and detecting vibrations. These two functions require so-called sensory patches (known as cristae, saccules, and utricles) that are made of mechanosensory hair cells and surrounding support cells (reviewed in Nicolson, 2005a, 2005b). While a set of three cristae sense the position of the head and angular acceleration by detecting fluid flow through the semicircular canals, the saccule has a more pronounced role in hearing; as for the cristae, the utricle seems devoted to vestibular function. Hair cells in these sensory patches synapse with neurons of the SAG, the axons of which project to nuclei in the hindbrain. While morphogenesis of this highly complex structure has been studied, here we will concentrate only on the initial steps of the process (placode formation and cavitation). Similarly, patterning within the otic vesicle leading to the emergence of the neural (SAG) and nonneural components of the inner ear (hair and support cells) has been intensively studied. Here, however, we will only focus on what is known concerning the formation of the SAG.

As for the olfactory and trigeminal placodes mentioned above, the formation of the otic placode requires coordinated convergence movements within the PPR. Using a *pax2a:GFP* reporter transgene to label the posterior PPR, otic morphogenesis has been investigated in living embryos (Bhat & Riley, 2011). Results from these studies highlight that, unlike the placodes described in previous sections, the convergence of cells of the future otic placode undergo several oriented steps of migration—first medially, then centripetally, and finally anteroposteriorly. Despite this complication, similar molecules appear to be involved. For instance, reducing Itga5 function affects otic placode convergence (Bhat & Riley, 2011); Itga5 appears to works with the FGF target gene *erm* (*etv5b*) in this process. Finally, while the chemokine *cxcl14* is expressed in otic placodes, no role for chemokines signaling has yet been reported during morphogenesis of the ear (Long, Quint, Lin, & Ekker, 2000).

Unlike the olfactory and trigeminal placodes, after convergence of the otic placodes, a lumen develops giving rise to the otic vesicle. Using high-resolution 4D imaging, it has been demonstrated that otic lumenogenesis can be divided into two phases, early lumen assembly (13−17 hpf) and lumen expansion (17−23 hpf) (Hoijman, Rubbini, Colombelli, & Alsina, 2015). Morphogenetic mechanisms driving these phases include active thinning of the epithelium combined with fluid loss from cells of the otic epithelium, which drives expansion of the newly formed lumen. Concomitantly, mitotic rounding during cell division contributes mechanically to the expansion of the lumen by orienting the contraction of the epithelium (Hoijman et al., 2015). The *lethal giant larvae 2* (*lgl2*) gene has been implicated

in controlling lumenogenesis of the otic vesicle and other luminal structures (Tay et al., 2013). How defects that arise in luminogenesis due the loss of function of *lgl2* relate to the two phases described by Hoijman et al. remains an open question.

It is well known that extrinsic signals from surrounding tissues are integrated by cells of the otic vesicle contributing to the complex three-dimensional organization of the organ and the generation of the stereotyped pattern of sensory neuron progenitors, hair cells, and supporting cells at specific positions in the otic vesicle (Bok, Bronner-Fraser, & Wu, 2005; Schneider-Maunoury & Pujades, 2007; Whitfield & Hammond, 2007). The generation of sensory neurons of the future SAG is restricted to an anteromedial subdomain of the otic vesicle in a process that depends on FGF, Notch, BMP, Hedgehog signaling, and RA (Alsina et al., 2004; Haddon, Jiang, Smithers, & Lewis, 1998; Hammond & Whitfield, 2011; Léger & Brand, 2002; Maier & Whitfield, 2014; Millimaki, Sweet, Dhason, & Riley, 2007). Using an inducible labeling of *pax2* expressing cells (PioTrack method), it was elegantly shown that *pax2* positive cells contribute to the neurogenesis domain (Hans, Irmscher, & Brand, 2013) (Fig. 4D). Downstream of these signals, transcription factors such as Tpaf2a, Foxi1, and Tbx1 are required to specify the otic neurogenic territory (Hans et al., 2013; Kantarci, Edlund, Groves, & Riley, 2015; Radosevic, Robert-Moreno, Coolen, Bally-Cuif, & Alsina, 2011). After specification, neuronal precursors delaminate as neuroblasts that will give rise to the SAG in a *neurog1*-dependent fashion (Adamska et al., 2000; Andermann et al., 2002; Bermingham et al., 1999; Haddon & Lewis, 1996; Ma, Chen, del Barco Barrantes, de la Pompa, & Anderson, 1998; Rubel & Fritzsch, 2002). Upon delamination from the otic epithelium, neuroblasts quickly switch from expressing *neurog1* to expressing a second bHLH transcription factor, *neurod*, as well as the homeodomain encoding gene *hmx3a* (Adamska et al., 2000; Andermann et al., 2002; Korzh, Sleptsova, Liao, He, & Gong, 1998). *neurod1* expressing cells comprise a so-called transit-amplifying pool of proliferative progenitors that will differentiate into mature neurons after a limited number of cell divisions (Camarero et al., 2003).

As during the olfactory and trigeminal neurogenesis, there are two waves of otic neurogenesis along the anteroposterior axis within the SAG that correlate with topographic position of the sensory epithelia in the otic vesicle (Kantarci et al., 2015; Sapède & Pujades, 2010; Vemaraju, Kantarci, Padanad, & Riley, 2012). Deciphering the conservation of signaling networks and cell behaviors, underlying these two waves of neuron production among these different placodes provides an interesting challenge for future research.

CONCLUSIONS

Cranial sensory placodes generate key organs required for vertebrates to decode their environment accurately. Since the middle of the 19th century, elegant studies using chick, *Xenopus*, and mice have shed light on the developmental programs that control cranial placode specification and differentiation. More recently, studies

in the zebrafish have highlighted the utility of this model for studying placode development. Thanks to state-of-the-art imaging techniques, important contributions to our understanding of cranial placode development have been made using the zebrafish model (Fig. 4). Indeed, the generation of transgenic zebrafish lines enabling temporally controlled gene overexpression or specific cell types/domain labeling has greatly contributed to the study of signaling pathways and gene regulatory networks controlling trigeminal, olfactory, and otic placode development (Table 1). Similarly, mutant lines generated in classical forward genetic screens or with recently developed genome editing strategies have also helped in understanding placode development (Table 2). This said, specific genetic tools are still lacking to label particular placodal cell types and early ectodermal domains. Hopefully, the advent of Crispr-Cas9 knock-in tools and others will soon provide us with a complete set of approaches for understanding cranial sensory placode development (for reviews Auer, Duroure, De Cian, Concordet, & Del Bene, 2014; Gonzales & Yeh, 2014).

ACKNOWLEDGMENTS

This work was supported by the Centre National de la Recherche Scientifique (CNRS); the Institut National de la Santé et de la Recherche Médicale (INSERM); Université de Toulouse III (UPS); Fondation pour la Recherche Médicale (FRM; DEQ20131029166); Fédération pour la Recherche sur le Cerveau (FRC); Association pour la Recherche sur le Cancer (ARC; SFI20101201699 and PJA 20131200173); and the Ministère de la Recherche. Authors apologize to the many authors whose research has not been cited.

REFERENCES

Adamska, M., Léger, S., Brand, M., Hadrys, T., Braun, T., & Bober, E. (2000). Inner ear and lateral line expression of a zebrafish Nkx5-1 gene and its downregulation in the ears of FGF8 mutant, ace. *Mechanisms of Development, 97*(1−2), 161−165. Retrieved from: http://www.ncbi.nlm.nih.gov/pubmed/11025218.

Ahrens, K., & Schlosser, G. (2005). Tissues and signals involved in the induction of placodal Six1 expression in *Xenopus laevis*. *Developmental Biology, 288*(1), 40−59. http://dx.doi.org/10.1016/j.ydbio.2005.07.022.

Ahuja, G., Bozorg Nia, S., Zapilko, V., Shiriagin, V., Kowatschew, D., Oka, Y., & Korsching, S. I. (2014). Kappe neurons, a novel population of olfactory sensory neurons. *Scientific Reports, 4*, 4037. http://dx.doi.org/10.1038/srep04037.

Ahuja, G., Ivandic, I., Saltürk, M., Oka, Y., Nadler, W., & Korsching, S. I. (2013). Zebrafish crypt neurons project to a single, identified mediodorsal glomerulus. *Scientific Reports, 3*, 2063. http://dx.doi.org/10.1038/srep02063.

Akimenko, M. A., Ekker, M., Wegner, J., Lin, W., & Westerfield, M. (1994). Combinatorial expression of three zebrafish genes related to distal-less: part of a homeobox gene code for the head. *The Journal of Neuroscience: The Official Journal of the Society for Neuroscience, 14*(6), 3475−3486. Retrieved from: http://www.ncbi.nlm.nih.gov/pubmed/7911517.

Alsina, B., Abelló, G., Ulloa, E., Henrique, D., Pujades, C., & Giraldez, F. (2004). FGF signaling is required for determination of otic neuroblasts in the chick embryo. *Developmental Biology, 267*(1), 119−134. http://dx.doi.org/10.1016/j.ydbio.2003.11.012.

Andermann, P., Ungos, J., & Raible, D. W. (2002). Neurogenin1 defines zebrafish cranial sensory ganglia precursors. *Developmental Biology, 251*(1), 45−58. Retrieved from: http://www.ncbi.nlm.nih.gov/pubmed/12413897.

Auer, T. O., Duroure, K., De Cian, A., Concordet, J.-P., & Del Bene, F. (2014). Highly efficient CRISPR/Cas9-mediated knock-in in zebrafish by homology-independent DNA repair. *Genome Research, 24*(1), 142−153. http://dx.doi.org/10.1101/gr.161638.113.

Bailey, A. P., Bhattacharyya, S., Bronner-Fraser, M., & Streit, A. (2006). Lens specification is the ground state of all sensory placodes, from which fgf promotes olfactory identity. *Developmental Cell, 11*(4). http://dx.doi.org/10.1016/j.devcel.2006.08.009.

Bailey, A. P., & Streit, A. (2006). Sensory organs: making and breaking the pre-placodal region. *Current Topics in Developmental Biology, 72*, 167−204. Retrieved from: http://www.ncbi.nlm.nih.gov/pubmed/16564335.

Baker, C. V., & Bronner-Fraser, M. (2001). Vertebrate cranial placodes I. Embryonic induction. *Developmental Biology, 232*(1), 1−61. http://dx.doi.org/10.1006/dbio.2001.0156.

Bandell, M., Story, G. M., Hwang, S. W., Viswanath, V., Eid, S. R., Petrus, M. J., & Patapoutian, A. (2004). Noxious cold ion channel TRPA1 is activated by pungent compounds and bradykinin. *Neuron, 41*(6), 849−857. Retrieved from: http://www.ncbi.nlm.nih.gov/pubmed/15046718.

Bazáes, A., Olivares, J., & Schmachtenberg, O. (2013). Properties, projections, and tuning of teleost olfactory receptor neurons. *Journal of Chemical Ecology, 39*(4), 451−464. http://dx.doi.org/10.1007/s10886-013-0268-1.

Bendall, A. J., & Abate-Shen, C. (2000). Roles for Msx and Dlx homeoproteins in vertebrate development. *Gene, 247*(1−2), 17−31. Retrieved from: http://www.ncbi.nlm.nih.gov/pubmed/10773441.

Bermingham, N. A., Hassan, B. A., Price, S. D., Vollrath, M. A., Ben-Arie, N., Eatock, R. A., & Zoghbi, H. Y. (1999). Math1: an essential gene for the generation of inner ear hair cells. *Science (New York, N.Y.), 284*(5421), 1837−1841. Retrieved from: http://www.ncbi.nlm.nih.gov/pubmed/10364557.

Bhat, N., Kwon, H.-J. J., & Riley, B. B. (2013). A gene network that coordinates preplacodal competence and neural crest specification in zebrafish. *Developmental Biology, 373*(1), 107−117. http://dx.doi.org/10.1016/j.ydbio.2012.10.012.

Bhat, N., & Riley, B. B. (2011). Integrin-α5 coordinates assembly of posterior cranial placodes in zebrafish and enhances Fgf-dependent regulation of otic/epibranchial cells. *PLoS One, 6*(12). http://dx.doi.org/10.1371/journal.pone.0027778.

Bhattacharyya, S., Bailey, A. P., Bronner-Fraser, M., & Streit, A. (2004). Segregation of lens and olfactory precursors from a common territory: cell sorting and reciprocity of Dlx5 and Pax6 expression. *Developmental Biology, 271*(2), 403−414. http://dx.doi.org/10.1016/j.ydbio.2004.04.010.

Bhattacharyya, S., & Bronner, M. E. (2013). Clonal analyses in the anterior pre-placodal region: implications for the early lineage bias of placodal progenitors. *The International Journal of Developmental Biology, 57*(9−10), 753−757. http://dx.doi.org/10.1387/ijdb.130155mb.

Bhattacharyya, S., & Bronner-Fraser, M. (2008). Competence, specification and commitment to an olfactory placode fate. *Development (Cambridge, England), 135*(24), 4165−4177. http://dx.doi.org/10.1242/dev.026633.

Bishop, K. M., Garel, S., Nakagawa, Y., Rubenstein, J. L., & O'Leary, D. D. (2003). Emx1 and Emx2 cooperate to regulate cortical size, lamination, neuronal differentiation, development

of cortical efferents, and thalamocortical pathfinding. *The Journal of Comparative Neurology, 457*(4), 345−360. http://dx.doi.org/10.1002/cne.10549.

Bok, J., Bronner-Fraser, M., & Wu, D. K. (2005). Role of the hindbrain in dorsoventral but not anteroposterior axial specification of the inner ear. *Development (Cambridge, England), 132*(9), 2115−2124. http://dx.doi.org/10.1242/dev.01796.

Bouchard, M., de Caprona, D., Busslinger, M., Xu, P., & Fritzsch, B. (2010). Pax2 and Pax8 cooperate in mouse inner ear morphogenesis and innervation. *BMC Developmental Biology, 10*, 89. http://dx.doi.org/10.1186/1471-213X-10-89.

Breau, M., & Schneider-Maunoury, S. (2014). Mechanisms of cranial placode assembly. *The International Journal of Developmental Biology, 58*(1), 9−19. http://dx.doi.org/10.1387/ijdb.130351mb.

Breau, M., & Schneider-Maunoury, S. (2015). Cranial placodes: models for exploring the multifacets of cell adhesion in epithelial rearrangement, collective migration and neuronal movements. *Developmental Biology, 401*(1), 25−36. http://dx.doi.org/10.1016/j.ydbio.2014.12.012.

Bricaud, O., & Collazo, A. (2006). The transcription factor six1 inhibits neuronal and promotes hair cell fate in the developing zebrafish (*Danio rerio*) inner ear. *The Journal of Neuroscience: The Official Journal of the Society for Neuroscience, 26*(41), 10438−10451. http://dx.doi.org/10.1523/JNEUROSCI.1025-06.2006.

Brugmann, S. A., Pandur, P. D., Kenyon, K. L., Pignoni, F., & Moody, S. A. (2004). Six1 promotes a placodal fate within the lateral neurogenic ectoderm by functioning as both a transcriptional activator and repressor. *Development (Cambridge, England), 131*(23), 5871−5881. http://dx.doi.org/10.1242/dev.01516.

Burton, Q., Cole, L. K., Mulheisen, M., Chang, W., & Wu, D. K. (2004). The role of Pax2 in mouse inner ear development. *Developmental Biology, 272*(1), 161−175. http://dx.doi.org/10.1016/j.ydbio.2004.04.024.

Camarero, G., Leon, Y., Gorospe, I., De Pablo, F., Alsina, B., Giraldez, F., & Varela-Nieto, I. (2003). Insulin-like growth factor 1 is required for survival of transit-amplifying neuroblasts and differentiation of otic neurons. *Developmental Biology, 262*(2), 242−253. Retrieved from: http://www.ncbi.nlm.nih.gov/pubmed/14550788.

Caron, S. J. C., Prober, D., Choy, M., & Schier, A. F. (2008). In vivo birthdating by BAPTISM reveals that trigeminal sensory neuron diversity depends on early neurogenesis. *Development, 135*(19), 3259−3269. http://dx.doi.org/10.1242/dev.023200.

Cau, E., Casarosa, S., & Guillemot, F. (2002). Mash1 and Ngn1 control distinct steps of determination and differentiation in the olfactory sensory neuron lineage. *Development (Cambridge, England), 129*(8), 1871−1880. Retrieved from: http://www.ncbi.nlm.nih.gov/pubmed/11934853.

Cau, E., Gradwohl, G., Fode, C., & Guillemot, F. (1997). Mash1 activates a cascade of bHLH regulators in olfactory neuron progenitors. *Development (Cambridge, England), 124*(8), 1611−1621. Retrieved from: http://www.ncbi.nlm.nih.gov/pubmed/9108377.

Cavodeassi, F. (2014). Integration of anterior neural plate patterning and morphogenesis by the Wnt signaling pathway. *Developmental Neurobiology, 74*(8), 759−771. http://dx.doi.org/10.1002/dneu.22135.

Chen, L., Gu, Y., & Huang, L. Y. (1995). The mechanism of action for the block of NMDA receptor channels by the opioid peptide dynorphin. *The Journal of Neuroscience: The Official Journal of the Society for Neuroscience, 15*(6), 4602−4611. Retrieved from: http://www.ncbi.nlm.nih.gov/pubmed/7540680.

Chen, Y., Pollet, N., Niehrs, C., & Pieler, T. (2001). Increased XRALDH2 activity has a posteriorizing effect on the central nervous system of *Xenopus* embryos. *Mechanisms of*

Development, 101(1−2), 91−103. Retrieved from: http://www.ncbi.nlm.nih.gov/pubmed/11231062.

Choi, P. S., Zakhary, L., Choi, W.-Y. Y., Caron, S., Alvarez-Saavedra, E., Miska, E. A., & Dulac, C. (2008). Members of the miRNA-200 family regulate olfactory neurogenesis. *Neuron, 57*(1), 41−55. http://dx.doi.org/10.1016/j.neuron.2007.11.018.

Christophorou, N. A., Mende, M., Lleras-Forero, L., Grocott, T., & Streit, A. (2010). Pax2 coordinates epithelial morphogenesis and cell fate in the inner ear. *Developmental Biology, 345*(2), 180−190. http://dx.doi.org/10.1016/j.ydbio.2010.07.007.

Cornell, R. A., & Eisen, J. S. (2002). Delta/Notch signaling promotes formation of zebrafish neural crest by repressing neurogenin 1 function. *Development (Cambridge, England), 129*(11), 2639−2648. Retrieved from: http://www.ncbi.nlm.nih.gov/pubmed/12015292.

Couly, G., & Le Douarin, N. M. (1990). Head morphogenesis in embryonic avian chimeras: evidence for a segmental pattern in the ectoderm corresponding to the neuromeres. *Development (Cambridge, England), 108*(4), 543−558. Retrieved from: http://www.ncbi.nlm.nih.gov/pubmed/2387234.

Couly, G. F., & Le Douarin, N. M. (1987). Mapping of the early neural primordium in quail-chick chimeras. II. The prosencephalic neural plate and neural folds: implications for the genesis of cephalic human congenital abnormalities. *Developmental Biology, 120*(1), 198−214. Retrieved from: http://www.ncbi.nlm.nih.gov/pubmed/3817289.

Cutforth, T., Moring, L., Mendelsohn, M., Nemes, A., Shah, N. M., Kim, M. M., & Axel, R. (2003). Axonal ephrin-As and odorant receptors: coordinate determination of the olfactory sensory map. *Cell, 114*(3), 311−322. Retrieved from: http://www.ncbi.nlm.nih.gov/pubmed/12914696.

Davies, A. M. (1988). The trigeminal system: an advantageous experimental model for studying neuronal development. *Development (Cambridge, England), 103*(Suppl.), 175−183. Retrieved from: http://www.ncbi.nlm.nih.gov/pubmed/3074907.

Dempsey, W. P., Fraser, S. E., & Pantazis, P. (2012). PhOTO zebrafish: a transgenic resource for in vivo lineage tracing during development and regeneration. *PLoS One, 7*(3). http://dx.doi.org/10.1371/journal.pone.0032888.

Devos, N., Deflorian, G., Biemar, F., Bortolussi, M., Martial, J. A., Peers, B., & Argenton, F. (2002). Differential expression of two somatostatin genes during zebrafish embryonic development. *Mechanisms of Development, 115*(1−2), 133−137. Retrieved from: http://www.ncbi.nlm.nih.gov/pubmed/12049777.

Duggan, C. D., DeMaria, S., Baudhuin, A., Stafford, D., & Ngai, J. (2008). Foxg1 is required for development of the vertebrate olfactory system. *The Journal of Neuroscience, 28*(20), 5229−5239. http://dx.doi.org/10.1523/JNEUROSCI.1134-08.2008.

Dutta, S., Dietrich, J.-E. E., Aspöck, G., Burdine, R. D., Schier, A., Westerfield, M., & Varga, Z. M. M. (2005). pitx3 defines an equivalence domain for lens and anterior pituitary placode. *Development (Cambridge, England), 132*(7), 1579−1590. http://dx.doi.org/10.1242/dev.01723.

Esterberg, R., & Fritz, A. (2009). dlx3b/4b are required for the formation of the preplacodal region and otic placode through local modulation of BMP activity. *Developmental Biology, 325*(1), 189−199. http://dx.doi.org/10.1016/j.ydbio.2008.10.017.

Esteves, F. F., Springhorn, A., Kague, E., Taylor, E., Pyrowolakis, G., Fisher, S., & Bier, E. (2014). BMPs regulate msx gene expression in the dorsal neuroectoderm of Drosophila and vertebrates by distinct mechanisms. *PLoS Genetics, 10*(9). http://dx.doi.org/10.1371/journal.pgen.1004625.

Feledy, J. A., Beanan, M. J., Sandoval, J. J., Goodrich, J. S., Lim, J. H., Matsuo-Takasaki, M., & Sargent, T. D. (1999). Inhibitory patterning of the anterior neural plate in *Xenopus* by

homeodomain factors Dlx3 and Msx1. *Developmental Biology, 212*(2), 455–464. http://dx.doi.org/10.1006/dbio.1999.9374.

Garnett, A. T., Square, T. A., & Medeiros, D. M. (2012). BMP, Wnt and FGF signals are integrated through evolutionarily conserved enhancers to achieve robust expression of Pax3 and Zic genes at the zebrafish neural plate border. *Development (Cambridge, England), 139*(22), 4220–4231. http://dx.doi.org/10.1242/dev.081497.

Gayoso, J., Castro, A., Anadón, R., & Manso, M. J. J. (2012). Crypt cells of the zebrafish *Danio rerio* mainly project to the dorsomedial glomerular field of the olfactory bulb. *Chemical Senses, 37*(4), 357–369. http://dx.doi.org/10.1093/chemse/bjr109.

Glavic, A., Honoré, S., Feijóo, C., Bastidas, F., Allende, M. L., & Mayor, R. (2003). Role of BMP signaling and the homeoprotein iroquois in the specification of the cranial placodal field. *Developmental Biology, 272*(1). http://dx.doi.org/10.1016/j.ydbio.2004.04.020.

Golling, G., Amsterdam, A., Sun, Z., Antonelli, M., Maldonado, E., Chen, W., & Hopkins, N. (2002). Insertional mutagenesis in zebrafish rapidly identifies genes essential for early vertebrate development. *Nature Genetics, 31*(2), 135–140. http://dx.doi.org/10.1038/ng896.

Gonzales, A., & Yeh, J.-R. (2014). Chapter eighteen—cas9-based genome editing in zebrafish. *Methods in Enzymology, 546*. http://dx.doi.org/10.1016/B978-0-12-801185-0.00018-0.

Grocott, T., Tambalo, M., & Streit, A. (2012). The peripheral sensory nervous system in the vertebrate head: a gene regulatory perspective. *Developmental Biology, 370*(1). http://dx.doi.org/10.1016/j.ydbio.2012.06.028.

Groves, A. K., & LaBonne, C. (2013). Setting appropriate boundaries: fate, patterning and competence at the neural plate border. *Developmental Biology, 389*(1). http://dx.doi.org/10.1016/j.ydbio.2013.11.027.

Guillemot, F., Lo, L. C., Johnson, J. E., Auerbach, A., Anderson, D. J., & Joyner, A. L. (1993). Mammalian achaete-scute homolog 1 is required for the early development of olfactory and autonomic neurons. *Cell, 75*(3), 463–476. Retrieved from: http://www.ncbi.nlm.nih.gov/pubmed/8221886.

Haddon, C., Jiang, Y. J., Smithers, L., & Lewis, J. (1998). Delta-Notch signalling and the patterning of sensory cell differentiation in the zebrafish ear: evidence from the mind bomb mutant. *Development (Cambridge, England), 125*(23), 4637–4644. Retrieved from: http://www.ncbi.nlm.nih.gov/pubmed/9806913.

Haddon, C., & Lewis, J. (1996). Early ear development in the embryo of the zebrafish, *Danio rerio*. *The Journal of Comparative Neurology, 365*(1), 113–128. http://dx.doi.org/10.1002/(SICI)1096-9861(19960129)365:1<113::AID-CNE9>3.0.CO;2–6.

Hamburger, V. (1961). Experimental analysis of the dual origin of the trigeminal ganglion in the chick embryo. *The Journal of Experimental Zoology, 148*, 91–123. Retrieved from: http://www.ncbi.nlm.nih.gov/pubmed/13904079.

Hammond, K. L., & Whitfield, T. T. (2011). Fgf and Hh signalling act on a symmetrical prepattern to specify anterior and posterior identity in the zebrafish otic placode and vesicle. *Development (Cambridge, England), 138*(18), 3977–3987. http://dx.doi.org/10.1242/dev.066639.

Hanashima, C., Fernandes, M., Hebert, J. M., & Fishell, G. (2007). The role of Foxg1 and dorsal midline signaling in the generation of Cajal-Retzius subtypes. *The Journal of Neuroscience: The Official Journal of the Society for Neuroscience, 27*(41), 11103–11111. http://dx.doi.org/10.1523/JNEUROSCI.1066-07.2007.

Hanashima, C., Li, S. C., Shen, L., Lai, E., & Fishell, G. (2004). Foxg1 suppresses early cortical cell fate. *Science (New York, N.Y.), 303*(5654), 56–59. http://dx.doi.org/10.1126/science.1090674.

Hans, S., Irmscher, A., & Brand, M. (2013). Zebrafish Foxi1 provides a neuronal ground state during inner ear induction preceding the Dlx3b/4b-regulated sensory lineage. *Development, 140*(9), 1936−1945. http://dx.doi.org/10.1242/dev.087718.

Hansen, A., & Zielinski, B. S. (2005). Diversity in the olfactory epithelium of bony fishes: development, lamellar arrangement, sensory neuron cell types and transduction components. *Journal of Neurocytology, 34*(3−5), 183−208. http://dx.doi.org/10.1007/s11068-005-8353-1.

Harden, M. V., Pereiro, L., Ramialison, M., Wittbrodt, J., Prasad, M. K., McCallion, A. S., & Whitlock, K. E. (2012). Close association of olfactory placode precursors and cranial neural crest cells does not predestine cell mixing. *Developmental Dynamics: An Official Publication of the American Association of Anatomists, 241*(7), 1143−1154. http://dx.doi.org/10.1002/dvdy.23797.

Hibi, M., & Shimizu, T. (2012). Development of the cerebellum and cerebellar neural circuits. *Developmental Neurobiology, 72*(3), 282−301. http://dx.doi.org/10.1002/dneu.20875.

Hoijman, E., Rubbini, D., Colombelli, J., & Alsina, B. (2015). Mitotic cell rounding and epithelial thinning regulate lumen growth and shape. *Nature Communications, 6*, 7355. http://dx.doi.org/10.1038/ncomms8355.

Hong, C.-S. S., & Saint-Jeannet, J.-P. P. (2007). The activity of Pax3 and Zic1 regulates three distinct cell fates at the neural plate border. *Molecular Biology of the Cell, 18*(6), 2192−2202. http://dx.doi.org/10.1091/mbc.E06-11-1047.

Huang, X., Hong, C.-S. S., O'Donnell, M., & Saint-Jeannet, J.-P. P. (2005). The doublesex-related gene, XDmrt4, is required for neurogenesis in the olfactory system. *Proceedings of the National Academy of Sciences of the United States of America, 102*(32), 11349−11354. http://dx.doi.org/10.1073/pnas.0505106102.

Ikeda, K., Watanabe, Y., Ohto, H., & Kawakami, K. (2002). Molecular interaction and synergistic activation of a promoter by Six, Eya, and Dach proteins mediated through CREB binding protein. *Molecular and Cellular Biology, 22*(19), 6759−6766. Retrieved from: http://www.ncbi.nlm.nih.gov/pubmed/12215533.

Itoh, M., Kudoh, T., Dedekian, M., Kim, C.-H. H., & Chitnis, A. B. (2002). A role for iro1 and iro7 in the establishment of an anteroposterior compartment of the ectoderm adjacent to the midbrain-hindbrain boundary. *Development (Cambridge, England), 129*(10), 2317−2327. Retrieved from: http://www.ncbi.nlm.nih.gov/pubmed/11973265.

Jordt, S.-E. E., Bautista, D. M., Chuang, H.-H. H., McKemy, D. D., Zygmunt, P. M., Högestätt, E. D., & Julius, D. (2004). Mustard oils and cannabinoids excite sensory nerve fibres through the TRP channel ANKTM1. *Nature, 427*(6971), 260−265. http://dx.doi.org/10.1038/nature02282.

Kaji, T., & Artinger, K. B. (2004). dlx3b and dlx4b function in the development of Rohon-Beard sensory neurons and trigeminal placode in the zebrafish neurula. *Developmental Biology, 276*(2), 523−540. http://dx.doi.org/10.1016/j.ydbio.2004.09.020.

Kantarci, H., Edlund, R. K., Groves, A. K., & Riley, B. B. (2015). Tfap2a promotes specification and maturation of neurons in the inner ear through modulation of bmp, fgf and notch signaling. *PLoS Genetics, 11*(3). http://dx.doi.org/10.1371/journal.pgen.1005037.

Kiecker, C., & Lumsden, A. (2012). The role of organizers in patterning the nervous system. *Annual Review of Neuroscience, 35*, 347−367. http://dx.doi.org/10.1146/annurev-neuro-062111-150543.

Knaut, H., Blader, P., Strähle, U., & Schier, A. F. (2005). Assembly of trigeminal sensory ganglia by chemokine signaling. *Neuron, 47*(5). http://dx.doi.org/10.1016/j.neuron.2005.07.014.

Kobayashi, M., Osanai, H., Kawakami, K., & Yamamoto, M. (2000). Expression of three zebrafish Six4 genes in the cranial sensory placodes and the developing somites.

Mechanisms of Development, 98(1−2), 151−155. Retrieved from: http://www.ncbi.nlm.nih.gov/pubmed/11044620.

Korzh, V., Sleptsova, I., Liao, J., He, J., & Gong, Z. (1998). Expression of zebrafish bHLH genes ngn1 and nrd defines distinct stages of neural differentiation. *Developmental Dynamics: An Official Publication of the American Association of Anatomists, 213*(1), 92−104. http://dx.doi.org/10.1002/(SICI)1097-0177(199809)213:1<92::AID-AJA9>3.0.CO;2-T.

Kozlowski, D. J., Murakami, T., Ho, R. K., & Weinberg, E. S. (1997). Regional cell movement and tissue patterning in the zebrafish embryo revealed by fate mapping with caged fluorescein. *Biochemistry and Cell Biology = Biochimie et Biologie Cellulaire, 75*(5), 551−562. Retrieved from: http://www.ncbi.nlm.nih.gov/pubmed/9551179.

Kozlowski, D. J., Whitfield, T. T., Hukriede, N. A., Lam, W. K., & Weinberg, E. S. (2005). The zebrafish dog-eared mutation disrupts eya1, a gene required for cell survival and differentiation in the inner ear and lateral line. *Developmental Biology, 277*(1), 27−41. http://dx.doi.org/10.1016/j.ydbio.2004.08.033.

Krauss, S., Johansen, T., Korzh, V., & Fjose, A. (1991). Expression pattern of zebrafish pax genes suggests a role in early brain regionalization. *Nature, 353*(6341), 267−270. http://dx.doi.org/10.1038/353267a0.

Kudoh, T., Concha, M. L., Houart, C., Dawid, I. B., & Wilson, S. W. (2004). Combinatorial Fgf and Bmp signalling patterns the gastrula ectoderm into prospective neural and epidermal domains. *Development (Cambridge, England), 131*(15), 3581−3592. http://dx.doi.org/10.1242/dev.01227.

Kudoh, T., Wilson, S. W., & Dawid, I. B. (2002). Distinct roles for Fgf, Wnt and retinoic acid in posteriorizing the neural ectoderm. *Development (Cambridge, England), 129*(18), 4335−4346. Retrieved from: http://www.ncbi.nlm.nih.gov/pubmed/12183385.

Kwon, H.-J. J., Bhat, N., Sweet, E. M., Cornell, R. A., & Riley, B. B. (2010). Identification of early requirements for preplacodal ectoderm and sensory organ development. *PLoS Genetics, 6*(9). http://dx.doi.org/10.1371/journal.pgen.1001133.

Laclef, C., Souil, E., Demignon, J., & Maire, P. (2003). Thymus, kidney and craniofacial abnormalities in Six 1 deficient mice. *Mechanisms of Development, 120*(6), 669−679. Retrieved from: http://www.ncbi.nlm.nih.gov/pubmed/12834866.

Lakhina, V., Marcaccio, C. L., Shao, X., Lush, M. E., Jain, R. A., Fujimoto, E., & Raper, J. A. (2012). Netrin/DCC signaling guides olfactory sensory axons to their correct location in the olfactory bulb. *The Journal of Neuroscience: The Official Journal of the Society for Neuroscience, 32*(13), 4440−4456. http://dx.doi.org/10.1523/JNEUROSCI.4442-11.2012.

Langenau, D. M., Palomero, T., Kanki, J. P., Ferrando, A. A., Zhou, Y., Zon, L. I., & Look, A. T. (2002). Molecular cloning and developmental expression of Tlx (Hox11) genes in zebrafish (*Danio rerio*). *Mechanisms of Development, 117*(1−2), 243−248. Retrieved from: http://www.ncbi.nlm.nih.gov/pubmed/12204264.

Lecaudey, V., Anselme, I., Dildrop, R., Rüther, U., & Schneider-Maunoury, S. (2005). Expression of the zebrafish Iroquois genes during early nervous system formation and patterning. *The Journal of Comparative Neurology, 492*(3), 289−302. http://dx.doi.org/10.1002/cne.20765.

Léger, S., & Brand, M. (2002). Fgf8 and Fgf3 are required for zebrafish ear placode induction, maintenance and inner ear patterning. *Mechanisms of Development, 119*(1), 91−108. Retrieved from: http://www.ncbi.nlm.nih.gov/pubmed/12385757.

Lele, Z., Folchert, A., Concha, M., Rauch, G.-J. J., Geisler, R., Rosa, F., & Bally-Cuif, L. (2002). parachute/n-cadherin is required for morphogenesis and maintained integrity of the zebrafish neural tube. *Development (Cambridge, England), 129*(14), 3281−3294. Retrieved from: http://www.ncbi.nlm.nih.gov/pubmed/12091300.

Li, X., Oghi, K. A., Zhang, J., Krones, A., Bush, K. T., Glass, C. K., & Rosenfeld, M. G. (2003). Eya protein phosphatase activity regulates Six1-Dach-Eya transcriptional effects in mammalian organogenesis. *Nature, 426*(6964), 247−254. http://dx.doi.org/10.1038/nature02083.

Lin, Z., Cantos, R., Patente, M., & Wu, D. K. (2005). Gbx2 is required for the morphogenesis of the mouse inner ear: a downstream candidate of hindbrain signaling. *Development (Cambridge, England), 132*(10), 2309−2318. http://dx.doi.org/10.1242/dev.01804.

Litsiou, A., Hanson, S., & Streit, A. (2005). A balance of FGF, BMP and WNT signalling positions the future placode territory in the head. *Development (Cambridge, England), 132*(18), 4051−4062. http://dx.doi.org/10.1242/dev.01964.

Liu, L., Korzh, V., Balasubramaniyan, N. V., Ekker, M., & Ge, R. (2002). Platelet-derived growth factor A (pdgf-a) expression during zebrafish embryonic development. *Development Genes and Evolution, 212*(6), 298−301. Retrieved from: http://www.ncbi.nlm.nih.gov/pubmed/12211169.

Lleras-Forero, L., & Streit, A. (2012). Development of the sensory nervous system in the vertebrate head: the importance of being on time. *Current Opinion in Genetics & Development, 22*(4), 315−322. http://dx.doi.org/10.1016/j.gde.2012.05.003.

Lleras-Forero, L., Tambalo, M., Christophorou, N., Chambers, D., Houart, C., & Streit, A. (2013). Neuropeptides: developmental signals in placode progenitor formation. *Developmental Cell, 26*(2). http://dx.doi.org/10.1016/j.devcel.2013.07.001.

Long, Q., Quint, E., Lin, S., & Ekker, M. (2000). The zebrafish scyba gene encodes a novel CXC-type chemokine with distinctive expression patterns in the vestibulo-acoustic system during embryogenesis. *Mechanisms of Development, 97*(1−2), 183−186. http://dx.doi.org/10.1016/S0925-4773(00)00408-1.

Ma, Q., Chen, Z., del Barco Barrantes, I., de la Pompa, J. L., & Anderson, D. J. (1998). neurogenin1 is essential for the determination of neuronal precursors for proximal cranial sensory ganglia. *Neuron, 20*(3), 469−482. Retrieved from: http://www.ncbi.nlm.nih.gov/pubmed/9539122.

Mackereth, M. D., Kwak, S.-J. J., Fritz, A., & Riley, B. B. (2005). Zebrafish pax8 is required for otic placode induction and plays a redundant role with Pax2 genes in the maintenance of the otic placode. *Development (Cambridge, England), 132*(2), 371−382. http://dx.doi.org/10.1242/dev.01587.

Madelaine, R., Garric, L., & Blader, P. (2011). Partially redundant proneural function reveals the importance of timing during zebrafish olfactory neurogenesis. *Development, 138*(21), 4753−4762. http://dx.doi.org/10.1242/dev.066563.

Maier, E. C., Saxena, A., Alsina, B., Bronner, M. E., & Whitfield, T. T. (2014). Sensational placodes: neurogenesis in the otic and olfactory systems. *Developmental Biology, 389*(1). http://dx.doi.org/10.1016/j.ydbio.2014.01.023.

Maier, E. C., & Whitfield, T. T. (2014). RA and FGF signalling are required in the zebrafish otic vesicle to pattern and maintain ventral otic identities. *PLoS Genetics, 10*(12). http://dx.doi.org/10.1371/journal.pgen.1004858.

Mandal, A., Rydeen, A., Anderson, J., Sorrell, M. R., Zygmunt, T., Torres-Vázquez, J., & Waxman, J. S. (2013). Transgenic retinoic acid sensor lines in zebrafish indicate regions of available embryonic retinoic acid. *Developmental Dynamics: An Official Publication of the American Association of Anatomists, 242*(8), 989−1000. http://dx.doi.org/10.1002/dvdy.23987.

Martin, K., & Groves, A. K. (2006). Competence of cranial ectoderm to respond to Fgf signaling suggests a two-step model of otic placode induction. *Development (Cambridge, England), 133*(5), 877−887. http://dx.doi.org/10.1242/dev.02267.

Maulding, K., Padanad, M. S., Dong, J., & Riley, B. B. (2014). Mesodermal Fgf10b cooperates with other fibroblast growth factors during induction of otic and epibranchial placodes in zebrafish. *Developmental Dynamics: An Official Publication of the American Association of Anatomists, 243*(10), 1275−1285. http://dx.doi.org/10.1002/dvdy.24119.

McCabe, K. L., & Bronner-Fraser, M. (2009). Molecular and tissue interactions governing induction of cranial ectodermal placodes. *Developmental Biology, 332*(2), 189−195. http://dx.doi.org/10.1016/j.ydbio.2009.05.572.

McCarroll, M. N., Lewis, Z. R., Culbertson, M., Martin, B. L., Kimelman, D., & Nechiporuk, A. V. (2012). Graded levels of Pax2a and Pax8 regulate cell differentiation during sensory placode formation. *Development, 139*(15), 2740−2750. http://dx.doi.org/10.1242/dev.076075.

Millimaki, B. B., Sweet, E. M., Dhason, M. S., & Riley, B. B. (2007). Zebrafish atoh1 genes: classic proneural activity in the inner ear and regulation by Fgf and Notch. *Development (Cambridge, England), 134*(2), 295−305. http://dx.doi.org/10.1242/dev.02734.

Miyasaka, N., Knaut, H., & Yoshihara, Y. (2007). Cxcl12/Cxcr4 chemokine signaling is required for placode assembly and sensory axon pathfinding in the zebrafish olfactory system. *Development (Cambridge, England), 134*(13), 2459−2468. http://dx.doi.org/10.1242/dev.001958.

Miyasaka, N., Sato, Y., Yeo, S.-Y., Hutson, L. D., Chien, C.-B., Okamoto, H., & Yoshihara, Y. (2005). Robo2 is required for establishment of a precise glomerular map in the zebrafish olfactory system. *Development, 132*(6), 1283−1293. http://dx.doi.org/10.1242/dev.01698.

Miyasaka, N., Wanner, A. A., Li, J., Mack-Bucher, J., Genoud, C., Yoshihara, Y., & Friedrich, R. W. (2013). Functional development of the olfactory system in zebrafish. *Mechanisms of Development, 130*(6−8), 336−346. http://dx.doi.org/10.1016/j.mod.2012.09.001.

Moody, S. A., & LaMantia, A.-S. S. (2015). Transcriptional regulation of cranial sensory placode development. *Current Topics in Developmental Biology, 111*, 301−350. http://dx.doi.org/10.1016/bs.ctdb.2014.11.009.

Moro, E., Vettori, A., Porazzi, P., Schiavone, M., Rampazzo, E., Casari, A., & Argenton, F. (2013). Generation and application of signaling pathway reporter lines in zebrafish. *Molecular Genetics and Genomics: MGG, 288*(5−6), 231−242. http://dx.doi.org/10.1007/s00438-013-0750-z.

Neave, B., Holder, N., & Patient, R. (1997). A graded response to BMP-4 spatially coordinates patterning of the mesoderm and ectoderm in the zebrafish. *Mechanisms of Development, 62*(2), 183−195. Retrieved from: http://www.ncbi.nlm.nih.gov/pubmed/9152010.

Nguyen, V. H., Schmid, B., Trout, J., Connors, S. A., Ekker, M., & Mullins, M. C. (1998). Ventral and lateral regions of the zebrafish gastrula, including the neural crest progenitors, are established by a bmp2b/swirl pathway of genes. *Developmental Biology, 199*(1), 93−110. http://dx.doi.org/10.1006/dbio.1998.8927.

Nica, G., Herzog, W., Sonntag, C., Nowak, M., Schwarz, H., Zapata, A. G., & Hammerschmidt, M. (2006). Eya1 is required for lineage-specific differentiation, but not for cell survival in the zebrafish adenohypophysis. *Developmental Biology, 292*(1), 189−204. http://dx.doi.org/10.1016/j.ydbio.2005.12.036.

Nicolay, D. J., Doucette, J. R., & Nazarali, A. J. (2006). Transcriptional regulation of neurogenesis in the olfactory epithelium. *Cellular and Molecular Neurobiology, 26*(4−6), 803−821. http://dx.doi.org/10.1007/s10571-006-9058-4.

Nicolson, T. (2005a). Fishing for key players in mechanotransduction. *Trends in Neurosciences, 28*(3), 140−144. http://dx.doi.org/10.1016/j.tins.2004.12.008.

Nicolson, T. (2005b). The genetics of hearing and balance in zebrafish. *Annual Review of Genetics, 39*, 9−22. http://dx.doi.org/10.1146/annurev.genet.39.073003.105049.

Ogino, H., Fisher, M., & Grainger, R. M. (2008). Convergence of a head-field selector Otx2 and Notch signaling: a mechanism for lens specification. *Development (Cambridge, England), 135*(2), 249−258. http://dx.doi.org/10.1242/dev.009548.

Ozaki, H., Watanabe, Y., Ikeda, K., & Kawakami, K. (2002). Impaired interactions between mouse Eyal harboring mutations found in patients with branchio-oto-renal syndrome and Six, Dach, and G proteins. *Journal of Human Genetics, 47*(3), 107−116. http://dx.doi.org/10.1007/s100380200011.

Padanad, M. S., Bhat, N., Guo, B., & Riley, B. B. (2012). Conditions that influence the response to Fgf during otic placode induction. *Developmental Biology, 364*(1), 1−10. http://dx.doi.org/10.1016/j.ydbio.2012.01.022.

Padanad, M. S., & Riley, B. B. (2011). Pax2/8 proteins coordinate sequential induction of otic and epibranchial placodes through differential regulation of foxi1, sox3 and fgf24. *Developmental Biology, 351*(1), 90−98. http://dx.doi.org/10.1016/j.ydbio.2010.12.036.

Patthey, C., Schlosser, G., & Shimeld, S. M. (2014). The evolutionary history of vertebrate cranial placodes−I: cell type evolution. *Developmental Biology, 389*(1), 82−97. http://dx.doi.org/10.1016/j.ydbio.2014.01.017.

Phillips, B. T., Bolding, K., & Riley, B. B. (2001). Zebrafish fgf3 and fgf8 encode redundant functions required for otic placode induction. *Developmental Biology, 235*(2), 351−365. http://dx.doi.org/10.1006/dbio.2001.0297.

Phillips, B. T., Kwon, H.-J. J., Melton, C., Houghtaling, P., Fritz, A., & Riley, B. B. (2006). Zebrafish msxB, msxC and msxE function together to refine the neural-nonneural border and regulate cranial placodes and neural crest development. *Developmental Biology, 294*(2), 376−390. http://dx.doi.org/10.1016/j.ydbio.2006.03.001.

Pieper, M., Ahrens, K., Rink, E., Peter, A., & Schlosser, G. (2012). Differential distribution of competence for panplacodal and neural crest induction to non-neural and neural ectoderm. *Development (Cambridge, England), 139*(6), 1175−1187. http://dx.doi.org/10.1242/dev.074468.

Pieper, M., Eagleson, G. W., Wosniok, W., & Schlosser, G. (2011). Origin and segregation of cranial placodes in *Xenopus laevis*. *Developmental Biology, 360*(2), 257−275. http://dx.doi.org/10.1016/j.ydbio.2011.09.024.

Radosevic, M., Fargas, L., & Alsina, B. (2014). The role of her4 in inner ear development and its relationship with proneural genes and notch signalling. *PLoS One, 9*(10). http://dx.doi.org/10.1371/journal.pone.0109860.

Radosevic, M., Robert-Moreno, À., Coolen, M., Bally-Cuif, L., & Alsina, B. (2011). Her9 represses neurogenic fate downstream of Tbx1 and retinoic acid signaling in the inner ear. *Development, 138*(3), 397−408. http://dx.doi.org/10.1242/dev.056093.

Raible, F., & Brand, M. (2004). Divide et Impera−the midbrain-hindbrain boundary and its organizer. *Trends in Neurosciences, 27*(12), 727−734. http://dx.doi.org/10.1016/j.tins.2004.10.003.

Ramel, M.-C., & Hill, C. S. (2012). Spatial regulation of BMP activity. *FEBS Letters, 586*(14). http://dx.doi.org/10.1016/j.febslet.2012.02.035.

Reichert, S., Randall, R. A., & Hill, C. S. (2013). A BMP regulatory network controls ectodermal cell fate decisions at the neural plate border. *Development, 140*(21). http://dx.doi.org/10.1242/dev.098707.

Rhinn, M., Lun, K., Ahrendt, R., Geffarth, M., & Brand, M. (2009). Zebrafish gbx1 refines the midbrain-hindbrain boundary border and mediates the Wnt8 posteriorization signal. *Neural Development, 4*, 12. http://dx.doi.org/10.1186/1749-8104-4-12.

Rhinn, M., Lun, K., Luz, M., Werner, M., & Brand, M. (2005). Positioning of the midbrain-hindbrain boundary organizer through global posteriorization of the neuroectoderm

mediated by Wnt8 signaling. *Development (Cambridge, England), 132*(6), 1261−1272. http://dx.doi.org/10.1242/dev.01685.

Rubel, E. W., & Fritzsch, B. (2002). Auditory system development: primary auditory neurons and their targets. *Annual Review of Neuroscience, 25*, 51−101. http://dx.doi.org/10.1146/annurev.neuro.25.112701.142849.

Saint-Amant, L., & Drapeau, P. (1998). Time course of the development of motor behaviors in the zebrafish embryo. *Journal of Neurobiology, 37*(4), 622−632. Retrieved from: http://www.ncbi.nlm.nih.gov/pubmed/9858263.

Saint-Jeannet, J.-P. P., & Moody, S. A. (2014). Establishing the pre-placodal region and breaking it into placodes with distinct identities. *Developmental Biology, 389*(1), 13−27. http://dx.doi.org/10.1016/j.ydbio.2014.02.011.

Sapède, D., & Pujades, C. (2010). Hedgehog signaling governs the development of otic sensory epithelium and its associated innervation in zebrafish. *The Journal of Neuroscience, 30*(10), 3612−3623. http://dx.doi.org/10.1523/JNEUROSCI.5109-09.2010.

Sato, Y., Miyasaka, N., & Yoshihara, Y. (2005). Mutually exclusive glomerular innervation by two distinct types of olfactory sensory neurons revealed in transgenic zebrafish. *The Journal of Neuroscience, 25*(20), 4889−4897. http://dx.doi.org/10.1523/JNEUROSCI.0679-05.2005.

Saxena, A., Peng, B. N., & Bronner, M. E. (2013). Sox10-dependent neural crest origin of olfactory microvillous neurons in zebrafish. *eLife, 2*(0). http://dx.doi.org/10.7554/eLife.00336.

Schlosser, G. (2005). Induction and specification of cranial placodes. *Developmental Biology, 294*(2). http://dx.doi.org/10.1016/j.ydbio.2006.03.009.

Schlosser, G. (2007). How old genes make a new head: redeployment of Six and Eya genes during the evolution of vertebrate cranial placodes. *Integrative and Comparative Biology, 47*(3), 343−359. http://dx.doi.org/10.1093/icb/icm031.

Schlosser, G. (2010). Making senses development of vertebrate cranial placodes. *International Review of Cell and Molecular Biology, 283*, 129−234. http://dx.doi.org/10.1016/S1937-6448(10)83004-7.

Schlosser, G. (2014). Early embryonic specification of vertebrate cranial placodes. *Wiley Interdisciplinary Reviews. Developmental Biology, 3*(5), 349−363. http://dx.doi.org/10.1002/wdev.142.

Schlosser, G. (2015). Vertebrate cranial placodes as evolutionary innovations−the ancestor's tale. *Current Topics in Developmental Biology, 111*, 235−300. http://dx.doi.org/10.1016/bs.ctdb.2014.11.008.

Schneider-Maunoury, S., & Pujades, C. (2007). Hindbrain signals in otic regionalization: walk on the wild side. *The International Journal of Developmental Biology, 51*(6−7), 495−506. http://dx.doi.org/10.1387/ijdb.072345ss.

Schumacher, J. A., Hashiguchi, M., Nguyen, V. H., & Mullins, M. C. (2011). An intermediate level of BMP signaling directly specifies cranial neural crest progenitor cells in zebrafish. *PLoS One, 6*(11). http://dx.doi.org/10.1371/journal.pone.0027403.

Schwarting, G. A., Kostek, C., Ahmad, N., Dibble, C., Pays, L., & Püschel, A. W. (2000). Semaphorin 3A is required for guidance of olfactory axons in mice. *The Journal of Neuroscience: The Official Journal of the Society for Neuroscience, 20*(20), 7691−7697. Retrieved from: http://www.ncbi.nlm.nih.gov/pubmed/11027230.

Shen, L., Nam, H.-S. S., Song, P., Moore, H., & Anderson, S. A. (2006). FoxG1 haploinsufficiency results in impaired neurogenesis in the postnatal hippocampus and contextual memory deficits. *Hippocampus, 16*(10), 875−890. http://dx.doi.org/10.1002/hipo.20218.

Shi, X., Bosenko, D. V., Zinkevich, N. S., Foley, S., Hyde, D. R., Semina, E. V., & Vihtelic, T. S. (2005). Zebrafish pitx3 is necessary for normal lens and retinal development. *Mechanisms of Development, 122*(4), 513−527. http://dx.doi.org/10.1016/j.mod.2004.11.012.

Shiotsugu, J., Katsuyama, Y., Arima, K., Baxter, A., Koide, T., Song, J., & Blumberg, B. (2004). Multiple points of interaction between retinoic acid and FGF signaling during embryonic axis formation. *Development (Cambridge, England), 131*(11), 2653−2667. http://dx.doi.org/10.1242/dev.01129.

So, J.-H., Chun, H.-S., Bae, Y.-K., Kim, H.-S., Park, Y.-M., Huh, T.-L., & Yeo, S.-Y. (2009). Her4 is necessary for establishing peripheral projections of the trigeminal ganglia in zebrafish. *Biochemical and Biophysical Research Communications, 379*(1), 22−26. http://dx.doi.org/10.1016/j.bbrc.2008.11.149.

Solomon, K. S., & Fritz, A. (2002). Concerted action of two dlx paralogs in sensory placode formation. *Development (Cambridge, England), 129*(13), 3127−3136. Retrieved from: http://www.ncbi.nlm.nih.gov/pubmed/12070088.

Stark, M. R. (2014). Vertebrate neurogenic placode development: historical highlights that have shaped our current understanding. *Developmental Dynamics: An Official Publication of the American Association of Anatomists, 243*(10), 1167−1175. http://dx.doi.org/10.1002/dvdy.24152.

Steventon, B., Mayor, R., & Streit, A. (2012). Mutual repression between Gbx2 and Otx2 in sensory placodes reveals a general mechanism for ectodermal patterning. *Developmental Biology, 367*(1), 55−65. http://dx.doi.org/10.1016/j.ydbio.2012.04.025.

Streit, A. (2002). Extensive cell movements accompany formation of the otic placode. *Developmental Biology, 249*(2), 237−254. Retrieved from: http://www.ncbi.nlm.nih.gov/pubmed/12221004.

Stuhlmiller, T. J., & García-Castro, M. I. I. (2012). Current perspectives of the signaling pathways directing neural crest induction. *Cellular and Molecular Life Sciences: CMLS, 69*(22), 3715−3737. http://dx.doi.org/10.1007/s00018-012-0991-8.

Suzuki, A., Ueno, N., & Hemmati-Brivanlou, A. (1997). *Xenopus* msx1 mediates epidermal induction and neural inhibition by BMP4. *Development (Cambridge, England), 124*(16), 3037−3044. Retrieved from: http://www.ncbi.nlm.nih.gov/pubmed/9272945.

Taniguchi, M., Nagao, H., Takahashi, Y. K., Yamaguchi, M., Mitsui, S., Yagi, T., & Shimizu, T. (2003). Distorted odor maps in the olfactory bulb of semaphorin 3A-deficient mice. *The Journal of Neuroscience: The Official Journal of the Society for Neuroscience, 23*(4), 1390−1397. Retrieved from: http://www.ncbi.nlm.nih.gov/pubmed/12598627.

Tay, H. G., Schulze, S. K., Compagnon, J., Foley, F. C., Heisenberg, C.-P. P., Yost, H. J., & Amack, J. D. (2013). Lethal giant larvae 2 regulates development of the ciliated organ Kupffer's vesicle. *Development (Cambridge, England), 140*(7), 1550−1559. http://dx.doi.org/10.1242/dev.087130.

Theveneau, E., Steventon, B., Scarpa, E., Garcia, S., Trepat, X., Streit, A., & Mayor, R. (2013). Chase-and-run between adjacent cell populations promotes directional collective migration. *Nature Cell Biology, 15*(7), 763−772. http://dx.doi.org/10.1038/ncb2772.

Torres, M., Gómez-Pardo, E., Dressler, G. R., & Gruss, P. (1995). Pax-2 controls multiple steps of urogenital development. *Development (Cambridge, England), 121*(12), 4057−4065. Retrieved from: http://www.ncbi.nlm.nih.gov/pubmed/8575306.

Torres-Paz, J., & Whitlock, K. E. (2014). Olfactory sensory system develops from coordinated movements within the neural plate. *Developmental Dynamics, 243*(12), 1619−1631. http://dx.doi.org/10.1002/dvdy.24194.

Tribulo, C., Aybar, M. J., Nguyen, V. H., Mullins, M. C., & Mayor, R. (2003). Regulation of Msx genes by a Bmp gradient is essential for neural crest specification. *Development (Cambridge, England), 130*(26), 6441−6452. http://dx.doi.org/10.1242/dev.00878.

Tucker, J. A., Mintzer, K. A., & Mullins, M. C. (2008). The BMP signaling gradient patterns dorsoventral tissues in a temporally progressive manner along the anteroposterior axis. *Developmental Cell, 14*(1), 108−119. http://dx.doi.org/10.1016/j.devcel.2007.11.004.

Vemaraju, S., Kantarci, H., Padanad, M. S., & Riley, B. B. (2012). A spatial and temporal gradient of Fgf differentially regulates distinct stages of neural development in the zebrafish inner ear. *PLoS Genetics, 8*(11). http://dx.doi.org/10.1371/journal.pgen.1003068.

Viktorin, G., Chiuchitu, C., Rissler, M., Varga, Z. M. M., & Westerfield, M. (2009). Emx3 is required for the differentiation of dorsal telencephalic neurons. *Developmental Dynamics: An Official Publication of the American Association of Anatomists, 238*(8), 1984−1998. http://dx.doi.org/10.1002/dvdy.22031.

Whitfield, T. T., & Hammond, K. L. (2007). Axial patterning in the developing vertebrate inner ear. *The International Journal of Developmental Biology, 51*(6−7), 507−520. http://dx.doi.org/10.1387/ijdb.072380tw.

Whitlock, K. E. (2004). A new model for olfactory placode development. *Brain, Behavior and Evolution, 64*(3), 126−140. http://dx.doi.org/10.1159/000079742.

Whitlock, K. E. (2008). Developing a sense of scents: plasticity in olfactory placode formation. *Brain Research Bulletin, 75*(2−4), 340−347. http://dx.doi.org/10.1016/j.brainresbull.2007.10.054.

Whitlock, K. E., & Westerfield, M. (1998). A transient population of neurons pioneers the olfactory pathway in the zebrafish. *The Journal of Neuroscience: The Official Journal of the Society for Neuroscience, 18*(21), 8919−8927. Retrieved from: http://www.ncbi.nlm.nih.gov/pubmed/9786997.

Whitlock, K. E., & Westerfield, M. (2000). The olfactory placodes of the zebrafish form by convergence of cellular fields at the edge of the neural plate. *Development (Cambridge, England), 127*(17), 3645−3653. Retrieved from: http://www.ncbi.nlm.nih.gov/pubmed/10934010.

Winkler, C., Hornung, U., Kondo, M., Neuner, C., Duschl, J., Shima, A., & Schartl, M. (2004). Developmentally regulated and non-sex-specific expression of autosomal dmrt genes in embryos of the Medaka fish (*Oryzias latipes*). *Mechanisms of Development, 121*(7−8), 997−1005. http://dx.doi.org/10.1016/j.mod.2004.03.018.

Woda, J. M., Pastagia, J., Mercola, M., & Artinger, K. B. (2003). Dlx proteins position the neural plate border and determine adjacent cell fates. *Development (Cambridge, England), 130*(2), 331−342. Retrieved from: http://www.ncbi.nlm.nih.gov/pubmed/12466200.

Wu, M. Y., Ramel, M.-C. C., Howell, M., & Hill, C. S. (2011). SNW1 is a critical regulator of spatial BMP activity, neural plate border formation, and neural crest specification in vertebrate embryos. *PLoS Biology, 9*(2). http://dx.doi.org/10.1371/journal.pbio.1000593.

Xu, H., Dude, C. M., & Baker, C. V. (2008). Fine-grained fate maps for the ophthalmic and maxillomandibular trigeminal placodes in the chick embryo. *Developmental Biology, 317*(1), 174−186. http://dx.doi.org/10.1016/j.ydbio.2008.02.012.

Xu, P. X., Adams, J., Peters, H., Brown, M. C., Heaney, S., & Maas, R. (1999). Eya1-deficient mice lack ears and kidneys and show abnormal apoptosis of organ primordia. *Nature Genetics, 23*(1), 113−117. http://dx.doi.org/10.1038/12722.

Yamamoto, T. S., Takagi, C., & Ueno, N. (2000). Requirement of Xmsx-1 in the BMP-triggered ventralization of *Xenopus* embryos. *Mechanisms of Development, 91*(1−2), 131−141. Retrieved from: http://www.ncbi.nlm.nih.gov/pubmed/10704838.

Yao, D., Zhao, F., Wu, Y., Wang, J., Dong, W., Zhao, J., & Liu, D. (2014). Dissecting the differentiation process of the preplacodal ectoderm in zebrafish. *Developmental Dynamics: An Official Publication of the American Association of Anatomists, 243*(10), 1338−1351. http://dx.doi.org/10.1002/dvdy.24160.

Yeo, S.-Y. Y., Kim, M., Kim, H.-S. S., Huh, T.-L. L., & Chitnis, A. B. (2007). Fluorescent protein expression driven by her4 regulatory elements reveals the spatiotemporal pattern of Notch signaling in the nervous system of zebrafish embryos. *Developmental Biology, 301*(2), 555−567. http://dx.doi.org/10.1016/j.ydbio.2006.10.020.

Zheng, W., Huang, L., Wei, Z.-B. B., Silvius, D., Tang, B., & Xu, P.-X. X. (2003). The role of Six1 in mammalian auditory system development. *Development (Cambridge, England), 130*(17), 3989−4000. Retrieved from: http://www.ncbi.nlm.nih.gov/pubmed/12874121.

Zilinski, C. A., Shah, R., Lane, M. E., & Jamrich, M. (2005). Modulation of zebrafish pitx3 expression in the primordia of the pituitary, lens, olfactory epithelium and cranial ganglia by hedgehog and nodal signaling. *Genesis (New York, N.Y.: 2000), 41*(1), *33−40*. http://dx.doi.org/10.1002/gene.20094.

Zou, D., Silvius, D., Fritzsch, B., & Xu, P.-X. X. (2004). Eya1 and Six1 are essential for early steps of sensory neurogenesis in mammalian cranial placodes. *Development (Cambridge, England), 131*(22), 5561−5572. http://dx.doi.org/10.1242/dev.01437.

La mer
Les a bercés
Le long des golfes clairs
Et d'une chanson d'amour
La mer
A bercé mon cœur pour la vie

Charles Trenet, 1945

Résumé

La formation d'un organe repose sur la coordination spatio-temporelle du positionnement et de la différenciation de progéniteurs. La finalité de ces évènements permet la constitution structurelle de l'organe et la production de la diversité cellulaire nécessaire pour assurer ses fonctions. L'épithélium olfactif de l'embryon de poisson-zèbre est issu de la migration de progéniteurs qui vont générer entre autres les neurones olfactifs. Au cours de ma thèse je me suis intéressé aux bases génétiques et moléculaires de la coordination de la morphogenèse et de la neurogenèse de cet épithélium tout en étudiant l'origine de la diversité des types cellulaires olfactifs.

L'imagerie en temps réel m'a permis de caractériser la migration de ces progéniteurs en générant une carte morphométrique de leur déplacement. Mon travail de thèse révèle que le proneural Neurog1 régule directement l'expression de *cxcr4b*, un récepteur aux chimiokines, dans les progéniteurs olfactifs assurant leur positionnement. Ainsi, Neurog1 coordonnerait la position et l'identité des progéniteurs olfactifs via ses cibles transcriptionnelles.

Au sein de l'épithélium olfactif dans l'embryon, deux populations cellulaires (neurones à GnRH et neurones à microvillosités) ont été décrites comme provenant des crêtes neurales céphaliques (CNC). J'ai pu montrer que l'expression de marqueurs spécifiques de ces populations n'est pas affectée dans un contexte d'absence de différenciation des CNCs ($sox10^{-/-}$) suggérant que ces types cellulaires ne dérivent pas de ce territoire. Afin d'identifier leur territoire d'origine, j'ai développé une méthode d'imagerie en temps réel, le backtracking, qui m'a permis de déterminer que la région de la placode olfactive, et non les crêtes neurales, génère ces deux types cellulaires. Ainsi j'ai pu définir la source de ces deux populations neuronales tout en minimisant la contribution des crêtes neurales.

En conclusion mes résultats suggèrent que la diversité des neurones olfactifs serait produite localement et ceci conjointement à la morphogenèse de l'épithélium.